



Université du Québec
à Rimouski

**Étude des interactions bioénergétiques
entre le rorqual bleu *Balaenoptera musculus* et le krill
dans l'estuaire et le golfe du Saint-Laurent**

**Bioenergetic interactions
between the blue whale *Balaenoptera musculus* and krill
in the Estuary and Gulf of St. Lawrence**

Thèse présentée

dans le cadre du programme de doctorat en océanographie
en vue de l'obtention du grade de *Philosophiae Doctor* (Ph.D)

PAR

© MARIE GUILPIN

Novembre 2020

Composition du jury :

Dr. David Deslauriers, président du jury, Université du Québec à Rimouski, Canada

Dr. Véronique Lesage, directrice, Pêches et Océans Canada, Canada

Dr. Gesche Winkler, co-directrice, Université du Québec à Rimouski, Canada

Dr. Martin Biuw, examinateur externe, Institute of Marine Research, Norvège

Dépôt initial le 07 Août 2020

Dépôt final le 10 Novembre 2020

UNIVERSITÉ DU QUÉBEC À RIMOUSKI
Service de la bibliothèque

Avertissement

La diffusion de ce mémoire ou de cette thèse se fait dans le respect des droits de son auteur, qui a signé le formulaire « *Autorisation de reproduire et de diffuser un rapport, un mémoire ou une thèse* ». En signant ce formulaire, l'auteur concède à l'Université du Québec à Rimouski une licence non exclusive d'utilisation et de publication de la totalité ou d'une partie importante de son travail de recherche pour des fins pédagogiques et non commerciales. Plus précisément, l'auteur autorise l'Université du Québec à Rimouski à reproduire, diffuser, prêter, distribuer ou vendre des copies de son travail de recherche à des fins non commerciales sur quelque support que ce soit, y compris l'Internet. Cette licence et cette autorisation n'entraînent pas une renonciation de la part de l'auteur à ses droits moraux ni à ses droits de propriété intellectuelle. Sauf entente contraire, l'auteur conserve la liberté de diffuser et de commercialiser ou non ce travail dont il possède un exemplaire.



MQ 2020

« Faut qu'tu t'rappelles de tes rêves

pour pas t'noyer dedans »

Anaïs Barbeau-Lavalette

À ma famille

À mes parents, pour leur soutien infailible

À ma grand-mère Jeanne

À mon grand-père Michel

REMERCIEMENTS

Alors que s'achèvent ces six années de travail, je souhaite adresser mes sincères remerciements à mes directrices de thèse, Véronique Lesage et Gesche Winkler. Je mesure la chance d'avoir pu travailler sur un tel projet, accompagnée de vos précieux conseils, de votre disponibilité et de votre soutien. Gesche, ton humanité, ton mentorat et ton soutien moral m'ont portée tout au long de ces six années. Véro, ton soutien sur tous les plans m'a fait avancer et m'a conduit à me dépasser. Je suis reconnaissante à toutes deux de m'avoir fait confiance et laissé mener ma barque tout en étant présentes.

Je remercie vivement David Deslauriers de présider mon jury de thèse et Martin Biuw d'en faire partie également. *Thank you Martin for showing a great interest in evaluating my thesis and for accepting to be part of my jury.*

Je tiens également à remercier Céline Audet d'avoir fait partie de mon comité de thèse. Au travers de ce doctorat, j'ai eu la chance de collaborer avec de nombreuses personnes qui auront participé à faire grandir mes travaux de recherche, mes connaissances et mes compétences. J'adresse ainsi toute ma gratitude à Ian McQuinn pour avoir partagé son savoir sur le krill et les données hydroacoustiques ainsi que pour avoir toujours répondu présent. Je souhaite également remercier Thomas Doniol-Valcroze pour avoir fait partie de mon comité de thèse et pour des discussions toujours enrichissantes. *Many thanks to Jean Potvin for his help and guidance on the energy expenditure equations. Thank you for our discussions and for meeting me at Jeremy's lab. A big thank you to Jeremy Goldbogen for hosting me in his lab for five weeks in the spring of 2017, for his advices and fruitful discussions around delicious and artsy lattes.* Je n'oublie pas Tiphaine Jeanniard du Dot pour ses conseils et son aide et Pablo Brosset pour avoir toujours été disponible pour répondre à mes nombreuses questions ainsi que pour son aide. *A big big thank you to Enrico Pirota for accepting to be part of the third chapter. Thank you for all your help, for letting me pick your brain, and for*

always responding to all my questions. On top of being a great collaborator, thank you for being my friend for now over 10 years, since our MRes in St Andrews.

Mes recherches ont pu être menées grâce Gesche et au Conseil de recherches en sciences naturelles et en génie du Canada (CRSNG) qui m'ont fait bénéficier d'une bourse de doctorat mais aussi grâce à Véronique et son soutien financier. Je remercie le réseau Québec-Océan, l'Institut des Sciences de la mer et l'Université du Québec à Rimouski grâce à qui j'ai pu assister à de nombreux congrès et ateliers mais aussi financer mon stage dans le laboratoire de Jeremy Goldbogen à la Hopkins Marine Station–Stanford University.

Je souhaite remercier grandement Fred Paquet pour avoir préparé toutes les données hydroacoustiques et pour avoir toujours été disponible pour répondre à mes questions. Merci Fred pour ton amitié. Bye, là. Mes remerciements vont à Michel Moisan, l'équipe du GREMM et Véro pour deux étés passés sur le terrain à déployer des tags sur des *Balaenoptera fuitlasuce* dans la joie et la bonne humeur, et ça dès 5:30am. J'adresse aussi mes remerciements à l'équipe du Parc marin du Saguenay–St-Laurent. Merci également à toute l'équipe des mammifères marins de l'Institut Maurice-Lamontagne, et Véro de m'avoir donné l'opportunité de participer aux relevés aériens et par bateau. J'ai eu la chance de faire partie de l'équipe du projet stratégique krill. Il aura été très enrichissant de travailler sur un projet s'intégrant dans une problématique aussi vaste et complète que celle du projet krill. Merci à toutes les personnes du labo zoo à l'ISMER et particulièrement Jory, collègue de doc du projet krill et Angélique. Enfin, merci à Martine Belzile pour son aide précieuse.

Six ans de thèse, c'est aussi six ans de vie avec son lot de petits bonheurs et de difficultés. Durant ces six années des gens sont arrivés tandis que d'autres ont continué vers d'autres horizons. Je suis ainsi redevable à tous les gens qui sont passés par le bureau O-202 et surtout Blandine, Jory et David B., et plus largement à la troupe du bureau O-262 pour les lundis pâtisserie et leurs encouragements durant cette dernière année. Les sessions aquarelle avec Clémence et Sarah depuis presque un an ont été une bouffée d'air et je leur suis

reconnaissante pour leur soutien. Merci ainsi à Sarah pour sa présence précieuse, surtout durant cette fin de thèse sur ton de confinement et de pandémie de covid-19. Sophie et Laurie, mes belles amies et complices de poterie (cette échappatoire de créativité artistique), je vous remercie ! Un grand merci à David P., Sydni, Josiane, CAR, Fred, Alain, Katy, David G., Bertrand, Andrew, Leïla. Merci à mes amis proches en France, Ecosse, Irlande, *you know who you are and I am grateful for your friendship and moral support.*

Pablo, merci de ton aide, soutien et amitié. Tiphaine, merci pour ton soutien sans faille, tes encouragements, et ta précieuse amitié. Merci à Marie-Pier, mon amie et la meilleure coloc qui soit. Les fous rires, les discussions dans le cadre de porte, ton soutien continu et tes encouragements à toujours croire en moi ont été particulièrement précieux. Claudie, merci toé. Merci d'être mon amie, merci d'être là dans les joies comme dans les moments durs. Du fond du cœur, fanks fwen. Enfin, tes parents ont droit à ma reconnaissance pour leur bienveillance et d'être toujours si chaleureux envers moi, ma famille québécoise.

Merci à ma famille. C'est bien plus qu'un merci et toute ma gratitude que j'adresse à mes parents Catherine et Yves, ma sœur Anaïs, mes neveux, ma nièce et mon beau-frère Romain. Je suis si reconnaissante de votre soutien infaillible, de toujours répondre présent, de m'épauler continuellement, d'être une famille si soudée. Merci maman et papa d'avoir toujours cru et de ne jamais cesser de croire en moi, de respecter mes choix et de m'avoir toujours encouragée dans mes aventures, même si cela m'a souvent emmenée loin de vous. Merci à mes neveux, Marin et Numa et ma nièce, Garance. J'espère les rendre fiers de leur Tata baleine.

Merci maman, merci papa, merci ma sœur chérie. Je vous aime.



AVANT-PROPOS

Ce projet de doctorat portant sur l'énergétique des rorquals bleus s'insère dans un projet multidisciplinaire intitulé « la production du krill et son importance trophique dans l'estuaire et le golfe du Saint-Laurent : vers une gestion écosystémique des stocks de krill ». Ce projet CRNSG stratégique (CRNSG stratégique n°447363) a été initié en 2013 par le Dr. Gesche Winkler et le Dr. Stéphane Plourde dans le but d'évaluer la résilience des stocks de krill face à une potentielle exploitation commerciale. Ce projet à grande échelle est scindé en cinq grands thèmes de recherche : (1) la détermination de la distribution spatiotemporelle du krill, (2) l'étude des processus physiologiques individuels du krill, (3) le développement de modèles biophysiques pour étudier la dynamique de population du krill, 4) l'estimation de la consommation du krill par les rorquals qui en dépendent et (5) le développement de modèles écosystémiques regroupant tous les aspects précédents. Plus précisément, ce présent travail de doctorat s'intègre dans la partie 4 des thèmes de recherche et fournit des informations cruciales pour la paramétrisation des modèles du thème 5.

Le présent manuscrit est composé de trois chapitres correspondant aux différents articles scientifiques. Une introduction générale décrit les principaux concepts écologiques abordés dans les axes de recherche et présente le modèle biologique étudié, le site d'étude et les objectifs de recherche. L'introduction générale est suivie des chapitres 1 à 3 qui correspondent aux différentes études menées pendant ma thèse. Ces chapitres sont écrits en anglais et ont été publiés ou seront soumis prochainement dans différentes revues internationales soumises à l'évaluation par les pairs. La thèse se termine par une discussion générale reprenant les principaux résultats obtenus dans les trois chapitres et le fil conducteur qui les relie, et fait état de l'avancée des connaissances auxquelles ce travail aura contribué en replaçant les conclusions dans un contexte global. Finalement, le statut du rorqual bleu de l'Atlantique Nord-Ouest est discuté au vu des nouvelles connaissances disponibles, tout en

considérant les limites de la présente étude mais aussi, et surtout, les perspectives que celle-ci apporte. Le jury de thèse n'étant pas composé exclusivement de membres francophones, les schémas réalisés et figurant dans l'introduction générale et la conclusion générale sont présentés en anglais pour faciliter leur compréhension par tous les membres du jury.

Les fruits de cette thèse sont publiés ou en préparation sous forme d'article dans des revues internationales soumises à la révision par les pairs. La dissémination des résultats novateurs des différents chapitres s'est également faite au cours des dernières années au travers de présentations orales ou d'affiches lors de congrès nationaux et internationaux.

Présentations orales (5) :

- **Guilpin M.**, Lesage V., McQuinn I., Goldbogen J., Potvin J., Doniol-Valcroze T., Jeanniard du Dot T., Michaud R., Moisan M., Winkler G. 2018. De quelles densités de krill le rorqual bleu a-t-il besoin dans le Saint-Laurent? Scientific Symposium of the Saguenay-St. Lawrence Marine Park, Tadoussac, Canada.
- **Guilpin M.**, Lesage V., McQuinn I., Goldbogen J., Potvin J., Doniol-Valcroze T., Michaud R., Moisan M., Winkler G. 2017. Krill density requirements and foraging efficiency of Northwest Atlantic blue whales foraging in the Estuary and Gulf of St. Lawrence, Canada. International Arctic Change 2017 Conference, Québec city, Canada
- **Guilpin M.**, Lesage V., McQuinn I., Goldbogen J., Potvin J., Doniol-Valcroze T., Michaud R., Moisan M., Winkler G. 2017. Foraging energetics and prey density requirements of western North Atlantic blue whales foraging in the Estuary and Gulf of St. Lawrence, Canada. 22nd Biennial Conference on the Biology of Marine Mammals SMM, Halifax, Nova Scotia, Canada.
- **Guilpin M.** 2015. Comportements alimentaires des rorquals dans l'estuaire et le golfe du Saint-Laurent. Présentation publique de projet au Centre d'interprétation des mammifères marins–Groupe de Recherche et d'Éducation sur les Mammifères Marins, Tadoussac, Canada.

- **Guilpin M.**, Lesage V., McQuinn I., Michaud R., Ménard N., Winkler G. 2015. Stratégies d'alimentation et consommation de krill par les rorquals dans le golfe du Saint-Laurent. 83^e congrès international de l'Association pour le savoir francophone (ACFAS), Rimouski, Canada.

Présentations par affiche (7) :

- **Guilpin M.**, Lesage V., Brosset P., Jeanniard-du-Dot T., McQuinn I., Winkler G. 2020. Energetic consequences of human disturbances and changes in krill preyscape on blue whales foraging in the Estuary and Gulf of St. Lawrence, Canada. Annual Scientific Meeting of Quebec-Ocean, Beaupré, Canada.
- **Guilpin M.**, Lesage V., Brosset P., Jeanniard-du-Dot T., McQuinn I., Winkler G. 2019. Energetic consequences of human disturbances and changes in krill preyscape on blue whales foraging in the Estuary and Gulf of St. Lawrence, Canada. 2nd World Marine Mammals Conference, Barcelona, Spain.
- **Guilpin M.**, Lesage V., Winkler G. 2017. Impacts of changes in krill vertical distribution and density on foraging efficiency of Northwest Atlantic blue whales in the Estuary and Gulf of St. Lawrence, Canada. International Arctic Change 2017 Conference, Québec city, Canada
- **Guilpin M.**, Lesage V., Goldbogen J., McQuinn I., Michaud R., Winkler G. 2017. Foraging energetics and krill density requirements of Northwest Atlantic blue whales in the Estuary and Gulf of St. Lawrence, Canada. 16th General Annual Meeting of Québec-Océan, Rivière-du-Loup, Canada.
- **Guilpin M.**, Lesage V., Goldbogen J., McQuinn I., Michaud R., Winkler G. 2015. Bilan énergétique de l'activité d'alimentation et consommation de krill par le rorqual bleu dans l'estuaire et le golfe du Saint-Laurent. 14th General Annual Meeting of Québec-Océan, Québec, Canada.
- **Guilpin M.**, Lesage V., Winkler G. Poster presentation. 2015. Étudier les baleines sous la surface? Oui, mais comment? 12^e colloque de vulgarisation scientifique "La nature dans tous ses états", Rimouski, Canada.

- **Guilpin M.**, Lesage V., Goldbogen J., McQuinn I., Michaud R., Winkler G. 2014. Interactions between baleen whales and Krill in the St-Lawrence Gulf. 13th general annual meeting of Québec-Océan, Rivière-du-Loup, Canada.

ABSTRACT

Sufficient energy acquisition is essential for an animal in order to survive, grow and reproduce. Prey density is one of the main drivers of the foraging effort for a predator. The efficiency at which they forage determines their ability to accumulate energy reserves and improve body condition. Blue whales *Balaenoptera musculus* are considered capital breeders and therefore accumulate the majority of their energy reserves through efficient foraging during temporally and spatially distinct periods. Blue whales seasonally visit the estuary and gulf of St. Lawrence (EGSL) to feed on two predominant species of krill, namely the Arctic krill *Thysanoessa* spp. and the northern krill *Meganyctiphanes norvegica*. The western North Atlantic blue whale population is listed as endangered under the Canadian Species at Risk Act. The size of this population is unknown, but likely in the low hundreds, and the apparent low calving rate raises questions about the nutritional status of its individuals. It is therefore essential to understand the energy needs of individuals in terms of krill and the energetic costs of foraging in order to understand the status of this population and better manage its conservation. The objectives of the present thesis are to i) determine the energetic requirements of foraging blue whales in the EGSL in terms of krill density, ii) investigate the impact of changes in the krill density and disturbance from vessel proximity on the energy gain of foraging whales, and iii) investigate if the energy reserves would be sufficient to provide for both migration and reproduction by linking fine-scale energetics to large-scale processes. In order to achieve this goal, we developed a bioenergetic model on different temporal scales using behavioral data of foraging blue whales from data loggers and *in situ* measurements of krill densities from hydroacoustic surveys. Results are presented in the form of three chapters in which specific scientific objectives regarding the bioenergetic interactions between blue whales and krill were investigated.

The first chapter examined the energy expenditure of foraging blue whales and their prey density requirements. The absence of simultaneous hydroacoustic data with the feeding behaviors recorded by data loggers led to the development of an original and innovative approach. This allowed us to predict krill density requirements needed to meet or exceed energy demands for different theoretical feeding efficiencies. These density requirements were then compared to the krill densities measured *in situ* to conclude on the degree of suitability of the habitat for foraging blue whales. We have shown that the vast majority of krill aggregations contain densities lower than those required by blue whales to achieve neutral energy balance, with <1.5% of krill aggregations allowing energy storage.

The second chapter investigated the energetic consequences over a 10-h daytime foraging bout of a decrease in krill densities and of a demonstrated decrease in the dive duration of blue whales triggered by vessel proximity. We used Monte Carlo simulations on

a bioenergetic model parametrized with empirical data to assess the effects of these two changes and their combined effects. The magnitude of the effects increased with that of krill density reductions and duration of vessel proximity but also depended on the depths of the most beneficial peaks of krill density. A reduction $\geq 10\%$ in krill density resulted in a moderate to large effect on blue whale cumulated net energy gain. Vessels that were in close proximity for 3 h reduced cumulated net energy gain by as much as 25% and by up to 47–85% when continuously present for 10 h. A decrease in net energy gain through an altered krill preyscape or repeated vessel interactions is of particular concern for this endangered population.

The third chapter considered the energy reserves of a female blue whale accumulated over a complete reproductive cycle. We used a mechanistic simulation approach to model the dynamics of the energy reserves over several feeding seasons based on krill densities documented in the EGSL from hydroacoustic surveys. Costs associated with reproduction (i.e., gestation and lactation) but also migration, and time spent on wintering grounds were estimated and compared to accumulated reserves on the feeding grounds. Simulation results hinted at a need for whales to target the highest densities of *M. norvegica* given densities available in the EGSL, mainly to ensure sufficient energy reserves to successfully complete a reproductive cycle and wean a calf. The low krill densities measured in the EGSL might be a clue to the energetic status of blue whales.

In conclusion, the present thesis contributed to new knowledge about the bioenergetics of blue whales, their krill requirements when feeding in the EGSL and the quality of the EGSL as a feeding ground for this population. The results highlighted the complex bioenergetic interactions between blue whales and their prey, the krill. The results also showcased their vulnerability in the face of decreasing krill density, either as a result of climate change or a commercial krill exploitation, or of vessel proximity or other disruptive activity on their foraging behavior. The modelling of energetic reserves over a full reproductive cycle suggested that the low krill densities observed in the EGSL over the past several years might explain the apparent low calving rate. In addition, this study provides a better understanding of the nutritional status of individuals and new tools for the necessary conservation measures for the recovery of this endangered blue whale population.

Keywords: blue whale, bioenergetic modelling, energetic requirements, krill density, energetic reserves, estuary and gulf of St. Lawrence.

RÉSUMÉ

Une acquisition d'énergie suffisante est essentielle pour la survie, la croissance et la reproduction d'un animal. La densité des proies est l'un des principaux moteurs de l'effort de recherche de nourriture d'un prédateur. L'efficacité avec laquelle il s'alimente détermine sa capacité à accumuler des réserves d'énergie et à améliorer sa condition corporelle. Les rorquals bleus *Balaenoptera musculus* sont considérés comme des *capital breeders*, accumulant ainsi la majorité de leurs réserves d'énergie grâce à une alimentation efficace pendant des périodes temporellement et spatialement distinctes. Les rorquals bleus visitent de façon saisonnière l'estuaire et le golfe du Saint-Laurent (EGSL) pour se nourrir de deux espèces prédominantes de krill, à savoir le krill arctique *Thysanoessa* spp. et le krill nordique *Meganyctiphanes norvegica*. La population de rorquals bleus de l'Atlantique Nord-Ouest est considérée en voie de disparition en vertu de la Loi sur les Espèces en Péril au Canada. Cette population est estimée à environ 400 individus et la faible production de veaux soulève des questions sur l'état nutritionnel des individus. Il est donc essentiel de comprendre les besoins énergétiques des individus en termes de krill et les coûts énergétiques de la recherche de nourriture afin de comprendre l'état de cette population et de gérer plus efficacement sa conservation. Les objectifs de la présente thèse sont : i) de déterminer les besoins énergétiques des rorquals bleus en quête de nourriture dans l'EGSL en termes de densité de krill, ii) d'étudier l'impact des changements dans la densité de krill et la perturbation par la proximité des bateaux d'excursion sur le gain énergétique des baleines en alimentation, et iii) d'estimer si les réserves d'énergie sur une longue échelle temporelle seraient suffisantes pour assurer à la fois la migration et la reproduction. Afin d'atteindre cet objectif, nous avons développé un modèle bioénergétique à différentes échelles temporelles en utilisant des données comportementales de plongée des rorquals bleus à partir d'enregistreurs de données et des mesures *in situ* de densités de krill à partir de relevés hydroacoustiques. Les résultats sont présentés sous forme de trois chapitres dans lesquels des objectifs scientifiques spécifiques concernant les interactions bioénergétiques entre le rorqual bleu et le krill ont été étudiés.

Le premier chapitre a examiné la dépense énergétique des rorquals bleus en quête de nourriture et leurs besoins en termes de densité de proies. L'absence de données hydroacoustiques simultanées avec les comportements alimentaires enregistrés par les enregistreurs de données a mené au développement d'une approche originale et innovante. Cela nous a permis de prédire les densités de krill nécessaires aux rorquals bleus afin de satisfaire ou dépasser les demandes énergétiques en assumant différentes efficacités d'alimentation théoriques. Ces besoins en densité ont ensuite été comparés aux densités de krill mesurées *in situ* pour évaluer la qualité de l'habitat pour l'alimentation des rorquals bleus. Nous avons montré que la grande majorité des agrégations de krill contiennent des

densités inférieures à celles requises par les rorquals bleus pour atteindre un bilan énergétique neutre, avec <1,5% d'agrégations de krill permettant le stockage d'énergie.

Le deuxième chapitre a examiné les conséquences énergétiques sur une période d'alimentation de 10 h d'une diminution des densités de krill et d'une diminution démontrée de la durée de plongée des rorquals bleus engendrée par la proximité d'embarcations. Nous avons utilisé des simulations de Monte Carlo sur un modèle bioénergétique paramétré avec des données empiriques pour évaluer les effets de ces deux changements et leurs effets combinés. L'ampleur des effets augmentait avec celle des réductions de densité de krill et la durée de la proximité des embarcations, mais dépendait également de la profondeur des pics de densité de krill les plus bénéfiques. Une réduction de $\geq 10\%$ de la densité de krill a eu un effet modéré à important sur le gain énergétique net cumulé du rorqual bleu. Les embarcations qui étaient à proximité pendant 3 h ont réduit le gain d'énergie net cumulé de 25%, et de 47 à 85% lorsqu'elles étaient continuellement présentes pendant 10 h. Une diminution du gain énergétique net liée à une altération du paysage des proies ou à des interactions répétées avec les embarcations est particulièrement préoccupante pour cette population en voie de disparition.

Le troisième chapitre a examiné les réserves d'énergie d'une femelle rorqual bleu sur un cycle de reproduction complet. Nous avons utilisé une approche de simulation mécaniste pour modéliser la dynamique des réserves énergétiques sur plusieurs saisons d'alimentation en fonction des densités de krill documentées dans l'EGSL à partir de relevés hydroacoustiques. Les coûts liés à la reproduction (c'est-à-dire la gestation et la lactation), mais aussi la migration et le temps passé sur les aires d'hivernage ont été estimés et comparés aux réserves accumulées sur les aires d'alimentation. Les résultats des simulations ont suggéré que, étant donné les densités de krill disponibles dans l'EGSL, les baleines devraient cibler principalement les densités les plus élevées de *M. norvegica* pour assurer des réserves d'énergie suffisantes pour un cycle de reproduction réussi et le sevrage d'un veau. Les faibles densités de krill mesurées dans l'EGSL pourraient être un indice de l'état énergétique des rorquals bleus.

En conclusion, la présente thèse a contribué à de nouvelles connaissances sur la bioénergétique des rorquals bleus et leurs besoins en krill lorsqu'ils se nourrissent dans l'EGSL. Les résultats ont mis en évidence les interactions bioénergétiques complexes entre les rorquals bleus et leur proie, le krill. Les résultats ont également montré leur vulnérabilité face à la diminution de la densité de krill, soit potentiellement résultant du changement climatique ou d'une exploitation commerciale du krill, mais aussi de la proximité des bateaux d'excursion perturbant leur comportement d'alimentation. La modélisation des réserves énergétiques sur un cycle de reproduction complet semble indiquer que les faibles densités de krill observées dans l'EGSL pourraient expliquer l'apparente faible production de veau. De plus, cette étude fournit une meilleure compréhension de l'état nutritionnel des individus et de nouveaux outils pour les mesures de conservation nécessaires au rétablissement de la population de rorquals bleus de l'ouest de l'Atlantique Nord.

Mots clés : rorqual bleu, modélisation bioénergétique, besoins énergétiques, densité de krill, réserves énergétiques, estuaire et golfe du Saint-Laurent.

TABLE DES MATIÈRES

REMERCIEMENTS	xiii
AVANT-PROPOS	xvii
ABSTRACT	xxi
RÉSUMÉ.....	xxiii
TABLE DES MATIÈRES	xxvii
LISTE DES TABLEAUX.....	xxxii
LISTE DES FIGURES.....	xxxv
INTRODUCTION GÉNÉRALE	1
LA THEORIE DE L'APPROVISIONNEMENT OPTIMAL ET LE THEOREME DE LA VALEUR MARGINALE	1
RELATION PREDATEURS–PROIES – LA DISTRIBUTION DES PROIES.....	4
CONTRAINTES INTRINSEQUES	5
L'EMERGENCE DU BIOLOGGING	8
LES MODELES BIOENERGETIQUES	12
LE RORQUAL BLEU–POPULATION DE L'ATLANTIQUE NORD-OUEST.....	13
L'ESTUAIRE ET LE GOLFE DU SAINT-LAURENT (EGSL).....	16
LE KRILL DANS L'EGSL–THYSANOESSA SPP. ET MEGANYCTIPHANES NORVEGICA	19
OBJECTIFS DE RECHERCHE	22
OBJECTIFS SPECIFIQUES	23
CHAPITRE 1 FORAGING ENERGETICS AND PREY DENSITY REQUIREMENTS OF WESTERN NORTH ATLANTIC BLUE WHALES IN THE ESTUARY AND GULF OF ST. LAWRENCE, CANADA	29

1.1	ABSTRACT	31
1.2	RESUME	32
1.3	INTRODUCTION	33
1.4	MATERIALS AND METHODS	36
1.4.1	Tag data and foraging effort	36
1.4.2	Energy expenditure	39
1.4.3	Krill density requirements	41
1.4.4	Preyscape: <i>in situ</i> krill densities	46
1.5	RESULTS	48
1.5.1	Hourly foraging effort and energy expenditure	48
1.5.2	Krill density requirements	52
1.5.3	<i>In situ</i> krill preyscape.....	56
1.6	DISCUSSION	58
1.6.1	Hourly foraging effort and energy expenditure	58
1.6.2	Krill density requirements	61
1.6.3	Coupling energetic requirements and <i>in situ</i> krill densities.....	62
1.7	ACKNOWLEDGEMENTS	66
1.8	SUPPLEMENTARY INFORMATION (CHAPITRE 1)	67
1.8.1	Supplementary figures	67
CHAPITRE 2 REPEATED VESSEL INTERACTIONS AND CLIMATE- OR		
FISHERY-DRIVEN CHANGES IN PREY DENSITY LIMIT ENERGY		
ACQUISITION BY FORAGING BLUE WHALES		
2.1	ABSTRACT	71
2.2	RESUME	72
2.3	INTRODUCTION	73
2.4	MATERIALS AND METHODS	75
2.4.1	Model framework	78
2.4.2	Simulated scenario.....	82

2.4.3	Statistical analysis	86
2.5	RESULTS.....	88
2.6	DISCUSSION.....	95
2.7	AUTHORS CONTRIBUTIONS	103
2.8	FUNDING	103
2.9	ACKNOWLEDGEMENTS	103
2.10	SUPPLEMENTARY INFORMATION (CHAPITRE 2).....	105
2.10.1	Supplementary tables	105
2.10.2	Supplementary figures.....	112
2.10.3	Supplementary data: model parameters	115
CHAPITRE 3 PREY DENSITY MAY LIMIT THE REPRODUCTIVE CAPACITY OF THE ENDANGERED WESTERN NORTH ATLANTIC BLUE WHALE POPULATION.....		
		127
3.1	ABSTRACT.....	128
3.2	RESUME.....	129
3.3	INTRODUCTION.....	130
3.4	MATERIALS AND METHODS	133
3.4.1	Model Timescale	134
3.4.2	Preyscape–krill density	136
3.4.3	Energy balance over the feeding season	138
3.4.4	Costs of migration and movements on wintering grounds.....	141
3.4.5	Cost of reproduction.....	142
3.4.6	Full reproductive cycle.....	143
3.5	RESULTS.....	146
3.5.1	Preyscape–krill density	146
3.5.2	Energy balance over the feeding season	147
3.5.3	Costs of migration and movements on wintering grounds.....	151
3.5.4	Cost of reproduction.....	151

3.5.5	Overall reproductive cycle.....	152
3.6	DISCUSSION	156
3.6.1	Link between preyscape and energy reserves of whales	156
3.6.2	Study limitations–krill density and biomass.....	158
3.6.3	Study limitations–foraging effort parameters.....	160
3.6.4	Link between body condition and reproduction	161
3.6.5	Non-feeding migration periods and the 27-month reproduction cycle.....	163
3.7	ACKNOWLEDGEMENTS	164
3.8	SUPPLEMENTARY INFORMATION (CHAPITRE 3)	166
3.8.1	Supplementary tables.....	166
3.8.2	Supplementary figures.....	174
3.8.3	Supplementary data: model parameters.....	183
	CONCLUSION GÉNÉRALE	187
	CONTRIBUTION DE L’ETUDE	187
	LIMITATIONS ET PERSPECTIVES	195
	RÉFÉRENCES BIBLIOGRAPHIQUES	211

LISTE DES TABLEAUX

Table 1 : Input parameters, associated sampling distributions and/or values (mean \pm SD where applicable) and data sources for estimating blue whale krill density requirements. na: not applicable.	45
Table 2 : Summary of ‘grids’ and ‘spirals’ (see Figure 15 in Supplementary information) from hydroacoustic surveys used for krill patch characterization. GSL: Gulf of St. Lawrence; SLE: St. Lawrence Estuary.	46
Table 3 : Trends in various indices of foraging effort with time of day, based on generalized additive mixed model (GAMM) results, and using individual blue whale as a random effect. Results (<i>p</i> -values) of the likelihood ratio test (LRT) for model selection against the null model (random effect only) are also presented; edf: estimated degrees of freedom.	52
Table 4 : Characteristics of feeding dives and feeding rates (mean \pm SD) during daytime vs. nighttime. Nighttime includes dusk, night, and dawn. Statistical differences (Mann-Whitney <i>U</i> -test and Student’s <i>t</i> -test) are indicated with an asterisk ($*p < 0.05$).	52
Table 5 : Trends in required density for Arctic and northern krill at various foraging efficiencies (FE = 1 to 4) with time of day based on generalized additive model results. N = 24000 simulations for each model. Results (<i>p</i> -values) of the likelihood ratio test (LRT) for model selection against the null model (random effect only) are also presented.	54
Table 6 : Standardized regression coefficients (SRC), minimum and maximum 95% confidence intervals, biases and standard errors of the partial sensitivity analysis of the parameters used in Monte Carlo simulations. The largest contributors to the uncertainty in predicted krill density requirements are indicated in bold.	56
Table 7 : Input parameters, associated sampling distributions and/or values and, data sources used in the bioenergetic framework for estimating net energy gain. NA: not applicable.	87

Table 8 : Summary characteristics of scenarios and sets of Monte Carlo simulations. Scenarios were done for each region i.e., the St. Lawrence Estuary (SLE) and the northwestern Gulf of St. Lawrence (NWG) and both dominant krill species, <i>Thysanoessa</i> spp. (Tr) and <i>Meganyctiphanes norvegica</i> (Mn). Mean net energy gain and their percent change relative to baseline is given for each set of simulations. The effects on mean net energy gain were quantified using Cohen's <i>d</i> (Cohen 1977). Values of 0.2, 0.5 and 0.8 indicate small, moderate and large effect sizes, respectively (Cohen 1977).....	105
Table 9 : Input parameters, associated sampling distributions (where applicable) and/or values used in the model framework.	144
Table 10 : Mean (\pm SD; when applicable) of all the energetic costs involved in the 27-month reproductive cycle with the temporal periods to which each costs applied to. These costs included, the costs of migrating and time spent on the wintering grounds, gestation and lactation. The indirect costs of gestation represented by the increase in locomotion costs due to the burden of motherhood for cost of transport (COT), the foraging average active metabolic rate (RAAMR), and the resting metabolic rate (RMR) to each temporal periods. na: not applicable.	154
Table 11 : Characteristics of prey densities considered suitable for blue whales foraging in the EGSL, as determined from hydroacoustic surveys conducted yearly from 2008 to 2017. Densities deemed suitable were those allowing blue whales to achieve at least neutral energy balance, and corresponded to 19 g m^{-3} for <i>Thysanoessa</i> spp. and 16 g m^{-3} for <i>Meganyctiphanes norvegica</i> . Data are also presented while setting suitability at higher thresholds (i.e., 25 th , > 50 th , > 75 th percentiles). The number of bins above the threshold are relative to a distribution that includes all densities above 4 g m^{-3} (McQuinn et al. 2015).	166
Table 12 : Estimates of energy reserves accumulated after one feeding season, according to densities of two krill species documented using hydroacoustic surveys conducted in the EGSL from 2008–2017. Simulations were done assuming a diet composed of different ratios between the two krill species (<i>Thysanoessa</i> spp. and <i>M. norvegica</i>), and whales seeking to achieve either neutral energy balance, or foraging efficiencies that allow some accumulation of energy reserves (thresholds of > 25 th , > 50 th , > 75 th percentiles of the maximum suitable densities that were observed in a specific year).....	168

Table 13 : Mean (\pm SD) indirect costs of gestation represented by the increase in locomotion costs due to the burden of motherhood for cost of transport (COT), the forqual average active metabolic rate (RAAMR), and the resting metabolic rate (RMR) and the temporal periods to which these extra costs applied to. 173

LISTE DES FIGURES

- Figure 1 : Schéma représentant la théorie de l’approvisionnement optimal (OFT) et le théorème de la valeur marginale (MVT) dans (a) un environnement hétérogène dans la distribution et densité des agrégations de proies. (b) Le gain énergétique dépend de la qualité de l’agrégation à court terme (bonne qualité : courbe rouge, faible qualité : courbe bleue) et du temps passé par le prédateur à s’y alimenter. (c) Si la qualité de l’agrégation reste la même à court terme (courbe noire) mais que la qualité de l’environnement à long terme varie (rouge : bonne qualité, bleu : faible qualité), le MVT prédit un temps de résidence optimal dans l’agrégation afin de maximiser les gains énergétiques. Figure tirée de Watanabe et al. (2014). 2
- Figure 2 : Schéma illustrant les contraintes extrinsèques (liées au paysage des proies) et intrinsèques aux individus influençant le comportement alimentaire d’un prédateur marin. 3
- Figure 3 : Photo illustrant un rorqual bleu équipé d’un enregistreur de données VTDR (Velocity-Time-Depth-Recorder) en haut de figure et le type de données qui en résultent en bas de figure. Les capteurs de profondeur et vitesse permettent de reconstruire des patrons de plongées et événements d’alimentation (cercles blancs) (a) en profondeur et (b) en surface. Crédit photo DFO–GREMM, figure tirée de (Doniol-Valcroze et al., 2011). 11
- Figure 4 : Schéma illustrant le comportement alimentaire des rorquals bleus. Le nombre de *lunges* par plongées est d’autant plus grand que la profondeur d’alimentation augmente. Adapté de Acevedo-Gutiérrez et al. (2002) et (Doniol-Valcroze et al., 2011). 16
- Figure 5 : Aire d’étude et bathymétrie associée. Carte extraite de Galbraith et al. (2019). 17
- Figure 6 : Représentation schématique du réseau trophique de l’EGSL, centré sur le krill et sur ses principaux prédateurs. La taille des flèches pleines représente l’intensité de prédation. La flèche en pointillés indique une possible exploitation commerciale. Adaptée de Savenkoff et al. (2013). 21

Figure 7 : Distribution verticale pendant le jour des densités de krill pour les deux espèces <i>Thysanoessa</i> spp. (vert), <i>M. norvegica</i> (orange) et la classification mixte des deux (marron) dans (a) l'estuaire et (b) le nord-ouest du golfe du Saint-Laurent. Figure extraite de Plourde et al. (2014b).....	22
Figure 8 : Schéma conceptuel représentant la démarche scientifique et l'organisation du projet de doctorat, ainsi que la complémentarité des chapitres dans l'étude de la bioénergétique des rorquals bleus sur une échelle spatiotemporelle d'une année. Les signes « +/- » représentent l'ampleur du gain net d'énergie qui sera ensuite stockée sous forme de gras et potentiellement disponible pour le maintien, la croissance et, le cas échéant, la reproduction.....	26
Figure 9 : Predicted change in blue whale foraging effort with time of day in (a) feeding depth (m), (b) dive duration (s), (c) number of feeding dives, (d) number of lunges d ⁻¹ , and (e) number of lunges h ⁻¹ . Dark grey ribbons represent the 95% confidence intervals around the predicted response from generalized additive mixed models. Shaded areas are for nighttime (grey), dusk and dawn (light grey), and daytime (white). Points are data observations. (See Table 3 for full statistical results).	50
Figure 10 : Relationship between energy expenditure during feeding dives for 3 blue whale sizes (22, 25, and 27 m length) and (a) dive duration (s) (mean ± SE slope for 22 m: 122 ± 0.6; 25 m: 171 ± 0.9; 27 m: 205 ± 1), (b) maximum dive depth (m) (22 m: 650 ± 11; 25 m: 914 ± 15; 27 m: 1093 ± 19) and (c) number of lunges per dive (22 m: 14265 ± 148; 25 m: 20054 ± 210; 27 m: 23986 ± 252). Relationships were modeled using linear mixed models (all <i>p</i> < 0.05).	51
Figure 11 : Diel distribution of energy expenditure for a 22, 25, and 27 m blue whale. Box plots present the median (solid horizontal line), lower and upper quartiles (boxes), extreme values (whiskers) and outliers (points). Shaded areas are for nighttime (dark grey), dusk and dawn (light grey), and daytime (white). The large confidence interval at 08:00 h is a combination of natural variability among individuals in feeding effort and small sample size (n = 4).	51
Figure 12 : Diel variation in the predicted response of estimated krill density required for a foraging efficiency of 1 by blue whales feeding on Arctic and northern krill. The y-axis represents the predicted response from generalized additive models on the mean krill density (solid line), including the 95% confidence intervals (ribbons). Shaded areas are for nighttime (dark grey), dusk and dawn (light grey), and daytime (white). (See Table 5 for full statistical results).	54

- Figure 13 : Diel distribution of densities of (a) Arctic krill and (b) northern krill required by a 25 m blue whale feeding at foraging efficiencies varying from 1 to 4. Curves and bars represent the median and 90% confidence interval, respectively. Shaded areas are for nighttime (dark grey), dusk and dawn (light grey), and daytime (white). 55
- Figure 14 : Percentage of krill patches with 3-ping \times 0.5 m bins dense enough to allow blue whales to forage with efficiencies of 1 to 4 on Arctic krill and northern krill during daytime. Estimated krill density requirements ($\text{g wet weight} \cdot \text{m}^{-3}$) were used as thresholds for foraging efficiencies of 1–4. For Arctic krill, mean estimates were 29, 57, 86, and 113 $\text{g} \cdot \text{m}^{-3}$, respectively; for northern krill, these values were 24, 47, 70 and 94 $\text{g} \cdot \text{m}^{-3}$, respectively. Means are represented by a red dot. Boxplots present the median (solid horizontal line), lower and upper quartiles (boxes), extreme values (whiskers) and outliers (points). 57
- Figure 15 : Illustrations of hydroacoustic survey designs. (a) Rectangular “spirals” (concentric lines of increasing distance and length from the central starting point). (b) “Grid” (parallel equidistant lines). The size of “grids” and “spirals” varied among survey designs, locations, and within and between years. 67
- Figure 16 : Diel distribution of tag deployments. Shaded areas are for nighttime (dark grey), dusk and dawn (light grey), and daytime (white). 67
- Figure 17 : Diel distribution of densities for (a) Arctic krill, and (b) northern krill required by three sizes of whales (colors for 22, 25, and 27-m) at foraging efficiencies varying from 1 to 4 (symbols). Curves and bars represent the median and 90% confidence interval, respectively. Shaded areas are for nighttime (dark grey), dusk and dawn (overlapping light grey), and daytime (white). The offset between the different size is a result of the positive allometric scaling of engulfment volume with body size. 68
- Figure 18 : Vertical density profiles for Arctic krill (green) and northern krill (orange) for each hydroacoustic surveys. Vignettes (a) to (j) indicate the survey year, the hydroacoustic survey design (either grid [G] or spiral [S]) and the general location (either the Estuary or northern Gulf of St. Lawrence — called ‘Estuary’ and ‘Gulf’, respectively — or the Gaspé Bay, also in the northern Gulf of St. Lawrence). Solid line represents the mean, whereas the darker ribbon is 25–75% quantiles, medium ribbon is the 10–90% quantiles, and the light ribbon and dotted line are the 1-99% quantile. 69

- Figure 19 : Bioenergetic model framework to assess immediate effects on net energy gain of changes in preyscape as a result of ocean warming or in prey access as a result of vessel proximity. Parameters and their value are provided in Table 7..... 79
- Figure 20 : Two regions, i.e., the Estuary of the St. Lawrence (dark blue) and the northwestern Gulf of the St. Lawrence (yellow) including the Gaspé peninsula, used to determine *in-situ* vertical distributions of krill densities. 83
- Figure 21 : Vertical density profiles for (A) *Thysanoessa* spp. (green) and (B) *Meganyctiphanes norvegica* (orange) for the St. Lawrence Estuary (left) and the northwestern Gulf of St. Lawrence (right) with identified high density layers used as targeted feeding depth for simulated dive time-series (grey horizontal ribbons). Solid vertical lines represent the median, the dashed lines are the 75th percentiles and the coloured areas are the 5–95% quantiles..... 84
- Figure 22 : Net energy gain (mean and 5–95% CI) accumulated over a 10h foraging period when feeding on *M. norvegica* in the St. Lawrence Estuary, (A) under baseline conditions measured *in situ*, (B) when exposed to vessel proximity within 400 m for 3h (from hour 5 to hour 8) and 10 h, (C, E, G, I) under krill density reductions of 5%, 10% 25% or 50% relative to baseline, and (D, F, H, J) while foraging on reduced krill densities when exposed to vessel proximity. Patterns for *Thysanoessa* spp. and the NWG are presented in the Supplementary information. 89
- Figure 23 : Effect of the various scenarios on net energy gain after a 10 h foraging period of a blue whale feeding on (B,D) *Thysanoessa* spp. or (A,C) *M. norvegica*, (A,B) in the St. Lawrence Estuary and (C,D) in the North western Gulf of St. Lawrence. The red dashed lines represent the threshold values of Cohen’s *d* above which effects are considered small (0.2), medium (0.5), and large (> 0.8). Negative Cohen’s *d* value indicates a positive effect..... 94
- Figure 24 : Frequency (%) distribution of feeding depths when exposed to vessel proximity within 400 m while feeding, thus when dives are limited to 4 min or less..... 95
- Figure 25 : Net energy gain (mean and 5–95% CI) accumulated over a 10-h foraging period when feeding at peak density depth of *Thysanoessa* spp. in the St. Lawrence Estuary, (A) under baseline conditions measured *in situ*, (B) when exposed to vessel proximity within 400 m for 3 h (from hour 5 to hour 8) and 10 h, (C, E, G, I) under krill density reductions of 5%, 10% 25% or 50% relative to baseline, and (D, F, H, J) while exposed to vessel proximity and foraging on reduced krill densities. 112

Figure 26 : Net energy gain (mean and 5–95% CI) accumulated over a 10-h foraging period when feeding at peak density depth of <i>M. norvegica</i> in the northwestern Gulf of St. Lawrence, (A) under baseline conditions measured <i>in situ</i> , (B) when exposed to vessel proximity within 400 m for 3 h (from hour 5 to hour 8) and 10 h, (C, E, G, I) under krill density reductions of 5%, 10% 25 % or 50% relative to baseline, and (D, F, H, J) while exposed to vessel proximity and foraging on reduced krill densities.....	113
Figure 27 : Net energy gain (mean and 5–95% CI) accumulated over a 10 h foraging period when feeding at peak density depth of <i>Thysanoessa</i> spp. in the northwestern Gulf of St. Lawrence, (A) under baseline conditions measured <i>in situ</i> , (B) when exposed to vessel proximity within 400 m for 3 h (from hour 5 to hour 8) and 10 h, (C, E, G, I) under krill density reductions of 5%, 10% 25 % or 50% relative to baseline, and (D, F, H, J) while exposed to vessel proximity and foraging on reduced krill densities.....	114
Figure 28 : Depth-specific distribution of the number of lunges per dive, was either calculated from tag data analysis (blue) or predicted using the model developed by Doniol-Valcroze et al. (2011) (red). Errors bars for depths 0-130 m are from tag data analysis, and are extrapolated for depths > 130 m. The grey solid line represents the model predictions from Doniol-Valcroze et al. (2011).....	116
Figure 29 : Mean number of dives per hour as a function of feeding depth.....	118
Figure 30 : Depth-specific distribution of foraging effort (dives per hour).....	118
Figure 31 : Surface time (sec) as a function of feeding depth (m).....	119
Figure 32 : Depth-specific distribution of post-dive surface times with 95% point-wise confidence intervals.	120
Figure 33 : Frequency distribution (percentage) of the depth difference (m) between successive feeding dives within a bout (as defined by the bout-ending criterion method (Boyd, 1996) in Doniol-Valcroze and Lesage, unpublished data).....	121
Figure 34 : Locations of hydroacoustic surveys conducted from 2008 to 2015. Colored lines represent the transects for each survey year. The colored polygons represent the two main areas defined into regions: the St. Lawrence Estuary (dark blue) and the northwestern Gulf of St. Lawrence including the Gaspé Peninsula (yellow).....	122

- Figure 35 : Inter-annual variations in the mean (\pm SD) krill density (g wet weight m^{-3}) for *Thysanoessa* spp. (A) and *Meganyctiphanes norvegica* (B) from hydroacoustic surveys conducted in the northwestern Gulf of St. Lawrence and Gaspé Peninsula (NWG), and the St. Lawrence Estuary (SLE). Interannual variability was not significant (two-way ANOVAs: p -values > 0.1). 125
- Figure 36 : Model framework used to estimate the energy accumulated in the form of blubber mass by an adult female blue whale foraging for seven months in the Estuary and Gulf of St. Lawrence. Parameters and their values are provided in Table 9. 135
- Figure 37 : Timescale for time spent on feeding grounds (green), migrating (red), and time spent on wintering grounds (blue). Reproductive status of adult females is indicated as follow: pregnant (yellow) and lactating (orange). Key events of the reproduction (conception, parturition and weaning) are indicated with arrows and white labels. 136
- Figure 38 : Number of bins above each threshold ($> FE1$, $> 25^{th}$, 50^{th} and 75^{th} percentiles) for both krill species (*Thysanoessa* spp. and *M. norvegica*) from hydroacoustic surveys conducted yearly from 2008 to 2017. 147
- Figure 39 : Yearly variation in total energy stored in blubber (MJ) at the end of a 7-month foraging period according to year-specific krill densities measured during hydroacoustic surveys in the Estuary and Gulf of St. Lawrence. Results are presented for diets comprised of different ratios of *Thysanoessa* spp. (T. spp.) and *M. norvegica* (Mn) (panels) and assuming that whales target prey densities that allow neutral energy balance, or densities allowing higher foraging efficiencies ($> 25^{th}$, $> 50^{th}$, $> 75^{th}$ percentiles of maximum observed densities in a specific year). Boxplots present the median (solid horizontal line), lower and upper quartiles (boxes), extreme values (whiskers) and outliers (points). The black dotted lines indicate the initial range of blubber masses (8,000–15,000 kg or (~255,000–480,000 MJ) at the beginning of the simulations. Maximum energy reserves (equivalent to 22,000 kg of blubber or ~700,000 MJ) is indicated by the solid black line while minimum blubber proportion for survival (5% or 2,000 kg, or ~160,000 MJ) is indicated by the horizontal red solid line. Detailed simulation results for krill densities above all thresholds ($FE=1$, 25^{th} , 50^{th} and 75^{th}) are presented in Supplementary information..... 150
- Figure 40 : Blue whale blubber mass (kg) throughout the entire reproduction cycle for whales assumed to feed on densities of *M. norvegica* (ratio 0:100) above the 75^{th} percentile with reproductive cycle starting in (A) 2011 and (B) 2014. The reproductive

cycle starts at the first feeding season (2011 or 2014) and carries over in the following years until weaning of a calf. Maximum (35%), average (27%) and minimum (5%) blubber proportions are indicated with the horizontal black dashed lines. Vertical red dashed lines indicate key events such as start of pregnancy, birth and weaning of the calf. Green shaded areas are periods of time spent on the feeding grounds, red shaded areas represent the time spent migrating and blue shaded areas represent on the wintering grounds..... 155

Figure 41 : Locations of hydroacoustic surveys conducted in the Estuary and the North western Gulf of St. Lawrence, from 2008 to 2017. Colored lines represent the transects for each survey year. 174

Figure 42 : Probability density distribution of krill densities that exceeded (A) the threshold identified in Guilpin et al. (2019) for blue whale neutral energetic balance (i.e., 16 and 19 g · m⁻³) and year-specific (B) 25th, (C) 50th and (D) 75th percentiles thresholds, presented for each of the hydroacoustic surveys conducted between 2008 and 2017, and the two krill species *Thysanoessa* spp. (left panels) and *Meganyctiphanes norvegica* (right panels). Availability is expressed as probability density functions of densities (black line) with associated frequency distributions (colored histograms), and raw data (black vertical lines). 177

Figure 43 : Blue whale blubber mass (kg) accumulated over a seven-month foraging period, according to year-specific krill densities measured during hydroacoustic surveys conducted in the EGSL between 2008–2017 and for krill densities above the threshold identified in Guilpin et al. (2019) for blue whale neutral energetic balance, while assuming that whales fed on a range of ratios (A) *Thysanoessa* spp. 100:0, (B) 75:25, (C) 50:50, (D) 25:75 or (E) *M. norvegica* 0:100. Body condition in terms of blubber proportion when arriving on feeding grounds was allowed to vary between 16% (lower black dashed line) and the average blubber proportion for a blue whale (27%; upper black dashed line), with a potential maximum of 35% over the course of the seven months (black solid line) and a minimum of 5% blubber (dotted line). 178

Figure 44 : Blue whale blubber mass (kg) over a seven months foraging period on the feeding ground, according to year-specific krill densities measured during hydroacoustic surveys above the 25th percentile, while assuming that whales fed on a range of ratios (A) *Thysanoessa* spp. 100:0, (B) 75:25, (C) 50:50, (D) 25:75 or (E) *M. norvegica* 0:100. Body condition in terms of blubber proportion when arriving on feeding grounds was allowed to vary between 16% (lower black dashed line) and the average blubber proportion for a blue whale (27%; upper black dashed line), with a

potential maximum of 35% over the course of the seven months (black solid line) and a minimum of 5% blubber (dotted line). 179

Figure 45 : Blue whale blubber mass (kg) over a seven months foraging period on the feeding ground, according to year-specific krill densities measured during hydroacoustic surveys above the 50th percentile, while assuming that whales fed on a range of ratios (A) *Thysanoessa* spp. 100:0, (B) 75:25, (C) 50:50, (D) 25:75 or (E) *M. norvegica* 0:100. Body condition in terms of blubber proportion when arriving on feeding grounds was allowed to vary between 16% (lower black dashed line) and the average blubber proportion for a blue whale (27%; upper black dashed line), with a potential maximum of 35% over the course of the seven months (black solid line) and a minimum of 5% blubber (dotted line). 180

Figure 46 : Blue whale blubber mass (kg) over a seven months foraging period on the feeding ground, according to year-specific krill densities measured during hydroacoustic surveys above the 75th percentile, while assuming that whales fed on a range of ratios (A) *Thysanoessa* spp. 100:0, (B) 75:25, (C) 50:50, (D) 25:75 or (E) *M. norvegica* 0:100. Body condition in terms of blubber proportion when arriving on feeding grounds was allowed to vary between 16% (lower black dashed line) and the average blubber proportion for a blue whale (27%; upper black dashed line), with a potential maximum of 35% over the course of the seven months (black solid line) and a minimum of 5% blubber (dotted line). 181

Figure 47 : (A) Cost of gestation (MJ) for the entire gestation period and (B) associated growth curve of the weight of foetus (kg). 182

Figure 48 : Increase in locomotion costs due to the burden of motherhood for the cost of transport (COT), the roqual average active metabolic rate (RAAMR), and the resting metabolic rate (RMR). Boxplots present the median (solid horizontal line), lower and upper quartiles (boxes), extreme values (whiskers) and outliers (points). 182

Figure 49 : Mean cost of lactation (MJ) (solid line) including the 95% confidence intervals (ribbon) estimated for 1000 simulated lactating females, with milk delivery variable between 90 and 220 kg of milk per day..... 183

Figure 50 : Frequency distribution the number of lunges performed per hour taken from Guilpin et al. 2019. 185

Figure 51 : Perspectives de recherche proposées basées sur le schéma conceptuel de la thèse. Les perspectives de recherches et leurs utilités afin de pallier aux

limitations/problématiques soulevées dans les différents chapitres sont proposées dans
les encadrés numérotés rouge..... 209

INTRODUCTION GÉNÉRALE

LA THÉORIE DE L'APPROVISIONNEMENT OPTIMAL ET LE THÉORÈME DE LA VALEUR MARGINALE

L'énergie, décrite par Kleiber (1975) comme « the fire of life », est essentielle pour la survie, croissance et reproduction de tout être vivant. L'acquisition de ressources constitue le fondement des relations proies-prédateurs inhérentes aux relations trophiques s'opérant dans un écosystème (Pyke et al., 1977). La survie et l'aptitude phénotypique d'un prédateur dépendent de sa capacité à évaluer les possibilités qui s'offrent à lui afin d'identifier les sources de nourriture selon leur profitabilité (Pyke, 1984). La théorie de l'approvisionnement optimal « optimal foraging strategy » (OFT) prédit l'exploitation judicieuse d'une source de nourriture par un prédateur en un temps alloué afin de maximiser le gain net d'énergie, c'est à dire le gain énergétique tenant compte des dépenses énergétiques, tout en minimisant les coûts liés à l'effort de recherche et d'alimentation (MacArthur and Pianka, 1966; Charnov, 1976; Houston and Carbone, 1992; Mori, 1998). Le théorème de la valeur marginale « marginal value theorem » (MVT) vient préciser l'OFT en y ajoutant qu'un prédateur devrait ajuster son effort d'alimentation, c'est-à-dire le temps investi dans la quête alimentaire, afin d'optimiser l'exploitation d'agrégations distinctes et non-hétérogènes de proies et indique qu'un prédateur devrait quitter une agrégation lorsque le gain énergétique décroît par rapport au coût énergétique (Charnov, 1976). Ultiment, ces théories ont pour objectif de prédire le comportement qu'un prédateur devrait adopter afin de maximiser son aptitude phénotypique, ou *fitness*, dans un environnement stochastique (Figure 1).

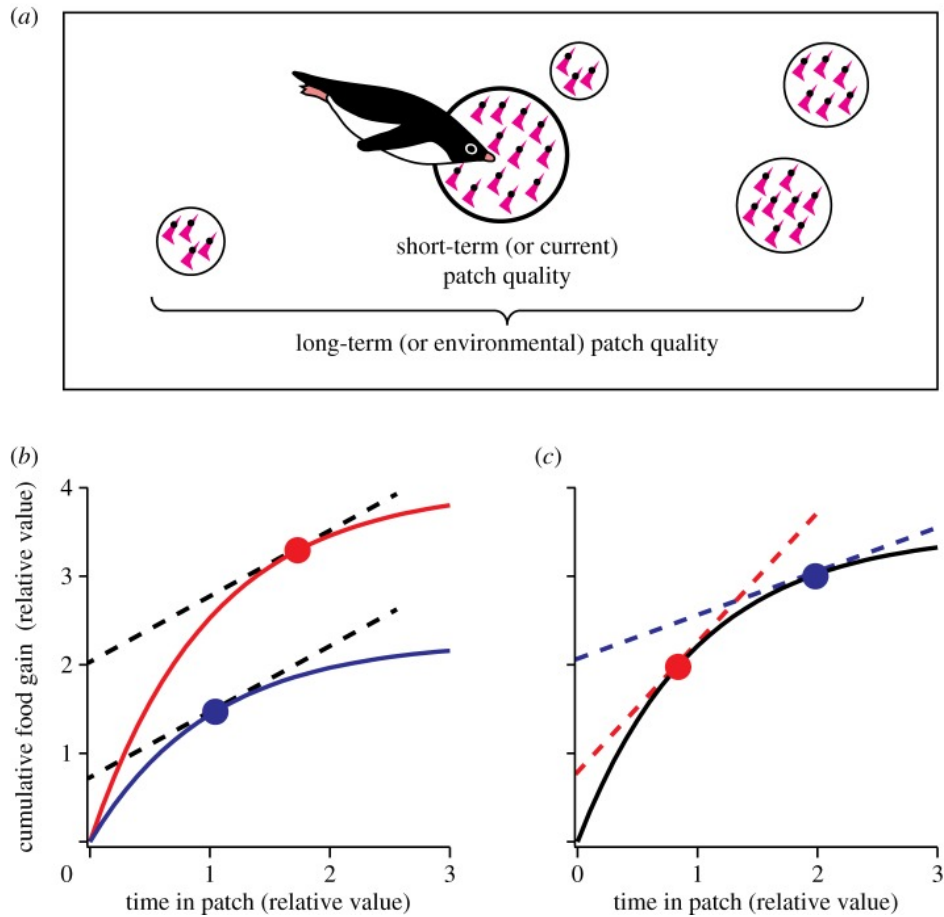


Figure 1 : Schéma représentant la théorie de l’approvisionnement optimal (OFT) et le théorème de la valeur marginale (MVT) dans (a) un environnement hétérogène dans la distribution et densité des agrégations de proies. (b) Le gain énergétique dépend de la qualité de l’agrégation à court terme (bonne qualité : courbe rouge, faible qualité : courbe bleue) et du temps passé par le prédateur à s’y alimenter. (c) Si la qualité de l’agrégation reste la même à court terme (courbe noire) mais que la qualité de l’environnement à long terme varie (rouge : bonne qualité, bleu : faible qualité), le MVT prédit un temps de résidence optimal dans l’agrégation afin de maximiser les gains énergétiques. Figure tirée de Watanabe et al. (2014).

L’efficacité d’alimentation d’un prédateur est représentée de manière quantitative par le ratio entre le gain énergétique brut et la dépense énergétique (Krebs et al., 1977; Stephens and Krebs, 1986). L’énergie absorbée dépend de la capacité d’assimilation du prédateur mais aussi du type de proies ciblées, de leur distribution et de la densité des agrégations. L’énergie

dépensée comprend l'énergie utilisée pour le métabolisme basal, la digestion et excrétion et égestion, le transport, ainsi que la recherche et la capture de proies (Krebs et al., 1977; Stephens and Krebs, 1986). Des contraintes extrinsèques et intrinsèques à l'individu ou à l'espèce peuvent s'exercer et affecter l'application de la théorie de l'approvisionnement optimal (Figure 2). Plus spécifiquement, les contraintes intrinsèques imposées sur le prédateur incluent des facteurs tels que ses capacités physiologiques (incluant la plongée dans le cas des mammifères marins), ses stratégies alimentaires, ses capacités digestives, son stade de vie et statut reproducteur, ses besoins énergétiques, son régime alimentaire et les pressions de prédation (Figure 2). Les contraintes extrinsèques des relations proies-prédateurs concernent essentiellement tous les paramètres faisant référence aux proies tels que leur distribution (verticale, horizontale et temporelle), densité et biomasse (MacArthur and Pianka, 1966) (Figure 2) et les caractéristiques de l'environnement dans lequel ils évoluent.

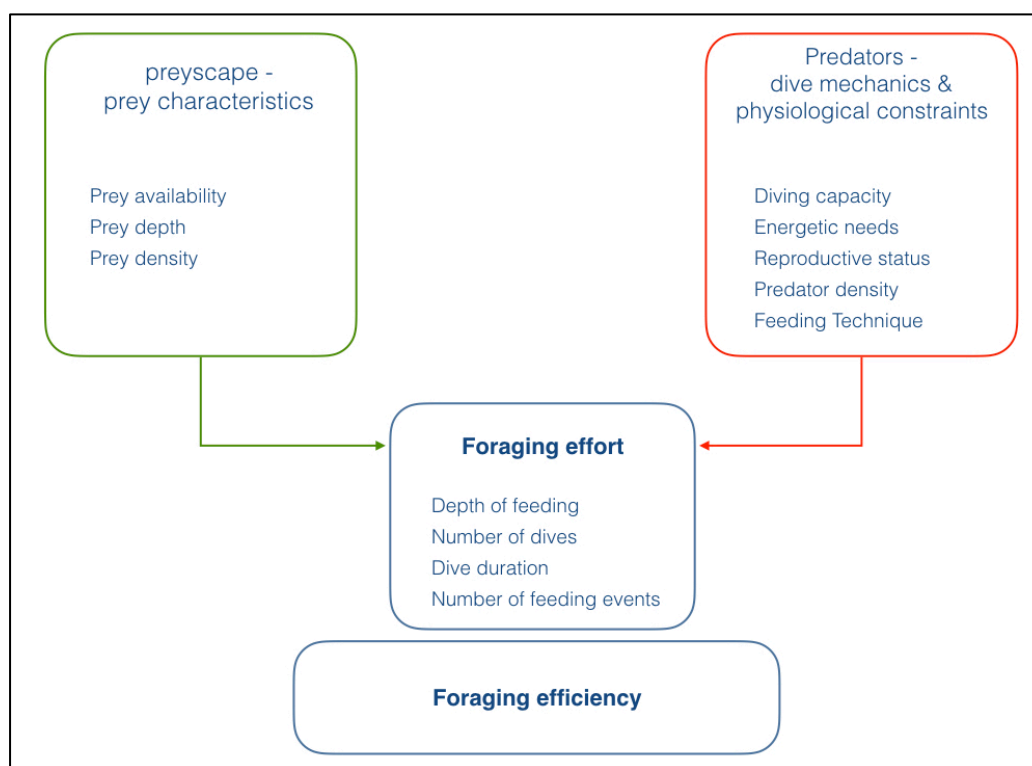


Figure 2 : Schéma illustrant les contraintes extrinsèques (liées au paysage des proies) et intrinsèques aux individus influençant le comportement alimentaire d'un prédateur marin.

RELATION PRÉDATEURS—PROIES – LA DISTRIBUTION DES PROIES

Les schémas d'acquisition de ressources et de stratégie d'alimentation d'un prédateur sont directement influencées par la distribution verticale et horizontale des proies sur lesquelles ils se nourrissent et illustrent certaines contraintes extrinsèques auxquelles les mammifères marins doivent faire face. Dans les systèmes prédateurs-proies, la distribution des prédateurs suit la plupart du temps une courbe sigmoïdale en relation avec la disponibilité des proies, suggérant que la distribution des prédateurs est en lien direct avec la distribution de leurs proies (Holling, 1965). La répartition des ressources au sein d'un écosystème est hétérogène dans le temps et l'espace (MacArthur, 1966), et le régime alimentaire des espèces dépend évidemment des proies disponibles. L'effort de recherche, c'est-à-dire le temps et l'énergie investis, le type de proies visées et les techniques d'alimentation employées par un prédateur vont être influencés par la distribution hétérogène des agrégations de densités de proies exploitables, par exemple le krill (MacArthur and Pianka, 1966; Iwasa et al., 1981; Bowen et al., 2002; Watanabe et al., 2014). Dans le cadre de relation entre des prédateurs et leur proies, la taille des agrégations, leur densité, leur distribution sont autant de facteurs qui influencent le degré d'interactions trophiques. En deçà d'un certain seuil, le coût énergétique associé à l'acquisition de nourriture dépasse le bénéfice de l'exploitation de l'agrégation. Ce seuil peut être atteint spatialement en fonction des densités de proies rencontrées, ou temporellement après que la densité d'une agrégation de nourriture préalablement considérée comme bénéfique passe, suite à son exploitation par le prédateur ou par des phénomènes océanographiques, sous la barre du niveau bénéfique.

Pour des prédateurs marins et les mammifères marins en particulier, le temps de plongée et le temps de résidence dans une agrégation de proies devrait dépendre du rendement énergétique (Mori, 1998). Les mammifères marins, tels que les rorquals, ont la capacité de moduler l'effort d'alimentation en variant la durée de plongée, la profondeur d'alimentation ou le nombre d'événements d'alimentation par plongée, ou *lunges* (Doniol-Valcroze et al., 2011; Ware et al., 2011; Friedlaender et al., 2016). Chez les rorquals par exemple, les baleines à bosse *Megaptera novaeangliae* dans les eaux antarctiques favorisent

les agrégations de krill moins denses mais situées plus haut dans la colonne d'eau (< 100 m) plutôt que les agrégations plus denses mais plus profondes (> 200 m), ce qui leur permet ainsi d'augmenter le taux d'alimentation (c'est à dire le nombre de *lunes* par plongée) et donc l'efficacité d'alimentation (Friedlaender et al., 2016). De même, les rorquals bleus *Balaenoptera musculus* dans l'océan Pacifique adoptent deux stratégies d'alimentation en fonction de la densité et de la distribution des proies : les individus tendent à minimiser leur consommation d'oxygène lorsque le krill se trouve en agrégation plus diffuse mais proche de la surface, alors que la maximisation du gain brut énergétique est préférée lorsque des densités de krill plus élevées se trouvent à de plus grandes profondeurs (Hazen et al., 2015). Le prédateur peut choisir de moduler les caractéristiques de ses plongées (durée, temps en profondeur, nombre de *lunes*, trajectoire) dans les limites de ses capacités physiologiques de plongée, en fonction de ses besoins énergétiques et de la distribution inégale des proies afin de maximiser le ratio gain énergétique brut/dépense énergétique grâce à la maximisation du gain brut énergétique (Thompson and Fedak, 2001; Heaslip et al., 2014).

CONTRAINTES INTRINSÈQUES

- *Contraintes physiologiques*

Les mammifères marins ont l'obligation de retourner à la surface pour respirer. Ils doivent maximiser leurs performances d'alimentation lors de plongées sans apport continu d'oxygène (Butler and Jones, 1997). La surface de l'eau peut être, dans ce contexte, considérée comme une place centrale à partir de laquelle se fait l'approvisionnement en énergie (Houston, 1985; Houston and McNamara, 1985). Le temps de récupération passé à la surface afin de reconstituer les réserves d'oxygène augmente rapidement et disproportionnellement avec le temps de plongée de l'animal et ne constitue donc pas du temps passé pour l'activité d'alimentation (Kooyman and Ponganis, 1998). La capacité de stockage de l'oxygène est positivement corrélée à la taille de l'animal (Croll et al., 2001), ce qui devrait se traduire par des capacités de plongée plus grandes pour des individus de plus

grande taille puisque le taux métabolique spécifique à la masse (taux métabolique par unité de masse de l'individu) diminue avec la taille de l'individu (Peters, 1983; Goldbogen et al., 2012a), permettant ainsi aux espèces de grande taille d'effectuer leurs activités à moindre coût (Kleiber, 1975). Paradoxalement pour les rorquals, le coût de l'activité d'alimentation résultant de la technique adoptée, augmente avec la taille de l'individu jusqu'à limiter les capacités de plongée de celui-ci (Croll et al., 2001; Acevedo-Gutiérrez et al., 2002; Goldbogen et al., 2012). De ce fait, les plus grands rorquals ont fait le choix d'abandonner leur plus grande capacité de plongée pour se nourrir plus efficacement en adoptant des techniques d'alimentation, certes plus coûteuses en énergie, mais en adéquation avec le type de proies ciblées et leur distribution (Acevedo-Gutiérrez et al., 2002; Goldbogen et al., 2012).

- *La technique d'alimentation*

La technique alimentaire adoptée par un prédateur est un des paramètres influençant la dépense énergétique lors de l'alimentation (Emlen, 1966). Le coût énergétique de l'activité d'alimentation dépend de trois composantes majeures constituant de l'activité puisque tout prédateur doit chercher sa nourriture, la poursuivre le cas échéant et la capturer (Griffiths, 1980). L'importance relative donnée à chaque composante dépend du type de prédateurs et du type de proies ciblées. Un prédateur chasseur investira davantage d'énergie dans la poursuite active et la capture de sa proie tandis qu'un prédateur filtreur ou brouteur investira plus d'énergie dans la recherche de nourriture (Griffiths, 1980; Webb, 1984; Riisgård and Larsen, 1995). De manière similaire, le coût énergétique de l'activité d'alimentation sera relatif à la taille des proies et ainsi corrélé positivement avec celle-ci (Labarbera, 1984). Ainsi, certaines familles d'espèces regroupant les plus grands animaux aquatiques (mysticètes, rhincodontidés, cétorhinidés) se nourrissent de petites proies multiples, tandis que de plus petits individus se nourrissent sur des proies uniques mais de plus grande taille et dont la manipulation requiert davantage d'énergie (Case, 1979; Griffiths, 1980). Les rorquals sont des prédateurs filtreurs possédant des sillons ventraux allant de leur bouche à leur nombril, et formant ainsi une poche extensible (Pivorunas, 1979). Ils ont également une

mâchoire inférieure capable de se désarticuler afin de permettre une ouverture buccale maximale (Goldbogen et al., 2010, 2012; Potvin et al., 2012). Ces caractéristiques anatomiques permettent aux rorquals d'engouffrer une importante quantité d'eau et de proies en une seule gorgée lorsqu'ils s'élancent à haute vitesse dans une agrégation de krill ou un banc de poissons (Pivorunas, 1979; Goldbogen et al., 2007). Les proies sont piégées grâce aux fanons puis avalées (Lambertsen et al., 1995; Goldbogen et al., 2006, 2007). Le volume engouffré par un rorqual est déterminé par la taille de la poche extensible ainsi que par la taille des os du crâne et des mâchoires ayant une croissance allométrique positive (Goldbogen et al., 2010), c'est-à-dire qui n'est pas proportionnelle, et dans ce cas-ci plutôt plus rapide relativement à la croissance globale de l'individu.

- *Besoins énergétiques–cycle de vie*

Pour sa survie, le gain net d'énergie d'un individu doit être, de manière évidente, supérieur à la perte nette d'énergie (Costa, 2009). Les mammifères marins se situent sur un continuum de stratégies de reproduction selon leurs traits d'histoire de vie et leur capacité à accumuler et stocker de l'énergie (Costa, 1993; Lockyer, 2007). Les *income breeders* répondent aux besoins de leurs petits en se nourrissant pendant les périodes de reproduction et d'allaitement, tandis que les *capital breeders* fournissent en théorie l'énergie nécessaire à la reproduction et la migration principalement à partir de réserves endogènes acquises précédemment pendant une saison d'alimentation intense (Jonsson, 1997; Madsen and Shine, 1999; Houston et al., 2007; Wheatley et al., 2008). Les baleines à fanons, dont le rorqual bleu, peuvent être considérées dans une certaine mesure comme des *capital breeders*, c'est-à-dire qu'elles assurent la gestation et au moins une partie de la lactation à partir de réserves préalablement acquises et stockées (Mate et al., 1999; Irvine et al. 2017). Elles rétablissent leurs réserves lipidiques durant la période estivale d'alimentation (Brodie, 1975). Cette évolution est sans doute liée à l'exploitation de zones très productives limitées dans le temps et dans l'espace, de ce fait l'acquisition de réserves d'énergie sur une période de temps limitée est cruciale. La migration ou les mouvements entre les habitats permettent aux *capital*

breeders d'exploiter des ressources qui varient dans l'espace, le temps et les saisons (Shaw and Couzin, 2013; Avgar et al., 2014). Il a été montré que les grand rorquals synchronisent leurs migrations avec les efflorescences zooplanctoniques (Visser et al., 2011; Szesciorka et al., 2019). Ils utilisent d'ailleurs leur mémoire pour suivre la disponibilité des ressources (Abrahms et al., 2019; Fagan, 2019). Par conséquent, lorsque les rorquals rejoignent leur site estival d'alimentation, leurs réserves énergétiques sont au plus bas (Vikingsson, 1990), même si des variations sont attendues en fonction de l'âge, du sexe ou du statut reproducteur (Miller et al., 2011).

L'énergie acquise en surplus est stockée sous forme de graisse et est ensuite disponible à un moment ultérieur lorsque la demande d'énergie dépasse l'approvisionnement énergétique (Lockyer, 2007). Les rorquals ont une grande capacité de stockage de lipides dans le gras, les muscles et la cavité abdominale (Lockyer, 1986). La condition corporelle, le ratio entre la masse maigre et la masse grasseuse, est liée à la disponibilité et à la qualité des proies chez les baleines grises *Eschrichtius robustus* (Soledade Lemos et al., 2020) et à la densité de proies chez les rorquals communs *Balaenoptera physalus* (Lockyer, 2007). La condition corporelle des femelles, donc la taille des réserves énergétiques, est liée au succès reproducteur qui englobe la fécondité, la croissance et la survie des veaux (Lockyer, 2007; Christiansen et al., 2014, 2016). La reproduction est l'une des fonctions les plus énergétiquement exigeantes, en particulier la phase de la lactation chez les mammifères, et dépend des réserves d'énergie de la femelle (Gittleman and Thompson, 1988; Crocker et al., 2001; Lewis and Kappeler, 2005).

L'ÉMERGENCE DU BIOLOGGING

Dans le but d'étudier les comportements, l'écologie et le fonctionnement physiologique d'espèces terrestres et aquatiques qui ne sont pas toujours à notre portée, des instruments qui permettent de les étudier à distance ont été développés (Kooyman, 2004; Ropert-coudert and Wilson, 2004). De nombreux taxons ont fait l'objet de ce genre d'études comme par exemple les oiseaux, les grands félidés, les poissons ou encore les mammifères marins (Naito, 2004).

L'accès à ces précieux outils pour l'étude des mammifères marins s'est révélé innovant et a permis d'élargir de façon exponentielle le champ de nos connaissances sur ces animaux (Boyd et al., 2004). En effet, l'étude des mammifères marins est bornée par des contraintes liées au vaste environnement en trois dimensions dans lequel ils évoluent. Les premiers dispositifs permettant l'étude de phénomènes hors de notre champ d'observation remontent aux années 60 (Kooyman, 1965). Depuis les avancées technologiques ont permis la miniaturisation et la sophistication des outils de recherche (Ropert-Coudert and Wilson, 2005). Dans le domaine de la science du biologging, une distinction est possible entre les instruments permettant l'enregistrement de données qu'il faut ensuite récupérer communément appelés « enregistreurs de données » et les instruments d'ordre télémétrique qu'il n'est pas nécessaire de recouvrer puisque les données sont transmises par satellite (Kooyman, 2004; Naito, 2004). Les premiers enregistreurs de données enregistraient la température et la profondeur à intervalles donnés (Womble et al., 2013). Ces enregistreurs VTDR (Velocity-Time-Depth-Recorders) sont toujours utilisés aujourd'hui dans l'étude du comportement de plongée d'organismes appartenant à différents taxons (Naito, 2004; Womble et al., 2013). Leur digitalisation a permis leur réduction en taille et par conséquent la diminution de leurs impacts sur les organismes étudiés (Naito, 2004). L'ajout de sondes mesurant la vitesse, l'accélération ou l'orientation dans les trois axes participe à l'étude des comportements de plongée de manière plus complexe (Kooyman, 2004; Naito, 2004). Il ne s'agit plus d'avoir une image en deux dimensions du comportement d'un animal sous la surface de l'eau mais d'en avoir une image en trois dimensions.

L'écologie alimentaire peut quant à elle être étudiée par observation directe de l'activité d'alimentation d'individus. Cependant, cela n'est pas toujours possible quand les individus ne sont pas directement observables comme les mammifères marins par exemple (Rutz and Hays, 2009; Hindell et al., 2010). Plusieurs techniques indirectes sont alors utilisées pour inférer ou interpréter les événements d'alimentation comme l'utilisation de caméras, de balises acoustiques passives ou de suivis focaux. Ceux-ci donnent des informations sur les activités d'alimentation de surface ou les événements ayant lieu à de faibles profondeurs (Rutz and Hays, 2009; Hindell et al., 2010). L'utilisation d'enregistreurs

VTDR permet la reconstruction des patrons de plongée en deux dimensions et des temps de surface effectués par les individus (Figure 3). La résolution temporelle, dépendante de la fréquence d'échantillonnage des différents paramètres, est un facteur critique pour la reconstruction des patrons de plongée. La durée entre deux enregistrements de paramètres doit être plus courte que la durée de l'événement afin de capter les changements dans le comportement de l'individu (Hindell et al., 2010). De telles données empiriques sont cruciales dans la paramétrisation réaliste de modèles bioénergétiques, par exemple.

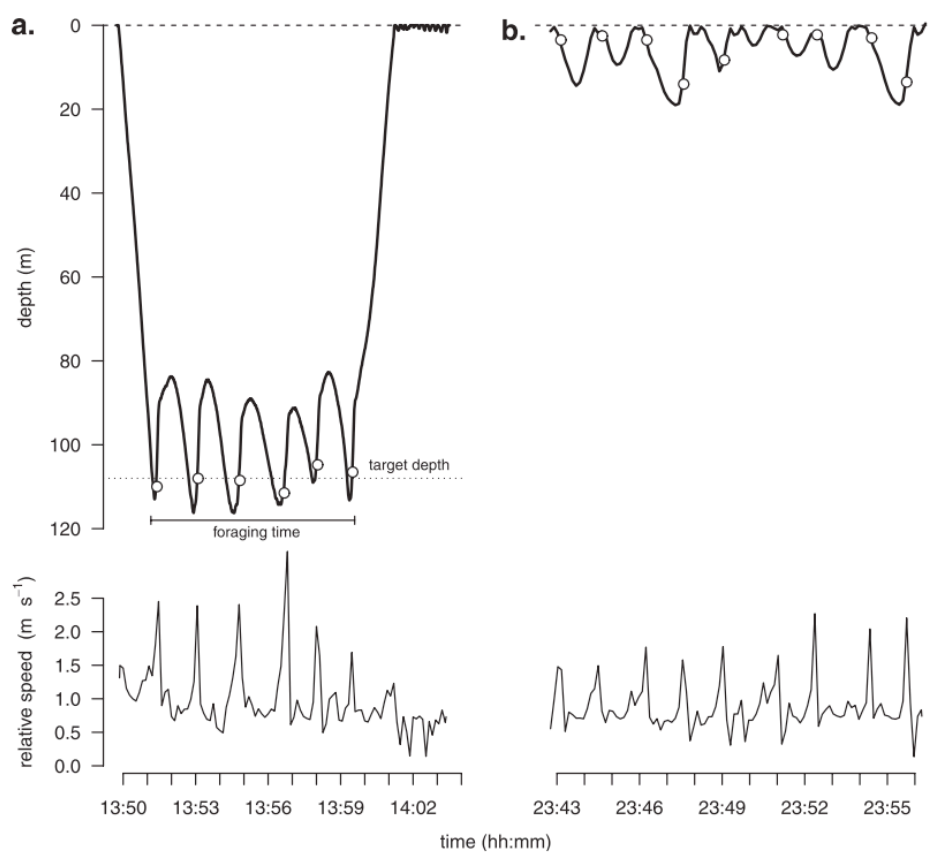


Figure 3 : Photo illustrant un rorqual bleu équipé d'un enregistreur de données VTDR (Velocity-Time-Depth-Recorder) en haut de figure et le type de données qui en résultent en bas de figure. Les capteurs de profondeur et vitesse permettent de reconstruire des patrons de plongées et événements d'alimentation (cercles blancs) (a) en profondeur et (b) en surface. Crédit photo DFO-GREMM, figure tirée de (Doniol-Valcroze et al., 2011).

LES MODÈLES BIOÉNERGÉTIQUES

Quantifier la consommation énergétique des individus n'est pas toujours directement possible. L'utilisation de modèles bioénergétiques permet, dans ce cas, de comprendre et prédire les interactions bioénergétiques entre les prédateurs et leur environnement. Les besoins énergétiques vont varier selon le budget d'activité de chaque individu mais aussi selon les besoins énergétiques dictés par le statut du cycle de vie de l'individu (p. ex. statut reproducteur). L'utilisation de modèles bioénergétiques pour estimer la consommation d'énergie a été appliquée à plusieurs espèces de cétacés et pinnipèdes (e.g., Winship et al., 2002 ; Hammill et al., 2010 ; Noren et al., 2012). L'exactitude et la précision de l'estimation des coûts énergétiques passent par l'application des taux métaboliques spécifiques selon le budget d'activité et le type d'activité (Jeanniard-du-Dot et al., 2016; Bejarano et al., 2017). En effet, l'utilisation de paramètres avec une incertitude associée trop grande peuvent diminuer la validité ou la confiance du modèle (Winship et al., 2002). L'ajout de paramètres issus de données empiriques est d'autant plus encouragé lorsque de telles données existent ou peuvent être acquises.

En plus d'estimer la consommation d'énergie d'un prédateur, les modèles énergétiques permettent d'investiguer l'impact de changements anthropiques ou naturels sur la balance énergétique des individus (New et al., 2013b). Les modèles développés dans le cadre du PCod « Population Consequences of Disturbances » permettent d'étudier l'impact de dérangements non seulement au point de vue comportemental, mais aussi énergétique et physiologique, sur des échelles temporelles de courte ou longue durée, à l'échelle de l'individu et de la population (King et al., 2015; Pirotta et al., 2018a; Booth et al., 2020). Le cadre du PCoD préalablement majoritairement centré sur les conséquences de dérangements tels que la présence de bateaux d'excursion, ou de source acoustique peut aussi intégrer des changements dans le paysage de proies (densité, disponibilité, accessibilité) qui ont aussi des conséquences énergétiques en affectant le gain énergétique ou le comportement de recherche alimentaire (Pirotta et al., 2018a). D'autres modèles de programmation dynamique stochastique « stochastic dynamic programming equations » permettent d'investiguer ce type

de changements à plus long terme et les décisions optimales qu'un individu devrait adopter, comme par exemple ce qui a été fait pour les rorquals bleus de la côte ouest du Pacifique (Pirota et al., 2018b, 2019).

LE RORQUAL BLEU—POPULATION DE L'ATLANTIQUE NORD-OUEST

Le rorqual bleu est le plus grand animal vivant sur la planète. Il fait partie de la famille des mysticètes et est cosmopolite à tous les océans (Yochem and Leatherwood, 1985). Cependant différents stocks peuvent être identifiés. Les rorquals bleus de l'Atlantique Nord-Ouest sont considérés comme une population à part entière et reconnus comme en voie de disparition en vertu de la Loi sur les espèces en péril du Canada mais aussi de la Loi sur les espèces en voie de disparition des États-Unis d'Amérique. En effet, les efforts de photo-identification indiquent un faible taux d'échange entre les individus du Nord-Ouest et du Nord-Est Atlantique (Sears et al., 2015). Notamment, une observation transatlantique rapporte l'observation d'un individu photo-identifié en septembre 2010 et 2017 dans le golfe du Saint-Laurent, puis aux Açores en mai 2015 (R. Sears and Mingan Island Cetacean Studies, données non publiées). Dans l'est du Canada, les rorquals bleus sont observés dans l'estuaire et le golfe du Saint-Laurent (EGSL), le sud de Terre-Neuve et le plateau néoécossais, et des observations font état de leur présence jusqu'à la côte ouest du Groenland (Sears et al., 1990; Kingsley and Reeves, 1998; Doniol-Valcroze et al., 2007; Lesage et al., 2007). Leur occurrence tout au long de l'année dans l'EGSL est rapportée acoustiquement, cependant qu'ils s'agisse d'adultes matures et au repos ou des juvéniles est encore incertain (Simard et al., 2016). Les rorquals bleus semblent utiliser le détroit de Cabot comme porte d'entrée et de sortie de l'EGSL (Simard et al., 2016; Lesage et al., 2017a). Le monitoring par acoustique passive rapporte la présence d'individus sur le plateau néo-écossais tout au long de l'année avec un pic d'occurrence en été et hiver (Moors-Murphy et al., 2019). Les patrons de migration de la population de rorqual bleu de l'Atlantique Nord-Ouest sont encore mal connus même si une étude de télémétrie satellite indique que tous les individus marqués avaient quitté l'EGSL en décembre au plus tard (Lesage et al., 2017a). Deux balises

téléométriques ont duré plusieurs mois, donnant les premières informations concernant leurs déplacements durant la période hivernale (Lesage et al., 2017a). Les individus se sont rendus jusqu'au large de la Caroline du Nord et autour des monts sous-marins de la Nouvelle-Angleterre aux États-Unis (Lesage et al., 2017a). L'exploitation commerciale, entre la fin du 19^{ème} siècle et son interdiction en 1966, a réduit de 70% le nombre de rorquals bleus présents dans l'Atlantique Nord, avec au moins 1500 des 11000 individus chassés provenant de la côte est du Canada (Sergeant, 1966; Sigurjónsson and Gunnlaugsson, 1990; Beauchamps, 2009). Cette population dont la taille est inconnue, est aujourd'hui estimée à quelques centaines d'individus (Sears and Calambokidis, 2002). En 40 ans d'observation, 28 paires de mère-veau ont été observées dans l'EGSL indiquant un faible taux de natalité (R. Sears and Mingan Island Cetacean Studies, données non publiées). Si l'exploitation commerciale du 20^e siècle est en grande partie responsable du statut de cette population, celle-ci fait face à de nombreuses menaces en plus de la mortalité naturelle telles que, le risque de prise dans les glaces, de collision avec les bateaux d'excursion, d'empêchement dans des engins de pêches ou encore de dégradation de l'habitat par les bruits anthropiques (Beauchamp et al., 2009; Lesage et al., 2018). D'autres menaces telles que les variations dans les communautés zooplanctoniques, en particulier le krill, leur principale proie, en réponse aux changements climatiques pourraient affecter le rétablissement de cette population.

Les rorquals bleus de l'Atlantique Nord-Ouest visitent de manière saisonnière l'EGSL pour se nourrir et reconstituer leurs réserves énergétiques (Sears and Calambokidis, 2002). Le régime alimentaire des rorquals bleus dans cette région, de 1999 à 2009, était constitué à 70% de krill arctique *Thysanoessa raschii* et à 30% de krill nordique *Meganyctiphanes norvegica* d'après une étude isotopique (Gavrilchuk et al., 2014). Dans l'estuaire du Saint-Laurent, les rorquals bleus, qui se nourrissent dans quatre types d'habitats (pente inférieure, pente supérieure, plateau et offshore) variant en termes de profondeur, adoptent des comportements alimentaires différents dans chacun d'eux, dépendamment du cycle de marée (Doniol-Valcroze et al., 2012). Ces quatre types d'habitats ont été déterminés grâce aux comportements de plongée des rorquals bleus et leurs géolocalisations (Doniol-Valcroze et al., 2012). De manière générale, la distribution des plongées des rorquals bleus suit une

distribution de profondeurs qui est bimodale, comprenant des plongées effectuées près de la surface et d'autres à des profondeurs entre 50 et 100 mètres (Doniol-Valcroze et al., 2012). Le nombre de *lunges* effectués par plongée par les rorquals bleus suivent les règles de la théorie de l'approvisionnement optimal (Doniol-Valcroze et al., 2011). En effet, ils effectuent plus de *lunges* par plongée lorsque la profondeur de plongée augmente et ont un plus haut taux d'alimentation lorsqu'ils se nourrissent près de la surface (Doniol-Valcroze et al., 2011) (Figure 4). Cependant cette étude est basée seulement sur le temps de plongée et la profondeur ciblée, et même si celles-ci devraient être représentatives de la profondeur des proies ingérées, la densité de proies ciblée joue un rôle majeur dans la stratégie d'alimentation adoptée par un prédateur. L'utilisation d'enregistreurs de données déployés sur les rorquals bleus en alimentation dans l'estuaire du Saint-Laurent a donc permis l'acquisition d'importantes connaissances sur leur comportement de recherche de nourriture (Doniol-Valcroze et al., 2011, 2012). Cependant, il n'existe pas d'études examinant l'aspect énergétique du comportement alimentaire des rorquals bleus dans l'EGSL. De plus, le faible nombre de veaux observés chaque année soulève des questions quant à l'état nutritionnel des individus et des femelles adultes en particulier. Il est donc essentiel d'estimer, par le biais de modélisations bioénergétiques, les coûts énergétiques associés à l'alimentation et de quantifier leurs besoins en krill afin de comprendre les facteurs limitant le rétablissement de cette population et ainsi mieux assurer sa conservation.

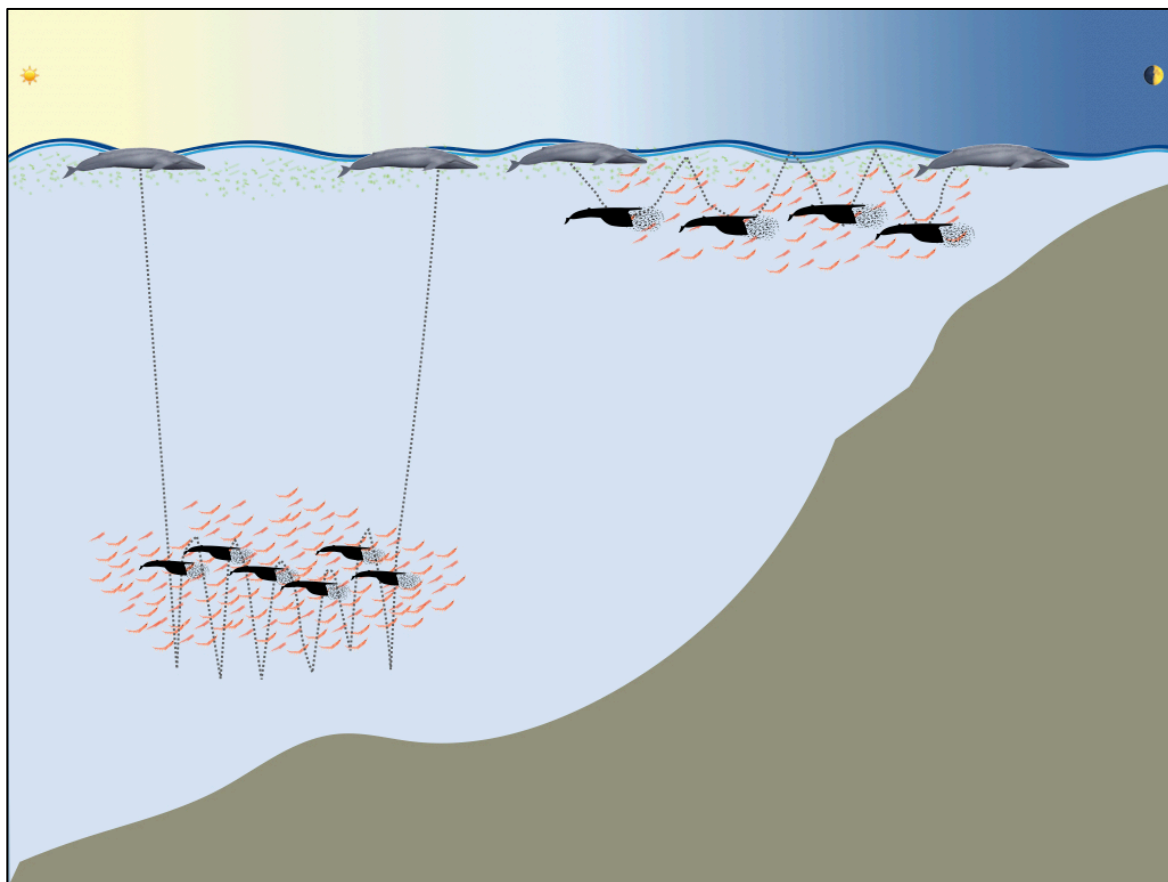


Figure 4 : Schéma illustrant le comportement alimentaire des rorquals bleus. Le nombre de *lunes* par plongées est d'autant plus grand que la profondeur d'alimentation augmente. Adapté de Acevedo-Gutiérrez et al. (2002) et (Doniol-Valcroze et al., 2011).

L'ESTUAIRE ET LE GOLFE DU SAINT-LAURENT (EGSL)

L'EGSL abrite une vingtaine d'espèces de mammifères marins, résidents ou saisonniers, qui viennent pour s'y nourrir et/ou s'y reproduire (Lesage et al., 2007). Parmi ces espèces se trouvent sept espèces de pinnipèdes et 12 espèces de cétacés dont le rorqual bleu, le rorqual commun, le rorqual à bosse et le petit rorqual (Lesage et al., 2007). L'EGSL, situé sur la côte est du Canada, est une mer semi-fermée de 240 000 km² de superficie (Galbraith et al., 2019) ouverte sur la mer du Labrador par le détroit de Belle-Isle et sur l'océan Atlantique par le détroit de Cabot situé entre l'île du Cap-Breton en Nouvelle-Écosse

et la côte sud de Terre-Neuve (Saucier et al., 2003) (Figure 5). Par ces deux points d'entrée, l'EGSL est influencé par des masses d'eaux froides provenant de l'Arctique et des masses d'eaux plus tempérées venant de l'Atlantique qui jouent un rôle majeur sur les communautés qui s'y retrouvent (Blais et al., 2019; Galbraith et al., 2019). Le courant du Labrador, le courant du Gulf Stream et les courants de marées influent fortement les processus physicochimiques et biologiques du golfe du Saint-Laurent (El-Sabh, 1990).

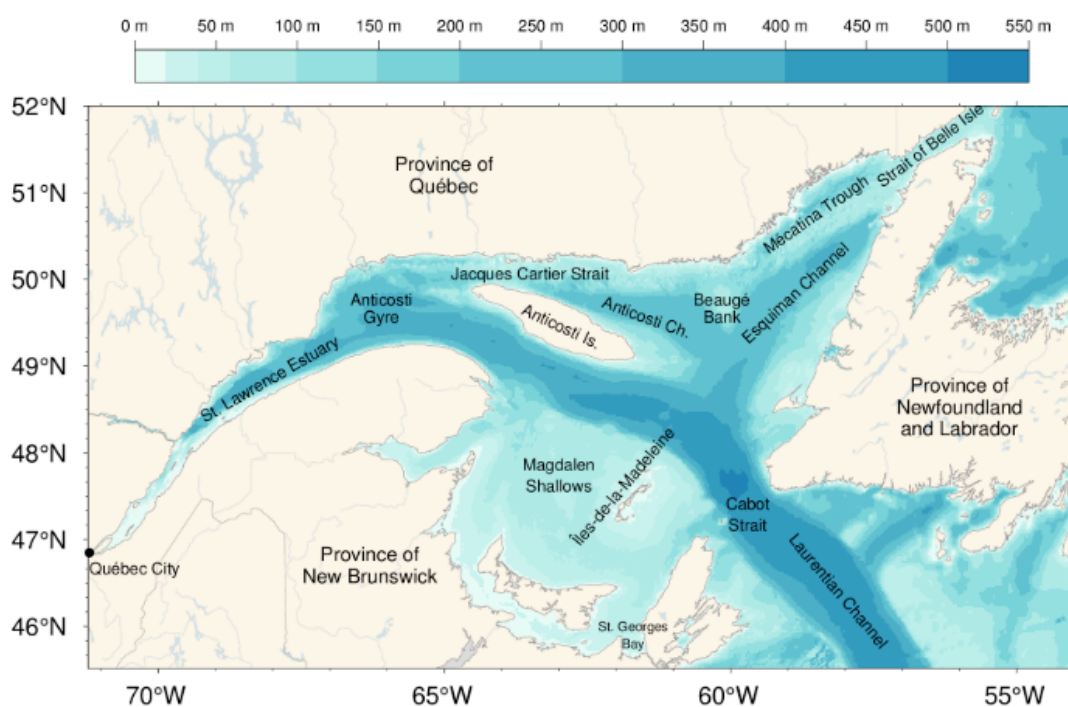


Figure 5 : Aire d'étude et bathymétrie associée. Carte extraite de Galbraith et al. (2019).

L'EGSL est caractérisé par une forte stratification des conditions physico-chimiques, comme la salinité, la température, le couvert de glace et la circulation (Koutitonsky et al., 1991; Saucier et al., 2003; Galbraith et al., 2019). Le système présente une importante stratification verticale des masses d'eaux suivant un cycle saisonnier selon la température et la salinité, qui influencent la densité des masses d'eaux (Galbraith et al., 2019). En été, le

système est formé de trois couches distinctes : une couche de surface, une couche intermédiaire froide ($< -1^{\circ}\text{C}$) et une couche profonde ($\sim 6^{\circ}\text{C}$). À l'automne, la couche de surface se refroidit et finit par se mélanger avec la couche intermédiaire froide pour ne donner qu'un système à deux couches en hiver : une couche de surface froide et une couche de fond plus salée et plus chaude influencée par les masses d'eaux de l'océan Atlantique. Au printemps, la fonte des glaces qui entraîne un important apport d'eau douce s'ajoute au réchauffement de la couche de surface, qui finit par isoler la couche intermédiaire froide et redonne un système à trois couches (Galbraith et al., 2019). Cette stratification des masses d'eau influence la distribution des proies ectothermes, comme le krill. De plus, la grande variabilité de la topographie, des masses d'eaux, et la présence de zones de résurgences à la tête du chenal Laurentien font de l'EGSL un milieu riche et productif (Morissette et al., 2009; Dufour et al., 2010).

Le réchauffement des eaux de l'EGSL, et notamment de la couche de surface, s'intensifie chaque année (Galbraith et al., 2019). Une augmentation de $0.6\text{--}1.2^{\circ}\text{C}$ de la température de l'EGSL est prédite pour les 50 prochaines années (Hutchings et al., 2012; Long et al., 2016; Blais et al., 2019) et pourrait être accompagnée d'une diminution de la couche intermédiaire froide (Galbraith et al., 2019). Des changements de communautés zooplanctoniques (mésozooplancton) sont déjà observés depuis les dernières décennies (Richardson, 2008; Blais et al., 2019). Néanmoins l'effet que de tels changements, en plus de la variabilité saisonnière, pourraient avoir sur les communautés de krill dans l'EGSL sont encore mal connus. Compte tenu de la distribution verticale et des niches de températures optimales des espèces de krill de l'EGSL (Plourde et al., 2014b), des conséquences sur la distribution et la dynamique de population du krill et des espèces qui en dépendent, comme particulièrement le rorqual bleu, sont à envisager.

LE KRILL DANS L'EGSL—THYSANOESSA SPP. ET MEGANYCTIPHANES NORVEGICA

Le krill, du nom générique d'origine norvégienne, représente un ensemble d'espèces holoplanctoniques appartenant au macrozooplancton de l'ordre des Euphausiacés (*Euphausiacea*). Le krill est une espèce clé des réseaux trophiques marins (Sourisseau et al., 2006; Savenkoff et al., 2013). En effet, le krill se nourrit de producteurs primaires (c'est-à-dire phytoplancton) et secondaires (c'est-à-dire mésozooplancton) et permet le transfert d'énergie vers les niveaux trophiques supérieurs (Falk-Petersen et al., 2000). Le krill effectue des migrations verticales nyctémérales durant lesquelles il migre vers la surface pendant la nuit pour s'y nourrir (Mauchline and Fisher, 1980). Ces migrations journalières leur permettent d'éviter stratégiquement les prédateurs mais celles-ci ont aussi lieu lors de comportements liés à la reproduction ou à la mue (Tarling et al., 1999; Plourde et al., 2014b). Le krill est une ressource hautement hétérogène dans le temps et l'espace (Miller and Hampton, 1989; Siegel and Kalinowski, 1994; Siegel, 2000), avec de petites unités denses (dizaines de km²) nichées à l'intérieur d'agrégations beaucoup vastes (centaines de km²) (Watkins and Murray, 1998; McQuinn et al., 2015). La distribution à plus large échelle des communautés de krill est généralement dictée par la salinité qui influence la pénétration de la lumière, température de l'eau, présence de glace, et disponibilité et abondance de leurs proies (Richardson, 2008; Plourde et al., 2014b). De plus, la topographie des fonds marins affecte la circulation de surface et la formation d'agrégations de krill, générant ainsi des zones d'agrégations récurrentes (Maps et al., 2012; McQuinn et al., 2015).

Dans l'Atlantique Nord-Ouest, on retrouve deux espèces prédominantes de krill, le krill nordique *Meganyctiphanes norvegica* et le krill arctique *Thysanoessa* spp. (incluant *Thysanoessa raschii* et *Thysanoessa inermis*) (Mauchline and Fisher, 1980; Simard et al., 1986a) dont les rorquals bleus se nourrissent (Figure 6). Ces deux espèces de krill diffèrent dans leurs comportements agrégatifs, la profondeur à laquelle ils se situent, leurs contenus énergétiques mais aussi leur niches écologiques optimales (Plourde et al., 2014b; McQuinn et al., 2015; Cabrol et al., 2019b). *Thysanoessa* spp. est plus petit que *M. norvegica* (longueur

moyenne = 22,0 vs. 35,7 mm, respectivement ; McQuinn et al. 2013) et son contenu énergétique est 21% plus bas que celui de *M. norvegica* ($4,3 \pm 0,6$ versus $5,2 \pm 0,4$ kJ · g⁻¹, respectivement ; D. Chabot, données non publiées). Ces deux espèces se chevauchent dans leurs distributions verticales, cependant *M. norvegica* est généralement retrouvée à de plus grandes profondeurs que *Thysanoessa* spp. (Plourde et al., 2014b; McQuinn et al., 2015) (Figure 7). Les estimations de la biomasse et de la densité de ces deux espèces de krill sont de plus en plus précises avec l'utilisation de relevés hydroacoustiques multifréquences et le développement d'algorithmes spécifiques de classification des espèces (McQuinn et al., 2013). Les densités mesurées des deux espèces par relevés hydroacoustiques sont variables à la fois spatialement et temporellement (McQuinn et al., 2015). Le ratio de la biomasse des deux espèces était estimé à 60:40 pour *Thysanoessa* spp. dans la période 2000–2009 (McQuinn et al., 2015). Les changements climatiques ne sont pas sans impacts sur les communautés zooplanctoniques. En effet, l'augmentation de la température de l'eau peut influencer la distribution, la condition physiologique, la reproduction et la survie des individus (Flores et al., 2012; McBride et al., 2014). Dans l'EGSL, une augmentation de la température de l'eau pourrait favoriser une espèce tempérée à boréale comme *M. norvegica* (Sameoto, 1976) plutôt qu'une espèce adaptée à des environnements plus froids comme *Thysanoessa* spp. (Mauchline and Fisher, 1980). Des changements quant à leurs abondances relatives et densités peuvent être envisagés en réponse, notamment, à l'augmentation de la température de l'eau et au changement d'habitats qui seraient alors occasionnés. De plus, les pressions de pêche exercées sur le krill comme par exemple dans l'hémisphère sud (Nicol and Foster, 2003; Nicol et al., 2012) ne sont pas sans possibles effets sur la structure trophique des écosystèmes et les consommateurs de krill (Nicol and Endo, 1999; Alonzo et al., 2003). Dans l'estuaire et le golfe du Saint-Laurent des pêches exploratoires ont eu lieu en 1991 et 1992 (Runge and Joly, 1995). Néanmoins, selon le principe de précaution et en l'absence de connaissances scientifiques suffisantes, un moratoire a été établi concernant une pêche commerciale du krill nordique dans l'EGSL depuis 1997 (DFO, politique sur la gestion des espèces fourragères). De ce fait, en raison de l'intérêt sporadique mais récurrent pour l'exploitation commerciale du krill à nos latitudes, à des fins d'aquaculture, de production de

cosmétiques et de dérivés nutraceutiques, il est primordial de mieux comprendre la dynamique de cette ressource afin d'en assurer sa pérennité.

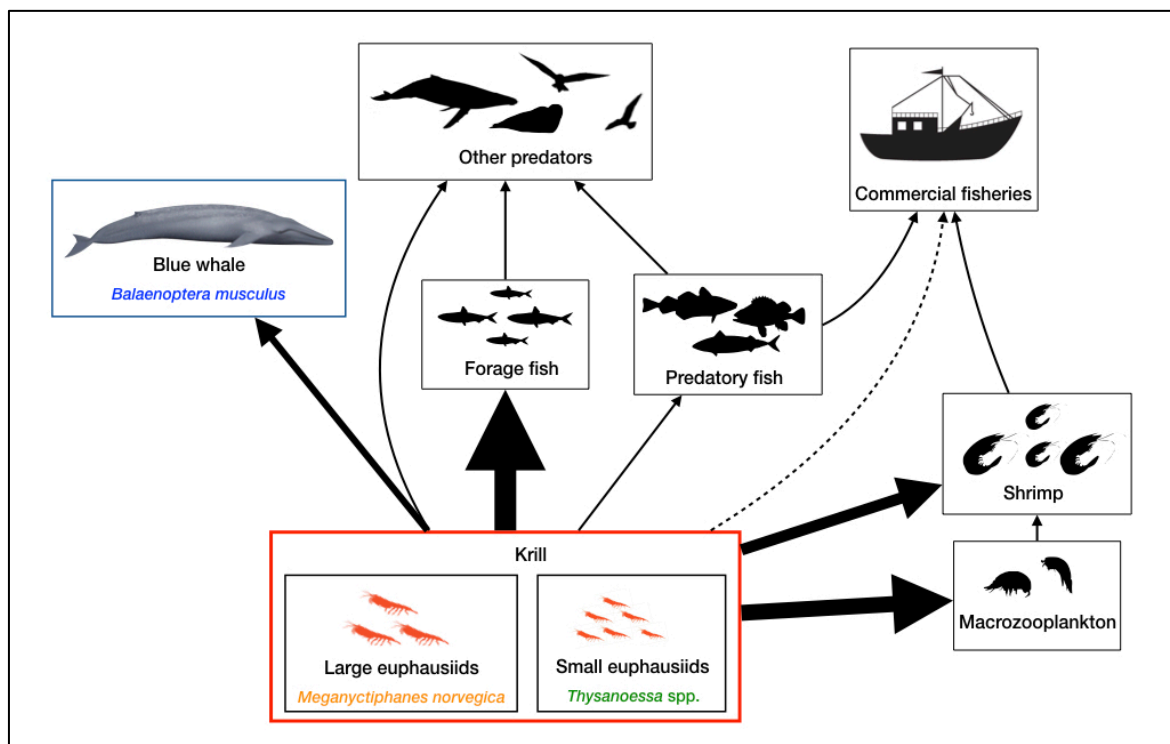


Figure 6 : Représentation schématique du réseau trophique de l'EGSL, centré sur le krill et sur ses principaux prédateurs. La taille des flèches pleines représente l'intensité de prédation. La flèche en pointillés indique une possible exploitation commerciale. Adaptée de Savenkoff et al. (2013).

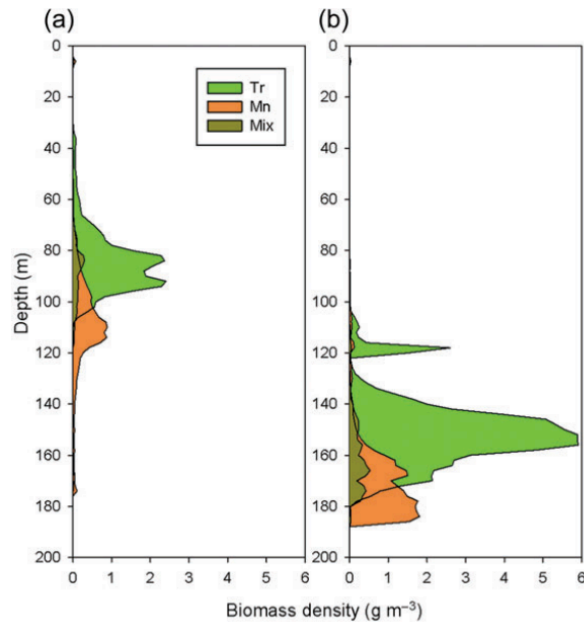


Figure 7 : Distribution verticale pendant le jour des densités de krill pour les deux espèces *Thysanoessa* spp. (vert), *M. norvegica* (orange) et la classification mixte des deux (marron) dans (a) l'estuaire et (b) le nord-ouest du golfe du Saint-Laurent. Figure extraite de Plourde et al. (2014b).

OBJECTIFS DE RECHERCHE

L'objectif général de cette thèse est d'évaluer **les besoins énergétiques du rorqual bleu afin de caractériser la qualité de l'EGSL afin de répondre aux besoins de la population de rorquals bleus de l'Atlantique Nord-Ouest**. Ce projet allie des données de plongées provenant d'archivistes (*biologgers*) et des données *in situ* des densités de krill mesurées par relevés hydroacoustiques. De plus, l'étude de l'écologie alimentaire d'espèces de rorquals en fonction de biomasses de proies *in situ*, et non à partir d'estimations tirées de la littérature a rarement été réalisée et cette étude, représente une approche inédite dans l'estuaire et le golfe du Saint-Laurent. Le projet s'articule autour de trois axes de recherche s'appuyant sur les besoins énergétiques des rorquals bleus à différentes échelles spatiotemporelles (c.f. schéma conceptuel en Figure 8).

OBJECTIFS SPÉCIFIQUES

Axe 1: Déterminer les densités de krill requises par le rorqual bleu à partir de ses besoins énergétiques et identifier les seuils en deçà desquels des agrégations de krill deviennent non-bénéfiques.

Chapitre 1

Le chapitre 1 vise à examiner le comportement de recherche de nourriture et la bioénergétique des rorquals bleus de l'Atlantique Nord-Ouest, en déterminant la capacité de ces individus à répondre à leurs besoins énergétiques dans l'environnement dans lequel ils se nourrissent. Ce chapitre constitue la première étude bioénergétique concernant la population de rorquals bleus de l'Atlantique Nord-ouest. L'approche utilisée est une approche intégrative basée sur le comportement de recherche de nourriture des rorquals bleu à l'aide des données comportementales provenant d'archiveurs de données (déployées sur le dos des rorquals grâce à des ventouses) et de mesures *in situ* des densités des deux principales espèces de krill dont ils se nourrissent effectuées à l'aide de relevés hydroacoustiques. L'absence de données hydroacoustiques simultanées aux comportements d'alimentation enregistrés par les balises télémétriques a conduit à développer une approche originale et novatrice. Ceci nous a permis de prédire les exigences de densité de krill pour répondre ou dépasser les demandes énergétiques associées à différentes efficacités théoriques d'alimentation en utilisant des modèles bioénergétiques basés sur les données empiriques comportementales. Ces exigences de densité ont ensuite été comparées aux densités de krill mesurées *in situ* pour conclure sur le degré d'aptitude de l'habitat à combler les besoins énergétiques des rorquals bleus. Les résultats de cette étude permettent de comprendre davantage l'état nutritionnel des individus et constituent de nouveaux outils dans les efforts de conservation de cette population. Cette étude a été publiée en août 2019 dans la revue Marine Ecology Progress Series.

Axe 2 : Déterminer les conséquences énergétiques d'une réduction des densités de krill qui pourraient survenir en raison d'une exploitation commerciale ou des changements climatiques ou encore du du temps passé à s'alimenter en raison de la présence répétée de bateaux d'excursion.

Chapitre 2

Le chapitre 2 vise à examiner les conséquences énergétiques de changements découlant d'activités anthropiques sur le comportement alimentaire et le gain net d'énergie des rorquals bleus se nourrissant dans l'EGSL. Les rorquals bleus font face à une multitude de pressions et les changements investigués dans ce chapitre se séparent en deux types : des changements liés aux proies, et survenant en raison par exemple d'une exploitation commerciale ou des changements climatiques, et des changements liés au comportement alimentaire et notamment une diminution du temps passé à s'alimenter induit par la présence répétée de bateaux d'excursion. Le modèle bioénergétique est basé sur des données empiriques du comportement alimentaire des rorquals bleus et sur des mesures *in situ* de krill obtenues par relevés hydroacoustiques. L'utilisation de simulations et de scénarios permettent d'investiguer les conséquences des changements illustrés ci-dessus sur l'acquisition d'énergie des rorquals bleus. Ce chapitre est primordial pour une meilleure compréhension des conséquences de changements anthropiques sur le comportement alimentaire et l'énergétique des rorquals bleus et offre une première quantification de la façon dont de tels changements peuvent influencer la balance énergétique des rorquals bleus de l'Atlantique Nord-Ouest. Cette étude a été publiée en août 2020 dans la revue *Frontiers in Marine Science*.

Axe 3 : Déterminer la capacité du rorqual bleu à accumuler l'énergie nécessaire à la reproduction selon la qualité de l'estuaire et du golfe du Saint-Laurent comme site d'alimentation.

Chapitre 3

Le chapitre 3 est une première quantification de l'énergie potentiellement accumulée, sous forme de réserves énergétiques, par les rorquals bleus pendant une saison d'alimentation complète en fonction de densités de krill mesurées *in situ* dans l'EGSL. Ce troisième chapitre utilise une approche de simulation mécanistique pour estimer les réserves d'énergie d'une femelle adulte au cours d'une saison d'alimentation. Ces travaux de modélisation reposent sur des données empiriques du comportement alimentaire des rorquals bleus et des densités de krill *in situ* spécifiques au site d'étude, mais aussi de paramètres issus de la littérature. Afin d'investiguer si les réserves énergétiques accumulées par une femelle adulte mature seraient adéquates pour couvrir les coûts énergétiques associés à la reproduction, ceux-ci ont été modélisés sur un cycle de reproduction complet, permettant ainsi de déterminer si les densités de krill dans la zone d'étude pourraient être l'un des facteurs explicatifs du faible taux de mise bas observé dans cette population en voie de disparition. Les résultats de cette étude seront soumis pour publication à l'automne 2020.

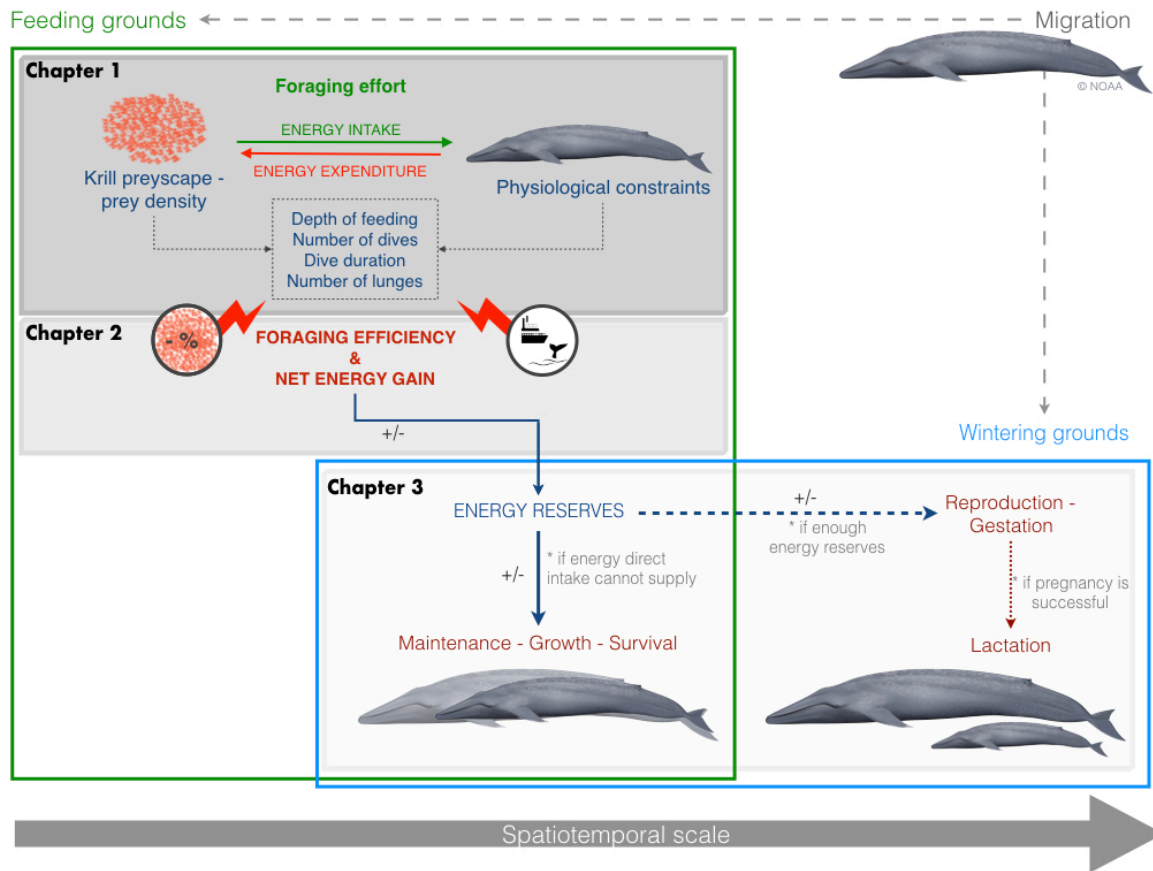


Figure 8 : Schéma conceptuel représentant la démarche scientifique et l'organisation du projet de doctorat, ainsi que la complémentarité des chapitres dans l'étude de la bioénergétique des rorquals bleus sur une échelle spatiotemporelle d'une année. Les signes « +/- » représentent l'ampleur du gain net d'énergie qui sera ensuite stockée sous forme de gras et potentiellement disponible pour le maintien, la croissance et, le cas échéant, la reproduction.

Ce projet, en combinant des approches à différentes échelles temporelles (heure, jour, mois, année) permettra de capter les besoins énergétiques des rorquals dans leur globalité (Figure 8). Les résultats obtenus contribueront à parfaire nos connaissances de la bioénergétique des rorquals bleus et de leurs besoins en krill lorsqu'ils s'alimentent dans l'EGSL. Ces résultats permettront de guider la mise en place de mesure de gestion d'une pêche éventuelle ou de règlement de l'industrie d'observation des baleines, en plus d'offrir une assise solide pour d'éventuelles études écosystémiques ou pour mieux appréhender les

conséquences d'un éventuel changement de structure des communautés dans le contexte actuel des changements climatiques sur les espèces qui dépendent du krill, comme les rorquals bleus.

CHAPITRE 1
FORAGING ENERGETICS AND PREY DENSITY REQUIREMENTS OF
WESTERN NORTH ATLANTIC BLUE WHALES IN THE ESTUARY AND
GULF OF ST. LAWRENCE, CANADA

Authors:

Marie Guilpin^{1,2}, Véronique Lesage¹, Ian McQuinn¹, Jeremy A. Goldbogen³, Jean Potvin⁴,
Tiphaine Jeanniard-du-Dot¹, Thomas Doniol-Valcroze⁵, Robert Michaud⁶, Michel Moisan⁶,
Gesche Winkler²

¹Lamontagne Institute, Fisheries and Oceans Canada, 850 route de la Mer, Mont-Joli, QC
G5H 3Z4, Canada

² Marine Science Institute, Quebec-Ocean–University of Quebec in Rimouski, 310 Allée des
Ursulines, Rimouski, QC G5L 3A, Canada

³Department of Biology, Hopkins Marine Station, Stanford University, Pacific Grove, CA
93950, USA

⁴Department of Physics, Saint Louis University, 3450 Lindell Boulevard, Saint Louis, MO
63103, USA

⁵Pacific Biological Station, Fisheries and Oceans Canada, 3190 Hammond Bay Rd,
Nanaimo, BC V9T 6N7, Canada

⁶Group of Research and Education on Marine Mammals, 108 de la Cale Sèche, Tadoussac,
QC G0T 2A0, Canada

Published in Marine Ecology Progress Series in August 2019

doi: 10.3354/meps13043

1.1 ABSTRACT

Foraging efficiency (FE) is determined by the ratio of energy intake to energy expenditure and represents a metric for estimating the capacity to store energy. Blue whales *Balaenoptera musculus* rely mostly on stored energy reserves for reproduction. They feed almost exclusively on krill, which vary in density and abundance both spatially and temporally. We used 10 depth–velocity archival tags deployed on blue whales foraging in the St. Lawrence Estuary, Canada, to identify feeding events. We modeled krill densities required to equal or exceed energy expenditures and allow energy storage. During the daytime, blue whales generally dove deeper and performed fewer but longer feeding dives than at other times of the diel cycle (10 vs. 28 feeding dives h^{-1}); however, they performed more lunges per dive during daytime (3 vs. 1 lunge dive^{-1}), which resulted in a stable feeding rate around the clock. Only 11.7 and 5.5% of the Arctic and northern krill patches measured *in situ* contained densities allowing blue whales to achieve neutral energetic balance (FE = 1); less than 1.5% of patches allowed FE of ≥ 3 . While FE leading to successful reproduction and adequate fitness is unknown, these results underscore the necessity for blue whales to seek the highest densities within patches to reach neutral balance or allow energy storage. These findings further our understanding of blue whale foraging ecology and habitat suitability, and may help predict the effects of climate and natural variability or of potential fisheries on krill densities and blue whale condition.

Keywords: blue whale, *Balaenoptera musculus*, energetics, foraging efficiency, krill density, prey requirements, foraging

1.2 RÉSUMÉ

L'efficacité de recherche de nourriture (FE) est déterminée par le rapport entre l'apport énergétique et la dépense énergétique et représente une métrique pour estimer la capacité de stockage d'énergie. Les rorquals bleus *Balaenoptera musculus* dépendent principalement des réserves énergétiques stockées pour la reproduction. Ils se nourrissent presque exclusivement de krill, dont la densité et l'abondance varient à la fois spatialement et temporellement. Nous avons utilisé 10 enregistreurs de profondeur-vitesse déployés sur des rorquals bleus en quête de nourriture dans l'estuaire du Saint-Laurent, au Canada, pour identifier les événements d'alimentation. Nous avons modélisé les densités de krill nécessaires pour égaler ou dépasser les dépenses énergétiques et permettre le stockage d'énergie. Pendant la journée, les rorquals bleus plongeaient généralement plus profondément et effectuaient moins de plongées mais des plongées plus longues qu'à d'autres moments du cycle de la journée (10 vs 28 plongées · h⁻¹); cependant, ils effectuaient plus de *lunes* par plongée pendant la journée (3 vs 1 *lunge* par plongée), ce qui a entraîné un taux d'alimentation stable tout au long de la journée. Seuls 11,7 et 5,5% des bancs de krill arctique et nordique mesurés *in situ* contenaient des densités permettant aux rorquals bleus d'atteindre un équilibre énergétique neutre (FE = 1); moins de 1,5% des patches permettaient une FE ≥ 3. Bien que l'efficacité d'alimentation conduisant à une reproduction réussie et à une forme physique adéquate soit inconnue, ces résultats soulignent la nécessité pour les rorquals bleus de rechercher les densités les plus élevées dans les agrégations de krill pour atteindre un équilibre neutre ou permettre le stockage d'énergie. Ces résultats approfondissent notre compréhension de l'écologie alimentaire du rorqual bleu et de la qualité de l'habitat, et pourront aider à prédire les effets du climat et de la variabilité naturelle ou issue de pêches potentielles sur les densités de krill et la condition corporelle du rorqual bleu.

Mots clés : rorqual bleu, *Balaenoptera musculus*, énergétique, efficacité d'alimentation, densité de krill, besoins en proies, quête alimentaire

1.3 INTRODUCTION

Marine predators face many obstacles to forage effectively in an environment where food resources most often exhibit a patchy, heterogeneous distribution in 3 dimensions. Diving mammals and birds have the additional constraint of having to regularly return to the water surface to replenish oxygen stores and remove metabolic by-products. They can therefore be considered central-place foragers with the surface as their essential return point (Houston, 1985; Houston and McNamara, 1985). Since they usually feed at depth, they allocate a significant amount of time and energy transiting to and from the surface, and have to factor this into their foraging decision process (Hoskins and Arnould, 2013). A key assumption of the marginal value theorem is that, for a given time spent in a food patch, a predator requires access to higher prey densities when the patch is located further from its central point to offset the greater energy costs of reaching a more distant patch (MacArthur and Pianka, 1966; Charnov, 1976; Piatt and Methven, 1992; Sparling et al., 2007). Central-place foragers should adjust their foraging effort using information acquired while foraging to select strategies that will maximize the energy gained per unit of energy expended (Caraco, 1980; Rosenberg and McKelvey, 1999). This capacity to modulate foraging time, or number of feeding events, with feeding depth or distance from the water surface or colony, has been shown in diving seabirds, pinnipeds, and cetaceans (Boyd, 1996; Doniol-Valcroze et al., 2011; Ware et al., 2011; Watanabe et al., 2014).

In large free-ranging species, it is often difficult to calculate energy expenditure directly, especially since animals routinely engage in a multitude of activities in which each differs in energetic costs (Jeanniard-du-dot et al., 2017a). However, isotopic (doubly-labeled water) or respiratory frequency approaches and, more recently, methods based on acceleration data from biologging devices have enabled estimating energy expenditure in a wide range of large species in relation to their foraging effort (Arnould et al., 1996; Fahlman et al., 2016; Ware et al., 2016). Energy expenditures measured in this way provide a basis as to how much energy animals need to extract from their environment when feeding to at least balance their metabolic costs. Given these metabolic rates, foraging efficiency (FE), i.e. the

ratio between energy gain and energy expenditure, is expected to change with prey encounter rate and density (MacArthur and Pianka, 1966): the higher the prey encounter rate or prey density, the greater the FE. Consequently, FE determines the energy available for the different life-history costs, influencing, for example, reproductive success and by extension population fitness (Costa, 1993; Braithwaite et al., 2015; Jeanniard-du-Dot et al., 2017b, 2018). At $FE = 1$, i.e. the critical prey density threshold, the energy gained balances the energy spent with no energy surplus accumulation. This means that animals are capable of supporting their own growth and maintenance costs, but it is then unlikely that they would have enough energy surplus to allocate to reproduction (Houston et al., 2007).

Marine mammals vary in life-history traits, reproduction strategies, and capacity for energy acquisition and storage (Costa, 1993; Lockyer, 2007). Income breeders need to forage throughout the breeding and nursing periods to provision their offspring adequately. Capital breeders fuel these life functions exclusively through endogenous reserves acquired and assimilated prior to breeding (Jonsson, 1997; Madsen and Shine, 1999; Houston et al., 2007; Wheatley et al., 2008). This means that species on the capital breeding end of the continuum of reproductive strategies rely on sufficient food supplies and resources to store the required fat reserves to maintain their basal body requirements, grow, and fuel reproduction (Brodie, 1975; Costa, 1993; Lockyer, 2007). Poor body condition, when resources are scarce or when the environment is less profitable, lead to low female reproductive success in a number of marine mammal species (Arnould et al., 1996; Braithwaite et al., 2015; Seyboth et al., 2016; Jeanniard-du-Dot et al., 2017b). The capacity to accumulate energy is thus determinant for successful pregnancy and offspring survival, i.e. for individual fitness (Emlen, 1966; Pyke et al., 1977), and therefore for population dynamics. In circumstances where the availability of high-quality food resources is ephemeral or limited to a short time window, predators are expected to adopt strategies that maximize FE and accumulation of surplus energy (Thompson et al., 1993; Jonsson, 1997).

Blue whales *Balaenoptera musculus* are considered capital breeders, as they tend to acquire the critical energy reserves necessary for winter breeding and calving during the

summer foraging period (Schoenherr, 1991; Mate et al., 1999; Lesage et al., 2017a). However, they may not fully fit this classical depiction of the annual cycle of capital breeders, as blue whales may take advantage of locally favorable feeding conditions when migrating (Bailey et al., 2009; Silva et al., 2013; Lesage et al., 2017a). They are air-breathing mammals and thus central-place foragers that feed almost exclusively on aggregations of krill (*Euphausiacea*) (Kawamura, 1980). Krill are heterogeneously distributed both in time and space, such that high-density patches at small scales (tens of km²) are nested within low-density patches at larger scales (thousands of km²) (Watkins and Murray, 1998; McQuinn et al., 2015, 2016). These rapidly changing prey fields require that bulk filter feeders such as blue whales adopt foraging strategies that maximize FE under various scenarios (Goldbogen et al., 2015). A study of the mechanics, hydrodynamics, and energetics of foraging blue whales suggests that they need to target extremely high-density krill patches to forage efficiently (Goldbogen et al., 2011). When they do, they can attain significantly higher FEs than other marine mammals, regardless of prey patch depth (Goldbogen et al., 2011). Blue whales have also been shown to adapt to the variability in prey depth and density by modulating their feeding rate and fine-scale maneuvers (Goldbogen et al., 2015). In the St. Lawrence Estuary in Canada, for instance, blue whales increased foraging time and number of feeding events as feeding depth increased, and fed nearer to the water surface when possible to reduce transit time, following the rules of optimal foraging (Doniol-Valcroze et al., 2011).

The western North Atlantic blue whale population is estimated to be in the low hundreds (Sears and Calambokidis, 2002), and there are concerns that the calving rate might be low in this population (Beauchamp et al., 2009; C. Ramp unpubl. data). A low calving rate could be an indication of poor nutritional state and an incapacity for individuals to accumulate enough energy to carry a pregnancy to term. The Estuary and Gulf of St. Lawrence (EGSL) encompasses important summer feeding habitats for western North Atlantic blue whales. In this region, their diet consists on average of 70% Arctic krill *Thysanoessa raschii* and 30% northern krill *Meganyctiphanes norvegica* (Gavrilchuk et al., 2014). These 2 species vary in patch density, preferred water temperature, and depth of

aggregation, as well as energy content (Plourde et al., 2014b; McQuinn et al., 2015; Cabrol et al., 2019b). Consequently, choosing one or the other will likely affect blue whale foraging energetics and efficiency. Hence, this can impact their capacity to accumulate energy stores to successfully reproduce and survive, and ultimately their population dynamics. The western North Atlantic blue whale population has been listed as ‘endangered’ under the Canadian Species at Risk Act since 2002. Therefore, there is a pressing need to better understand the prey densities that blue whales require not only to maintain homeostasis, but also to accumulate energy for reproduction or other purposes.

The objective of this study was to estimate the krill densities required by blue whales in their environment to meet or exceed energy demands and achieve $FE \geq 1$. We first determined energy requirements of the blue whales using depth-specific foraging effort obtained from archival tag data of previous studies (Doniol-Valcroze et al., 2011, 2012) along with parameters from mechanistic and bio-energetic models (Goldbogen et al., 2011; Potvin et al., 2012). Given these energy expenditures and measurements of krill energy content, we then estimated the krill densities required for different FE scenarios. Lastly, we compared these krill densities to *in situ* acoustically measured krill densities to assess the range of FEs blue whales are likely to reach in this region when feeding on Arctic krill or northern krill. Results will improve our understanding of habitat and prey requirements for these animals and provide insights into potential effects of a warming climate on the quality of one of their main feeding habitats in the western North Atlantic.

1.4 MATERIALS AND METHODS

1.4.1 Tag data and foraging effort

Nine velocity-time-depth recorders (VTDRs Mk8; Wildlife Computers) and 1 digital acoustic recording tag (D-tag; Johnson and Tyack, 2003), along with radio-transmitters, were deployed on blues whales in the St. Lawrence Estuary (SLE, Quebec, Canada, 48° 18' N, 69°

20° W) during August and September of 2002 to 2009. Tags were temporarily attached to whales with suction cups, and deployed from a 5 m rigid-hulled inflatable boat using a hand-held pole or a crossbow. A high-power directional VHF antenna and multiple observers allowed tracking of the whales from a distance (500–1000 m) to minimize boat disturbance. Tagged whales were tracked until nightfall or until tag detachment through the corrosion of a magnesium cap as a suction release system (Doniol-Valcroze et al., 2011, 2012). The swim velocity (measured from a pressure transducer resolution of 0.25 m), diving depth, and water temperature were sampled every second (1 Hz). Estimates of swim speed for the D-tag were obtained from flow noise data (sampling rate 1 Hz) following Goldbogen et al. (2008).

A dive was defined as a vertical excursion below 0.25 m (Doniol-Valcroze et al., 2011, 2012). Lunges or feeding events and depths at which they occurred were identified from swimming speed patterns alone using a robust technique developed by Doniol-Valcroze et al. (2011). This algorithm exploits the abrupt changes in swim speed, characteristic of lunge feeding, occurring during the acceleration phase and subsequent mouth opening (Croll et al., 2001; Goldbogen et al., 2006). Dives including at least 1 feeding attempt were labeled ‘feeding dives.’ Dives with no feeding events were considered ‘non-feeding dives’ and included non-foraging behaviors (e.g. traveling or resting dives), surface breathing, and exploratory dives. Other parameters were also extracted from the dive data, including dive duration and maximum depth, as well as the number of lunges and depths at which they occurred, i.e. depth at which mouth opening was maximum and marked by a sharp decrease in swim speed, for feeding dives.

Given that energetic costs vary between ascending, descending, and lunge feeding, dives were separated into more energetically homogeneous segments. For feeding dives, descent was the period between the start of a dive (i.e. below 0.25 m depth) and the first lunge; ascent was the period following the last lunge but prior to reaching the surface. Transit was the combination of both descent and ascent. Foraging time corresponded to the period between the start of the first lunge and end of the last lunge within a dive. For non-feeding

dives, the period when animals remained within 80 and 100% of their maximum dive depth corresponded to the bottom phase. Descent and ascent preceded and followed this phase.

Foraging effort was examined on an hourly basis and was described in terms of feeding depth, dive duration, and feeding rate. The latter was expressed as the number of lunges h^{-1} , number of feeding dives h^{-1} , and number of lunges $\text{dive}^{-1} \text{h}^{-1}$. We used general additive mixed models (GAMMs) in the ‘mgcv’ package (Wood 2006) in R (v3.3.3; R Development Core Team 2017) to investigate hourly variability in 5 response variables: feeding depth, dive duration, and 3 feeding rate indices, i.e. number of lunges h^{-1} , number of feeding dives h^{-1} , and number of lunges $\text{dive}^{-1} \text{h}^{-1}$. Hour of the day, the only covariate included in the model, was incorporated as a smoothed term using cyclic cubic regression splines ($k = 24$, or 1h^{-1}) and modeled against each of the 5 response variables in separate GAMMs. Individual whales were set as a random effect. Sex was not included as an explanatory variable, as it was unknown for 2 of the 10 tagged whales; including this variable would have resulted in a reduction of an already small sample size. Interannual variations in diving patterns were also not investigated given that only 1 blue whale was tagged per year except in 2004 (4 tagged whales). We assessed the significance of covariates using a likelihood ratio test comparing each model against the null model which included only the random effect. We assessed homogeneity of variances in the models from plots of residuals versus fitted values, and normality of the residuals using quantile-quantile plots and residual histograms. Hourly mean foraging effort was compared among periods of the day using either a Student’s t -test or a Mann-Whitney U -test, depending on normality of the data. Periods of the day were date-specific to account for variations in sunrise and sunset times during the study period. Daytime strictly included daylight hours; dusk and dawn were defined by the nautical twilight times; night included hours after sunset and before sunrise. We pooled dusk, dawn, and night hours together (referred to as ‘nighttime hours’ hereafter) for comparison against daytime hours.

1.4.2 Energy expenditure

Accurate estimates of gross energy expenditure require activity-specific metabolic rates (Jeanniard-du-dot et al., 2017a). These parameters are difficult to measure in free-ranging cetaceans, especially large-sized species such as blue whales. In these species, mass-specific basal metabolic rate (BMR, in $J \cdot s^{-1}$) and active metabolic rate (AMR, in $J \cdot s^{-1}$) have been calculated by scaling values obtained from terrestrial animals and smaller marine mammals (Kleiber 1975; Croll et al., 2001). Recently, Goldbogen et al. (2006) and Potvin et al. (2012) used hydrodynamic and mechanistic models to predict AMR for rorquals. They defined the lunge/filter metabolic rate (hereafter LFMR, in $J \cdot s^{-1}$), which takes into account the extra power required to overcome the drag created by the expanded ventral pouch during the engulfment phase of lunge feeding. Mass-specific BMR, where M represents body mass in kg, was obtained following Kleiber (1975), whereas AMR and LFMR were based on scaled equations of Potvin et al. (2012):

$$\text{BMR} = 2 \times (4 \times M^{0.75}) \quad (1)$$

$$\text{AMR} = 3 \times \text{BMR} \quad (2)$$

$$\text{LFMR} = 1.6 \times \text{AMR} \quad (3)$$

We modeled energy expenditure for each dive, and separately for each dive type (feeding or non-feeding) and dive phase (descent, ascent, bottom, and foraging in the case of foraging dives). Blue whale foraging dives typically consist of a descent where passive gliding occurs on average 40% of the time, one or multiple lunges at depth, and an ascent powered by steady swimming (Goldbogen et al., 2011). Gliding is a key energy-saving strategy for diving marine mammals, the use of which depends on maximum dive depth, dive duration, and body condition of the animals (Williams et al., 2000; Miller et al., 2012; Narazaki et al., 2018) and thus is also expected to occur in non-feeding dives. A study of

diving cost-efficiency indicates that blue whales are negatively buoyant and start gliding at depths of approximately 18 m from the surface when diving at depths of 36 to 88 m (Williams et al., 2000). In our analysis, we considered this strategy as being part of the descent phase for both foraging and non-foraging dives with maximum depths exceeding 18 m. Accordingly, the energy expenditure of non-feeding dives (in kJ) at depths of 18 m or more was calculated as follows:

$$\text{Energy expenditure}_{(\text{non-feeding dive} > 18 \text{ m})} = (0.60 \text{ Descent time} \times \text{AMR} + 0.40 \text{ Descent time} \times \text{BMR} + \text{Bottom time} \times \text{AMR} + \text{Ascent time} \times \text{AMR}) / 1000 \quad (4)$$

The energy expenditure of non-feeding dives (in kJ) shallower than or equal to 18 m was calculated based on total dive duration as follows:

$$\text{Energy expenditure}_{(\text{non-feeding dive} \leq 18 \text{ m})} = (\text{Dive time} \times \text{AMR}) / 1000 \quad (5)$$

The energy expenditure of feeding dives (in kJ) was calculated similarly as for non-feeding dives deeper than 18 m, while accounting for extra costs during the foraging phase:

$$\text{Energy expenditure}_{(\text{feeding dive} > 18 \text{ m})} = (0.60 \text{ Descent time} \times \text{AMR} + 0.40 \text{ Descent time} \times \text{BMR} + \text{Foraging time} \times \text{LFMR} + \text{Ascent time} \times \text{AMR}) / 1000 \quad (6)$$

The energy expenditure of feeding dives (in kJ) shallower than or equal to 18 m was calculated in a similar way as for feeding dives deeper than 18 m, except without taking gliding into consideration:

$$\text{Energy expenditure}_{(\text{feeding dive} \leq 18 \text{ m})} = (\text{Descent time} \times \text{AMR} + \text{Foraging time} \times \text{LFMR} + \text{Ascent time} \times \text{AMR}) / 1000 \quad (7)$$

Potvin et al. (2012) calculated specific metabolic rates for different phases of a lunge (prey approach, engulfment, filtering) through biomechanical and hydrodynamic modeling. Engulfment is the costliest part of a lunge but only accounts for approximately 6% of the total lunge duration; the prey approach/filter metabolic rates and LFMR are of the same order of magnitude. The limited number of tag sensors prevented us from obtaining the kinematic details needed to apply specific metabolic rate to filtration, engulfment, and prey approach times. The application of LFMR to the entire foraging time during a dive was a reasonable assumption when calculating foraging costs over extended periods of time that included multiple lunges and dives, as it balanced the overestimated costs of filtering with the underestimated costs of lunging. To reflect changes in metabolic rate with body size, energy expenditure was calculated for 3 body lengths, i.e. 22, 25 and 27 m. These values reflect the size of sexually mature blue whales from the northern hemisphere (21–23 m for females, approximately 22 m for males; Sears and Calambokidis, 2002), and are within the range of the maximum of 27 m documented for the North West Atlantic Ocean (Sears and Perrin, 2009).

The relationship between energy expenditure and dive duration, maximum dive depth, and number of lunges was examined using linear mixed effects (LME) models in the ‘nlme’ package in R (Pinheiro et al. 2013) and checked for model assumptions, with individual whales as a random effect. We examined potential temporal variation in hourly energy expenditure with GAMMs, using the approach and validation process described previously.

1.4.3 Krill density requirements

Depth-specific foraging effort and linked energy expenditure while foraging in the SLE were used to estimate the krill densities required by blue whales to meet or exceed energy demands and thus build energy reserves. A key assumption of our approach is that the foraging effort observed in the 10 tagged individuals is assumed to represent the best strategies chosen by the animals and adapted to the foraging conditions for that depth and

time of day. We estimated krill density requirements ($\text{g wet weight} \cdot \text{m}^{-3}$; hereafter, all weights indicated are wet weights, unless otherwise noted) for i , the i^{th} hour, using energy expenditure (from Eqs. 4–7), and a set of fixed FEs (i.e. 1, 2, 3, 4):

$$\text{Krill density}_i = \frac{\text{Foraging Efficiency}_i \times \text{Energy Expenditure}_i}{\text{Ve} \times \text{Feeding rate}_i \times \text{Kec} \times \text{Ae} \times \text{Sr}} \quad (8)$$

where Ve is the volume of engulfment (in m^3), feeding rate is estimated by the number of lunges h^{-1} , Kec is the krill energy content ($\text{kJ} \cdot \text{g}^{-1}$), Ae is the assimilation efficiency, and Sr is success rate (see Table 1 for specific values). An FE of 1 indicates a neutral balance between gross energy intake and expenditure, and represents the theoretical krill density threshold below which foraging is no longer beneficial. Efficiencies above 1 indicate a capacity to build energy reserves. We used the FE ratio, i.e. the ratio between energy intake and energy expenditure, for each time bin (i) of 1 h as the starting point of our estimations (Goldbogen et al., 2011):

$$\text{Foraging Efficiency}_i = \frac{\text{Energy Intake}_i}{\text{Energy Expenditure}_i} \quad (9)$$

We calculated energy expenditure (kJ) from the dive data using the procedure outlined above. Energy intake (in kJ) needed to be estimated using information on a number of variables, including the number of lunges h^{-1} (feeding rate), volume of engulfment in m^3 (Ve), krill density in $\text{g} \cdot \text{m}^{-3}$, krill energy content in $\text{kJ} \cdot \text{g}^{-1}$ (Kec), the assimilation efficiency (Ae), and success rate (Sr) using the following equation (Goldbogen et al., 2011):

$$\text{Energy intake}_i = \text{Ve} \times \text{Feeding rate}_i \times \text{Krill density} \times \text{Kec} \times \text{Ae} \times \text{Sr} \quad (10)$$

Krill densities estimated in Eq. (5) represented the density required to cover the cost of any feeding and non-feeding dives performed during each 1 h time bin i (i.e. $FE = 1$) or the density required to cover these costs and to store surplus energy (i.e. $FE > 1$). We ran Monte Carlo simulations to estimate krill density requirements while incorporating uncertainty of input parameters. Uncertainties around each input parameter were either data-driven or taken from the literature, and were described with sampling distributions that best captured the inherent variability associated with biological data (Table 1). Parameter values were randomly drawn from their assigned distributions in each model iteration. Sets of 10 000 iterations were run for each of the defined FEs, for each whale length, and for each hour of the day to obtain a mean, standard deviation (SD), and a 90% confidence interval (CI) around estimated krill density requirements.

Energy expenditure h^{-1} and feeding rate (number of lunges h^{-1}) were fitted with gamma distributions for each hour of the day. A gamma distribution is well suited for highly variable, continuous, and strictly positive data. However, the gamma distribution of feeding rates needed to be constrained between 1 lunge and a maximum of 60 lunges h^{-1} for physiological consistency, since a lunge lasts between 60 and 98 s (Goldbogen et al., 2006, 2008, 2011; Potvin et al., 2012). The upper bound of the gamma distribution of energy expenditure was constrained to a cost equivalent to 60 lunges. Distributions for both parameters were defined by shape and scale parameters, which were parameterized from the mean and SD with shape = $mean^2/SD^2$ and scale = $SD^2/mean$. Engulfment volume is allometric to body length (Potvin et al., 2010; Goldbogen et al., 2012) and was calculated for the 3 selected body lengths following Potvin et al. (2012) (Table 1).

Assimilation efficiency was assumed to be uniformly distributed from 0.84 to 0.93 (Table 1). The assimilation efficiency of 0.84 from (Lockyer, 1981, 2007) has been commonly used in studies on rorqual FE (Goldbogen et al., 2011). The highest value (0.93) was based on digestive efficiency documented for krill in minke whales *Balaenoptera acutorostrata* (Mårtensson et al., 1994).

Arctic krill *Thysanoessa raschii* and to a lesser extent *T. inermis* represent up to 70% of blue whale diet in the EGSL, the rest being northern krill *Meganyctiphanes norvegica* (Gavrilchuk et al., 2014). Arctic krill are generally found higher in the water column and form denser patches than northern krill in this ecosystem (McQuinn et al., 2015). Krill density requirements were modeled assuming a 100% diet of either Arctic or northern krill. Species-specific energy content was obtained by bomb calorimetry ($\text{kJ} \cdot \text{g}^{-1}$) (Phillipson, 1964) using krill sampled in the EGSL during the blue whale feeding period, i.e. from May to September. A normal distribution was fitted to the data to represent all krill body lengths, life stages, and seasonal changes of lipid content Table 1).

Prey capture success rate is difficult to measure in free-ranging animals, and has yet to be measured for bulk filter feeders like rorquals. The feeding techniques exhibited by blue whales suggest a high degree of specialization to maximize prey capture and minimize the escape of individual krill. For example, the rolling behavior of blue whales (Goldbogen et al., 2013a) is thought to be a way of anticipating the escape response of krill (Potvin et al., 2012) and maximizing prey capture. Considering the speed at which a whale lunges (Potvin et al., 2010) and documented feeding maneuvers (Goldbogen et al., 2013a; Cade et al., 2016), krill escapement was assumed negligible and therefore krill capture success rate was assumed to be 1.

We assessed hourly variations of krill density requirements using a generalized additive model (GAM) in the ‘mgcv’ package in R (Wood 2006). Cyclic cubic regression splines were applied to the temporal variable, i.e. hour of the day. Model selection was done using a likelihood ratio test comparing our model against the null model. Equal variance and normality of the residuals were assessed through scatter plots of residuals versus fitted values, quantile-quantile plots, and residual histograms. Model sensitivity to uncertainty in input parameters was explored for each parameter using a partial correlation coefficient sensitivity analysis and the ‘pcc’ function of the R package ‘sensitivity’ (Pujol et al. 2016). This method accounted for the correlation between feeding rate and energy expenditure. Data analysis was conducted under the R programming language (R Development Core Team 2017).

Table 1 : Input parameters, associated sampling distributions and/or values (mean \pm SD where applicable) and data sources for estimating blue whale krill density requirements. na: not applicable.

Parameter	Description (units)	Value	Distribution	Source
FE	Foraging efficiency	1, 2, 3, 4	Fixed parameter	
Energy expenditure_i	Size-specific energy expended (kJ · h ⁻¹)	Hour-specific	Gamma	Tag data, this study
Feeding rate_i	Number of lunges h ⁻¹	Hour-specific	Gamma	Tag data, this study
Ve	Length (<i>L</i>)-specific engulfment volume (m ³)	(1.023 × <i>L</i> ^{3.65}) / 1025	na	(Goldbogen et al., 2010)
M	Length-specific body mass (kg)	61318 (22 m), 96568 (25 m), 122605 (27 m)	na	(Croll et al., 2001)
Kec_{tr}	Krill energy content (kJ · g ⁻¹ wet weight) <i>Thysanoessa raschii</i>	4.3 ± 0.58	Normal	D. Chabot (unpubl. data), V. Lesage (unpubl. data)
Kec_{mn}	Krill energy content (kJ · g ⁻¹ wet weight) <i>Meganyctiphanes norvegica</i>	5.2 ± 0.45	Normal	D. Chabot (unpubl. data), V. Lesage (unpubl. data)
Ae	Assimilation efficiency	0.84–0.93	Uniform	(Martensson et al., 1994; Olsen et al., 2000; Goldbogen et al., 2011)
Sr	Success rate	1	Fixed	

1.4.4 Preyscape: *in situ* krill densities

Hydroacoustic data were collected during surveys conducted between 2009 and 2015 in the EGSL (Quebec, Canada, 49° 43' N–65° 11' W) (Table 2). Data were recorded during daytime using a calibrated (Demer et al., 2015) Simrad® EK60 multifrequency echosounder (38, 70, 120, and 200 kHz). Systematic hydroacoustic sampling was performed whenever blue whales were present and repeatedly seen (but not tagged) by trained onboard marine mammal observers. Sampling was either in the form of a rectangular ‘spiral’ (concentric lines of increasing distance and length from the center starting point; see Figure 15a in Supplementary information) or a ‘grid’ (parallel equidistant lines; Figure 15b in Supplementary information) of ~0.5 km spacing grid size. Both designs, totaling 8 to 128 km² of sampled area, provided adequate spatial resolution to characterize the krill patches.

Table 2 : Summary of ‘grids’ and ‘spirals’ (see Figure 15 in Supplementary information) from hydroacoustic surveys used for krill patch characterization. GSL: Gulf of St. Lawrence; SLE: St. Lawrence Estuary.

Survey	Location	Year	Type	Area covered (km ²)	Number of lines
C1522	GSL	2015	Grid	16	6
			Spiral	14	7
C1410	GSL	2014	Grid	24	4
C1223	GSL	2012	Spiral	8	3
			Spiral	38	3
			Grid	60	5
			Grid	16	3
C0962	SLE	2009	Grid	64	6
			Grid	126	6
			Grid	128	10

Hydroacoustic data were edited to remove non-biological echoes and noise from the surface to the seabed reflection. We echo-integrated data into high-definition bins of 3 pings on the horizontal axis by 0.5 m depth on the vertical axis. Acoustic classification of prey was done using species-specific multifrequency algorithms developed for the western GSL

(McQuinn et al., 2013). Biological echoes were classified between the 2 species of krill, namely Arctic and northern krill.

We used the classified volume backscattering coefficient (S_v in $\text{m}^2 \cdot \text{m}^{-3}$) and its logarithmic form, mean volume backscattering strength (MVBS or S_v in dB re $1 \text{ m}^2 \cdot \text{m}^{-3}$) to infer species-specific krill density (g m^{-3}) for each echo-integrated bin. Krill biomass density was calculated using a weight-based target strength (TS_W) function:

$$\text{TS}_W = \text{TS}_N - 10\text{Log}(W) \quad (11)$$

where W is the mean wet weight (g) of an individual krill (i.e. 56.2 and 298 mg for Arctic and northern krill, respectively). TS_N is the length-based modeled target strength (McQuinn et al., 2013) for each species assuming average length, and TS_W is -70.0 and -69.0 dB $\cdot \text{g}^{-1}$ for Arctic krill and northern krill, respectively. From this relationship, krill density (D_k) was calculated as:

$$D_k = S_v / 10^{(\text{TS}_W / 10)} \quad (12)$$

To account for the anisotropy of krill distribution in relation to the shoreline (Simard and Lavoie, 1999; McQuinn et al., 2015), only transects perpendicular to the slope were used in the estimation of patch density and distribution. We used a threshold of $4 \text{ g} \cdot \text{m}^{-3}$ to discriminate between weakly aggregated krill, which includes empty bin cells, and aggregated krill patches (McQuinn et al., 2015). For each grid or spiral sampled, the mean, maximum, minimum, and quantiles of krill densities ($\text{g} \cdot \text{m}^{-3}$) were used to describe the vertical distributions of bins containing aggregated Arctic and northern krill. For each patch, estimated *in situ* krill densities during daytime were compared to those modeled for the same period, while estimating the percentage of density bins that exceeded each FE threshold. This analysis allowed us to determine the likelihood of a blue whale finding and exploiting krill

patches meeting the different FE thresholds, as well as the potential FE that a blue whale is likely to reach when foraging in the EGSL.

1.5 RESULTS

The 9 VTDR and the 1 D-Tag deployed on blue whales provided data for 2 to 25 h (average 13 h), and a total of 139 h. Tagging efforts were initiated early after sunrise but tags were often only successfully deployed later in the day. As a result, data were unevenly distributed during the day, with a larger coverage of the period between noon and sunset compared with early in the day (Figure 16 in Supplementary information). Feeding dives ($N = 1718$) were recorded from all whales, although some variability in feeding activity was noted among individuals. Whales performed on average (\pm SD) 172 ± 147 feeding dives and 271 ± 203 lunges during the tracking period, but these numbers varied from 9 to 390 feeding dives and from 40 to 576 lunges. Another 4115 dives corresponded to the shallow dives performed in-between surface breaths, i.e. inter-breath intervals (average per whale: 412 ± 331 ; range: 57–972), and 844 dives (average per whale: 85 ± 68 ; range: 3–196) corresponded to underwater behaviors other than feeding.

1.5.1 Hourly foraging effort and energy expenditure

Significant diel variations were detected in feeding depth, feeding dive duration, number of feeding dives h^{-1} , number of lunges dive^{-1} , and number of lunges h^{-1} (Fig.1, Table 3). Generally, blue whales fed at deeper depths (Mann-Whitney $U = 143$, $p < 0.0001$) and performed longer dives during daytime compared to nighttime (including dusk, night and dawn, Mann-Whitney $U = 141$, $p < 0.0001$; Figure 9, Table 4). Feeding dives were 2.5 times less frequent during daytime (Student's t -test, $df = 21$, $p < 0.0001$), but had 3 times more lunges than dives performed during nighttime (Student's t -test, $df = 21$, $p < 0.0001$).

However, when examined on an hourly basis (thus including transit and surface times), feeding rate expressed as the number of lunges per hour was approximately 25% less during daytime compared to nighttime (Figure 9).

Energy expenditure during feeding dives increased significantly (LMEs, all $p < 0.05$) with maximum dive depth, dive duration, and the number of lunges d^{-1} , but more rapidly as whale size increased (i.e. steeper slope for the relationship; Figure 10). However, when examined on an hourly basis rather than a dive by dive basis, energy expenditure remained relatively unchanged throughout the day (edf = 22; $F = 0$, $p = 0.48$), with an average 455206 ± 111604 kJ expended during daytime hours vs. 456583 ± 95112 kJ during nighttime (Figure 11).

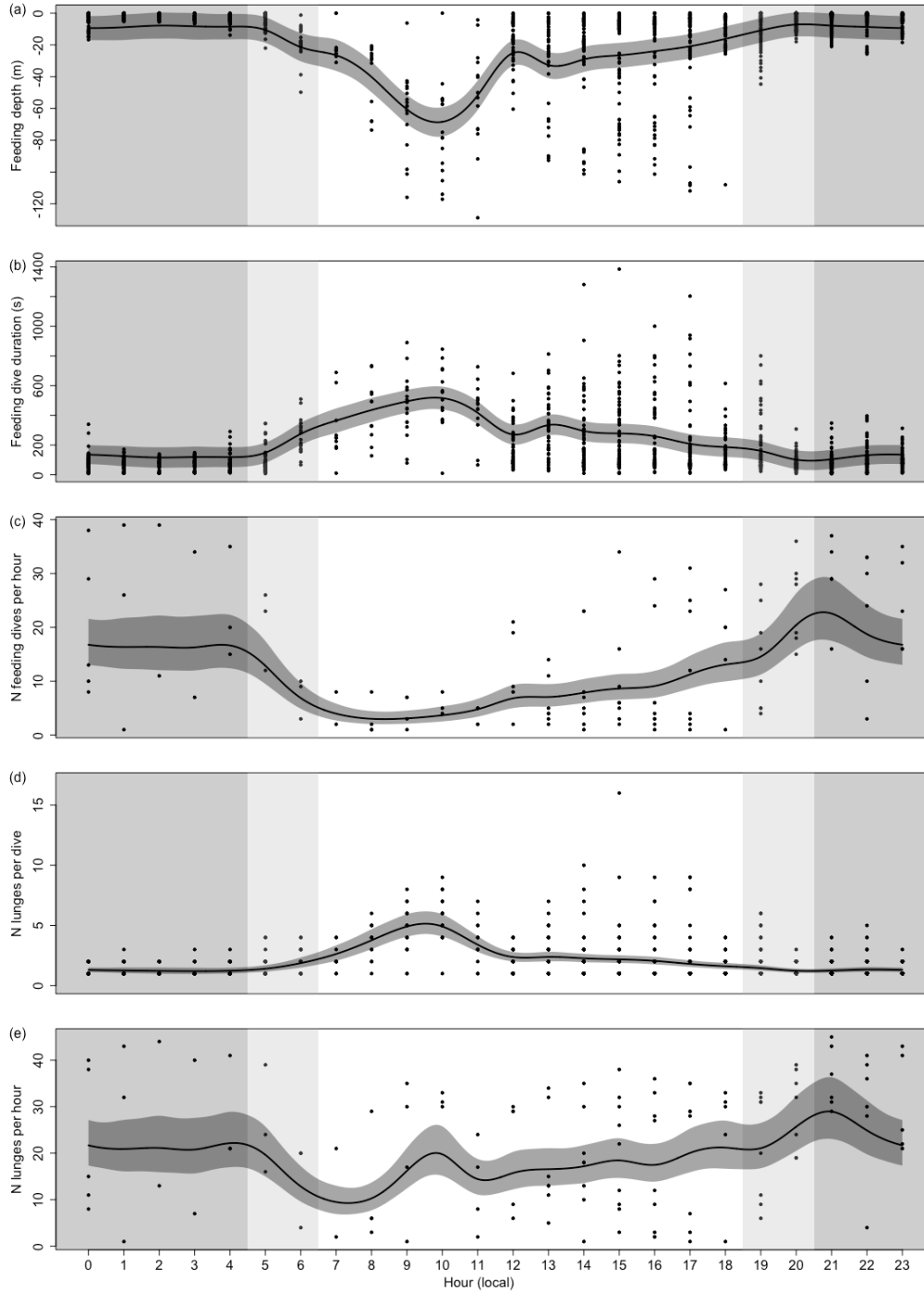


Figure 9 : Predicted change in blue whale foraging effort with time of day in (a) feeding depth (m), (b) dive duration (s), (c) number of feeding dives, (d) number of lunges d^{-1} , and (e) number of lunges h^{-1} . Dark grey ribbons represent the 95% confidence intervals around the predicted response from generalized additive mixed models. Shaded areas are for nighttime (grey), dusk and dawn (light grey), and daytime (white). Points are data observations. (See Table 3 for full statistical results).

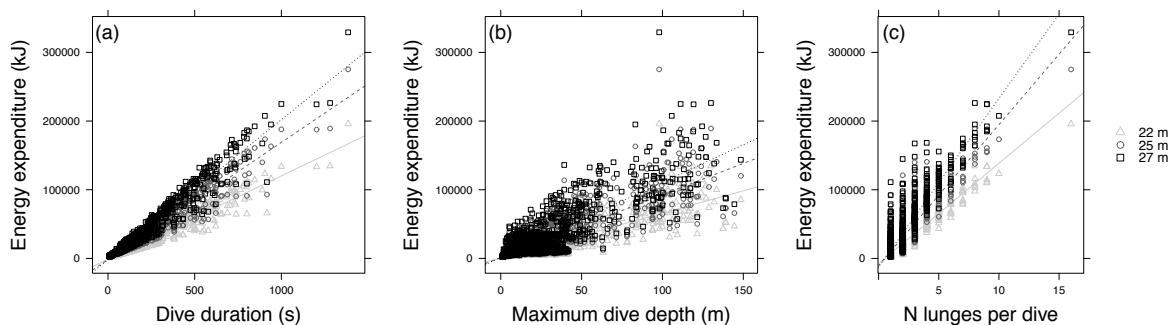


Figure 10 : Relationship between energy expenditure during feeding dives for 3 blue whale sizes (22, 25, and 27 m length) and (a) dive duration (s) (mean \pm SE slope for 22 m: 122 ± 0.6 ; 25 m: 171 ± 0.9 ; 27 m: 205 ± 1), (b) maximum dive depth (m) (22 m: 650 ± 11 ; 25 m: 914 ± 15 ; 27 m: 1093 ± 19) and (c) number of lunges per dive (22 m: 14265 ± 148 ; 25 m: 20054 ± 210 ; 27 m: 23986 ± 252). Relationships were modeled using linear mixed models (all $p < 0.05$).

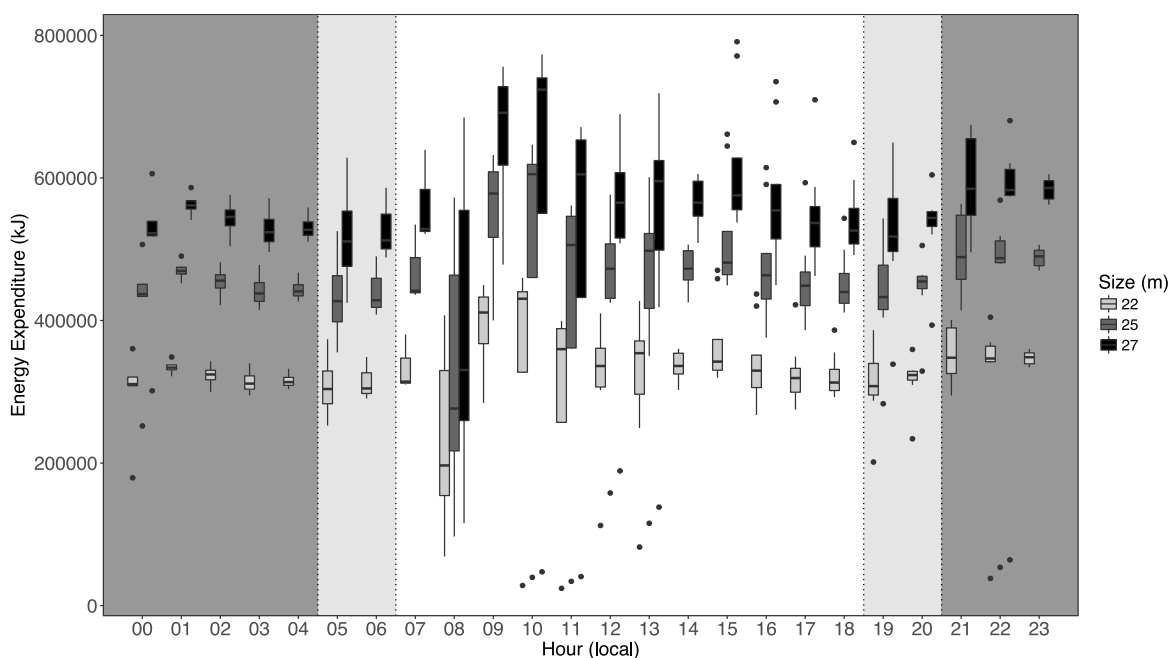


Figure 11 : Diel distribution of energy expenditure for a 22, 25, and 27 m blue whale. Box plots present the median (solid horizontal line), lower and upper quartiles (boxes), extreme values (whiskers) and outliers (points). Shaded areas are for nighttime (dark grey), dusk and dawn (light grey), and daytime (white). The large confidence interval at 08:00 h is a combination of natural variability among individuals in feeding effort and small sample size ($n = 4$).

Table 3 : Trends in various indices of foraging effort with time of day, based on generalized additive mixed model (GAMM) results, and using individual blue whale as a random effect. Results (p -values) of the likelihood ratio test (LRT) for model selection against the null model (random effect only) are also presented; edf: estimated degrees of freedom.

Response variable	N	Adjusted R ²	p	edf	F	LRT
Feeding depth (m)	1718	0.385	<0.001	18.3	44.4	<0.0001
Feeding dive duration (s)	1718	0.316	<0.001	16.9	34.9	<0.0001
Total number of feeding dives	137	0.267	<0.001	12.8	19.7	<0.0001
Number of lunges per feeding dive	1718	0.282	<0.001	11.3	16.3	<0.0001
Total number of lunges	137	0.087	<0.001	14.7	11.4	<0.0001

Table 4 : Characteristics of feeding dives and feeding rates (mean \pm SD) during daytime vs. nighttime. Nighttime includes dusk, night, and dawn. Statistical differences (Mann-Whitney U -test and Student's t -test) are indicated with an asterisk ($*p < 0.05$).

Parameter	Day	Night
Feeding depth (m) *	39.8 \pm 19.6	4.9 \pm 3.1
Feeding dive duration (s) *	371.9 \pm 115.8	95.8 \pm 44.8
No. of feeding dives h ⁻¹ *	9.9 \pm 4.7	27.9 \pm 4.2
No. of lunges per feeding dive *	3.1 \pm 1.2	1.3 \pm 0.2
No. of lunges h ⁻¹ *	23.2 \pm 4.7	30.6 \pm 4.1

1.5.2 Krill density requirements

Krill density requirements for feeding blue whales varied depending on time of day, but in a similar fashion when feeding on Arctic krill or northern krill (Figure 12, Table 5). Density requirements tended to be higher in the early morning than at other times of day or night; this corresponded to the period when whales were diving deeper and for longer, and were performing a larger number of lunges dive⁻¹ (Figures 9d & 13). Globally, krill densities

that a 25 m blue whale required to balance energy expenditures were higher during daytime feeding than at night, and when feeding on Arctic krill rather than on northern krill (Mann-Whitney $U = 50085 \times 10^5$ and 20428×10^6 ; both $p < 0.0001$; Figures 12 & 13). Mean \pm SD density requirements were $40.9 \pm 49.8 \text{ g m}^{-3}$ for Arctic krill and $33.3 \pm 39.3 \text{ g} \cdot \text{m}^{-3}$ for northern krill, when feeding during daytime, compared to 31.7 ± 38.1 and $25.8 \pm 31.0 \text{ g} \cdot \text{m}^{-3}$, respectively, when feeding at nighttime (including night, dusk, and dawn; Figure 13).

Krill densities need to be considerably higher in order for blue whales to reach higher FEs and accumulate reserves (Kruskal-Wallis test, $df = 3$, $p < 0.0001$; Figure 13). For instance, median required Arctic krill densities, which varied for a 25 m whale from 14 to $40 \text{ g} \cdot \text{m}^{-3}$ depending on time of day, would need to increase to 56–159 $\text{g} \cdot \text{m}^{-3}$ for this whale to reach an FE of 4 (Figure 13a). The predicted required krill density of northern krill for a 25 m blue whale to balance its energy expenditures (FE = 1) followed similar patterns as for Arctic krill, and ranged from a median of 11 to $33 \text{ g} \cdot \text{m}^{-3}$ depending on time of day (Figure 13b). To achieve an FE of 4, northern krill median densities would need to reach values ranging from 46 to $131 \text{ g} \cdot \text{m}^{-3}$ depending on time of day (Figure 13b). These results indicate that while krill density requirements varied similarly with FE among the 2 krill species, higher densities were required when feeding on the smaller, and energetically less rewarding, Arctic krill than northern krill. Density requirements according to FE and krill species followed a similar pattern for a 22 or 27 m whale as for a 25 m whale, but were offset as a result of the positive allometric scaling of engulfment volume with whale size (Figure 17 in Supplementary information).

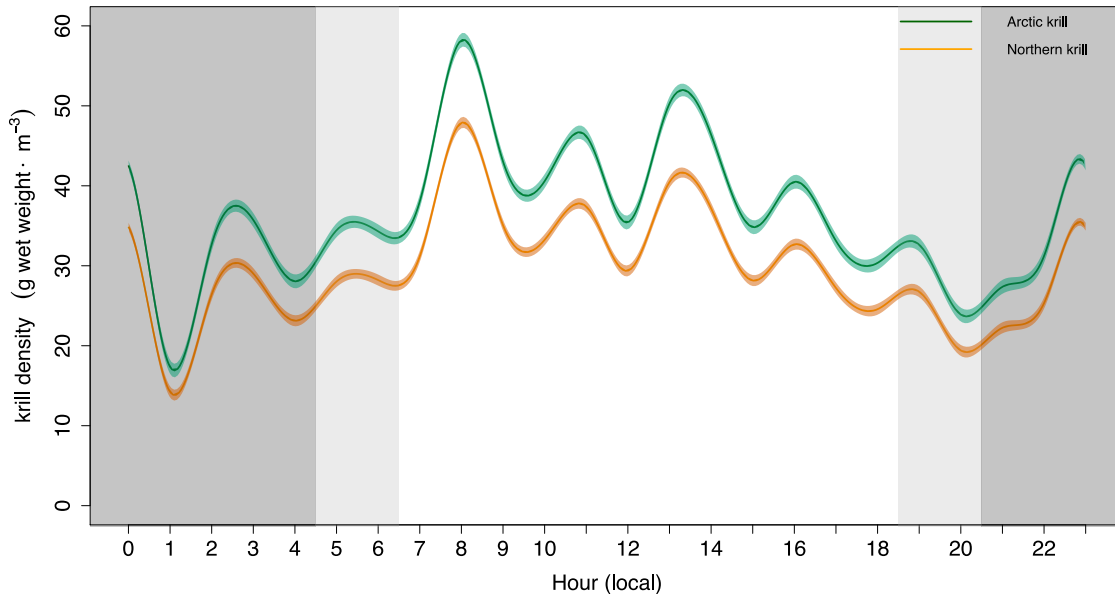


Figure 12 : Diel variation in the predicted response of estimated krill density required for a foraging efficiency of 1 by blue whales feeding on Arctic and northern krill. The y-axis represents the predicted response from generalized additive models on the mean krill density (solid line), including the 95% confidence intervals (ribbons). Shaded areas are for nighttime (dark grey), dusk and dawn (light grey), and daytime (white). (See Table 5 for full statistical results).

Table 5 : Trends in required density for Arctic and northern krill at various foraging efficiencies (FE = 1 to 4) with time of day based on generalized additive model results. N = 24000 simulations for each model. Results (p -values) of the likelihood ratio test (LRT) for model selection against the null model (random effect only) are also presented.

Response variable	Adjusted R ²	p	edf	F	LRT
Arctic krill density					
FE = 1	0.036	0.001	21.95	417.6	<0.0001
FE = 2	0.039	0.001	21.95	445.2	<0.0001
FE = 3	0.039	0.001	21.95	446.5	<0.0001
FE = 4	0.040	0.001	21.95	457.6	<0.0001
Northern krill density					
FE = 1	0.040	0.001	21.94	458.9	<0.0001
FE = 2	0.039	0.001	21.95	449.3	<0.0001
FE = 3	0.040	0.001	21.95	457.4	<0.0001
FE = 4	0.037	0.001	21.95	428	<0.0001

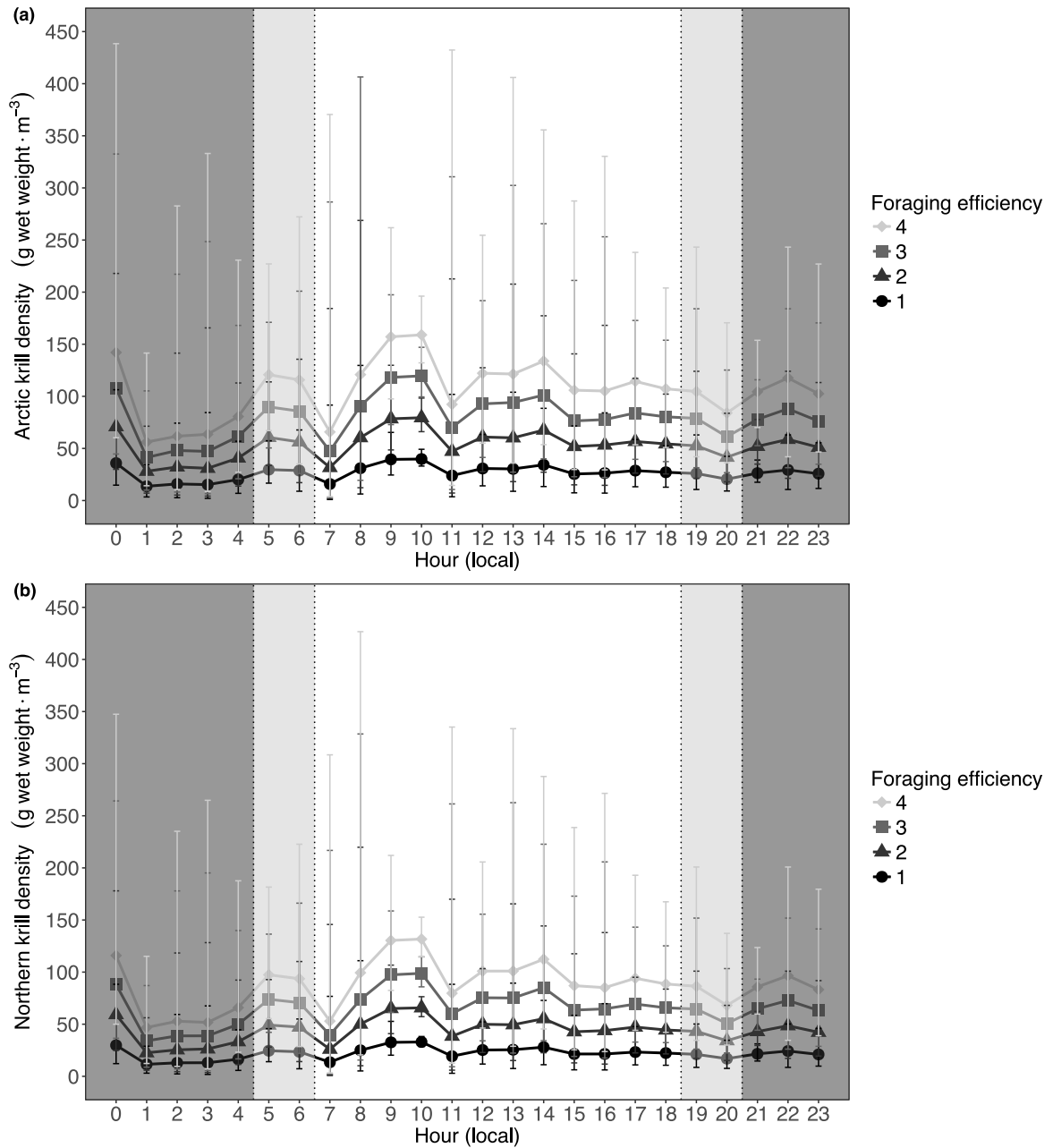


Figure 13 : Diel distribution of densities of (a) Arctic krill and (b) northern krill required by a 25 m blue whale feeding at foraging efficiencies varying from 1 to 4. Curves and bars represent the median and 90% confidence interval, respectively. Shaded areas are for nighttime (dark grey), dusk and dawn (light grey), and daytime (white).

The sensitivity analysis highlighted the feeding rate (number of lunges h^{-1}) and energy expenditure as the largest contributors to the uncertainty in predicted krill density requirements (Table 6).

Table 6: Standardized regression coefficients (SRC), minimum and maximum 95% confidence intervals, biases and standard errors of the partial sensitivity analysis of the parameters used in Monte Carlo simulations. The largest contributors to the uncertainty in predicted krill density requirements are indicated in bold.

Parameter	SRC	95% CI		Bias	SE
		Min.	Max.		
Success rate	-0.002	-0.025	0.004	2.8×10^{-3}	0.010
Assimilation efficiency	-0.020	-0.038	-0.001	-8.6×10^{-5}	0.009
Krill energy content ($\text{kJ} \cdot \text{g}^{-1}$ wet weight)	-0.103	-0.124	-0.081	-3.5×10^{-5}	0.011
Feeding rate (no. of lunges h^{-1})	-0.503	-0.520	-0.484	-5.5×10^{-4}	0.009
Energy expenditure (kJ)	0.480	0.463	0.499	3.8×10^{-4}	0.009
Volume engulfed (m^3)	0.002	-0.005	0.025	-2.2×10^{-3}	0.010

1.5.3 *In situ* krill preyscape

Ten ‘spirals’ or ‘grids’ were performed during hydroacoustic krill surveys when blue whales were seen but not tagged. They were made between mid-May and the end of August in the EGSL (specifically in the SLE and the Gaspé Peninsula regions). Daytime vertical distributions for both krill species and for each survey are shown in Figure 18 in Supplementary information. Generally, Arctic krill was located higher (50–110 m) in the water column than northern krill (100–150 m). Densities of Arctic krill were more uniformly distributed across depths than northern krill, which showed a spikier pattern (Figure 18 in Supplementary information). Depth-specific mean densities of Arctic krill ranged from 4 to $50 \text{ g} \cdot \text{m}^{-3}$ across surveys, with the 99th percentile reaching 4 to $250 \text{ g} \cdot \text{m}^{-3}$ depending on the

survey. Depth-specific mean densities of northern krill varied across a wider range of values among surveys, with densities varying from 4 to $76 \text{ g} \cdot \text{m}^{-3}$; however, northern krill reached similar maximum densities as Arctic krill, with 99th percentiles varying from 4 to $260 \text{ g} \cdot \text{m}^{-3}$ depending on the survey.

Among krill patches ($4 \text{ g} \cdot \text{m}^{-3}$ or above) detected during these 10 surveys, an average \pm SD of $11.7 \pm 13.0\%$ of those comprised of Arctic krill and $5.5 \pm 7.4\%$ of those comprised of northern krill contained bins ($3 \text{ pings} \times 0.5 \text{ m}$ deep) that just met the densities required for a 25 m blue whale to achieve neutral energetic balance ($\text{FE} = 1$; Figure 14). Only $1.7 \pm 2.5\%$ of Arctic krill patches and $2.1 \pm 3.4\%$ of northern krill patches allowed blue whales to forage with an efficiency of 2, and less than 1.5% allowed blue whales to reach $\text{FE} \geq 3$ (Figure 14).

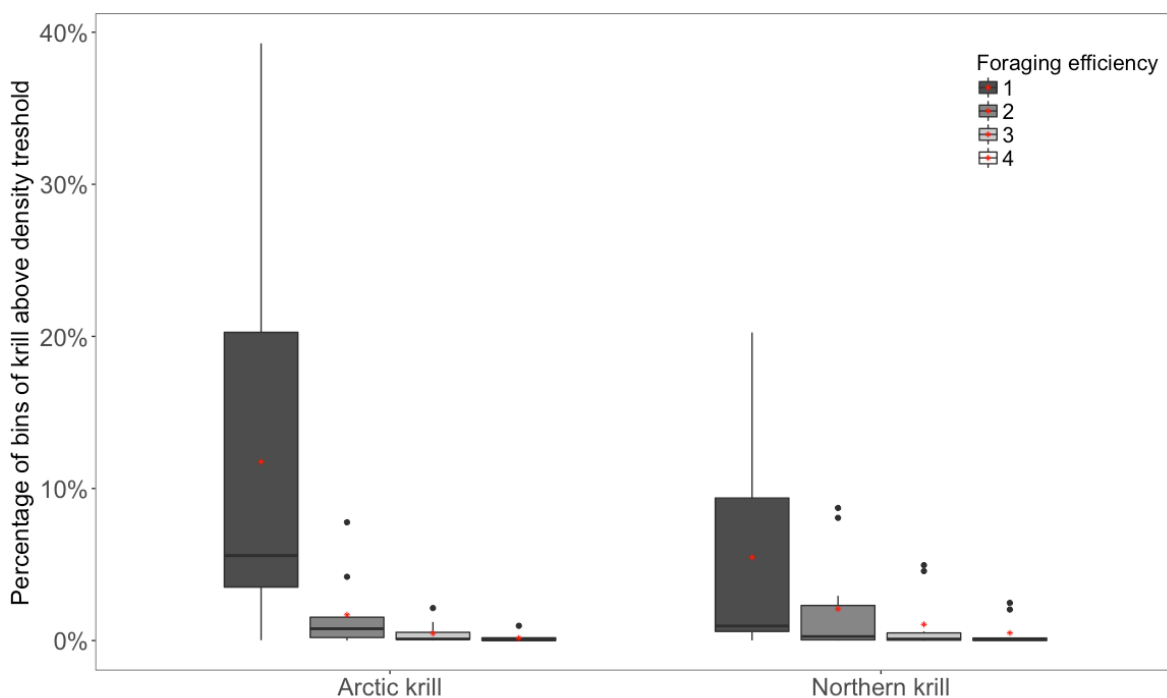


Figure 14 : Percentage of krill patches with $3\text{-ping} \times 0.5 \text{ m}$ bins dense enough to allow blue whales to forage with efficiencies of 1 to 4 on Arctic krill and northern krill during daytime. Estimated krill density requirements ($\text{g wet weight} \cdot \text{m}^{-3}$) were used as thresholds for foraging efficiencies of 1–4. For Arctic krill, mean estimates were 29, 57, 86, and $113 \text{ g} \cdot \text{m}^{-3}$, respectively; for northern krill, these values were 24, 47, 70 and $94 \text{ g} \cdot \text{m}^{-3}$, respectively. Means are represented by a red dot. Boxplots present the median (solid horizontal line), lower and upper quartiles (boxes), extreme values (whiskers) and outliers (points).

1.6 DISCUSSION

Prey density is the main driver of foraging effort, which together determine the FE at which an animal forages (MacArthur and Pianka, 1966). For capital breeders, maximizing FE allows maximizing energy storage to fuel survival, growth, and reproduction (Costa, 1993). We used foraging effort inferred from biologging data and the resulting energy expenditures to estimate krill density requirements of blue whales foraging in the EGSL. Our study indicated that blue whales modulate their foraging effort throughout the day while maintaining stable energy expenditures. We estimated that during daytime, blue whales require minimum mean krill densities of 40.9 and 33.3 $\text{g} \cdot \text{m}^{-3}$ depending on whether they feed on Arctic krill or northern krill. At night, they require lower mean densities of these 2 species to achieve this state, i.e. 31.7 and 25.8 $\text{g} \cdot \text{m}^{-3}$, respectively. *In situ* measures of krill densities suggest that blue whales only sporadically find krill patches that allow for energy storage.

1.6.1 Hourly foraging effort and energy expenditure

The distribution of predators, and variations in their foraging effort throughout the day, likely reflect changes in the diel vertical distribution, density, and accessibility of their prey (Croll et al., 2005). For example, penguins adjust their residency time in a food patch according to their rate of energy gain (Watanabe et al., 2014), while krill-feeding humpback whales in Antarctica track the diel vertical migration of their prey and adjust their foraging effort accordingly (Friedlaender et al., 2016). In the latter study, humpback whales exhibited a higher number of lunges dive^{-1} during daytime when feeding at depth than at night when feeding closer to the surface (Friedlaender et al., 2013, 2016), a similar pattern to what was observed in blue whales foraging in the SLE (Doniol-Valcroze et al., 2011; this study). Blue whales optimize FE by adjusting their foraging behavior according to vertical distributions and densities of krill (Hazen et al., 2015). In the northern Pacific Ocean, blue whales either

feed close to the surface and breathe more often (thereby decreasing the risk of costly anaerobic metabolism as well as optimizing oxygen replenishment time) in low-density krill patches or increase their rate of energy gain in high-density krill patches by increasing the number of lunges dive^{-1} (Hazen et al., 2015). Blue whales in the SLE follow a similar pattern and increase the number of lunges dive^{-1} when feeding at increasingly deeper depths (Doniol-Valcroze et al., 2011).

Longer and deeper dives with several lunges are energetically more costly than shallower dives with a single mouthful (Acevedo-Gutiérrez et al., 2002; this study). Considering that hourly foraging effort exhibited by blue whales varied throughout the day, the associated hourly energy expenditure was expected to follow the same pattern. We had thus hypothesized that blue whale shallow feeding at night would reduce energy costs of transit, and result in lower hourly energy expenditures at that time of day. However, while significant diel variations were noted in hourly foraging effort, overall the average energy expenditure remained stable throughout the day, leading us to reject our initial hypothesis. This relative stability in energy expenditure on an hourly basis was the result of the extra cost of diving deeper during daytime being counterbalanced by the combination of the increase in feeding rate at night and the high energetic cost of lunging. By modulating feeding rate (e.g. number of feeding dives h^{-1} and number of lunges h^{-1}) and the number of lunges dive^{-1} according to feeding depth, blue whales were able to achieve a nearly constant hourly energy expenditure. This means that blue whales can maximize net energy intake and FE by intensifying foraging when and where the energy return is expected to be the highest, i.e. at higher prey densities or shallower depths.

Unlike blue whales in the Pacific Ocean, which are known to feed at depths up to 250–300 m (Goldbogen et al., 2015; Hazen et al., 2015; Deruiter et al., 2017), blue whales in the SLE were not observed feeding at depths deeper than 100 m (Doniol-Valcroze et al., 2012) even though water depths can reach 300 to 500 m, depending on location. This indicates that blue whale foraging effort is likely driven by krill density, accessibility, and availability within that depth range. Krill vertical distribution data from hydroacoustic surveys in the

EGSL show that the densest patches of the two studied krill species are generally located within the first 180 m of the water column during daytime (Plourde et al., 2014b; McQuinn et al., 2015). Blue whales in the SLE also feed almost continuously (T. Doniol-Valcroze and V. Lesage unpubl. data); this is in contrast with krill-feeding humpback whales in Antarctica, which stop feeding in the morning when patches reach their deepest depths (>100 m depth; Friedlaender et al., 2016). These differences in behavior among whale species may in part be related to size- and shape-specific metabolic considerations (Potvin et al., 2012). They may also arise from differences in krill densities among regions, with potentially lower krill densities in the St. Lawrence compared to Antarctica, possibly forcing a near-continuous feeding in the St. Lawrence in order for blue whales to accumulate fat reserves. Alternatively, it is possible that if krill also reach their deepest depths in the morning in the SLE, the perception of continuous feeding behavior arises from the small number of tags that were deployed early enough in the morning, or that lasted overnight to capture these early morning resting periods (V. Lesage unpubl. data).

Blue whales and other balaenopterids display a wide range of foraging strategies by modifying the kinematics of lunge feeding (e.g. speed, body orientation, inter-lunge intervals), in relation to prey density and the depth at which they feed to maximize prey intake and FE (Goldbogen et al., 2015; Cade et al., 2016). They perform more maneuvers when feeding on low-density and patchily distributed krill (Goldbogen et al., 2015). Also, the speed at which whales lunge likely affects energy expenditure since most of the cost arises from associated power and drag generated by a lunge (Goldbogen et al., 2012; Potvin et al., 2012; Potvin and Werth, 2017). In this study, we could not account for the kinematics and maneuvering associated with feeding strategies due to the limited sensors available on our tags. Hence if whales lunge at lower speeds when feeding at shallow depths or on krill patches of lesser density, energy expenditure might be overestimated for these types of dives. The use of data loggers with supplementary sensors such as tri-axial accelerometers and magnetometers would provide more details about feeding maneuvering, and would help refine and improve the accuracy of energetic cost estimates related to foraging.

1.6.2 Krill density requirements

The sensitivity analyses revealed that the greatest uncertainty in our bioenergetics model output lay with the number of lunges h^{-1} , which was propagated to hourly energy expenditure. This parameter varied among individuals, possibly as a result of the heterogeneity of tag deployment duration and natural variation in blue whale activity budget and behavior. Increasing sample size might lower this uncertainty. However, the high variability observed in the hourly foraging effort (number of feeding dives h^{-1} , number of lunges $dive^{-1} h^{-1}$, number of lunges h^{-1}) could also be ecologically relevant. Individuals of different sex, age, and reproductive status have different energetic requirements (Winship et al., 2002; Hammill et al., 2010; Fortune et al., 2013; Villegas-Amtmann et al., 2015) and are expected to display different behavioral patterns and foraging strategies (Hoskins and Arnould, 2013; Hückstädt et al., 2018).

Krill density requirements were predicted based on the feeding rate (number of lunges h^{-1}), thus both are expected to be linked. For a given FE, whales required lower prey densities to meet the same energetic demands when performing more lunges (Figs. 1d,e, 4, & 5). In the morning when whales were observed diving deeper and for longer, krill density requirements were generally estimated to be higher. This is consistent with previous findings that fine-scale prey density, as opposed to prey biomass at a larger scale, is one of the most deterministic parameters in the foraging decision process when optimizing FE (Croll et al., 2005; Friedlaender et al., 2006). The minimum krill density thresholds required for a blue whale to achieve neutral balance was estimated at 14 to 40 $g \cdot m^{-3}$ for Arctic krill and 11 to 33 $g \cdot m^{-3}$ for northern krill, depending on time of day. This range of values encompasses the 12 $g \cdot m^{-3}$ estimated by Hazen et al. (2015) off the Californian coast, where whale foraging behavior differs as a result of dense krill swarms occurring at deeper depths. This provides confidence in our model predictions. However, our estimate is lower than the mean density threshold below which blue whales reject swarms of krill in Antarctica, i.e. 110 $g \cdot m^{-3}$ (range: 75–750) (Wiedenmann et al., 2011). In their study, Wiedenmann et al. (2011) fixed the number of lunges h^{-1} at 20, and limited feeding to daylight hours only. In our study, the

number of daytime lunges was similar, but we allowed an additional 30 lunges per h^{-1} during nighttime foraging. These differences in model parameterization, where all capital needs to be accumulated during daytime in the Antarctic, led to a higher density threshold for profitability in Antarctic compared to St. Lawrence blue whales.

Prey densities required to fulfill energy demands are likely to vary with the targeted prey species and their energy content (Lockyer, 2007). In our simulations, krill density requirements were slightly higher (22.8%) for Arctic krill than for northern krill, the latter of which have an energy content 21% higher than Arctic krill (5.2 ± 0.4 versus $4.3 \pm 0.6 \text{ kJ} \cdot \text{g}^{-1}$, respectively). Arctic krill is also much smaller than northern krill (mean length = 22.0 vs. 35.7 mm, respectively; McQuinn et al., 2013). The two krill species also differ in their aggregation behavior and 3-dimensional distribution (McQuinn et al., 2015). While the 2 species overlap in their vertical distributions, the center of mass of northern krill is typically found at depths 20–30 m deeper than that of Arctic krill (Plourde et al., 2014b; McQuinn et al., 2015). Northern krill on average form looser aggregations ($<8 \text{ g} \cdot \text{m}^{-3}$) than Arctic krill ($8\text{--}16 \text{ g} \cdot \text{m}^{-3}$) and are generally found in lower-density patches than Arctic krill (McQuinn et al., 2015). Therefore, a blue whale would need to expend more energy finding sufficiently dense patches or would need to perform more lunges per dive when seeking northern krill than Arctic krill.

1.6.3 Coupling energetic requirements and *in situ* krill densities

The hydroacoustic krill surveys were performed as close in time and space as possible to observed but not tagged feeding blue whales, but it is unknown how long the whales had been feeding in the surveyed area. Therefore, the krill densities that were measured might not reflect exactly those that were available to blue whales at the time they started to feed, and may have decreased over time. We used the krill patches in areas where blue whales were observed as a sample of the type of patches blue whales are susceptible to exploit, and more specifically, to characterize the vertical distribution and densities of krill in these

patches. We cannot exclude the possibility that denser patches occurred at locations where no blue whales were observed or at times when no hydroacoustic surveys were done. However, for the spatial aspect, the bias introduced in analysis of the availability of energetically suitable patches, if it exists, might be more toward an overrepresentation of higher-density patches than lower-density patches. Information currently available in the literature focuses on biomass density ($\text{g} \cdot \text{m}^{-2}$) rather than volumetric density ($\text{g} \cdot \text{m}^{-3}$) (e.g. Simard and Lavoie, 1999; Sourisseau et al., 2006; McQuinn et al., 2015), preventing us from evaluating the size and direction of a potential bias. The hydroacoustic surveys were also conducted only during daytime and thus, could not capture prey density during nighttime, when both species migrate to the surface and form more diffuse patches (Berkes, 1976; Simard et al., 1986b). Obtaining accurate information at night might be challenging given that hydroacoustic measures can be negatively biased due to the blind zone of a few meters below the echo sounders. Based on our hydroacoustic measurements, daytime krill densities that blue whales required to accumulate energy reserves were estimated to be scarce, suggesting that blue whales would need to seek the highest densities within krill patches to reach an FE above 2.

It is difficult to assess the FE value and period over which this FE needs to be maintained in order for free-ranging marine mammals to accumulate enough fat reserves to reproduce. Indications of adequate FE comes from two studies of income breeders (fur seals) showing an FE of 3.4 ± 0.4 on average in an increasing population (Antarctic fur seal) (Jeanniard-du-Dot et al., 2017b) and an FE of 2.2 ± 0.4 on average in a declining population (northern fur seal) (Jeanniard-du-Dot et al., 2018). In the declining population, ~45% of the studied individuals foraged at efficiencies close to or below 1 (Jeanniard-du-Dot et al., 2018). In North Atlantic right whales, lipid reserves have been linked to reproductive performances, with pre-pregnant and pregnant females showing significantly thicker blubber than males or non-pregnant females (Miller et al., 2011). If energy stores are low, physiological mechanisms responsible for energy allocation prioritize processes involved in an animal's survival rather than reproduction (Bronson 1989; Schneider, 2004). Our study indicates that blue whales in the EGSL may not often have the opportunity to forage at efficiencies higher

than 2 and appear to have lower FE than other populations due to comparatively low krill densities. Observations of females with calves have been rare in this population, with fewer than 28 reports of cow–calf pairs over the past 35 yr (Mingan Island Cetacean Studies unpubl. data). Without further studies coupling blue whale feeding success and krill densities, and an extension of such studies to other areas where blue whales are known to occur in the western North Atlantic (Lesage et al., 2017a), we can only speculate about a possible link between the low FEs predicted in our study and the low calving rate documented for this population (Mingan Island Cetacean Studies unpubl. data).

The EGSL, like several other marine systems in the world, is changing. Our study indicates that given the krill densities observed in this region, blue whales are more likely to achieve neutral energetic balance or accumulate body reserves by feeding on the highest available densities of Arctic krill than by feeding on the highest densities of northern krill. Currently, the krill biomass in the EGSL is dominated by Arctic krill, with a ratio between Arctic and northern krill of 60:40 (McQuinn et al., 2015). While *Thysanoessa inermis* also occurs in the EGSL and can be locally abundant, this species has not been documented as a significant contributor to total krill biomass in this region (Berkes, 1976). There are indications that blue whales in the EGSL tend to target Arctic krill preferentially (Gavrilchuk et al., 2014; McQuinn et al., 2016), and to forage within 100 m from the surface (Doniol-Valcroze et al., 2011; this study), a pattern consistent with the observed shallower mean center of mass for Arctic krill as compared to northern krill (McQuinn et al., 2015). However, northern krill can be more abundant than Arctic krill in some years (I. McQuinn unpubl. data); feeding on northern krill in these years would increase the energy expenditure associated with deeper diving. In other feeding areas of western North Atlantic blue whales, such as the Scotian Shelf, the krill species ratio is reversed, with northern krill forming the bulk of the krill biomass (Cochrane et al., 1991, 2000). Northern krill and Arctic krill differ in their thermal niche, with northern krill being a more temperate to boreal species and Arctic krill being better adapted to cold environments (Kulka et al., 1982; Simard et al., 1986b; Plourde et al., 2014b; McQuinn et al., 2015). With the prospect of a warming climate, the dominance ratio in the upper water column (above 100 m) between the 2 krill species is

expected to change, which may affect blue whale spatial distribution and FE. Specifically, it would be of interest to examine the effects of changes in the ratio of Arctic krill biomass to northern krill biomass, absolute densities of the two species, and their vertical distribution on blue whale FE.

Our study was limited to the time of year that blue whales spend in the SLE in the summer, and thus we lack information about potential food sources they may find in other regions or at other times (Houston et al., 2007). We modeled energy requirements over 24 h to investigate fine-scale foraging behavior, recognizing that blue whales have an entire feeding season to meet their energy demands. Findings from this study could be taken one step further in future studies to incorporate stochastic changes in food availability or accessibility and examine how blue whales balance short-term potential deficits or benefits in FE over longer time periods. Consequently, extending our estimates of energy requirements to other seasons and over the geographic range of migrating blue whales would be useful to assess FE in other areas and at other times of the year relative to the availability and accessibility of resources. However, the amount of energy required during their migration, and to fuel the different annual life history stages, is difficult to estimate, especially for such large animals. Pirotta et al. (2018b) developed a multi-annual bioenergetic model for blue whales in the western North Pacific. It highlighted the complex interaction between a female's energy budget and her ability to reproduce, which requires detailed knowledge of behavioral, physiological, and environmental parameters. In the western North Atlantic, little is known about blue whale distribution and migration patterns outside the SLE and western GSL (but see Lesage et al., 2017a). Quantifying their energy needs on a broader time scale, as well as estimating how far they can migrate and if reproduction is possible with the reserves they are accumulating, would be an essential next step.

In marine ecological studies, it is often logistically difficult to collect data on foraging effort and surrounding preyscape simultaneously. In this study, we used a reverse-engineering approach where preyscape and density requirements by a large marine predator were estimated from modeling energy expenditures derived from high-resolution diving

behavior data. This approach offers an interesting perspective to conservation studies, as it provides a framework for estimating potential bioenergetic consequences of scenarios where anthropogenic activities or environmental factors might alter to various degrees the behavior of a predator or availability or quality of their prey.

1.7 ACKNOWLEDGEMENTS

We thank M. Moisan for tag conception; Y. Morin, J. Giard, D. Lefebvre, M. Moisan, R. Pintiaux, J. Winn, and S. Thompson for tag deployments; B. Woodward for providing access to the D-tag data; the Canadian Coast Guard crew aboard the ‘Frederick G. Creed’ and the various marine mammal observers for blue whale tracking and field support for the hydro-acoustic surveys; F. Paquet for help with the hydroacoustic data; A. Mosnier and P. Brosset for advice on the analysis; and the editor and the 3 anonymous reviewers for providing constructive comments which greatly improved the manuscript. This study was supported by the Species at Risk and Oceans Management programs of Fisheries and Oceans Canada, and by the strategic partnership grant (STPGP 447363) from the Natural Sciences and Engineering Research Council of Canada (NSERC) awarded to G.W. and V.L. This work contributes to the Québec-Océan program (a strategic cluster funded by the Fonds de Recherche du Québec–Nature et Technologies, FRQNT). J.A.G. was supported in part by a Terman Fellowship from Stanford University.

1.8 SUPPLEMENTARY INFORMATION (CHAPITRE 1)

1.8.1 Supplementary figures

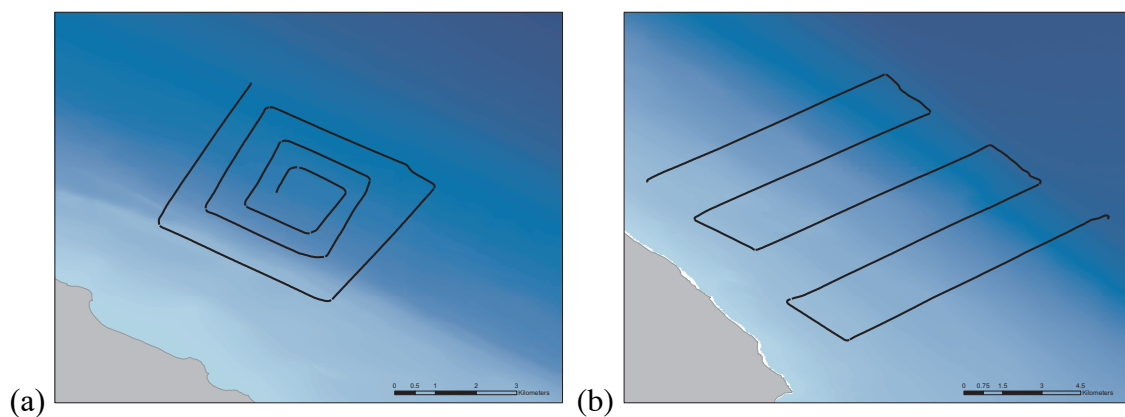


Figure 15 : Illustrations of hydroacoustic survey designs. (a) Rectangular “spirals” (concentric lines of increasing distance and length from the central starting point). (b) “Grid” (parallel equidistant lines). The size of “grids” and “spirals” varied among survey designs, locations, and within and between years.

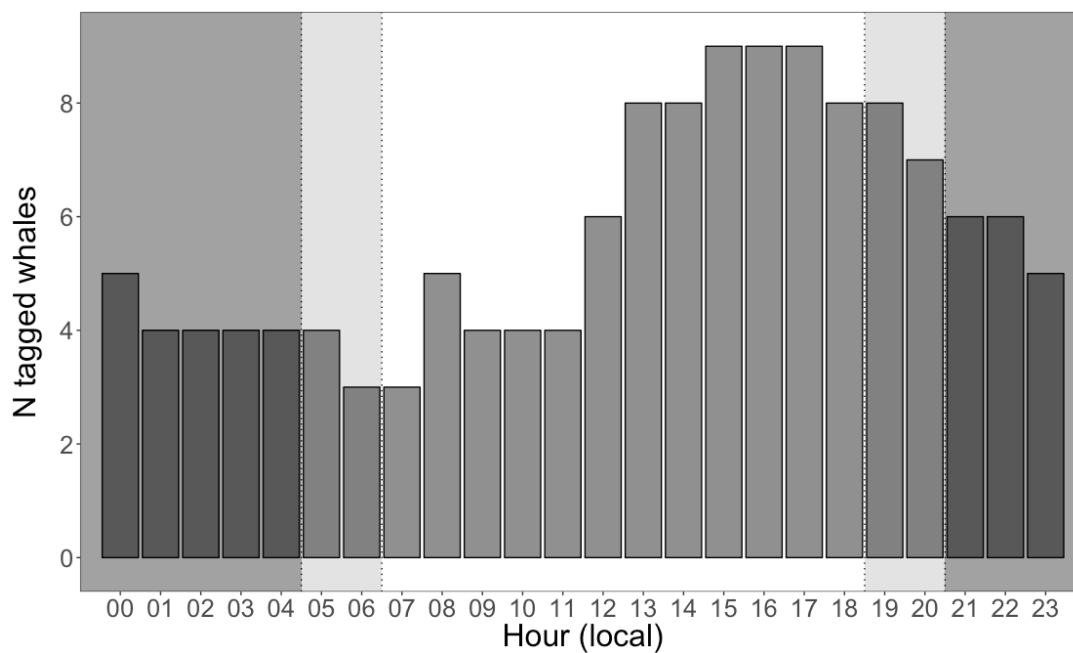


Figure 16 : Diel distribution of tag deployments. Shaded areas are for nighttime (dark grey), dusk and dawn (light grey), and daytime (white).

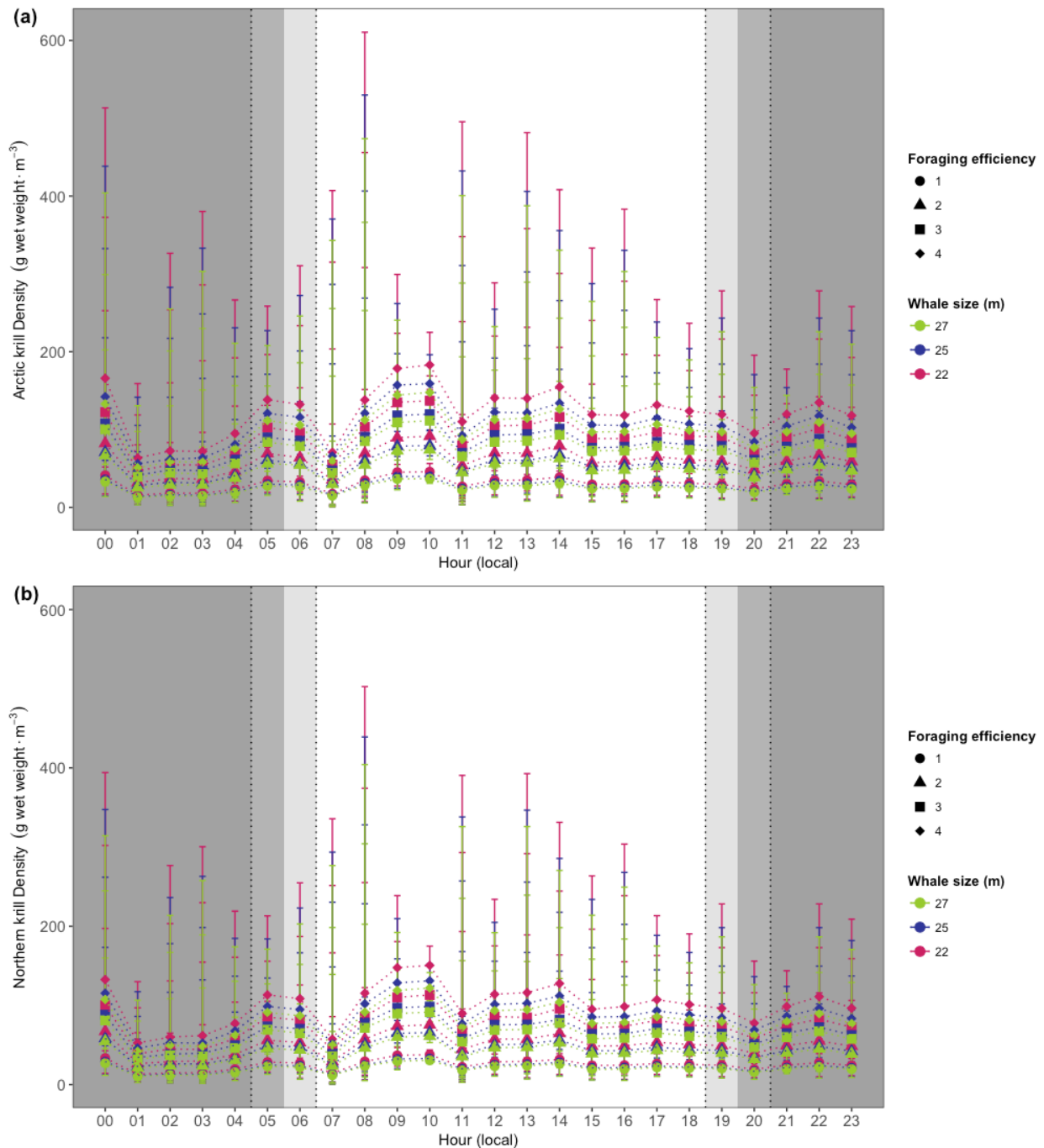


Figure 17 : Diel distribution of densities for (a) Arctic krill, and (b) northern krill required by three sizes of whales (colors for 22, 25, and 27-m) at foraging efficiencies varying from 1 to 4 (symbols). Curves and bars represent the median and 90% confidence interval, respectively. Shaded areas are for nighttime (dark grey), dusk and dawn (overlapping light grey), and daytime (white). The offset between the different size is a result of the positive allometric scaling of engulfment volume with body size.

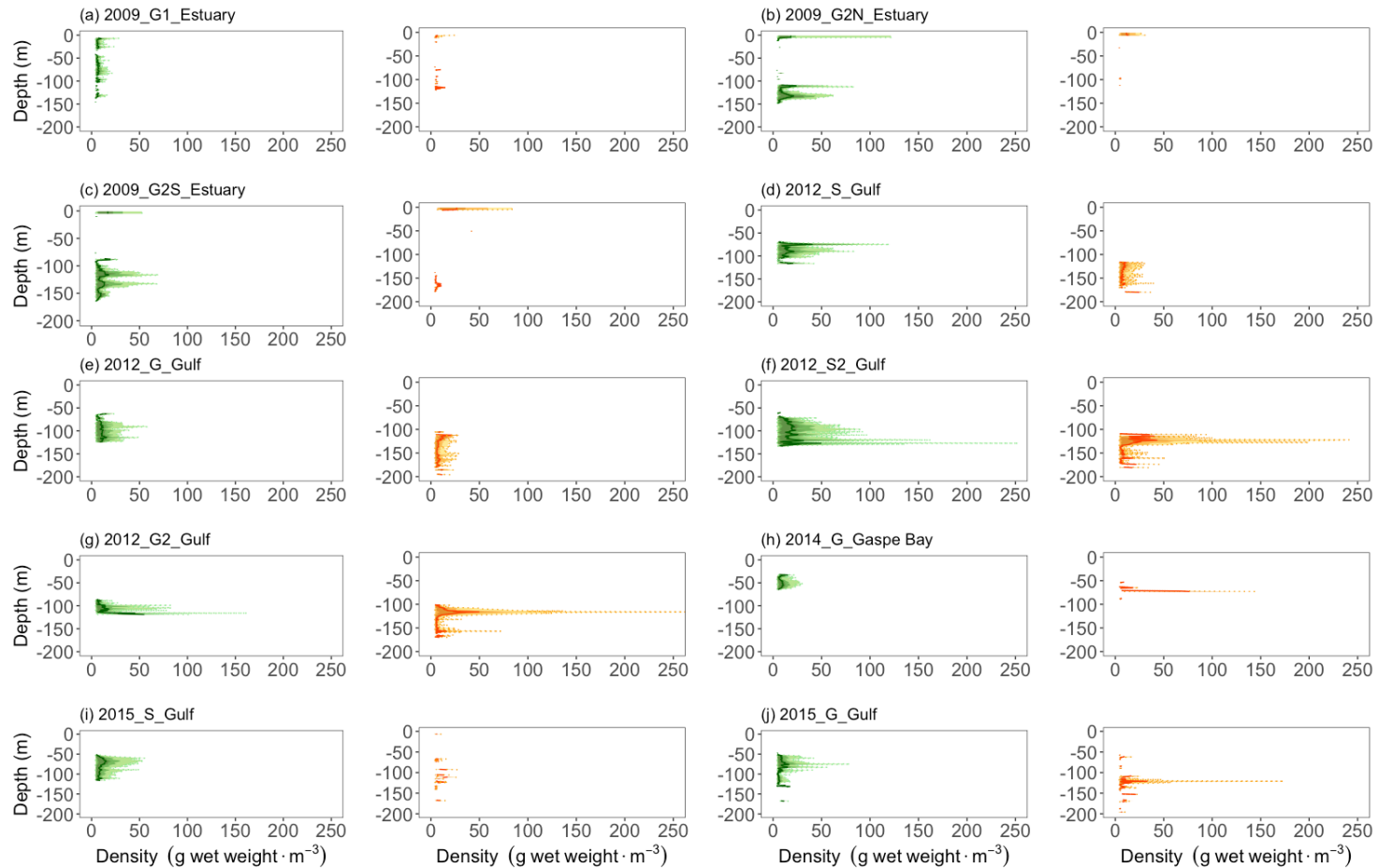


Figure 18 : Vertical density profiles for Arctic krill (green) and northern krill (orange) for each hydroacoustic surveys. Vignettes (a) to (j) indicate the survey year, the hydroacoustic survey design (either grid [G] or spiral [S]) and the general location (either the Estuary or northern Gulf of St. Lawrence — called ‘Estuary’ and ‘Gulf’, respectively — or the Gaspé Bay, also in the northern Gulf of St. Lawrence). Solid line represents the mean, whereas the darker ribbon is 25–75% quantiles, medium ribbon is the 10–90% quantiles, and the light ribbon and dotted line are the 1–99% quantile.

CHAPITRE 2
**REPEATED VESSEL INTERACTIONS AND CLIMATE- OR FISHERY-
DRIVEN CHANGES IN PREY DENSITY LIMIT ENERGY ACQUISITION
BY FORAGING BLUE WHALES**

Authors:

Marie Guilpin^{1,2}, Véronique Lesage¹, Ian McQuinn¹, Pablo Brosset¹, Thomas Doniol-Valcroze³, Tiphaine Jeanniard-du-Dot⁴ & Gesche Winkler²

¹Maurice Lamontagne Institute, Fisheries and Oceans Canada, Mont-Joli, Canada

²Institut des Sciences de la Mer, Québec-Océan–Université du Québec à Rimouski, Rimouski, Canada

³Pacific Biological Station, Fisheries and Oceans Canada, Nanaimo, Canada

⁴Centre d'Études Biologiques de Chizé, UMR 7372 CNRS–Université de la Rochelle,

Villiers-en-Bois, France

Published in *Frontiers in Marine Science* in August 2020

doi: 10.3389/fmars.2020.00626

2.1 ABSTRACT

Blue whale survival and fitness are highly contingent on successful food intake during an intense feeding season. Factors affecting time spent at the surface or at depth in a prey patch are likely to alter foraging effort, net energy gain, and fitness. We specifically examined the energetic consequences of a demonstrated reduction in dive duration caused by vessel proximity, and of krill density reductions potentially resulting from krill exploitation or climate change. We estimated net energy gain over a simulated 10-h foraging bout under baseline conditions, and three scenarios, reflecting krill density reductions, vessel interactions of different amplitudes, and their combined effects. Generally, the magnitude of the effects increased with that of krill density reductions and duration of vessel proximity. They were also smaller when peak densities were more accessible, i.e., nearer to the surface. Effect size from a reduction in krill density on net energy gain were deemed small to moderate at 5% krill reduction, moderate to large at 10% reduction, and large at 25 and 50% reductions. Vessels reduced cumulated net energy gain by as much as 25% when in proximity for 3 of a 10-h daylight foraging period, and by up to 47–85% when continuously present for 10 h. The impacts of vessel proximity on net energy gain increased with their duration. They were more important when whales were precluded from reaching the most beneficial peak densities, and when these densities were located at deeper depths. When krill densities were decreased by 5% or more, disturbing foraging blue whales for 3 h could reduce their net energy gain by $\geq 30\%$. For this endangered western North Atlantic blue whale population, a decrease in net energy gain through an altered krill preyscape or repeated vessel interactions is of particular concern, as this species relies on a relatively short feeding season to accumulate energy reserves and to fuel reproduction. This study highlights the importance of distance limits during whale-watching operations to ensure efficient feeding, as well as the vulnerability of this specialist to fluctuations in krill densities.

Keywords: net energy gain, foraging energetics, krill density, climate change, whale-watching interaction, Estuary and Gulf of St. Lawrence

2.2 RÉSUMÉ

La survie et le succès reproducteur du rorqual bleu dépendent de l'acquisition suffisante de nourriture pendant une saison d'alimentation intense. Les facteurs affectant le temps passé à la surface ou dans une agrégation de proies sont susceptibles de modifier l'effort de recherche de nourriture, le gain net d'énergie et le succès reproducteur d'un individu. Nous avons spécifiquement examiné les conséquences énergétiques d'une réduction démontrée de la durée de la plongée causée par la proximité des bateaux d'excursion et des réductions de la densité de krill résultant d'une potentielle exploitation du krill ou des changements climatiques. Nous avons estimé le gain net d'énergie sur une période simulée de 10 h de recherche de nourriture dans des conditions de base et trois scénarios, reflétant des réductions de densité de krill, des interactions avec des bateaux d'excursion de différentes durées et leurs effets combinés. D'une manière générale, l'ampleur des effets a augmenté avec celle des réductions de densité de krill et la durée de proximité des bateaux d'excursion. Les impacts étaient également moins importants lorsque les pics de densités étaient plus accessibles, c'est-à-dire plus proches de la surface. L'ampleur de l'effet d'une réduction de la densité de krill sur le gain net énergétique a été jugée petite à modérée pour une réduction de 5% du krill, modérée à grande avec une réduction de 10% et grande avec des réductions de 25 et 50%. Les bateaux d'excursion ont réduit le gain net d'énergie cumulé jusqu'à 25% lorsqu'ils se trouvaient à proximité des rorquals pendant 3 des 10 h de la période d'alimentation, et jusqu'à 47–85% lorsqu'ils étaient présents en continu pendant 10 h. Les impacts de la proximité des bateaux d'excursion sur le gain net énergétique ont augmenté avec leur durée. Ils étaient plus importants dans le cas où les rorquals ne pouvaient pas atteindre les densités de krill les plus bénéfiques et lorsque ces densités étaient situées à des profondeurs plus profondes. Lorsque les densités de krill diminuaient de 5% ou plus, la perturbation des rorquals bleus pendant 3 h pouvait réduire leur gain net énergétique de $\geq 30\%$. Pour cette population de rorquals bleus de l'Atlantique Nord-Ouest en voie de disparition, une diminution du gain net énergétique due à une altération du paysage du krill ou à des interactions répétées avec les bateaux d'excursion est particulièrement préoccupante,

car cette espèce dépend d'une saison d'alimentation relativement courte pour accumuler des réserves d'énergie nécessaires à la reproduction. Cette étude souligne l'importance des limites de distance lors des activités d'observation des baleines pour assurer une alimentation efficace, ainsi que la vulnérabilité de ce spécialiste aux fluctuations des densités de krill.

Mots clés : gain énergétique net, énergétique de la quête alimentaire, densité de krill, changement climatique, interaction avec l'industrie d'observations de baleines, estuaire et golfe du Saint-Laurent

2.3 INTRODUCTION

Sufficient food provisioning is essential to the growth, survival, and reproduction of individuals (Emlen, 1966; Pyke et al., 1977). In capital breeders and other migrating species, the vast majority of lipid accumulation relies on a spatiotemporally narrow window of food abundance. Accumulated energy reserves are then used for their yearly needs to sustain the individual during reproduction and periods of fasting or reduced food availability (Houston et al., 2007). Rorqual whales are capital breeders that adopt this strategy, although sporadic feeding has been documented during migration when suitable areas are encountered (McWilliams et al., 2004; Skagen, 2006; Silva et al., 2013; Owen et al., 2016). Rorquals feed on dense aggregations of zooplankton or small schooling fish using a distinct feeding strategy called lunge filter feeding (Goldbogen et al., 2011). However, the high energetic cost of lunge feeding, constrains rorquals to target dense prey patches to maintain high foraging efficiency and allow for fat accumulation (Goldbogen et al., 2011; Guilpin et al., 2019).

The blue whale, *Balaenoptera musculus*, is the largest of the rorquals. This species is ubiquitous to all oceans and feeds almost exclusively on euphausiids or krill, a keystone species of pelagic food webs that is heterogeneously distributed in space and time (Kawamura, 1980; Mauchline & Fisher, 1980; Watkins & Murray, 1998). Blue whales have been shown to follow optimality predictions when feeding on krill by increasing the number of lunges per dive with increasing feeding depth (Doniol-Valcroze et al., 2011). Additionally, they modulate their behavior both in response to krill density and foraging depth (Hazen et al., 2015). For instance, they tend to optimize oxygen consumption when krill densities are low or located at shallow depths and to maximize energy intake when krill densities are high or located at deeper depths (Hazen et al., 2015). Capital breeders such as blue whales might be particularly sensitive to alterations to their prey field or prey access, and in the context of climate change and worldwide increase in anthropogenic activity, there is a need to understand how animals cope with natural or human-induced changes to their environment.

In recent years, climate change and increased anthropogenic activity may be adding to the stochasticity and natural variability in krill availability, density and patchiness. By affecting water temperature, sea ice extent and other environmental factors, climate change has been acting on krill abundance and distribution, species composition, and life cycle in both hemispheres (Flores et al., 2012; McBride et al., 2014). Krill exploitation for use primarily as fish food in aquaculture, medical or pharmaceutical purposes, or for human consumption is a common activity in the Antarctic and around Japan, and its potential as a new fishery resource is periodically considered by different countries including Canada (Nicol et al., 2012). Decreases in krill abundance from climate change and fisheries have been shown to hinder foraging success in penguins (Alonzo et al., 2003; Cresswell et al., 2008). Given that prey density directly influences the rate of net energy gain, any reductions in the krill preyscape would impact blue whale energetics likewise.

In the western North Atlantic, blue whales seasonally visit the Estuary and Gulf of St. Lawrence (EGSL) to feed (Sears & Calambokidis, 2002). In this region from 1999-2009, their diet was composed on average of 70% of *Thysanoessa raschii*, and 30% of *Meganctiphanes norvegica* (Gavrillchuk et al., 2014), the two dominant krill species in the area. These two species differ in aggregative behavior, mean depth, temperature preferences, optimal ecological niche as well as energy content (Plourde et al., 2014b; McQuinn et al., 2015; Cabrol et al., 2019b). Surface salinity affects daytime distribution of the two species, while changing water temperature experienced by adult krill may have consequences for development, growth, and reproduction (Richardson, 2008; Plourde et al., 2014a, 2014c; Benkort et al., 2019), and ultimately biomass and density (Richardson 2008). With climate change, *M. norvegica* – a temperate to boreal species (Sameoto, 1976) – might be favored over *Thysanoessa* spp. (i.e. *T. raschii* and *T. inermis*) – adapted to cold environments (Mauchline and Fisher, 1980). A change in the relative abundance and density of the two krill species, or in the depth of their center of mass, is likely to affect the energetics and foraging efficiency of blue whales feeding in the EGSL. Similarly, operations such as the introduction of a krill fishery, that would reduce krill density and biomass, could lead to a

decrease in the number of krill patches with densities suitable for foraging blue whales and to an increased patchiness of blue whale habitat, affecting their foraging efficiency.

Other anthropogenic activities might also affect foraging efficiency by acting on prey access rather than density. This is the case for instance of anthropogenic disturbances related to marine traffic or whale-watching activities, underwater noise and vessel collision risk (Pirodda et al., 2018a) that interfere with normal behavior. Whale watching operations can reduce foraging activity of marine mammals by triggering avoidance responses and changing diving patterns (Lusseau et al., 2009; Christiansen et al., 2013; Senigaglia et al., 2016; Schuler et al., 2019). A reduction in net energy gain can lead not only to immediate physiological repercussions but also to long-term consequences on population dynamics (Pirodda et al., 2019). In the EGSL, marine traffic and whale-watching are industry sectors that generate thousands of transits through blue whale habitat annually (Chion et al., 2009; Aulanier et al., 2016). In this area, close proximity between vessels and blue whales occurs on a regular basis, and for prolonged periods during daytime, as the species is the target of whale-watching activities (Martins, 2012). Particularly when within 400 m, vessels have been shown to reduce blue whale feeding opportunities by decreasing their surface and dive times (Lesage et al., 2017b). The relative proportion of lost foraging time from vessel exposure also increased exponentially with prey depth (Lesage et al., 2017b). This lost foraging time through a decrease in the number of feeding lunges per dive has resulted in lesser net energy gain in other rorqual species (Christiansen et al. 2013; Di Clemente et al. 2018). Consequently, vessel proximity may be affecting the energetics and foraging efficiency of disturbed whales. These effects might be exacerbated when cumulated with other stressors such as fisheries or climate change on prey abundance and density.

Blue whales in the western North Atlantic are listed as endangered under the Species at Risk Act of Canada and the Endangered Species Act of the United States of America. Their low abundance and apparently low calving rate raise concerns about their nutritional status and cumulative impacts of the changes to their environment, either natural or man-induced, on their foraging efficiency, fitness and population size. In this study, we examined how

changes in krill density and reductions in time spent foraging affected net energy gain of foraging blue whales through model simulations based on empirical data of their foraging behavior. Ultimately, these results can help estimate the amount of additional pressure if any that this population can sustain in light of the long-term changes in climate, and chronic exposure to anthropogenic activity.

2.4 MATERIALS AND METHODS

We used model simulations to explore the energetic consequences of both human disturbances and variations in krill preyscape on blue whale energy gains. Each scenario comprised a set of simulations to investigate the effects of reductions in krill density, of reduced dive durations as a result of vessel proximity, and of the combined effect of both while accounting for foraging depths. Consequences on blue whale energetics and the ability to accumulate energy were integrated over a 10-h daylight foraging bout, which corresponded to the maximum duration of whale-watching activities and potential vessel proximity in the study area during summer (Martins, 2012; Lesage et al., 2017b). However, we did not consider the longer term impacts of these energetic consequences because we lacked data on seasonal changes in blue whale behavior and on the strategies that blue whales may use to cope with energy deficits.

2.4.1 Model framework

We simulated individual time-series of foraging dives to investigate immediate and cumulated energetic consequences of the different scenarios. The model framework allowed the integration of dive-specific parameters such as feeding depth and depth-specific krill densities when calculating energy intake and expenditures (Figure 19). We used Monte Carlo methods to account for the uncertainty and variability in parameters, and for estimating net

energy gain. Dive parameters for the simulations were based on the literature or the analysis of data loggers (Table 7). We assumed that a whale initiating a foraging dive at a given depth foraged in the same way and in the same location for the 10-h foraging bout. We also did not take into account the time needed to fill the forestomach or its clearing rate given that our model was based on empirical diving rate data, which already incorporated these factors.

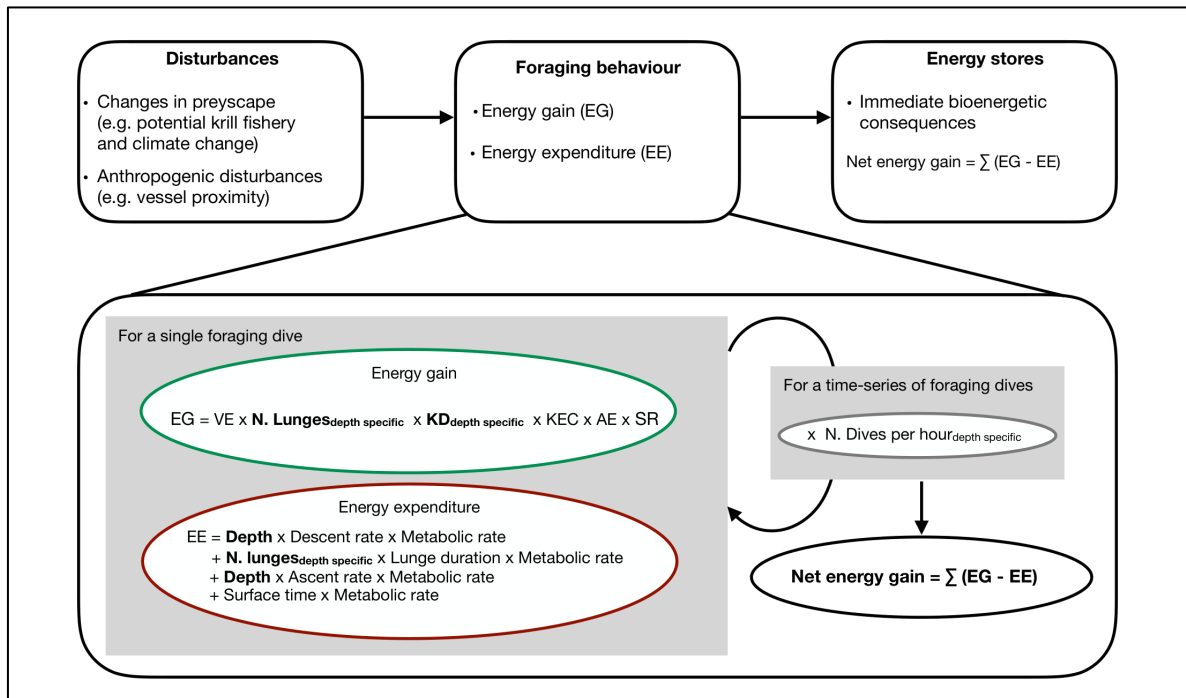


Figure 19 : Bioenergetic model framework to assess immediate effects on net energy gain of changes in preyscape as a result of ocean warming or in prey access as a result of vessel proximity. Parameters and their value are provided in Table 7.

We calculated the net energy gain (MJ) as the difference between the energy intake and energy expenditure cumulated over each hour of foraging (i):

$$\text{Net energy gain} = \left(\sum (\text{energy intake}_i - \text{energy expenditure}_i) \right) / 1000$$

(1)

The energy intake (kJ) during a dive was defined as:

$$\text{Energy intake} = (\text{VE} * \text{N lunges} * \text{KED} * \text{KEC} * \text{AE} * \text{SR}) \quad (2)$$

and accounts for the number of lunges per dive, which depends on feeding depth, body-length dependent volume of engulfment VE (m³), species-specific krill density KED (g wet weight · m⁻³), krill-specific energy content KEC (kJ · g wet weight⁻¹), the assimilation efficiency AE, and success rate SR.

The energy expended per dive depends on the targeted depth. Typically, blue whale foraging dives consist of a descent during which 40% is passive gliding, followed by one or more lunges at depth, a steadily-powered ascent phase and recovery time at the surface (Goldbogen et al., 2011). Blue whales are negatively buoyant and start gliding at a depth of about 18 m when targeting depths exceeding 36 m (Williams et al., 2000). Accordingly, the energy expended (kJ) during a foraging dive at depths of 36 m or more, was modelled as follows :

$$\begin{aligned} &\text{Energy expenditure}_{(\text{feeding dive} \geq 36 \text{ m})} \\ &= (0.60 * \text{Depth} * \text{Descent rate} * \text{AMR} + 0.40 \text{Depth} * \text{Descent rate} * \text{BMR} \\ &\quad + \text{N. lunges per dive} * \text{Lunge duration} * \text{LFMR} \\ &\quad + \text{Depth} * \text{Ascent rate} * \text{AMR})/1000 \\ &\quad + (\text{Surface time} * \text{RMR})/1000 \end{aligned} \quad (3)$$

where Depth (m) * Descent rate (m · s⁻¹) and Depth (m) * Ascent rate (m · s⁻¹) respectively represent the time (s) required to descend to the targeted depth or to ascend back to the surface, and where N. lunges per dives * Lunge duration represents the time (s) available for foraging at the targeted depth (m). Each feeding dive was followed by a period spent at the

surface, specific to feeding depth, and for which costs were calculated based on the resting metabolic rate. Recovery time at the surface was shown to increase with feeding depth of the preceding dive (Doniol-Valcroze et al., 2011), and therefore this relationship was extrapolated from empirical data.

The specific metabolic rates: basal metabolic rate (BMR), resting metabolic rate (RMR), active metabolic rate (AMR), and lunge/filter metabolic rate (LFMR) were taken from the literature (Hemmingsen, 1960; Kleiber, 1975; Croll et al., 2001; Goldbogen et al., 2006; Potvin et al., 2012). Values and sources for all parameters are presented in Table 7. The energy expended (kJ) when foraging at depths shallower than 36 m was modelled in the same way, but without considering passive gliding during descent:

Energy expenditure_(feeding dive < 36 m)

$$= (\text{Depth} * \text{Descent rate} * \text{AMR} + \text{N. lunges per dives} * \text{Lunge duration} * \text{LFMR} \\ + \text{Depth} * \text{Ascent rate} * \text{AMR})/1000 + (\text{Surface time} * \text{RMR})/1000 \quad (4)$$

Energy associated with urine production was assumed to be included in basal metabolism, which represents the energy needed for maintenance activities, including vital organs such as kidneys. Energy expenditure from the heat increment of feeding, i.e. energy associated with digesting food, depends on the size and composition of the meal, and should ideally be included as a separate parameter in bioenergetics models. However, given there is no value specific to large whales for this parameter, numerous studies investigating the energetics of large whales (e.g. right whales, blue whales) have not taken these costs into account (Wiedenmann et al., 2011; Fortune et al., 2013; Pirota et al., 2018b). Instead, heat increment of feeding has been assumed to be part of the active metabolic rate (Nordøy et al., 1995).

Details on other parameters, such as depth-specific diving rate or time spent at the surface after a dive, which were extracted from the analysis of biologging data, and on krill

densities obtained from systematic hydroacoustic surveys, are presented in the Supplementary information.

2.4.2 Simulated scenario

The energetic consequences of krill density reductions or of repeated vessel interactions were each examined under baseline conditions and three different scenarios using Monte Carlo simulations (Table 8 in Supplementary information). We proceeded with 1000 iterations, which were each comprised of a time-series of feeding dives performed over a 10-h foraging bout.

2.4.2.1 Scenario 1: Baseline

This scenario used vertical distributions of krill densities measured in two regions, i.e., the St. Lawrence Estuary (SLE) and the North western Gulf of St. Lawrence (NWG), during systematic hydroacoustic surveys conducted in August 2008-2015 in the EGSL (Quebec, Canada, 49° 43'N–65° 11'W) (Figure 20, data analysis is presented in details in the Supplementary information). Blue whales feed in three different habitats in the SLE (Doniol-Valcroze et al., 2012), the mean feeding depth of which corresponds well with the center of mass of krill patches documented in this region (i.e., 30, 80 and 130 m for *Thysanoessa* spp., and 60 and 80 m for *Meganyctiphanes norvegica*) (Figure 21, and McQuinn et al., 2015). While a comparable study documenting blue whale foraging depth does not exist for the NWG, the center of mass for *Thysanoessa* spp. and *M. norvegica* remain in the range of those plausible or documented in the SLE, or in other regions such as the Pacific (i.e., 30, 60, 120 and 160 m for *Thysanoessa* spp., and 60, 100, 140 and 180 m for *M. norvegica*) (Goldbogen et al., 2013b; Hazen et al., 2015; Irvine et al., 2019). Therefore, we ran simulations for feeding

depths corresponding to krill peak densities in each of the two regions, and separately for the two krill species (Figure 21).

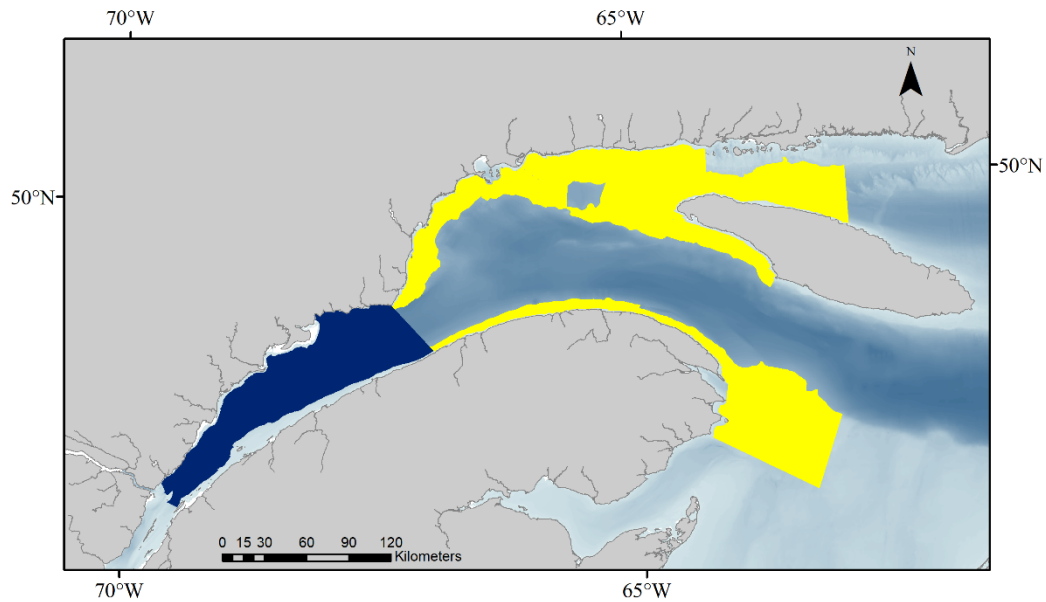


Figure 20 : Two regions, i.e., the Estuary of the St. Lawrence (dark blue) and the northwestern Gulf of the St. Lawrence (yellow) including the Gaspé peninsula, used to determine *in-situ* vertical distributions of krill densities.

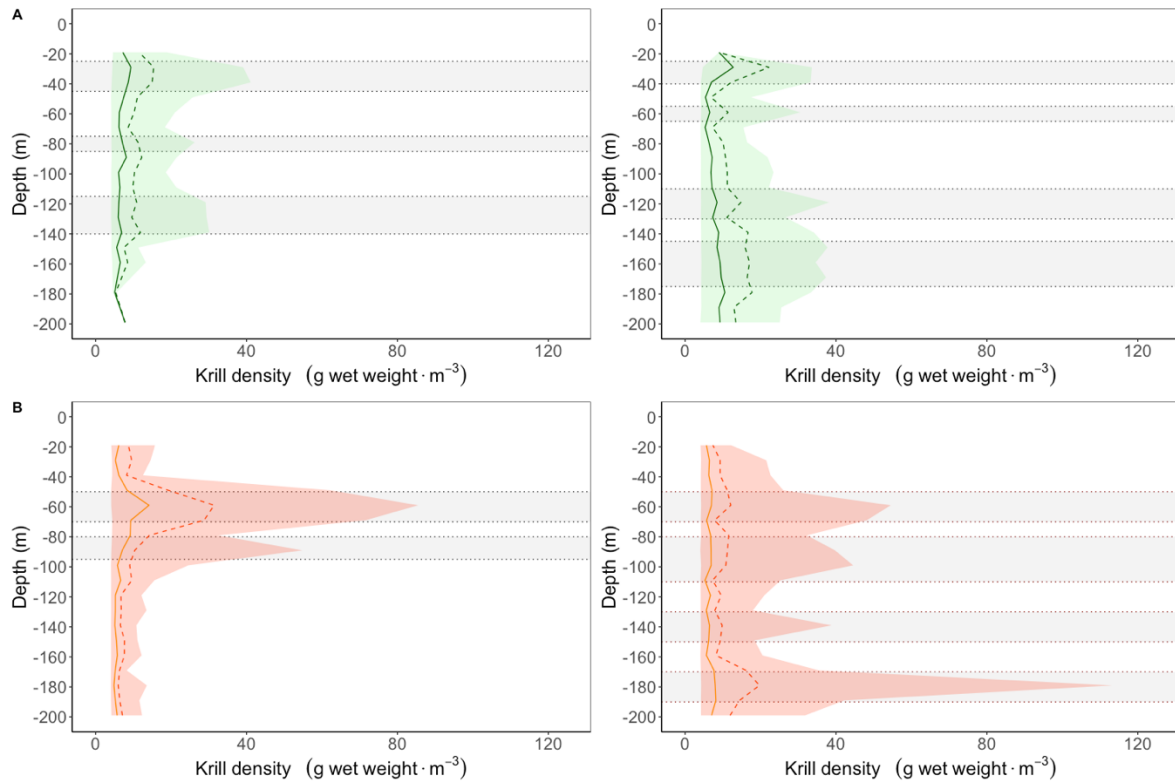


Figure 21: Vertical density profiles for (A) *Thysanoessa* spp. (green) and (B) *Meganyctiphanes norvegica* (orange) for the St. Lawrence Estuary (left) and the northwestern Gulf of St. Lawrence (right) with identified high density layers used as targeted feeding depth for simulated dive time-series (grey horizontal ribbons). Solid vertical lines represent the median, the dashed lines are the 75th percentiles and the coloured areas are the 5–95% quantiles.

2.4.2.2 Scenario 2: Reduction in krill biomass density

This scenario investigates the effect of reducing krill densities on net energy gain. We modelled a decrease in krill density relative to the baseline scenario for the two species separately and distributed this decrease homogeneously over the baseline vertical distribution. Hypothetical reductions in krill density of 5%, 10%, 25% and 50% were examined, each using a set of 1000 iterations.

2.4.2.3 Scenario 3: Disturbances from vessel proximity

A recent study indicated that the presence of vessels within 400 m of blue whales in the SLE resulted in a 36% reduction in dive time, equivalent to a mean dive duration of 4 min, and a maximum foraging effort of 12 dives per hour (Lesage et al., 2017b). In this scenario, we investigated the effect of limiting dive time to a maximum of 4 min on blue whale capacity to accumulate energy, while allowing reachable depth and number of lunges per dive to vary for each dive. In other words, disturbed whales were allowed to vary the number of lunges per dive according to feeding depth, but with the constraint of a maximum dive duration of 4 min. Krill density was depth-specific for each dive. We simulated conditions reflecting vessel proximity within 400 m of foraging blue whales for a portion (i.e., 3-h—from hour 5 to 8) and the full potential duration (10 h) of whale-watching activities in the St. Lawrence Estuary (Martins, 2012). Therefore in the scenario of a 3-h vessel proximity, a whale would be constrained to adjust feeding depth and exploit the highest densities that are reachable within the 4-min dive limit during these 3 hours. They would be allowed to resume foraging at the initial target depth for the next 7 hours. In the scenario where vessel proximity lasted for the full daytime foraging bout, i.e., 10 h, whales would be deprived from reaching certain deeper depths under the constraints of the 4-min dive limit for the entire period. While effects on net energy gain for a 3 h vessel proximity are presented relative to the baseline scenarios for the same depth categories, they are presented for the 10 h relative to the baseline scenario providing the highest net energy gain, i.e., they are not depth-specific.

2.4.2.4 Scenario 4: Combined effect of reduction in krill density and vessel disturbance

Reductions in krill density might occur in areas where vessel-related effects take place and thus, these two effects might be additive (Hin et al., 2019; Pirotta et al., 2019). To account for potential combined effects, we examined scenarios where krill density was reduced by

5%, 10%, 25% and 50% from baseline densities, while blue whales foraged in conditions of vessel proximity for 3 and 10 h.

2.4.3 Statistical analysis

We assessed the sensitivity of the energy gain function to the uncertainty in parameters using a partial correlation coefficient sensitivity analysis and the “pcc” function of the R package “sensitivity” (Pujol et al., 2016. Sensitivity: Global Sensitivity Analysis of Model Outputs. R package version 1.17.0). This method accounted for the correlation between feeding rate and energy expenditure, and identified parameters with the largest influence on energy gain, across all scenarios. While all parameters from the energy gain equations (Eq. 1 and 2) figured in the sensitivity analysis, the energy expenditure associated with each dive (Eq. 3) was entered as a single parameter, thereby incorporating variability associated with depth-specific feeding. This allowed the analysis to be focussed on uncertainty from krill density and number of lunges performed, while avoiding autocorrelation of multiple parameters associated with energy expenditure. Metabolic rates are weight-specific, and estimates from the literature are not associated with uncertainty and thus a single, fixed value, was used given our model was for a 25-m whale.

We assessed each scenario and its effect on blue whale net energy gain against the baseline scenario using Cohen’s d value, which represents the difference between the mean net energy gain of one of the krill-reduction and/or vessel-proximity scenarios and the baseline scenario scaled by their pooled standard deviation (Cohen, 1977). Cohen’s d values indicate a small (0.2-0.5), moderate (0.5-0.8) or large (> 0.8) effect size (Cohen, 1977). Simulations and statistical analyses were conducted under the R programming language (R Development Core Team 2017).

Table 7 : Input parameters, associated sampling distributions and/or values and, data sources used in the bioenergetic framework for estimating net energy gain. NA: not applicable.

Parameters	Description (units)	Value	Distribution	Source
<i>N lunges per dive</i>	Number of lunges per dive	Dive- and depth-specific	Gamma	Tag data, this study
<i>N dives per h</i>	Number of dives per hour	Depth-specific	Gamma	Tag data, this study
<i>VE</i>	Length (25 m) specific engulfment volume (m ³)	(1.023*L ^{3.65})/1,025	NA	Potvin et al. (2012)
<i>M</i>	Length (25 m) specific body weight (kg)	96568	NA	Croll et al. (2001)
<i>KD_T</i>	Krill density <i>Thysanoessa</i> spp. (g wet weight · m ⁻³)	Depth-specific– 75 th –95 th percentile	Uniform	Hydroacoustic surveys, this study
<i>KD_M</i>	Krill density <i>Meganyctiphanes norvegica</i> (g wet weight · m ⁻³)	Depth-specific– 75 th –95 th percentile	Uniform	Hydroacoustic surveys, this study
<i>KEC_T</i>	Krill energy content <i>Thysanoessa</i> spp. (kJ · g wet weight ⁻¹)	4.3 ± 0.58	Normal	D. Chabot (unpubl.data) V. Lesage (unpubl.data)
<i>KEC_M</i>	Krill energy content <i>M. norvegica</i> (kJ · g wet weight ⁻¹)	5.2 ± 0.45	Normal	D. Chabot (unpubl.data) V. Lesage (unpubl.data)
<i>AE</i>	Assimilation efficiency	0.84–0.93	Uniform	Goldbogen et al. (2011) Olsen et al. (2000) Martensson et al. (1994)
<i>SR</i>	Success rate	1	Fixed	
<i>Lunge duration</i>	Lunge duration (s)	75	Fixed	Doniol-Valcroze et al. (2011)
<i>BMR</i>	Basal metabolic rate (J · s ⁻¹)	2 * (4 * M ^{0.75})	NA	Kleiber (1975)
<i>RMR</i>	Resting metabolic rate (J · s ⁻¹)	2 * BMR	NA	Potvin et al. (2012)
<i>AMR</i>	Active metabolic rate (J · s ⁻¹)	3 * BMR	NA	Potvin et al. (2012)
<i>LFMR</i>	Lunge/filter metabolic rate (J · s ⁻¹)	1.6 * AMR	NA	Potvin et al. (2012)

2.5 RESULTS

Baseline simulations using *in-situ* krill vertical distributions indicated that blue whales had the potential to accumulate three times more energy by feeding on the most accessible peak of krill densities, i.e. nearest to the surface. For instance, mean net energy gain was more than 3 times higher in the SLE when feeding on peak densities of *M. norvegica* at 50–70 m versus 80–90 m (Figure 22A), or on peak densities of *Thysanoessa* spp. at 25–45 m versus 115–145 m (Figure 15A in Supplementary information). Only in the NWG, where peak densities of *M. norvegica* at 170–190 m were double those at 50–70 m, was net energy gain similar at the two feeding depths (Figure 26A in the NWG for *M. norvegica* Supplementary information). *M. norvegica* also offered a higher potential for net energy gain than *Thysanoessa* spp. in the two regions, regardless of feeding depth. This was particularly the case in the SLE, with mean net energy gain for blue whales reaching a maximum of 4,526 MJ and 2,772 MJ for *M. norvegica*, as opposed to 1,070 MJ and 675 MJ for *Thysanoessa* spp. in the SLE and NWG, respectively (Figures 22A and 25A, 26A, 27A, Table 8 in Supplementary information).

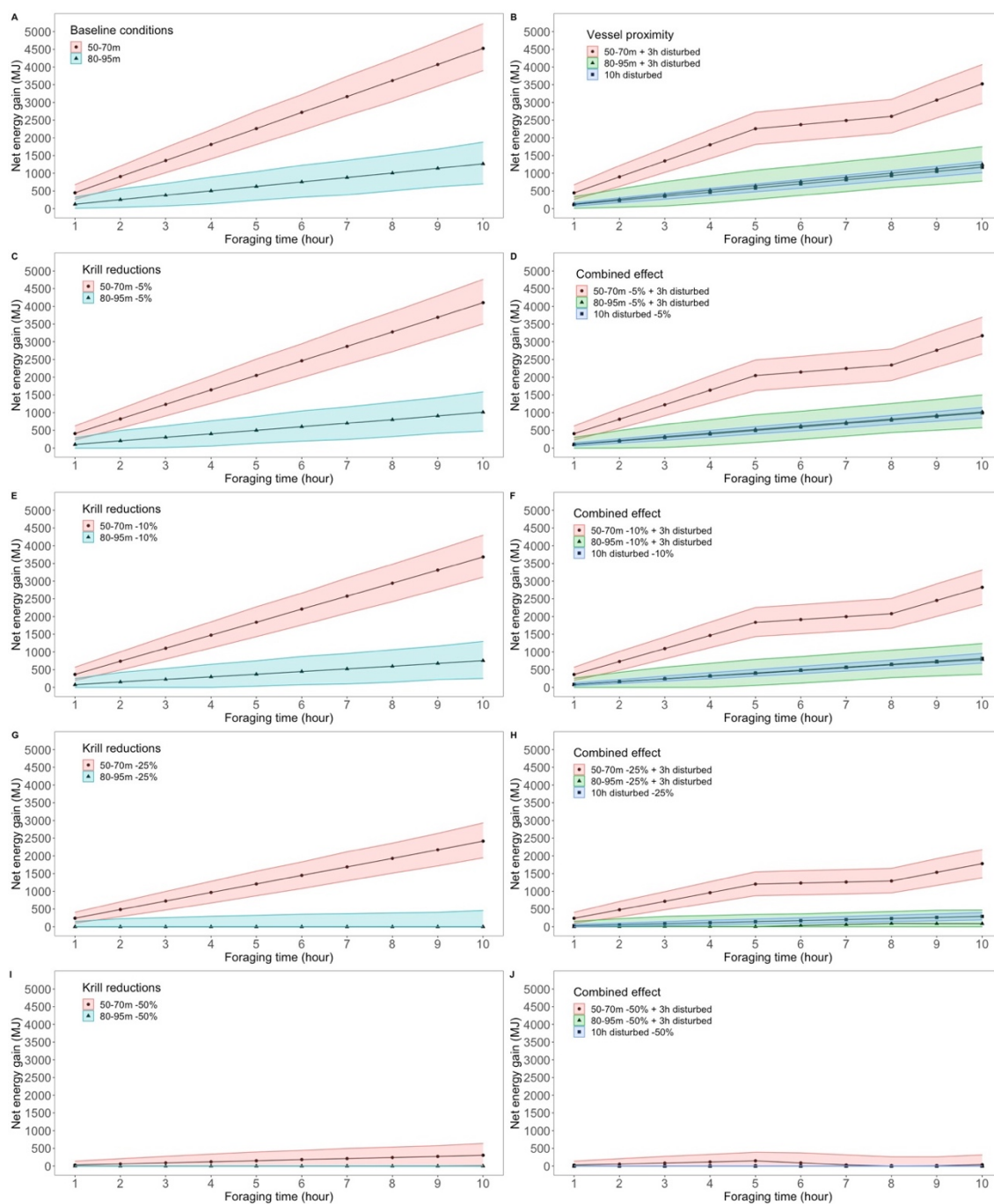


Figure 22 : Net energy gain (mean and 5–95% CI) accumulated over a 10h foraging period when feeding on *M. norvegica* in the St. Lawrence Estuary, (A) under baseline conditions measured *in situ*, (B) when exposed to vessel proximity within 400 m for 3h (from hour 5 to hour 8) and 10 h, (C, E, G, I) under krill density reductions of 5%, 10% 25% or 50% relative to baseline, and (D, F, H, J) while foraging on reduced krill densities when exposed to vessel proximity. Patterns for *Thysanoessa* spp. and the NWG are presented in the Supplementary information.

Simulations of various scenarios of krill reduction and vessel proximity highlighted significant differences in blue whale net energy gains made over a 10-h daylight foraging bout compared to the baseline. Generally, the magnitude of the effects increased with that of krill density reductions and the duration of vessel proximity. Trends in net energy gain as a result of krill density reduction and vessel proximity scenarios were similar for the two krill species, and the two regions, except for the particular case of *Thysanoessa* spp. in the SLE. Therefore, detailed results are presented only for the scenarios that involved *M. norvegica* in the SLE, with results for the other species and regions being presented in the Supplementary information. However, the relative range of the effect sizes of the different scenarios on net energy gain is presented below for both krill species and the two regions.

As expected, reducing krill density decreased the net energy potentially gained by a blue whale feeding at any depth compared to the baseline scenario. The energy deficit increased with the size of the krill density reduction, for the two species and regions (Figures 22C, E, G, I and 25C, E, G, I and 26C, E, G, I and 27C, E, G, I in Supplementary information). However, net energy losses were overall smaller both in absolute terms (in MJ) and in percentage for a given scenario when peak densities were more accessible, i.e., closer to the surface (Figures 22C, E, G, I and Figure 23). For instance, a reduction of 5% in *M. norvegica* densities in the SLE caused a 9% reduction in net energy gain when peak densities were at 50-70 m (422/4,526 MJ), compared to 20% (257/1,268 MJ) when peak densities were at deeper depths (80-90 m) (Table 8 in Supplementary information). In addition, large effects were observed when initial peak densities were low. In *Thysanoessa* spp. for instance, even small to moderate reductions in krill densities decreased net energy gain to 0 (Figures 21; Table 8, Figures 25C, E, G, I, and 27C, E, G, I in Supplementary information), with effect sizes considered moderate at 5% reduction (Cohen's d values >0.51) and large at 10%, 25% and 50% reduction (Cohen's d values >1.16 , Figure 23). In comparison, the effects of a decrease in krill density were considered small for *M. norvegica* at 5% reduction (Cohen's d values >0.28), moderate to large at 10% reduction (Cohen's d values >0.45) and large at 25% and 50% reduction (Cohen's d values >1.17 , Figure 23) depending on whether whales were feeding in the SLE or NWG.

Vessel proximity to foraging whales, with the limit they imposed on dive duration (4 min) and feeding rate (12 dives per h), led to the majority (70%) of dives being constrained to depths of 30 m or less (Figure 24). The impacts of vessel proximity on net energy gain of foraging whales increased with the duration of vessel interaction, were more important when whales were precluded from reaching the most beneficial krill density peaks and when these densities were located at deeper depths (Figure 22, 26B, 27B in Supplementary information and Figure 23). The impacts of vessel proximity also depended on initial feeding depth and associated peak densities. For instance, an undisturbed whale foraging in the SLE at intermediate depths (50–70 m) on densities of *M. norvegica* performed on average 10 dives and 25 lunges h⁻¹, and gained 4,526 MJ over the 10 h foraging bout. During the 3 h when vessels were in proximity, their feeding rate declined to 12 dives and 15 lunges h⁻¹, and whales were likely unable to reach depths where they were initially feeding. Adding the 7 h of undisturbed foraging (during which feeding depth, the number of dives, and the number of lunges were unconstrained) resulted in a 22.2 % reduction in net energy gain compared to the baseline over the 10-h foraging bout, i.e., 3,521 MJ (Table 8 in Supplementary information). In comparison, an undisturbed whale targeting less dense krill densities at deeper depths (80–95 m) was able to perform only 7 dives and 26 lunges h⁻¹, gaining nearly 3 times less energy than a similarly undisturbed whale feeding near the surface (1,268 MJ). In this case, vessel proximity over 3 h did not further constrain the whale feeding rate (which was already within the set limit of 12 dives h⁻¹), but it limited feeding depth to shallow waters through the 4-min dive limit where densities were lower than at deeper depths (Figure 21). Unconstrained diving to 80–195 m for the remaining 7 h led to no overall change in net energy gain in this scenario (i.e., 1,251 MJ, Table 8 in Supplementary information). Whales having vessels in proximity during most of their daytime foraging bout had their feeding rate limited for the full 10 h of vessel proximity, leading to net energy gains that were 74% lower compared to undisturbed whales feeding at depths allowing the highest energy accumulation, an effect considered large based on Cohen's *d* value (>1.8) (Figure 23, Table 8 in Supplementary information). There were scenarios where vessel proximity did not lead to a

negative effect on net energy gain, notably when undisturbed whales foraged near the surface (25–45 m) on the highest densities of *Thysanoessa* spp. in the SLE.

In the last scenario, effects from krill density reductions were combined with those from vessel proximity. As a result, effects on net energy gain generally reflected those from the two stressors separately. Specifically, vessel proximity and krill density reductions net energy losses were smaller when peak densities were high, and more accessible. Impacts of these two factors on net energy gain increased with krill density reductions, and with vessel proximity persistence over time (Figures 22D, F, H, J and Figure 23). For whales foraging on peak densities of *M. norvegica* in the SLE, a density reduction of 25% or more, combined with vessel proximity of 3 h or more, invariably resulted in a medium to large effect, equivalent to approximately 60–100% decrease in net energy gain depending on feeding depth (Figure 23, Table 8 in Supplementary information). A whale foraging optimally, i.e., on peak densities of *M. norvegica* nearest to the surface, but that have been reduced by 50%, with vessels in proximity for 3 h, would accumulate less than half the energy they would have acquired under the baseline scenario (mean net energy gain of 1,781 MJ versus 4,526 MJ under baseline) (Table 8 in Supplementary information). Extending this perturbation to 10 h would lead to a 60% reduction in energy accumulated over that period compared to baseline conditions (i.e., 2,747 MJ) (Table 8 in Supplementary information). For *M. norvegica* in the SLE and both species in the NWG, even a small reduction in krill densities (5%), when combined to medium (3 h) exposure to vessels can lead to a net energy deficit of 19–38% when feeding at intermediate or shallow depths. The scale of the effect varied for the two species and regions for a given depth and scenario according to krill densities and depths where net energy gain was the highest (see Supplementary information for further results). Comparing the effect size between the two stressors, a 3 h vessel proximity to a foraging blue whale would result in the same reduction in net energy gain as a 5% krill density reduction in most cases. Foraging during 10 h with vessels in continuous proximity would be equivalent to foraging on krill densities that are reduced by 5 to 10% (Figure 23).

The sensitivity analysis highlighted the number of lunges per dive, krill density and krill energy content as the three parameters contributing the most to the uncertainty in net energy gain (Sensitivity partial correlation coefficients: 0.96, 0.87 and 0.62, respectively).

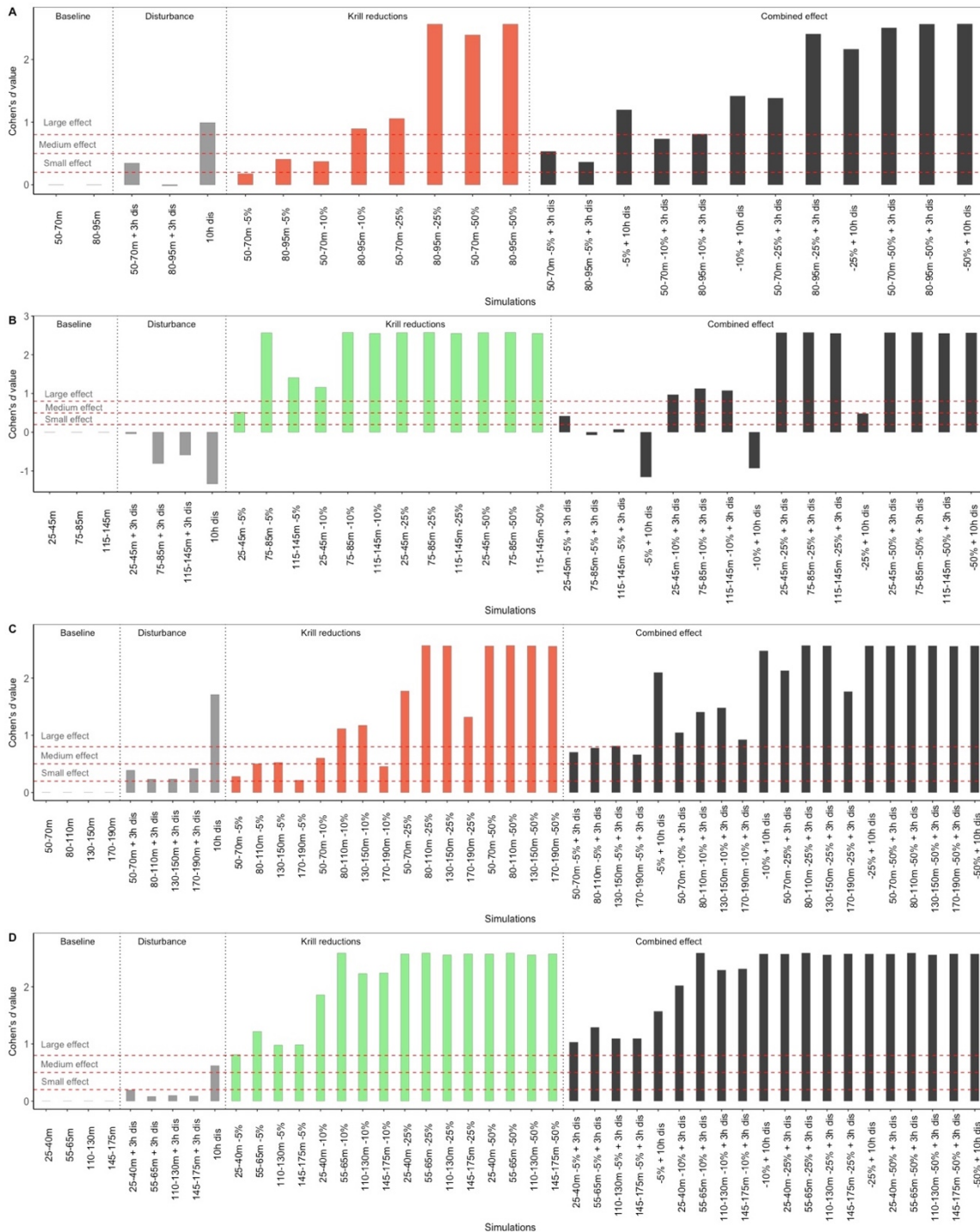


Figure 23 : Effect of the various scenarios on net energy gain after a 10 h foraging period of a blue whale feeding on (B,D) *Thysanoessa* spp. or (A,C) *M. norvegica*, (A,B) in the St. Lawrence Estuary and (C,D) in the North western Gulf of St. Lawrence. The red dashed lines represent the threshold values of Cohen's *d* above which effects are considered small (0.2), medium (0.5), and large (> 0.8). Negative Cohen's *d* value indicates a positive effect.

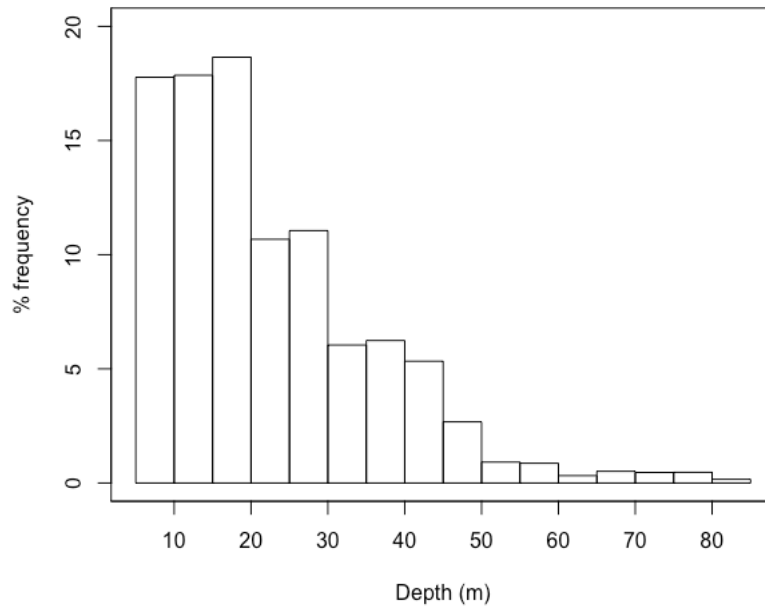


Figure 24 : Frequency (%) distribution of feeding depths when exposed to vessel proximity within 400 m while feeding, thus when dives are limited to 4 min or less.

2.6 DISCUSSION

Habitat degradation, either natural and/or human-induced, can have detrimental effects on foraging efficiency, fitness and population trends (Williams et al., 2006; Pirotta et al., 2018a). Blue whale foraging behavior in the SLE conforms to optimality predictions, with feeding dives near the surface yielding the highest feeding rates (Doniol-Valcroze et al. 2011). Adding to this that the krill densities measured *in situ* in the EGSL were generally denser at shallower depths than at deeper depths (Figure 21), we predicted that the highest potential for energy accumulation was when whales were feeding on these shallow peaks densities and were targeting *Meganyctiphanes norvegica* over *Thysanoessa* spp.. We also showed that the energy deficit caused by krill density reductions or vessel proximity, or their combination, can be significant, even when vessels are in proximity for relatively short

periods of time (3 h). Generally, effects varied with the density and depth of the krill peaks accessible to blue whales, and increased with the magnitude of krill density reductions, and with the duration of vessel proximity.

Krill densities, like any other marine resource, naturally fluctuate in abundance according to environmental conditions (Reid et al., 2010; Flores et al., 2012; Sydeman et al., 2013), and long-lived predators are particularly well adapted to cope with these fluctuations (Benoit-Bird et al., 2013; Abrahms et al., 2019; Dunn et al., 2020). Our simulations showed that blue whales are in all likelihood well adapted to cope with fluctuations of 5%, but that they may incur considerable energy loss at higher density fluctuations. A link between food availability and calving rate has been documented in several species including blue whales (e.g., Ward et al., 2009; Seyboth et al., 2016; Meyer-Gutbrod and Greene, 2018). In blue whales from Antarctica, a simulated reduction of 50% in mean swarm density during an entire feeding season of 120 days resulted in an estimated 80% decrease in calving rate (Wiedenmann et al., 2011). Blue whales appear to track food resource based on long-term stored information rather than short-term proximate cues (Abrahms et al., 2019), a behaviour that might limit their ability to respond and adjust to rapidly changing environmental conditions despite a certain degree of behavioral plasticity in blue whales (Abrahms et al., 2019) as in other marine predators (Ronconi & Burger, 2008). Behavioral plasticity might be particularly insufficient for mitigating the consequences of climate change, which are accelerating and exacerbating the natural variability of prey resources (Sydeman et al., 2013). Important foraging habitats for blue whales have been identified in several areas across eastern Canada, including the EGSL but also in Newfoundland waters and on the Scotian Shelf (Lesage et al., 2018). These regions offer a high diversity of habitats, and are heterogeneous in their seascape (Loncarevic et al., 1999; Galbraith et al., 2018), in vessel traffic density (e.g., Simard et al., 2014), and in krill densities (McQuinn et al., 2015; Plourde et al., 2016). In the case where krill densities would be inadequate in a given region, or where vessel exposure would limit energy gains, whales would theoretically have the opportunity to move to other areas of recurrent krill aggregations within the EGSL region or outside of

it, assuming of course that these habitats exist in these other regions at the time they are needed.

Changes in zooplankton community composition in the EGSL have been documented over the last two decades (Richardson, 2008; Blais et al., 2019). Although studies specifically examining climate change effects are still scarce for krill communities typical of the EGSL, changes in composition are also expected for the latter given the overlapping but distinct optimal temperature niche of the two main krill species (Sameoto, 1976; Mauchline and Fisher, 1980; Ollier et al., 2018). Water salinity through its effect on light penetration influences the vertical distribution and density of krill in the EGSL (Plourde et al., 2014b) as well as their temperature exposure, physiological state, condition, and survival (Flores et al., 2012; McBride et al., 2014). The forecasted 0.6–1.2 °C increase in seawater temperature the EGSL over the next 50 years (Long et al., 2016; Hutchings et al., 2012; Galbraith et al., 2018) might lead to a niche expansion of the more temperate species, *M. norvegica* (Sameoto, 1976). Although the effects of a potential increase in species-specific krill density are not explicitly addressed in this study, their general trend could be derived directly from the percent changes presented in the Supplementary information (by making them positive).

M. norvegica offered a higher potential for net energy gain than *Thysanoessa* spp., with particularly high energetic benefits when peak densities were near the surface. While blue whales are known to feed on both *M. norvegica* and *Thysanoessa* spp., their diet is likely to vary across their range depending on local availability (Lesage et al., 2018). *M. norvegica* is the dominant krill species in other, warmer blue whale foraging areas such as the Scotian shelf or the waters off southern Newfoundland (Cochrane et al., 1991, 2000) and is likely to represent their main prey, although specific blue whale diet is unknown for these areas. In the EGSL, *Thysanoessa* spp. comprised 70% of blue whale diet between 1995–2009 according to quantitative isotopic models (Gavrilchuk et al., 2014). This is in agreement with the stronger spatial association of this krill species with blue whale observations made during hydroacoustic surveys in 2009–2013 (McQuinn et al., 2016), and which suggests that *M. norvegica* densities worth exploiting might not be that common in the EGSL. Hydroacoustic

surveys used in our study to derive total krill densities were conducted in 2008–2015, i.e., mainly after the study on blue whale diet, and indicated densities that were similar for the two krill species or greater for *M. norvegica* since 2010 (Figure 21). However, *M. norvegica* peak densities are typically found at deeper depths than *Thysanoessa* spp. (Figure 21; McQuinn et al., 2015, 2016), reducing the relative benefit of exploiting this resource over *Thysanoessa* spp. Considering its higher energetic value, and that our results showed that blue whales accumulated the most energy when feeding on *M. norvegica*, a change in the dominance ratio with climate change in favor of *M. norvegica* might be beneficial to blue whales and therefore mitigate at least in part the reduced krill density in the EGSL.

We showed that the level of impact from vessel proximity is dependent on resource accessibility. If krill is present in sufficient densities near the surface, then the negative effects from close vessel proximity, which imposes a limit on dive time and dive rate, would not be as limiting as if adequate krill densities are only available at deeper depth, where they become out of reach with a dive-duration limit of 4 min (> 30 m). In the SLE, blue whales forage in four types of habitat that vary in feeding depth and whale behavior, and that are used differently depending on tidal phase (Doniol-Valcroze et al. 2012). Feeding depths follow a bimodal distribution, with a strong peak near the surface and a weaker peak between 50 and 100 m (Doniol-Valcroze et al., 2012). Indeed, blue whales in the SLE and NWG exhibited the strongest spatial association with shallow krill patches over deep aggregations between 2009-2013 (McQuinn et al., 2016). These results suggest that a given vessel-proximity event might have differential effects on blue whale foraging efficiency depending on where and when it occurs in their habitat. At times or in areas where krill densities that may allow for a positive net energy gain are unavailable near the surface, effects from vessel proximity on the blue whale capacity to accumulate energy reserves might be more important than depicted in our study, even for short periods of vessel exposure.

The timing of peak whale-watching activities is inextricably linked to the presence of whales. In the EGSL, the whale-watching fleet comprises over 20 vessels proposing multiple departures a day from May to October. Their activities result in prolonged and recurrent

vessel proximity to foraging blue whales (Martins 2012) and what might lead to negligible to major energy deficits per day. Whether the net energy deficits predicted in our study would have long-term effects on blue whale body condition is unknown, and depends on the nature and magnitude of the consequences (Houston et al., 2012; Pirotta et al., 2018a), which in turn depend on the recurrence of exposure and the whale's capacity to compensate for uncapitalized energy at other times. Individuals generally show resilience and plasticity by adjusting foraging effort to the naturally changing preyscape (Costa et al., 1989; Sigler et al., 2009). In the context of anthropogenic disturbance, this plasticity likely allows some degree of compensation for lost feeding opportunities. While some studies show a relatively high resilience to disturbance in some populations (e.g., New et al., 2013a, 2014), others provide strong support for a limited capacity to compensate for lost opportunities (e.g., New et al., 2013b; McHuron et al., 2018b). For example, a simulation study on Californian sea lions indicated that both short and infrequent disturbances (< 1 month, one year only) and prolonged and repetitive disturbances (lasting several months and occurring yearly) could have detrimental effects on recruitment and population size, depending on the severity of the behavioral response to disturbance (McHuron et al., 2018b). In the case of blue whales exposed to whale-watching activities, compensating for lost foraging opportunities and associated energetic shortcomings would need to occur on undisturbed day or daylight hours, during twilight and/or at night, or through an extension of their feeding season. Biologging data indicates that foraging accounts on average for 69% of the daily activity budget of blue whales in the SLE (Doniol-Valcroze and Lesage, unpublished data), thus leaving little time or opportunity for compensation. It is noteworthy that in scenarios of vessel proximity, we assumed based on Lesage et al. (2017b) that whales reduced time spent at depth and at the surface. However, their analysis was based on surface behavior only and was thus unsuitable for assessing whether the average reduction in dive time was caused by a reduction in the duration of foraging dives or by a change in behavior with total cessation of feeding (Lusseau et al., 2009). In the latter case, this would represent a total loss of foraging opportunity until whales find another suitable and undisturbed location to forage.

The availability of prey resources may also modulate the impacts of disturbances by acting synergistically. For example, a modelling exercise indicated that long-finned pilot whales should be able to withstand longer periods of disturbance when resources are abundant than when they are more scarce (Hin et al., 2019). Another simulation study involving blue whales further indicated that, beyond the instantaneous potential shortfall in net energy gain associated with a disturbance event, the recurrence of anthropogenic disturbances (e.g., every year) and its combined effect with poor environmental conditions might result in strong negative effects on their reproductive success, as they tend to prioritize their own survival over investment into an offspring (Pirodda et al., 2019). In our study area, whether the changes we modelled could affect blue whale's capacity to accumulate adequate energy reserves to reproduce successfully or to survive is unknown, and depends on the persistence of vessel interactions and on food abundance. However, there are indications of a low calving rate for this western North Atlantic blue whale population (Mingan Island Cetacean studies, Unpublished data), which may be an indication of difficulties in foraging. When food resources are limited, the additional pressure from short-term or prolonged vessel-proximity might exacerbate the negative effects of prey limitation on their net energy gain. Modelling the effects of vessel-proximity and food shortage over longer time periods (e.g. for annual life cycle or a reproductive cycle) would be evaluated best if cumulated over a feeding season or a full reproductive cycle and would help determine their biological significance for blue whales. However, this would require a model that incorporates energy gains from feeding at other times of day, search time for food patches and non-foraging behavior, and in the case of extrapolation over a full reproductive cycle, breeding and migration costs. The model would also need to incorporate the unknown mechanisms that blue whales implement for coping with energy deficits, which may include increased foraging effort that day, or an extension of the feeding season, assuming that the foraging schedule can accommodate these additions. Energy gains from these compensatory strategies would depend on a number of factors such as prey density and search time in-between food patches, parameters that vary directly with prey densities and thus which are dependent on one of the effects we are testing here (effect of a fishery or climate-driven change in prey

densities). We felt that the uncertainty associated with such predictions would be so high that they would be in the end, uninformative given the information currently available for parameterizing the model.

As a first attempt to quantify the energetic consequences of potential change in krill density and/or anthropogenic disturbances for this specific endangered blue whale population, we made a number of assumptions, which should be addressed in future work. For simplicity, we assumed continuous foraging for a period of 10 h during which whales stayed in the same foraging “mode”, i.e. they fed at the same depth for the entire period. However, foraging is often not continuous but rather organized in bouts of intense activity separated by periods of time allocated to other activities, or until foraging comes to a stop due to physiological requirements (e.g., clearing of the forestomach, digestion, replenishing oxygen stores) (Sibly et al., 1990; Boyd, 1996). While records in the Pacific indicate a median feeding-bout duration of 3.3 h for blue whales (range 0.2–34.9 h) (Irvine et al., 2019), a value similar to what has been observed in the SLE (2 h on average, range 0.1–13 h; Doniol-Valcroze and Lesage, Unpublished data), the long period spent foraging daily by SLE blue whales (average 69%, Doniol-Valcroze and Lesage, Unpublished data) suggests that pauses between foraging bouts are likely short. Individuals should theoretically end foraging when a prey patch is depleted, and resume foraging when they encounter another prey patch of sufficient density. However, both of these behavioral modes are time dependent and were not considered in our study (Mori, 1998; Watanabe et al., 2014). We assumed constant prey density while depletion of a food patch is inevitable and influences predator foraging decisions (Thompson and Fedak, 2001; Sparling et al., 2007; Thums et al., 2013; Akiyama et al., 2019), and did not allow a whale to find an alternative patch (Sims et al., 2006; Thums et al., 2011). The hydroacoustic surveys used covered most of the areas visited by blue whales over a feeding season (Lesage et al., 2017a) and provided us with a global krill vertical density distribution rather than densities of specific krill layers or swarms. It was therefore reasonable to assume that whales were feeding at the same general location for the 10-h foraging period. However, we might have overestimated net energy gain during this 10-h

portion of daylight foraging by not accounting for activities other than foraging (i.e., resting, travelling).

From a management perspective, the findings of this study are important as they transpose behavioral responses into energetic consequences for foraging blue whales. They also bring support to the currently applied regulations in the Saguenay-St. Lawrence Marine Park, which impose a 400-m exclusion zone for vessels around blue whales, as a way to mitigate potential impacts on this endangered species. In addition, they highlight the need to extend these limits to other important habitats for blue whales, where vessel interactions might be chronic. Our study also underscored the importance of limiting the duration of vessel proximity, especially if vessels are within 400 m of a blue whale and in conditions where krill densities might be reduced. In the Saguenay-St. Lawrence Marine Park, a single vessel has a one-hour viewing time limit, with a one-hour interval between successive observations (Regulations Saguenay-St. Lawrence Marine Park). A potential management measure could be to implement cumulative vessel time viewing limits around blue whales to decrease total duration of potential disturbance.

For a species like the blue whale, which relies on a limited feeding season for building energy reserves, changes in energy gain through an altered krill preyscape and/or anthropogenic disturbances is of concern. This study showed that these changes not only would have a detrimental effect on net energy gain, but there is the possibility of these changes to acting synergistically or exacerbating one another. Under conditions where krill densities would decrease due to climate change or krill exploitation, disturbing foraging blue whales would undoubtedly affect their capacity to accumulate energy stores over a feeding season. An estimation of the energy budget over a reproductive cycle of blue whales is needed to determine a threshold above which these changes would jeopardize their reproductive success. Although future work needs to investigate the fine scale diving behavior of disturbed individuals, our results to date could be integrated into models simulating the population consequences of disturbances to estimate their effect on vital rates

and population dynamics, providing a longer time-scale perspective on the energetics of this endangered population.

2.7 AUTHORS CONTRIBUTIONS

VL and MG conceived the model framework. MG led the data analysis, and wrote the manuscript. VL and GW obtained funding to support the research. IHM provided the hydroacoustic surveys data and guidance for the analysis of it. VL, GW, PB and TJJD provided guidance on the model and simulations. All authors provided guidance on model framework and reviewed the manuscript.

2.8 FUNDING

This work was financially supported by the Species at Risk and Oceans Management programs of Fisheries and Oceans Canada, and by the strategic partnership grant (STPGP 447363) from the Natural Sciences and Engineering Research Council of Canada (NSERC) awarded to G.W. and V.L. PB was funded by Fisheries Science and Ecosystem Research Program from the Government of Canada through an NSERC (Natural Sciences and Engineering Research Council of Canada) visiting fellowship.

2.9 ACKNOWLEDGEMENTS

We thank all DFO personnel and crewmembers aboard the *Frederick G. Creed* involved in the systematic hydroacoustic surveys. We thank F. Paquet for validating the hydroacoustic data as well as the editor and reviewers for their helpful suggestions which greatly improved the manuscript. This study is contributing to the program of Québec–

Océan, a strategic cluster of oceanography scientists and their partners, funded by the Fonds de Recherche du Québec–Nature et Technologie (FRQNT)

2.10 SUPPLEMENTARY INFORMATION (CHAPITRE 2)

2.10.1 Supplementary tables

Table 8 : Summary characteristics of scenarios and sets of Monte Carlo simulations. Scenarios were done for each region i.e., the St. Lawrence Estuary (SLE) and the northwestern Gulf of St. Lawrence (NWG) and both dominant krill species, *Thysanoessa* spp. (Tr) and *Meganyctiphanes norvegica* (Mn). Mean net energy gain and their percent change relative to baseline is given for each set of simulations. The effects on mean net energy gain were quantified using Cohen's *d* (Cohen 1977). Values of 0.2, 0.5 and 0.8 indicate small, moderate and large effect sizes, respectively (Cohen 1977).

Scenario	Feeding depth (m)	Krill density (g.m ⁻³)	Vessel proximity (h)	Disturbed dive duration (min)	Mean net energy gain (MJ)	% reduction compared to baseline	Cohen's d value	Cohen's d effect size	
1 Baseline	SLE_Tr	25–45	Depth specific– <i>in situ</i>	-	-	1,070	-	-	-
		75–85	Depth specific– <i>in situ</i>	-	-	206	-	-	-
		115–145	Depth specific– <i>in situ</i>	-	-	345	-	-	-
	SLE_Mn	50–70	Depth specific– <i>in situ</i>	-	-	4,526	-	-	-
		80–95	Depth specific– <i>in situ</i>	-	-	1,268	-	-	-
	NWG_Tr	25–40	Depth specific– <i>in situ</i>	-	-	675	-	-	-
		55–65	Depth specific– <i>in situ</i>	-	-	430	-	-	-
		110–130	Depth specific– <i>in situ</i>	-	-	487	-	-	-
		145–175	Depth specific– <i>in situ</i>	-	-	463	-	-	-
	NWG_Mn	50–70	Depth specific– <i>in situ</i>	-	-	2,099	-	-	-
		80–110	Depth specific– <i>in situ</i>	-	-	985	-	-	-
		130–150	Depth specific– <i>in situ</i>	-	-	887	-	-	-
170–190		Depth specific– <i>in situ</i>	-	-	2,772	-	-	-	

Table 8 continued

Scenario	Feeding depth (m)	Krill density (g.m ⁻³)	Vessel proximity (h)	Disturbed dive duration (min)	Mean net energy gain (MJ)	% reduction compared to baseline	Cohen's d value	Cohen's d effect size	
2 Reduction in krill density	SLE_Tr	25–45	-5%	-	-	800	-25.2	0.51	moderate
			-10%	-	-	530	-50.4	1.16	large
			-25%	-	-	0	-100	2.56	large
			-50%	-	-	0	-100	2.57	large
	75–85	-5%	-	-	0	-100	2.56	large	
		-10%	-	-	0	-100	2.56	large	
		-25%	-	-	0	-100	2.57	large	
		-50%	-	-	0	-100	2.57	large	
	115–145	-5%	-	-	139	-60	1.41	large	
		-10%	-	-	0	-100	2.57	large	
		-25%	-	-	0	-100	2.55	large	
		-50%	-	-	0	-100	2.55	large	
	SLE_Mn	50–70	-5%	-	-	4,104	-9.3	0.17	-
			-10%	-	-	3,682	-18.6	0.37	small
			-25%	-	-	2,416	-46.6	1.05	large
			-50%	-	-	305	-93.2	2.39	large
80–95		-5%	-	-	1,011	-20.3	0.40	moderate	
		-10%	-	-	785	-38	0.89	large	
		-25%	-	-	0	-100	2.56	large	
		-50%	-	-	0	-100	2.56	large	
NWG_Tr	25–40	-5%	-	-	423	-37.3	0.81	large	
		-10%	-	-	172	-74.5	1.85	large	
		-25%	-	-	0	-100	2.55	large	
		-50%	-	-	0	-100	2.57	large	
	55–65	-5%	-	-	206	-52	1.21	large	
		-10%	-	-	0	-100	2.58	large	
		-25%	-	-	0	-100	2.55	large	
		-50%	-	-	0	-100	2.58	large	

Table 8 continued

Scenario	Feeding depth (m)	Krill density (g.m ⁻³)	Vessel proximity (h)	Disturbed dive duration (min)	Mean net energy gain (MJ)	% reduction compared to baseline	Cohen's d value	Cohen's d effect size
	110–130	-5%	-	-	273	-43.9	0.98	large
		-10%	-	-	59	-87.8	2.23	large
		-25%	-	-	0	-100	2.55	large
		-50%	-	-	0	-100	2.55	large
	145–175	-5%	-	-	259	-44	0.98	large
		-10%	-	-	55	-88.1	2.24	large
		-25%	-	-	0	-100	2.57	large
		-50%	-	-	0	-100	2.57	large
NWG_Mn	50–70	-5%	-	-	1,797	-14.4	0.28	small
		-10%	-	-	1,495	-28.7	0.60	moderate
		-25%	-	-	589	-71.9	1.77	large
		-50%	-	-	0	-100	2.56	large
	80–110	-5%	-	-	745	-24.4	0.5	moderate
		-10%	-	-	505	-48.7	1.11	large
		-25%	-	-	0	-100	2.56	large
		-50%	-	-	0	-100	2.56	large
	130–150	-5%	-	-	660	-25.6	0.52	moderate
		-10%	-	-	434	-51.1	1.17	large
		-25%	-	-	0	-100	2.56	large
		-50%	-	-	0	-100	2.56	large
	170–190	-5%	-	-	2,461	-11.2	0.21	small
		-10%	-	-	2,150	-22.4	0.45	moderate
		-25%	-	-	1,218	-56.0	1.31	large
		-50%	-	-	0	-100	2.56	large

Table 8 continued

Scenario	Feeding depth (m)	Krill density (g.m ⁻³)	Vessel proximity (h)	Disturbed dive duration (min)	Mean net energy gain (MJ)	% reduction compared to baseline	Cohen's d value	Cohen's d effect size	
3 Vessel proximity	SLE_Tr	25–45 [‡]	Depth specific– <i>in situ</i>	3	4-min limit	1105	+	-0.03	-
		75–85 [‡]	Depth specific– <i>in situ</i>	3	4-min limit	500	+	-0.80	-
		115–145 [‡]	Depth specific– <i>in situ</i>	3	4-min limit	595	+	-0.58	-
		variable [†]	Depth specific– <i>in situ</i>	10	4-min limit	1170	+	-0.17	-
	SLE_Mn	50–70 [‡]	Depth specific– <i>in situ</i>	3	4-min limit	3,521	-22.2	0.34	small
		80–95 [‡]	Depth specific– <i>in situ</i>	3	4-min limit	1,251	-1.3	0	-
		variable [†]	Depth specific– <i>in situ</i>	10	4-min limit	1,169	-74	1.8	large
	NWG_Tr	25–40 [‡]	Depth specific– <i>in situ</i>	3	4-min limit	582	-13.7	0.19	-
		55–65 [‡]	Depth specific– <i>in situ</i>	3	4-min limit	408	-5.1	0.08	-
		110–130 [‡]	Depth specific– <i>in situ</i>	3	4-min limit	449	-7.8	0.09	-
		145–175 [‡]	Depth specific– <i>in situ</i>	3	4-min limit	432	-11.3	0.09	-
		variable [†]	Depth specific– <i>in situ</i>	10	4-min limit	355	-47.4	1.07	large
NWG_Mn	50–70 [‡]	Depth specific– <i>in situ</i>	3	4-min limit	1,578	-24.8	0.38	small	
	80–110 [‡]	Depth specific– <i>in situ</i>	3	4-min limit	825	-16.2	0.23	small	
	130–150 [‡]	Depth specific– <i>in situ</i>	3	4-min limit	743	-16.2	0.23	small	
	170–190 [‡]	Depth specific– <i>in situ</i>	3	4-min limit	2,030	-26.7	0.41	moderate	
	variable [†]	Depth specific– <i>in situ</i>	10	4-min limit	405	-85.4	2.56	large	

Table 8 continued

Scenario	Feeding depth (m)	Krill density (g.m ⁻³)	Vessel proximity (h)	Disturbed dive duration (min)	Mean net energy gain (MJ)	% reduction compared to baseline	Cohen's d value	Cohen's d effect size	
4 Combined effects	SLE_Tr 25–45‡	-5%	3	4-min limit	863	-19	0.41	small	
		-10%	3	4-min limit	621	-42	0.96	large	
		-25%	3	4-min limit	0	-100	2.56	large	
		-50%	3	4-min limit	0	-100	2.56	large	
	75–85‡	-5%	3	4-min limit	303	+	0	-	
		-10%	3	4-min limit	106	-48	1.12	large	
		-25%	3	4-min limit	0	-100	2.56	large	
		-50%	3	4-min limit	0	-100	2.56	large	
	115–145‡	-5%	3	4-min limit	398	+	0.07	-	
		-10%	3	4-min limit	202	-44	1.07	large	
		-25%	3	4-min limit	0	-100	2.56	large	
		-50%	3	4-min limit	0	-100	2.56	large	
	variable†	-5%	10	4-min limit	1,001	-6.2	0.12	small	
		-10%	10	4-min limit	824	-23	0.46	moderate	
		-25%	10	4-min limit	295	-72	1.7	large	
		-50%	10	4-min limit	0	-100	2.56	large	
	SLE_Mn	50–70‡	-5%	3	4-min limit	3,173	-29.9	0.53	moderate
			-10%	3	4-min limit	2,825	-37.5	0.73	moderate
			-25%	3	4-min limit	1,781	-60.6	1.34	large
			-50%	3	4-min limit	403	-91	2.5	large
80–95‡		-5%	3	4-min limit	1,018	-19.7	0.36	small	
		-10%	3	4-min limit	785	-38	0.81	large	
		-25%	3	4-min limit	87	-93.1	2.40	large	
		-50%	3	4-min limit	0	-100	2.56	large	
variable†		-5%	10	4-min limit	993	-78	1.96	large	
		-10%	10	4-min limit	818	-81.9	2.07	large	
		-25%	10	4-min limit	291	-98	2.4	large	
		-50%	10	4-min limit	0	-100	2.56	large	

Table 8 continued

Scenario	Feeding depth (m)	Krill density (g.m ⁻³)	Vessel proximity (h)	Disturbed dive duration (min)	Mean net energy gain (MJ)	% reduction compared to baseline	Cohen's d value	Cohen's d effect size
NWG_Tr	25–40 [‡]	-5%	3	4-min limit	352	-47.8	1.03	large
		-10%	3	4-min limit	122	-81.9	2.01	large
		-25%	3	4-min limit	0	-100	2.57	large
		-50%	3	4-min limit	0	-100	2.57	large
	55–65 [‡]	-5%	3	4-min limit	193	-55.2	1.29	large
		-10%	3	4-min limit	0	-100	2.58	large
		-25%	3	4-min limit	0	-100	2.58	large
		-50%	3	4-min limit	0	-100	2.58	large
	110–130 [‡]	-5%	3	4-min limit	245	-49.7	1.09	large
		-10%	3	4-min limit	42	-91.3	2.29	large
		-25%	3	4-min limit	0	-100	2.55	large
		-50%	3	4-min limit	0	-100	2.55	large
	145–175	-5%	3	4-min limit	236	-49	1.09	large
		-10%	3	4-min limit	39	-91.5	2.31	large
		-25%	3	4-min limit	0	-100	2.57	large
		-50%	3	4-min limit	0	-100	2.57	large
	variable [†]	-5%	10	4-min limit	176	-73.9	1.83	large
		-10%	10	4-min limit	0	-100	2.58	large
		-25%	10	4-min limit	0	-100	2.57	large
		-50%	10	4-min limit	0	-100	2.58	large
NWG_Mn	50–70 [‡]	-5%	3	4-min limit	1,313	-37.4	0.70	moderate
		-10%	3	4-min limit	1,049	-50	1.04	large
		-25%	3	4-min limit	255	-87.8	2.13	large
		-50%	3	4-min limit	0	-100	2.55	large
	80–110 [‡]	-5%	3	4-min limit	602	-38.8	0.77	moderate
		-10%	3	4-min limit	379	-61.5	1.40	large
		-25%	3	4-min limit	0	-100	2.55	large
		-50%	3	4-min limit	0	-100	2.55	large

Table 8 continued

Scenario	Feeding depth (m)	Krill density (g·m ⁻³)	Vessel proximity (h)	Disturbed dive duration (min)	Mean net energy gain (MJ)	% reduction compared to baseline	Cohen's d value	Cohen's d effect size
	130–150 [‡]	-5%	3	4-min limit	530	-40.2	0.81	large
		-10%	3	4-min limit	318	-64.1	1.47	large
		-25%	3	4-min limit	0	-100	2.55	large
		-50%	3	4-min limit	0	-100	2.55	large
	170–190 [‡]	-5%	3	4-min limit	1,760	-36.5	0.66	moderate
		-10%	3	4-min limit	1,490	-46.2	0.92	large
		-25%	3	4-min limit	680	-75.4	1.76	large
		-50%	3	4-min limit	0	-100	2.55	large
	variable [†]	-5%	10	4-min limit	225	-91.4	2.27	large
		-10%	10	4-min limit	45	-98.3	2.50	large
		-25%	10	4-min limit	0	-100	2.56	large
		-50%	10	4-min limit	0	-100	2.57	large

Note:

For scenarios where vessels are in proximity to whales during the entire foraging bout (10 h), the mean net energy gain is compared to the baseline scenario at the most beneficial depths for whales to accumulate energy.

[‡] During the period when vessels are in proximity to foraging whales, feeding depth corresponds to where the highest densities are reachable within the constraint of a 4-min limit to dive duration while feeding rate is limited to 12 feeding dives·h⁻¹. At other times, i.e., when vessels are absent, feeding depth and rate are unconstrained, and are assumed to resume at the discrete values indicated in the feeding depth column.

[†] Whales that are disturbed for the full 10-h foraging bout are unconstrained to a specific feeding depth, but are limited 70 % of the time to 12 feeding dives·h⁻¹ and to depths that can be reached in within 4 min, i.e., 30 m or less.

2.10.2 Supplementary figures

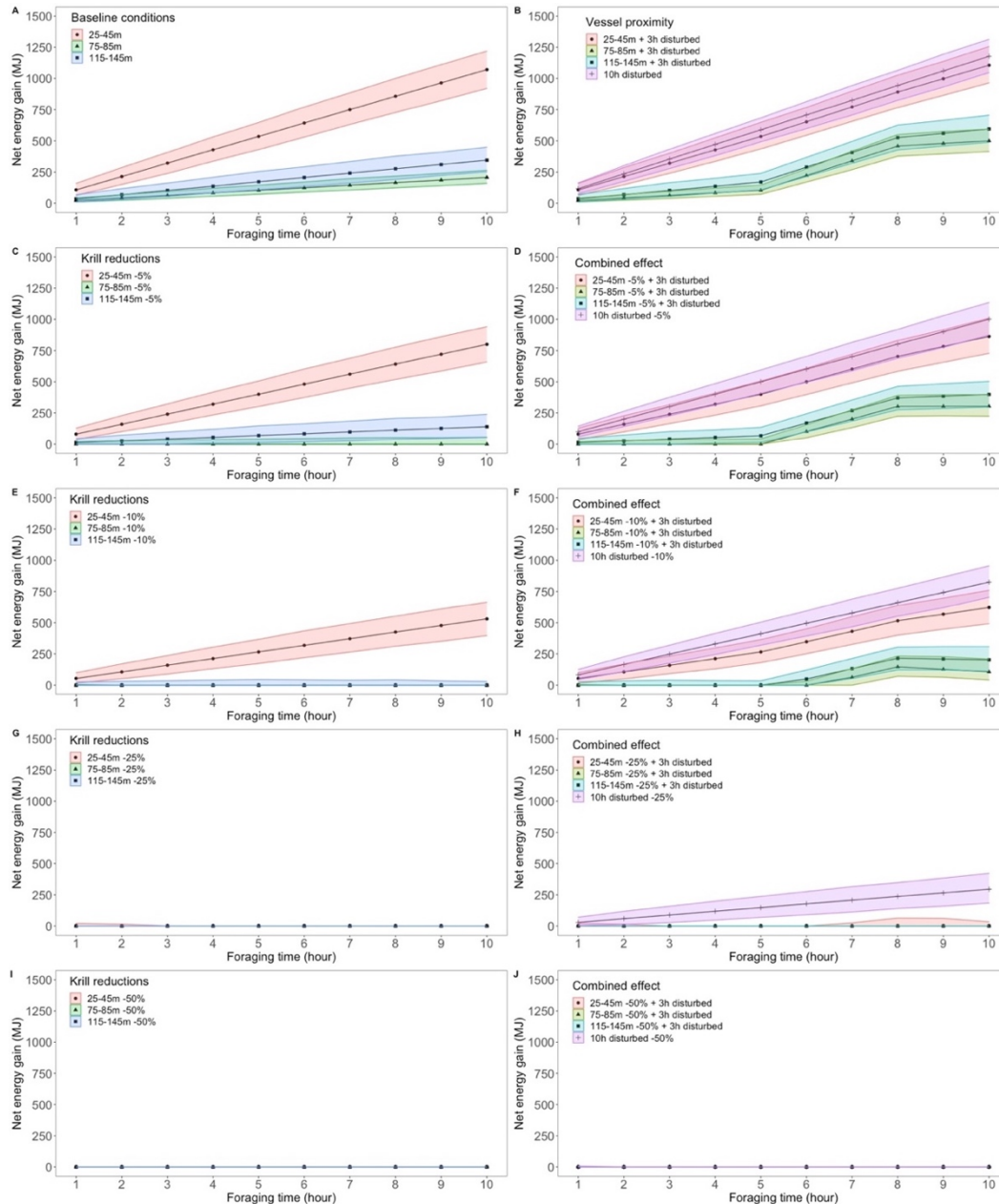


Figure 25 : Net energy gain (mean and 5–95% CI) accumulated over a 10-h foraging period when feeding at peak density depth of *Thysanoessa* spp. in the St. Lawrence Estuary, (A) under baseline conditions measured *in situ*, (B) when exposed to vessel proximity within 400 m for 3 h (from hour 5 to hour 8) and 10 h, (C, E, G, I) under krill density reductions of 5%, 10% 25% or 50% relative to baseline, and (D, F, H, J) while exposed to vessel proximity and foraging on reduced krill densities.

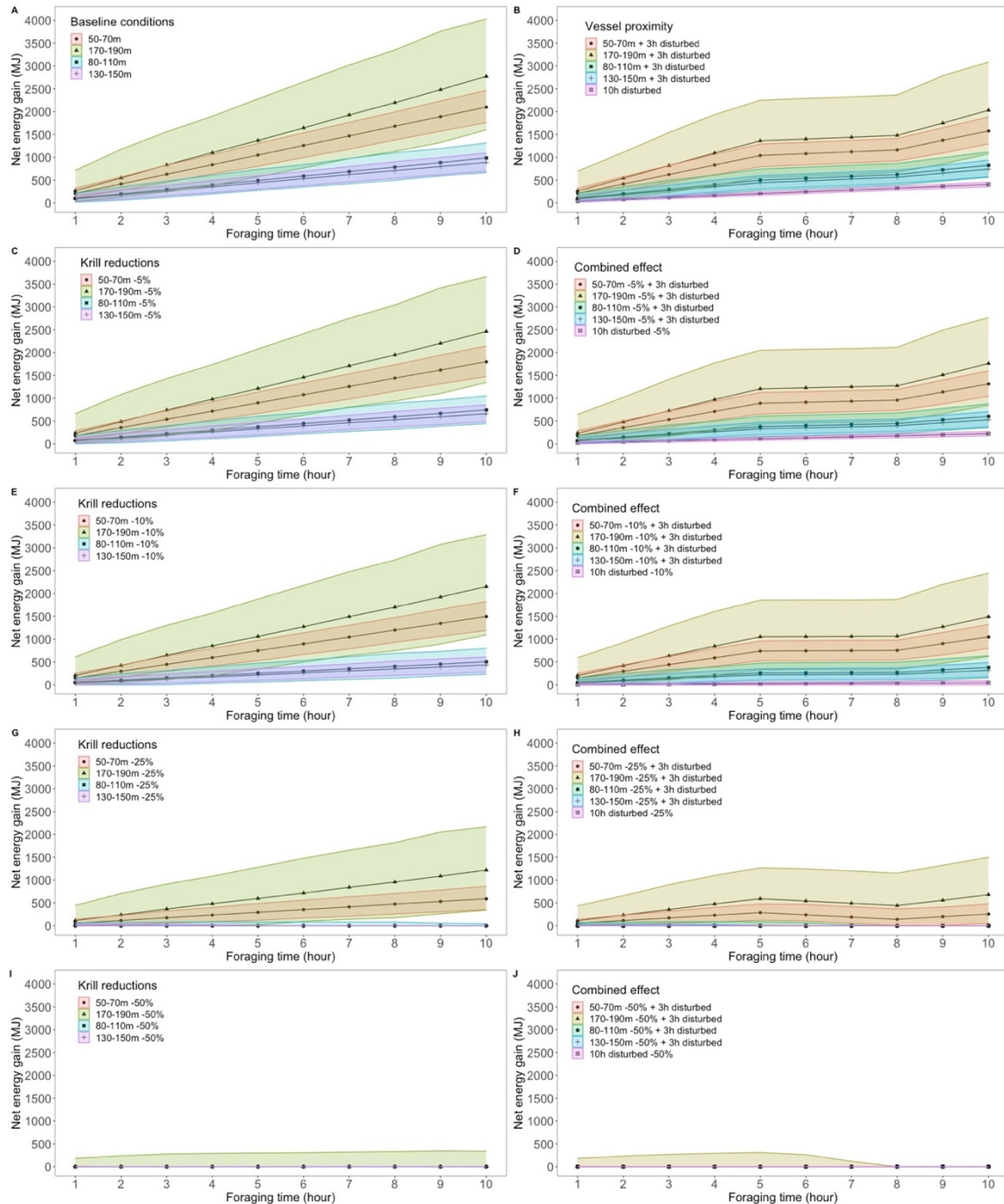


Figure 26 : Net energy gain (mean and 5–95% CI) accumulated over a 10-h foraging period when feeding at peak density depth of *M. norvegica* in the northwestern Gulf of St. Lawrence, (A) under baseline conditions measured *in situ*, (B) when exposed to vessel proximity within 400 m for 3 h (from hour 5 to hour 8) and 10 h, (C, E, G, I) under krill density reductions of 5%, 10% 25 % or 50% relative to baseline, and (D, F, H, J) while exposed to vessel proximity and foraging on reduced krill densities.

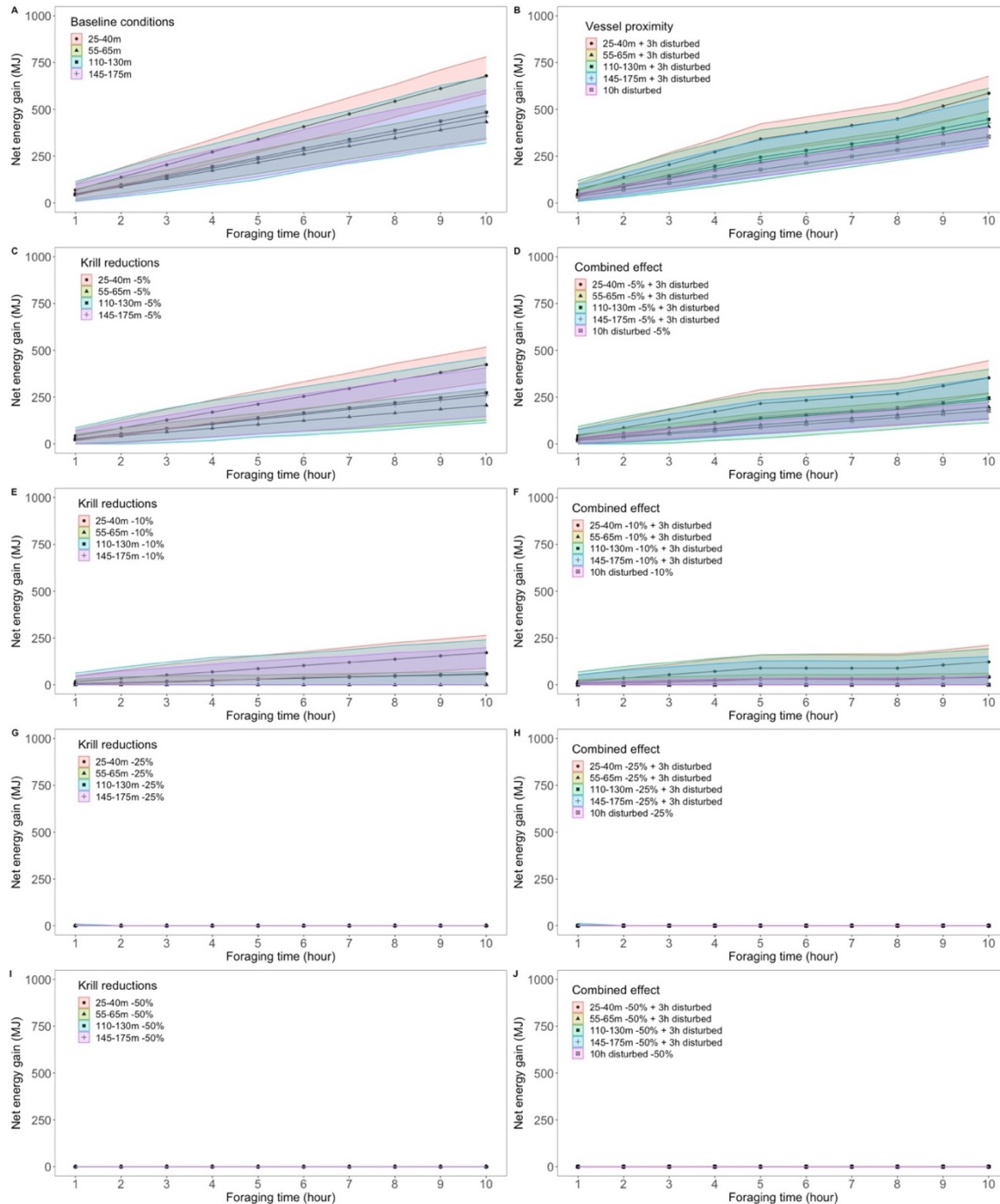


Figure 27 : Net energy gain (mean and 5–95% CI) accumulated over a 10 h foraging period when feeding at peak density depth of *Thysanoessa* spp. in the northwestern Gulf of St. Lawrence, (A) under baseline conditions measured *in situ*, (B) when exposed to vessel proximity within 400 m for 3 h (from hour 5 to hour 8) and 10 h, (C, E, G, I) under krill density reductions of 5%, 10% 25 % or 50% relative to baseline, and (D, F, H, J) while exposed to vessel proximity and foraging on reduced krill densities.

2.10.3 Supplementary data: model parameters

In this study, the number of lunges per dive and the number of dives·h⁻¹ are both depth-specific, and were drawn from distributions defined through the analysis of nine velocity-time-depth recorders (VTDR) from Wildlife Computers, Redmond, WA, and a D-tag (Johnson & Tyack 2003). Archival tags were deployed on ten blues whales in the St. Lawrence Estuary (Quebec, Canada, 48°18'N, 69°20'W) between July and September 2002–2009 (Doniol-Valcroze et al., 2011; 2012). Tags and radio transmitters were attached temporarily to whales with suction cups and detached via a suction release mechanism. Swim speed, depth and water temperature were sampled every second. Swim speeds from the D-tag were inferred from flow noise data sampled at 1 Hz (see procedure in Doniol-Valcroze et al. 2011). A vertical excursion > 0.25 m (greater than the depth resolution) defined a dive, and lunges were identified using a robust algorithm exploiting the acceleration and deceleration phases typical of this behaviour in large baleen whales (Doniol-Valcroze et al., 2011). Other variables including dive duration, dive depth, lunge depth, number of lunges and, descent/ascent rates were extracted from the dive data following Doniol-Valcroze et al. (2011, 2012). These dive characteristics were summarized for each individual in bins of one hour as described in Guilpin et al. (2019).

- Depth-specific number of lunges per dive

The number of lunges associated with a dive of a specific duration and made at a specific depth is a pivotal parameter both of energy gain and energy expenditure, with a lunge being the most energetically costly component of a dive. A study on foraging Pacific blue whales highlighted that the number of lunges per dive change according to krill density encountered, likely to optimize energy gain or oxygen consumption (Hazen et al., 2015). In a study conducted in the St. Lawrence Estuary (eastern Canada), Doniol-Valcroze et al. (2011) showed that blue whales followed the optimal foraging theory by adjusting the number of lunges per dive to feeding depth. We determined the mean (and SD) number of

lunges per dive by 10-m depth bins from empirical data. We used model predictions from Doniol-Valcroze et al. (2011) for depths where no tag data was available, i.e., beyond 130 m. The number of lunges per dive per depth bin showed variability, which is likely linked to the prey density encountered as shown by Hazen et al. (2015). The optimal model from Doniol-Valcroze et al. (2011) did not include variability, but we obtained associated standard deviations from analysis of the tag data. Therefore, for depth bins deeper than 130 m, we extrapolated the variability observed in the tag data to the model predictions (Figure 28). It allowed us to incorporate uncertainty in the number of lunges per dive inherent to inter-individual variability and foraging strategies. In our simulations, the number of lunges per dive was a mix of empirical data and model predictions. For each depth bin, the number of lunges per dive was drawn from a Gamma distribution, parameterized from the mean and standard deviation with $\text{shape} = \text{mean}^2/\text{SD}^2$ and $\text{scale} = \text{SD}^2/\text{mean}$. Gamma distributions are well suited for right-tailed strictly positive data.

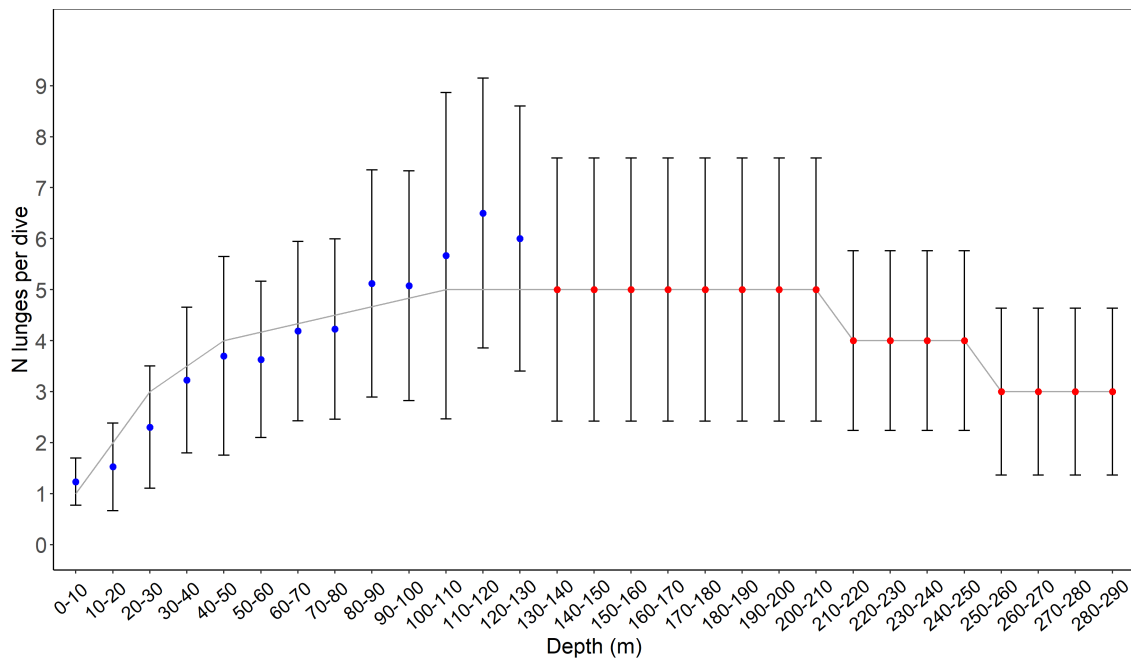


Figure 28 : Depth-specific distribution of the number of lunges per dive, was either calculated from tag data analysis (blue) or predicted using the model developed by Doniol-Valcroze et al. (2011) (red). Errors bars for depths 0-130 m are from tag data analysis, and are extrapolated for depths > 130 m. The grey solid line represents the model predictions from Doniol-Valcroze et al. (2011).

- Depth-specific number of dives per hour

The number of feeding dives made per hour depends on the target depth of successive dives. First, feeding dives were binned per hour for each tagged whale. We then determined the mean number of dives per hour of foraging from the analysis of tag data (Figure 29) although empirical data were restricted to depths < 100 m. We fitted a Generalized Additive Mixed Model (GAMM) to the number of dives per hour as a function of mean feeding depth using a thin plate regression spline smoother and $k = 3$. The model generated predictions for depths > 100 meters. The GAMM was fitted in the `mgcv` library (Wood 2006. Mixed GAM Computation Vehicle with Automatic Smoothness Estimation. R package version 1.8-17) in R (v3.3.3; R Development Core Team 2017). Individual whales were considered a random effect, with hours of the day and individual ID being used as factors in an autoregressive correlation structure of order 1 (`corAR1`) to account for temporal autocorrelation (Zuur et al., 2009). We assessed the significance of the covariate “feeding depth” by comparing model output to a null model including only a random effect using a likelihood ratio test. Homogeneity of variances in the model was assessed from plots of residuals versus fitted values, and normality of the residuals using Quantile-Quantile plots and residual histograms. Model predictions were made for depth bins > 100 m, but considering the lack of empirical data for these deeper depths, the uncertainty around the predicted values was unreliable. We chose to extrapolate the empirically-measured uncertainty to the number of dives per hour for depth bins > 100 m (Figure 30).

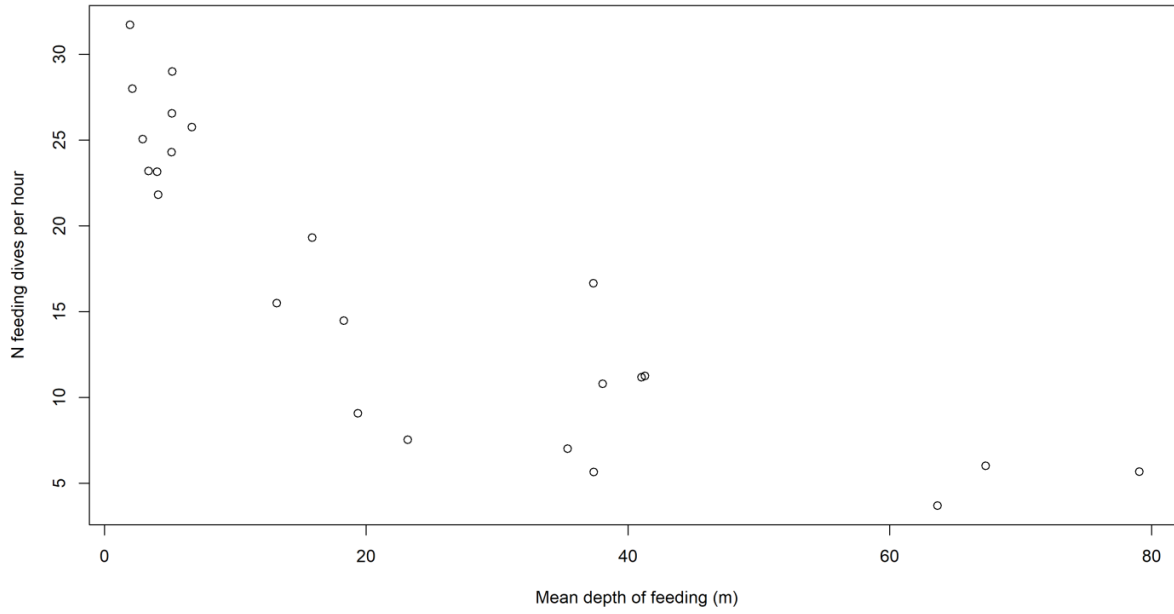


Figure 29 : Mean number of dives per hour as a function of feeding depth.

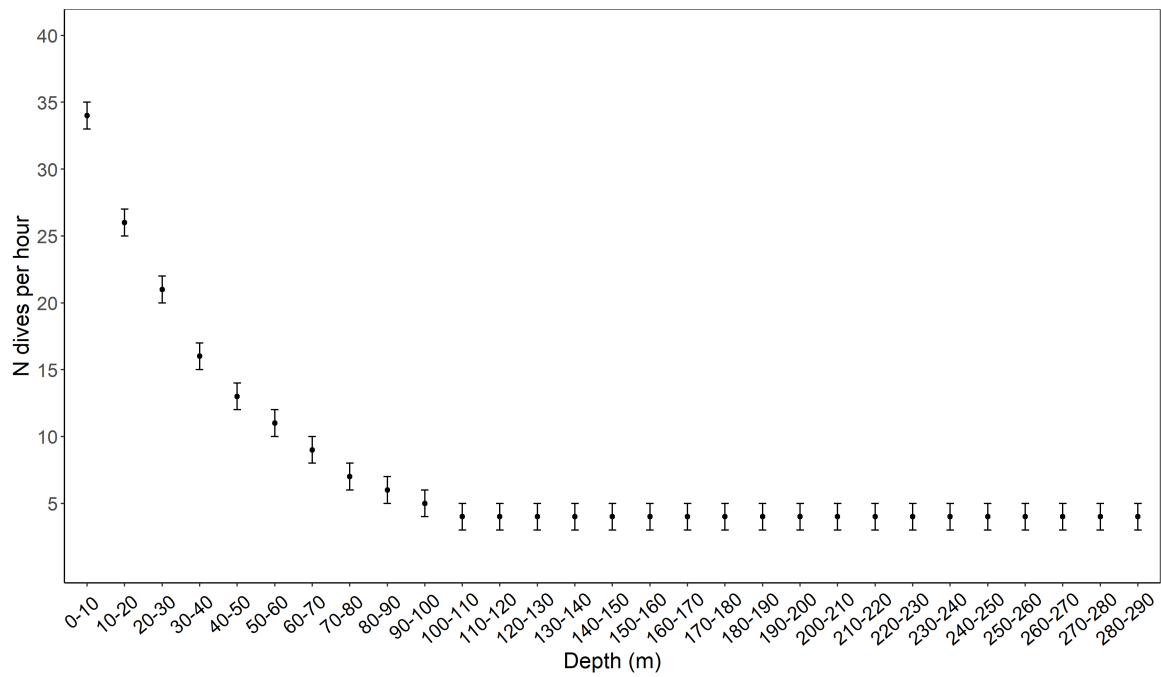


Figure 30 : Depth-specific distribution of foraging effort (dives per hour).

- Depth-specific post-dive surface time

Time spent at the surface following a dive depends on target depth. This parameter and uncertainty around it were estimated from tag data (Figure 31). For depths greater than 120 m where empirical data were lacking, uncertainty around surface time was estimated by extrapolating from the empirical measurements at shallower depths (Figure 32). A Generalized Additive Mixed Model (GAMM) was fitted to the post-dive surface time as a function of mean feeding depth using a thin plate regression spline smoother and $k = 3$ (number of knots for the smoother parameter), and individual whales as a random effect (Zuur et al., 2009). The GAMM was fitted using the R package *mgcv* (Wood 2006. Mixed GAM Computation Vehicle with Automatic Smoothness Estimation. R package version 1.8-17). We assessed the effect of feeding depth on surface time by comparing model output to a null model including only the random effect using a likelihood ratio test. Homogeneity of variances was visually assessed from plots of residuals versus fitted values, whereas normality of the residuals was assessed using Quantile-Quantile plots and residual histograms. Model predictions for depth bins > 120 m were considered unreliable considering the lack of empirical data for these deeper depths.

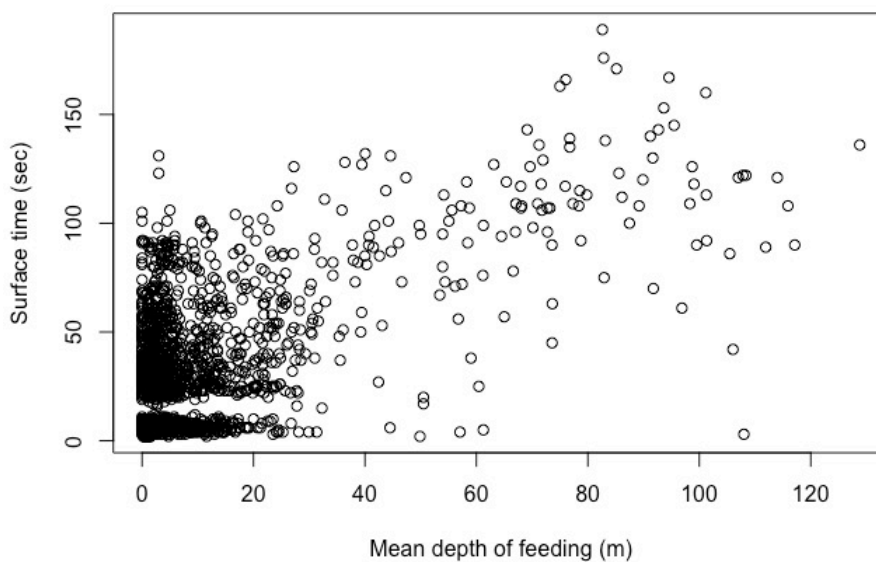


Figure 31 : Surface time (sec) as a function of feeding depth (m).

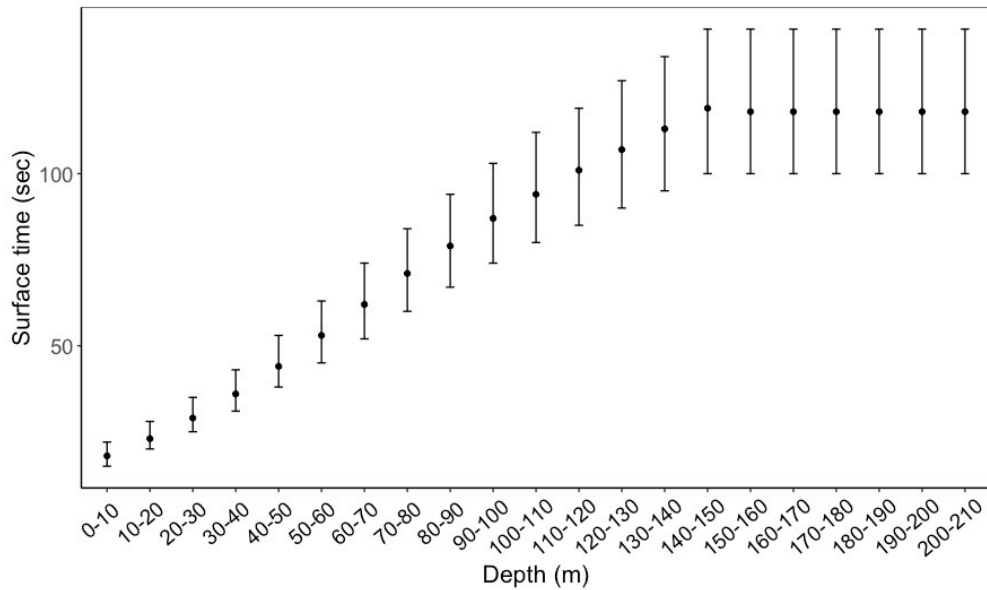


Figure 32 : Depth-specific distribution of post-dive surface times with 95% point-wise confidence intervals.

- Consecutive dives

Foraging is often organised into bouts of feeding dives of similar characteristics (Boyd et al., 1994; Sibly, Nott, & Fletcher, 1990). Consecutive dives are therefore correlated in time and in their characteristics (e.g. feeding depth). Feeding bouts were defined by Doniol-Valcroze and Lesage (unpublished data) using a bout ending criterion method (Boyd, 1996). The frequency distribution of depth difference between successive foraging dives within a bout indicated that 92% of the depth differences did not exceed 10 m (Figure 33). Therefore, we made the assumption that successive foraging dives within each hour of foraging did not differ in depth by more than 10 m.

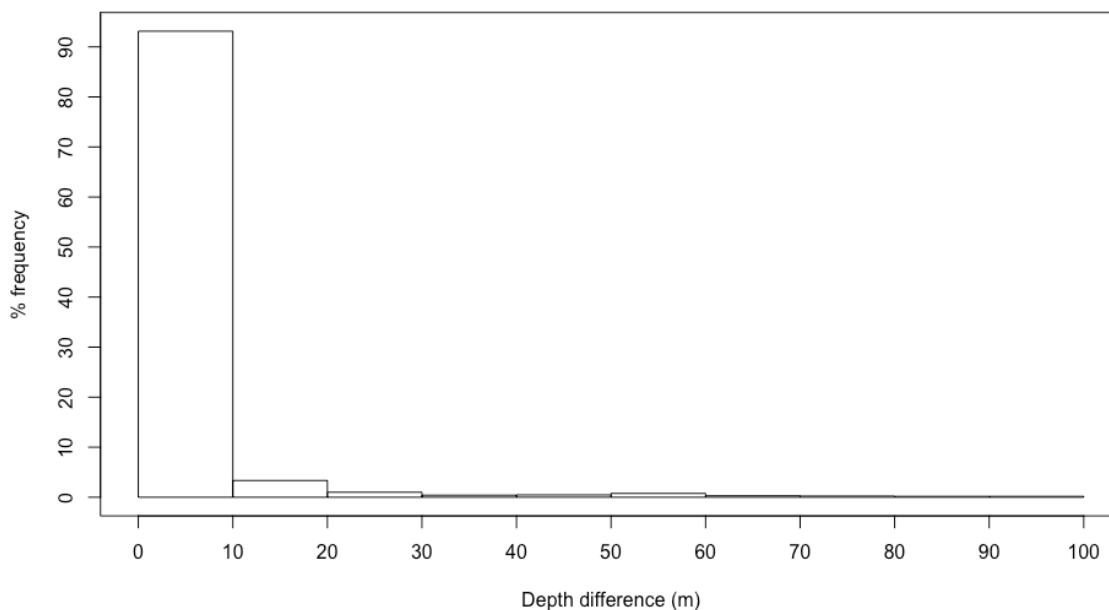


Figure 33 : Frequency distribution (percentage) of the depth difference (m) between successive feeding dives within a bout (as defined by the bout-ending criterion method (Boyd, 1996) in Doniol-Valcroze and Lesage, unpublished data).

- *In situ* preyscape

In-situ krill densities and vertical distributions were estimated from hydroacoustic data collected during systematic surveys conducted each August from 2008 to 2015 in the Estuary and Gulf of St. Lawrence (EGSL, Québec, Canada, 49° 43'N, 65° 11'W) (Figure 34). Two main regions were defined determined according to topographical habitats (i.e. shelf, slope and channel) and the similarity in the pattern of distribution of the centre of mass of krill in each area (McQuinn et al., 2015): the St. Lawrence Estuary (SLE) and the northwestern part of the Gulf of the St. Lawrence which includes the Gaspé Peninsula (NWG). Hydroacoustic data were recorded only during daytime using a calibrated (Demer et al., 2015) Simrad® EK60 multifrequency echosounder (38, 70, 120 and 200 kHz).

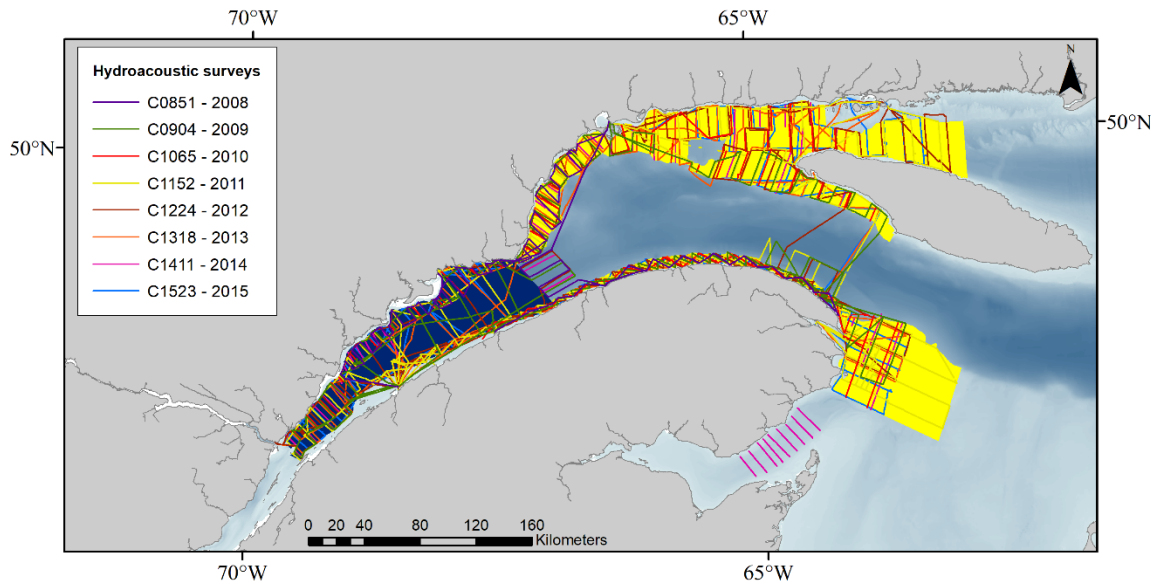


Figure 34 : Locations of hydroacoustic surveys conducted from 2008 to 2015. Colored lines represent the transects for each survey year. The colored polygons represent the two main areas defined into regions: the St. Lawrence Estuary (dark blue) and the northwestern Gulf of St. Lawrence including the Gaspé Peninsula (yellow).

Non-biological echoes and noise from the surface to the seabed reflection were edited from the hydroacoustic data. Echo-integration of the data was done by bins of 25 m on the horizontal axis by 10 m depth on the vertical axis. Prey were acoustically classified using multifrequency algorithms developed for the northwestern GSL (McQuinn et al., 2013). Biological echoes identified as krill were classified into two species, namely *Thysanoessa raschii* and *Meganyctiphanes norvegica*. Although these algorithms are specific for the two dominant species, they do not allow the differentiation between *T. raschii* and *T. inermis* (McQuinn et al., 2013), the latter being a physiologically-similar, yet much less abundant *Thysanoessa* species. Thus, we will be using *Thysanoessa* spp. when referring to krill densities from this genus.

To infer species-specific krill density ($\text{g wet weight m}^{-3}$) for each echo-integrated bin, we used the classified volume backscattering coefficient ($\text{sv in m}^2 \cdot \text{m}^{-3}$) and its logarithmic

form, the mean volume backscattering strength (MVBS or Sv in dB re 1 m²·m⁻³). Krill biomass density was calculated using a weight-based target strength (TS_w) function:

$$TS_w = TS_N - 10\text{Log}(W)$$

where W is the mean individual krill wet weight (g) for each species (56.2 mg and 298 mg for *T. raschii* and *M. norvegica*, respectively) (McQuinn et al., 2013). TS_N is the length-based modelled target strength (McQuinn et al., 2013) for each species assuming average length, and TS_w is -70.0 and -69.0 dB·g⁻¹ for *T. raschii* and *M. norvegica*, respectively. Krill density (D_k) was calculated as:

$$D_k = sv/10^{(TS_w/10)}$$

Krill distribution is anisotropic in relation to the shoreline (Simard & Lavoie 1999; McQuinn et al., 2015). To account for this specificity, only transects perpendicular to the slope were used in the estimation of krill density and krill vertical distribution. A threshold of 4 g wet weight·m⁻³ was used to discriminate between weakly aggregated krill (empty bin cells included), and aggregated krill patches or layers (McQuinn et al., 2015). For each survey, the mean, maximum, minimum and various quantiles of krill density (g wet weight·m⁻³) were used to describe the vertical distributions of bins containing aggregated *Thysanoessa* spp. and *M. norvegica*. Krill, *T. raschii* in particular, has a strong inter-seasonal distributional variability which was not taken into account since all surveys were carried out in August (McQuinn et al., 2015). Inter-region and interannual variability in the mean overall krill density were investigated with a two-way ANOVA. Both year and region had no significant effect on mean krill density for each species (ANOVA; *Thysanoessa* spp.: year: p = 0.09, region: p = 0.08; *M. norvegica*: year: p = 0.6, region: p = 0.6) (Figure 35). Graphical analysis of the vertical distribution of both krill species in each region for all years showed different patterns of vertical density distribution (Figure 21 in main document), albeit no significant differences are detected in overall mean krill density. The differences in the density distributions within the water column lie in the vertical distribution itself, and can be explained by the specificities of habitats encompassed in each region and the depths of center

of mass of each species in each region. As highlighted in McQuinn et al. (2015), the center of mass of each species is located higher in the water column in the Estuary compared to the northwestern part of the Gulf (~80 m vs. ~140 m for *Thysanoessa* spp. and ~110 m vs. ~160 m for *M. norvegica* in the Estuary and the Gulf, respectively). We then determined typical krill vertical density distributions per 10-m depth bin for each species which were considered baseline information in our scenarios. Guilpin et al. (2019) showed that blue whales need to seek out the highest densities of krill to forage efficiently. Therefore, for each depth bin, the krill density was drawn from a uniform distribution of each depth bin from the 75th to the 95th percentiles.

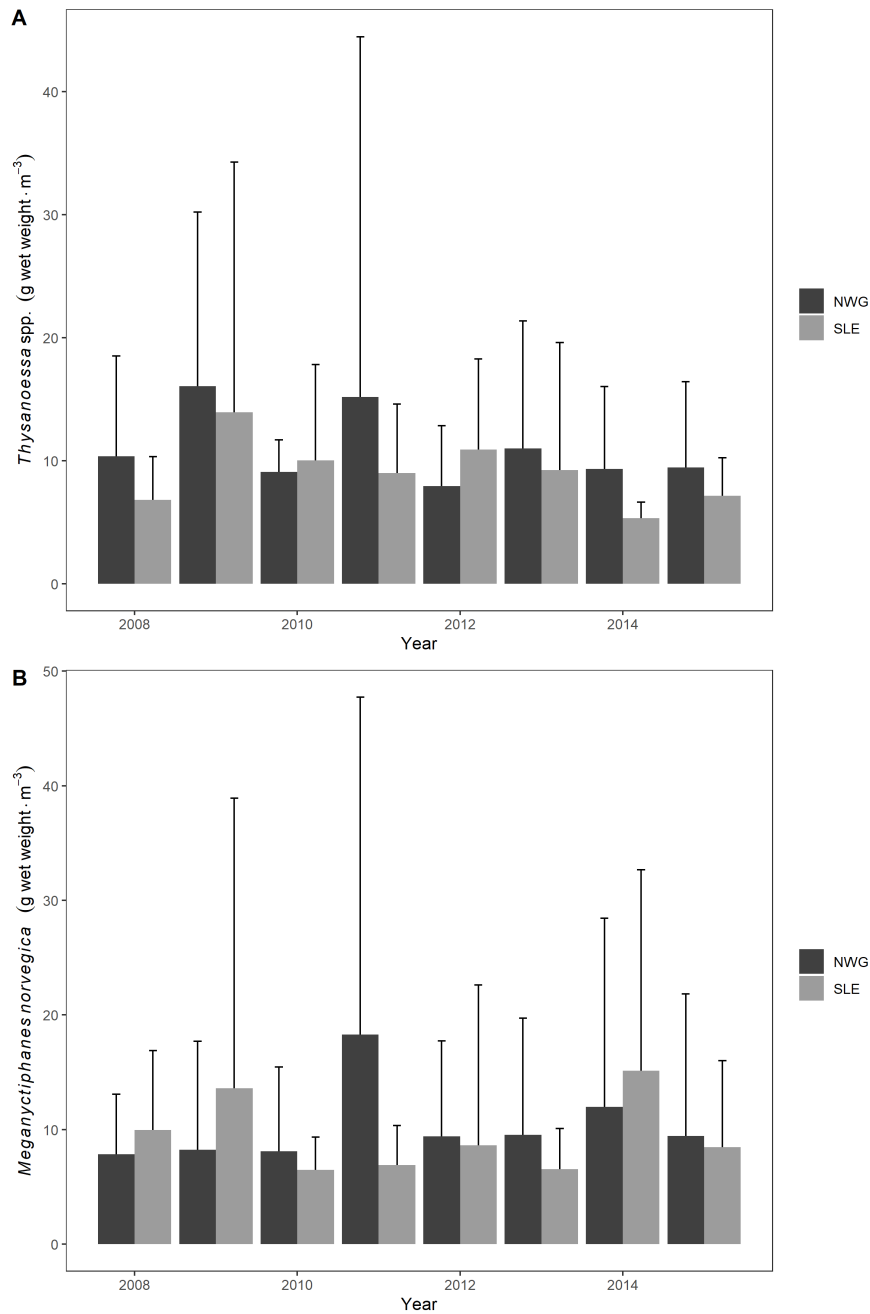


Figure 35 : Inter-annual variations in the mean (\pm SD) krill density (g wet weight m^{-3}) for *Thysanoessa* spp. (A) and *Meganyctiphanes norvegica* (B) from hydroacoustic surveys conducted in the northwestern Gulf of St. Lawrence and Gaspé Peninsula (NWG), and the St. Lawrence Estuary (SLE). Interannual variability was not significant (two-way ANOVAs: p -values > 0.1).

CHAPITRE 3
PREY DENSITY MAY LIMIT THE REPRODUCTIVE CAPACITY OF THE
ENDANGERED WESTERN NORTH ATLANTIC BLUE WHALE
POPULATION

Authors:

Marie Guilpin^{1,2}, Véronique Lesage², Enrico Pirotta^{3,4}, Ian McQuinn², Gesche Winkler¹

¹Institut des Sciences de la Mer, Québec-Océan–Université du Québec à Rimouski,
Rimouski, QC G5L 2Z9, Canada

²Maurice Lamontagne Institute, Fisheries and Oceans Canada, Mont-Joli, QC G5H 3Z4,
Canada

³Dept of Mathematics and Statistics, Washington State University, Vancouver, WA, USA.

⁴School of Biological, Earth and Environmental Sciences, University College Cork, Cork,
Ireland

In preparation

3.1 ABSTRACT

Prey density is one of the main drivers of the foraging behavior, which together with foraging effort determine the ability of individuals to accumulate energy reserves and improve body condition. Baleen whales, and capital breeders in general, accumulate the majority of their energy reserves through efficient foraging during temporally and spatially distinct periods. Blue whales visit the Estuary and Gulf of St. Lawrence (EGSL) seasonally to feed on two predominant krill species, *Thysanoessa spp.* and *Meganyctiphanes norvegica*. We used a mechanistic simulation approach to model the dynamics of the energy reserve accumulation of an adult female blue whale over a feeding season using krill densities documented in the EGSL between 2008 and 2017 from hydroacoustic surveys. Sets of simulations were obtained for each year independently, for five abundance ratios of the two krill species (*Thysanoessa spp.*: *M. norvegica*; 100:0, 75:25, 50:50, 25:75, 0:100), and for four krill density thresholds (> minimum density to achieve neutral energetic balance of diving, > 25th, > 50th, and > 75th percentile of observed densities). We also estimated the costs involved in reproduction (i.e., gestation and lactation), migration and time spent on wintering grounds. Given the krill densities available in the EGSL, whales would need to target mainly the highest densities of *M. norvegica* for their energy reserves to be sufficient to successfully complete a reproductive cycle and wean a calf. Considering that reproduction is one of the first functions to be suppressed by energy allocation mechanisms when energy reserves are sub-optimal, the apparent limited ability for individuals to accumulate adequate energy reserves within the EGSL is consistent with the small number of calves that have been reported over the past 40 years for this endangered population.

Keywords: bioenergetic modelling, energy reserves, krill densities, summer feeding, reproduction success, migration, Estuary and Gulf of St. Lawrence

3.2 RÉSUMÉ

La densité des proies est l'un des principaux moteurs du comportement de recherche de nourriture qui, avec l'effort de recherche déployé, détermine la capacité des individus à accumuler des réserves énergétiques et à améliorer leur condition corporelle. Les baleines à fanons, et les *capital breeders* en général, accumulent la majorité de leurs réserves d'énergie grâce à une alimentation efficace pendant des périodes temporellement et spatialement distinctes. Les rorquals bleus visitent de façon saisonnière l'estuaire et le golfe du Saint-Laurent (EGSL) pour se nourrir de deux espèces de krill prédominantes, *Thysanoessa* spp. et *Meganyctiphanes norvegica*. Nous avons utilisé une approche de simulation mécaniste pour modéliser la dynamique des réserves énergétiques d'un rorqual bleu femelle adulte au cours d'une saison d'alimentation en utilisant les densités de krill documentées dans l'EGSL de 2008 à 2017 à partir de relevés hydroacoustiques. Des séries de simulations ont été effectuées pour chaque année séparément, pour cinq ratios d'abondance des deux espèces de krill (*Thysanoessa* spp.: *M. norvegica*; 100: 0, 75:25, 50:50, 25:75, 0: 100) et pour quatre seuils de densité de krill (> densité minimale pour atteindre l'équilibre énergétique neutre d'une plongée d'alimentation, > 25^{ème}, > 50^{ème} et > 75^{ème} percentile des densités observées). Nous avons également estimé les coûts liés à la reproduction (c'est à dire, la gestation et la lactation), la migration et le temps passé dans les aires d'hivernage. Compte tenu des densités de krill disponibles dans l'EGSL, les rorquals bleus devraient cibler principalement les densités les plus élevées de *M. norvegica* pour que leurs réserves énergétiques soient suffisantes pour un cycle de reproduction réussi et le sevrage d'un veau. Considérant que la reproduction est l'une des premières fonctions à être supprimée par les mécanismes d'allocation d'énergie lorsque les réserves d'énergétiques sont sous-optimales, l'apparente difficulté des individus à accumuler suffisamment de réserves énergétiques adéquates est cohérente avec le petit nombre de veaux répertoriés au cours des 40 dernières années pour cette population en voie de disparition.

Mots clés : modélisation bioénergétique, réserves énergétiques, densités de krill, alimentation, succès reproducteur, migration, estuaire et golfe du Saint-Laurent.

3.3 INTRODUCTION

Energy, acquired through feeding, is an essential prerequisite for survival, growth and reproduction of all animals (Kleiber, 1975). Predators should maximize their foraging efficiency by increasing the energy gained per unit of time compared to energy expended (MacArthur and Pianka, 1966). They do so by adjusting their foraging effort to the prey density experienced while foraging, which can often change dynamically throughout and between feeding bouts (Caraco, 1980; Rosenberg and McKelvey, 1999). Diving predators, such as marine mammals and seabirds, have the capacity to modulate foraging time and effort by varying their feeding depth or the number of feeding attempts (Boyd, 1996; Doniol-Valcroze et al., 2011; Ware et al., 2011; Watanabe et al. 2014; Friedlaender et al., 2016). Therefore, favoring the exploitation of prey that are broadly distributed and in lesser densities but higher in the water column over denser but deeper aggregations, as observed in Antarctic humpback whales (Friedlaender et al., 2016). In addition, diving predators may display distinct feeding strategies depending on prey density and distribution: (1) they prioritize energy conservation when prey are found in more diffuse aggregations closer to the surface, or (2) they maximize gross energy gain when prey are in high densities but at deeper depths (e.g., Hazen et al., 2015). The ability of individuals to accumulate energy reserves and increase body condition consequently depends on the preyscape in their foraging environment and the foraging strategies adopted but also on a predator's ability to modulate these strategies in response to changing prey distribution and availability (Higginson et al., 2012; Higginson and Ruxton, 2015).

When acquired in excess of daily needs, energy is generally stored in the form of fat reserves to be available at a later time when energy demand exceeds intake and provide an indication of body condition (Biuw et al., 2007; Narazaki et al., 2018). For example, body condition has been linked to prey availability and quality in gray whales (*Eschrichtius robustus*) (Soledade Lemos et al., 2020) and harp seals (*Pagophilus groenlandicus*) (Øigård et al., 2013) and to food concentration in fin whales (Lockyer, 2007). Body condition of females, thus energy reserves, is linked to reproductive success, i.e. fecundity, calves growth

and survival (Lockyer, 2007; Christiansen et al., 2014, 2016). Reproduction is one of the most energetically demanding functions in adult female mammals and depends on energy reserves available being above a species-specific threshold (Crocker et al., 2001; Lewis and Kappeler, 2005). Reproductive costs encompass energetic costs associated with both, gestation and lactation, the latter being the most energetically demanding phase (Gittleman and Thompson, 1988). In poor environmental conditions (e.g. food shortage) resulting in poor physiological status (e.g. limited or insufficient blubber reserves), physiological mechanisms regulating energy allocation prioritize processes ensuring survival of the individual rather than growth and reproduction (Bronson, 1989; Schneider, 2004). Reproduction can then be postponed to a later breeding event, or, if mothers have already been inseminated, pregnancy can be terminated (Schneider, 2004). The occurrence of spontaneous abortions during pregnancy as a result of poor body condition has been documented in a number of pinniped species (Guinet et al., 1998; Pitcher et al., 1998; McKenzie et al., 2005; Gibbens et al., 2010). Evidence for an effect of body condition on reproduction come from studies of right whales (*Eubalaena glacialis*), whose ovulation occurred only when blubber reached a certain thickness (Miller et al., 2011), and of North Atlantic fin whales (*Balaenoptera physalus*), whose pregnancy rate declined when blubber thickness decreased and prey availability was low (Williams et al., 2013).

Marine mammals exhibit differences in life-history traits, reproductive strategy, and capacity to accumulate and store energy (Costa, 1993; Lockyer, 2007). Income breeders supply their offspring's energy needs by foraging during the breeding and nursing periods, whereas on the other side of the theoretical continuum, capital breeders fuel reproduction and migration mostly from endogenous reserves previously acquired during an intense feeding season (Jonsson, 1997; Madsen and Shine, 1999; Houston et al., 2007; Wheatley et al., 2008). Capital breeders have evolved physiological adaptations and behavioural strategies that successfully take advantage of relatively short and intense productive periods in specific feeding areas, usually far from their breeding sites in ways that maximize blubber accumulation over a limited time period (Shaw and Couzin, 2013; Avgar et al., 2014). Large

baleen whales, for example, time their migrations with seasonal zooplankton aggregations (Visser et al., 2011; Szesciorka et al., 2019) most likely using their memory of seasonally predictable resource availability (Abrahms et al., 2019; Fagan, 2019).

Blue whales are usually considered capital breeders in the spectrum of reproductive strategies (Schoenherr, 1991; Mate et al., 1999; Lesage et al., 2017a), although foraging and breeding may not always be totally separate (Silva et al., 2013, 2019; Bailey et al., 2009). They feed almost exclusively on aggregations of krill by means of an energetically costly but efficient feeding strategy, called lunge filter feeding (Goldbogen et al., 2011). To forage efficiently and accumulate energy reserves, they must find and target dense aggregations of their main prey, euphausiids or krill (Goldbogen et al., 2011; Guilpin et al., 2019). Blue whales in the western North Atlantic visit the EGSL seasonally to feed on two predominant genera of euphausiids, *Thysanoessa* spp. (including *Thysanoessa raschii* and *Thysanoessa inermis*) and *Meganyctiphanes norvegica* (Gavrilchuk et al., 2014). Krill is neither homogeneously distributed in time nor in space (Watkins and Murray, 1998; McQuinn et al., 2015).

The western North Atlantic blue whale population is listed as endangered by both the Canadian Species at Risk Act and the Endangered Species Act of the United States of America. Current population size is unknown, but is estimated to be in the low hundreds (Sears and Calambokidis, 2002). Only 28 calves have been sighted in over 40 years of observations suggesting an apparent low calving rate (Mingan Island Cetacean Studies unpubl. data). There are growing concerns about the capacity for western North Atlantic blue whales to accumulate sufficient energy reserves to reproduce, especially with environmental variability exacerbated by global warming and foraging disruptions from anthropogenic activities in certain parts of their feeding ground such as the St. Lawrence Estuary, Canada (Martins, 2012; Guilpin et al., 2020). It is thus hypothesized that the low number of calves over the past 40 years for the western North Atlantic blue whale population might be due to an inability to accumulate enough energy reserves to sustain successful reproduction. To investigate this question, we propose a first quantification of the amount of energy potentially

accumulated by blue whales during a feeding season in the EGSL using a simulation approach based on *in situ* measurements of krill densities. The dynamics of energy stores and expenditures was then examined while accounting for both migration and reproduction by linking fine-scale energetics to large-scale processes using available published information.

3.4 MATERIALS AND METHODS

We used a mechanistic simulation approach to estimate the energy reserves that an adult female blue whale can accumulate over a feeding season and which must be sufficient to sustain energetic needs throughout an entire reproductive cycle from pre-conception feeding to calf weaning (Figure 36 and Figure 37). The approach was adapted from the bioenergetics model developed by Pirotta et al. (2018b), and incorporated data on prey availability and blue whale foraging behavior that were specific to our study area, the Estuary and Gulf of St. Lawrence (EGSL). Specifically, krill densities came from hydroacoustic surveys conducted in 2008–2017, whereas behavioral data were obtained from archival tags deployed in an earlier study (e.g., Doniol-Valcroze et al., 2011, 2012). Cost estimates for the various parameters associated with foraging, migration, lactation and gestation were taken from the literature (Table 9), whereas migration patterns were based on satellite telemetry data from this specific population (Lesage et al., 2017a). Energy expenditures associated with each reproductive phase and the entire reproductive cycle were compared to the energy reserves accumulated over the corresponding periods to determine surplus energy accumulation and whether available krill densities were sufficient to support the accumulation of surplus energy reserves which are required for each reproductive phase and the reproduction cycle as a whole. Equations were adjusted from Pirotta et al. (2018b) for a 22-m adult and sexually mature female blue whale (Sears and Calambokidis, 2002). Analyses were conducted using the R programming language (R Development Core Team 2017).

3.4.1 Model Timescale

The exact duration of the feeding season, gestation and lactation is not well documented for blue whales from the Northern hemisphere. Blue whales likely mate in late fall in this region, and give birth in mid-winter of the following year (Sears and Calambokidis, 2002; Sears et al., 2013). Observations of cow-calf pairs are rare in the EGSL (28 cow-calf pairs observed in 40 years of observations), but they spread through part of the summer (8 observations in 2018 ranged from May to August) (R. Sears and Mingan Island Cetacean Studies, unpublished data). Lactation was estimated to last for seven months on average, but may extend over nine months (Lockyer, 1984; Yochem and Leatherwood, 1985).

Accordingly, we set the duration of a full reproductive cycle at 27 months, which included two and a half consecutive feeding seasons interspersed with periods of migration (Figure 37). Under this proposed timeline, a female would get pregnant in early winter after a first feeding season, would give birth to a calf the following winter after an 11-month gestation (Lockyer, 1984), and would wean the calf seven months later, about halfway through the third feeding season. Blue whales are reported acoustically in the EGSL throughout the year (Simard et al., 2016), and are observed more regularly from May to December (Sears and Calambokidis, 2002). We assumed that females migrated to and back from the breeding grounds each year. However, there is currently no data to determine if mature females at all reproductive stages leave the feeding grounds each year and thus, whether individuals overwintering in the EGSL include pregnant and resting adult females.

Satellite telemetry data indicates that migration to the breeding ground occurs generally in December (Lesage et al., 2017a), an observation supported by a peak in acoustic detections at the main passage to the EGSL in Cabot Strait in November-December (Simard et al., 2016). We assumed a return to the EGSL in April, based on limited satellite telemetry data (Lesage et al., 2017a) and peaks in blue whale ice-entrapments in March-April in the southeast Gulf of St. Lawrence near Cabot Strait (Moors-Murphy et al., 2019; Stenson and Lawson, unpubl. data). However, these satellite telemetry data are imprecise about the

duration of migration, which may last from three to five weeks (several records never reached the wintering grounds). We therefore assumed the migration to last one month on average, in April and December, leading to a seven month foraging season.

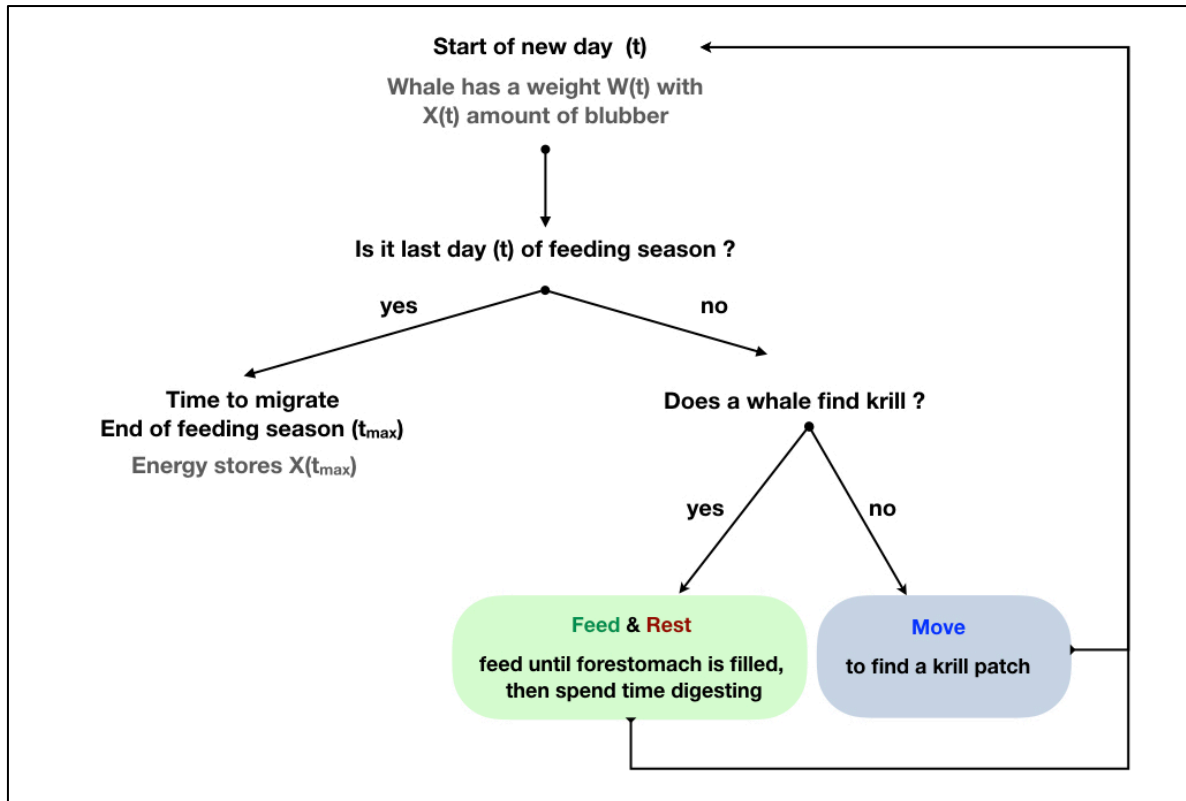


Figure 36 : Model framework used to estimate the energy accumulated in the form of blubber mass by an adult female blue whale foraging for seven months in the Estuary and Gulf of St. Lawrence. Parameters and their values are provided in Table 9.

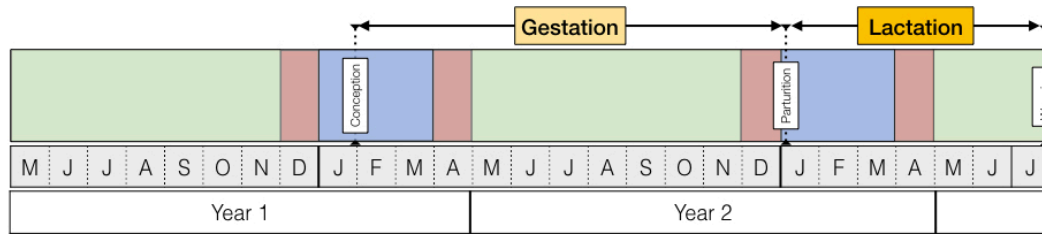


Figure 37 : Timescale for time spent on feeding grounds (green), migrating (red), and time spent on wintering grounds (blue). Reproductive status of adult females is indicated as follow: pregnant (yellow) and lactating (orange). Key events of the reproduction (conception, parturition and weaning) are indicated with arrows and white labels.

3.4.2 Preyscape–krill density

Krill aggregations are highly dynamic both in time and space (Miller and Hampton, 1989; Watkins and Murray, 1998; Maps et al., 2012; McQuinn et al., 2015). Capturing the complexity of krill aggregation densities and distribution throughout the blue whale foraging habitat and feeding season was beyond the scope of this paper. Species composition varies across the blue whale foraging habitat in the western North Atlantic (Cochrane et al., 1991, 2000; McQuinn et al., 2015). However, environmental factors driving yearly variations in krill densities likely act over regions that are larger than just the EGSL (Hutchings et al., 2012; Galbraith et al., 2019). Based on this assumption, we considered krill densities and inter-annual variability patterns documented in the EGSL from long-term hydroacoustic surveys to be representative of the variations that blue whales from this subpopulation likely encountered elsewhere in their feeding habitat.

The systematic hydroacoustic surveys span 10 years between 2008 and 2017 and covered the St. Lawrence Estuary and northwestern Gulf of St. Lawrence (Canada) (Figure 41 in Supplementary information). Although krill has a strong intra-seasonal distributional variability, this could not be taken into account since all surveys were carried out in August

(McQuinn et al., 2015). All hydroacoustic data were recorded using a calibrated (Demer et al., 2015) Simrad® EK60 multifrequency echosounder (38, 70, 120 and 200 kHz). To account for the anisotropic krill distribution in relation to the shoreline, only transects perpendicular to the continental slope were used in the estimation of krill density. Hydroacoustic data were edited to remove non-biological echoes and noise from the surface and seabed reflection. Data were echo-integrated into 25-m bins on the horizontal axis, and 10-m bins on the vertical axis. Biological echoes were classified using acoustic multifrequency algorithms developed for the study area, allowing the identification of euphausiids to the genus, namely *Thysanoessa* spp. (which includes *Thysanoessa raschii* and *Thysanoessa inermis*) and *Meganyctiphanes norvegica*. Bins without any krill echoes were excluded from the analysis. Species-specific krill densities ($\text{g wet weight} \cdot \text{m}^{-3}$) were inferred for each echo-integrated bin, by using the classified mean volume backscattering coefficient (s_v in m^{-1}) and its logarithmic form, the mean volume backscattering strength (MVBS or S_v in $\text{dB re } 1 \text{ m}^{-1}$). Krill density was calculated using a weight-based target strength (TS_W) function:

$$TS_W = TS_N - 10\text{Log}(M)$$

where M is mean individual krill wet weight (g) for each species (56.2 mg and 298 mg for *Thysanoessa* spp. and *M. norvegica*, respectively; McQuinn et al., 2013), TS_N is the length-based modelled target strength for each species assuming average length, and TS_W is -70.0 and -69.0 $\text{dB} \cdot \text{g}^{-1}$ for *Thysanoessa* spp. and *M. norvegica*, respectively (McQuinn et al., 2013). Krill density (j) per bin was calculated as follows:

$$j = sv/10^{(TS_W/10)}$$

Krill densities needed to be $\geq 4 \text{ g m}^{-3}$ to be considered an aggregation (McQuinn et al., 2015) and to be considered suitable prey aggregations available to foraging blue whales. We then generated a distribution of densities per bin ($\text{g} \cdot \text{m}^{-3}$) for each survey year and krill species to extract from the available habitat the densities that can lead at least to neutral energy balance in a 22-m blue whale. This was done by including only densities above $\sim 16 \text{ g} \cdot \text{m}^{-3}$ for *M. norvegica* and $\sim 19 \text{ g} \cdot \text{m}^{-3}$ for *Thysanoessa* spp. (Guilpin et al., 2019), and by

fitting the data with a gamma distribution, which allowed capturing the highest observed densities and their frequency of occurrence in our study area. These values represented the minimum krill density required to balance hourly energy expenditure of SLE blue whales when foraging (Guilpin et al., 2019). Note also that these thresholds likely represent underestimates of the krill densities required to maintain a positive energy balance over longer term, as they were strictly specific to foraging bouts, i.e., they did not take into account the energy expenditures associated with other behaviors, including resting, time spent searching for food or other non-foraging behaviours such as courtship or other physiological processes such as gestation or carrying a growing foetus (Guilpin et al., 2019).

3.4.3 Energy balance over the feeding season

The model was run so that on each day (t) of the feeding season, a female blue whale could either travel to find a food patch or forage in a patch with potentially suitable krill densities (Figure 36). The probability of a whale being in a foraging mode or searching mode on day t was based on the matrix of transition probabilities between the two behavioral modes estimated from satellite telemetry data collected in our study area (Lesage et al., 2017a). The probability of being in a specific mode depended on the behavioral mode on the previous day ($t - 1$) (Table 9). On days when whales were in foraging mode, their time was split between feeding and digesting/resting, proportions that were dependent on the density of krill they encountered and fed upon (Supplementary information). On days when whales were in searching mode, we assumed they travelled for the entire day.

The daily energy gain and expenditure associated with foraging (i.e. including feeding, digesting and searching for food patches) were estimated using bioenergetic equations parameterized for blue whales (Wiedenmann et al., 2011; Pirotta et al., 2018b). The blubber mass (kg) remaining after a day (t) spent searching for food was defined as in Pirotta et al. (2018b):

$$X(t + 1) = X(t) - \frac{COT(t) \cdot d \cdot W(t)}{u}$$

where $COT(t)$ is the cost of transport ($\text{kJ} \cdot \text{kg}^{-1} \cdot \text{km}^{-1}$) (Williams, 1999), d is the distance travelled (km), $W(t)$ is body weight (kg), and u is the usable energy in the blubber ($\text{kJ} \cdot \text{kg}^{-1}$). The swimming speed of a whale in transit mode was extracted from the satellite telemetry data (Lesage et al., 2017a). Specifically, a value of speed was drawn from a normal distribution centered on an average speed of $5.6 (\pm 2.5 \text{ km} \cdot \text{h}^{-1})$ for each simulated day, and used to calculate the distance d travelled over 24 h.

The resulted total blubber mass (kg) accumulated after a day spent foraging (t) on a given krill density drawn from the binned density distribution was defined as in Pirotta et al. (2018b):

$$X(t + 1) = X(t) + (y_j - C_f(t) - C_r(t))/u$$

where $C_f(t)$ is the cost of feeding (kJ), $C_r(t)$ is the cost of resting (kJ), $y(j)$ is the energy gain (kJ) obtained from feeding on krill density j , and u represents the amount of usable energy in the blubber ($\text{kJ} \cdot \text{kg}^{-1}$). Costs of feeding and resting depend on a number of parameters, and are presented in details in the Supplementary information. Given the energetic efficiency of blue whale movements, the costs of any small-scale movements within a foraging area were assumed to be comparable to the energy expended while resting (Williams, 1999). In cases where energy expenditures associated with feeding on a specific krill density surpassed energy gains, we assumed that the whale would not forage on that day, and that energy expenditures on that day would equal those associated with resting. The number of lunges per hour could not be linked to krill density and depth considering the absence of blue whale behavioural data simultaneous to hydroacoustic surveys. Therefore the number of lunges performed per hour was taken as the average from Guilpin et al. (2019) and fitted with a Weibull distribution (scale = 28, shape = 4) (Supplementary information).

The gross energy intake from feeding (kJ) was calculated as in (Pirotta et al. (2018):

$$y_j = n_j \cdot \Psi \cdot \rho \cdot A$$

where n_j is the number of times the forestomach can be filled in a day, which depends on the krill density j , Ψ is the whale length-specific forestomach capacity (kg), ρ is the krill energy content ($\text{kJ} \cdot \text{g}^{-1}$), and A is the assimilation efficiency (see Table 1 and Supplementary information for additional details on these parameters).

The total energy reserves (MJ) and the resulting blubber mass X (kg) (assuming that 1 kg of blubber corresponds to 31,798 MJ; Lockyer, 1981), at the end of the feeding season (t_{max}) resulted from the initial condition of an individual, the costs associated with days spent travelling searching for food, and the energy expenditures and gains associated with days of foraging. On average, 27% of a blue whale's total mass is blubber with 73% lean tissue (i.e., muscle, bone and viscera) (Lockyer, 1976). Sixteen percent has been the lowest blubber proportion reported in the literature (Lockyer, 1976, 1981), which likely represents the blubber proportion at the end of winter. It is unlikely that whales reach the feeding grounds with a blubber proportion higher than the average or lower than 16%. Therefore we drew the blubber percentage on the first day of the feeding season ($X(t=0)$) from a uniform distribution ranging between the lowest record and the average blubber proportion, i.e., 16 to 27%, which is equivalent to 8,000–15,000 kg of blubber proportion (equivalent to ~255,000–480,000 MJ) for a 22-m adult whale. We set the maximum quantity of blubber that a whale can accumulate (i.e. maximum energy storage capacity) to 35% of total mass, or 22,000 kg of blubber (~700,000 MJ) for a 22-m whale (Lockyer, 1976; Wiedenmann et al., 2011; Pirota et al., 2018b). The minimum blubber proportion was set to 5% (2,000 kg or ~160,000 MJ), representing a case of extreme leanness, at which the whale would be assumed to die from starvation (Pirota et al., 2018b). Although fat can accumulate in tissues other than blubber, such as muscle and viscera (Lockyer, 1984; Lockyer et al., 1985), we assumed that whales only stored and used energy from the blubber. All parameter values and sources are detailed in Table 9.

We ran simulations for different scenarios to account for potential changes in preyscape (i.e. simply the relative proportion of the two species) and species availability as a result of short-term or longer-term variability (e.g., Guilpin et al., 2020), and to examine the effect of

constraining feeding to densities that correspond to different foraging efficiencies (Guilpin et al. 2019). Specifically, we drew from species- and year-specific distributions that theoretically allowed achieving neutral energy balance (~ 16 or $\sim 19 \text{ g} \cdot \text{m}^{-3}$ depending on krill species), but also from distributions where species-specific krill densities exceeded the 25th, 50th, and 75th percentiles above the 16 or 19 $\text{g} \cdot \text{m}^{-3}$ thresholds. Simulations accounting for changes in preyscape had ratios of 100:0, 75:25, 50:50, 25:75, and 0:100 for *Thysanoessa* spp. and *M. norvegica*, respectively. For example, at a ratio of 75:25, we assumed the whale to feed each day on *Thysanoessa* spp. with a probability of 0.75 and on *M. norvegica* with a probability of 0.25. Sets of 1000 iterations were run for each scenario to obtain a mean, standard deviation (SD), and 95% confidence interval (CI) around the estimated energetic reserves that a 22-m female blue whale was likely to accumulate over the course of a feeding season.

3.4.4 Costs of migration and movements on wintering grounds

We estimated the costs of migration between feeding and wintering grounds, and of movements within wintering areas using satellite telemetry data from this population (Lesage et al., 2017a; Lesage, unpublished data). The migratory distance varied amongst tagged whales, as a result of destination and duration of tag deployment, and averaged $1,550 \pm 2,657$ km (range 99 to 11,918 km). We used distances travelled by the four whales with the longest tag deployments outside the feeding area (2-6 months corresponding to migratory distances of 2,466, 5,794, 5,804 and 11,918 km) to generate a distribution of daily travelled distances centered on an average of $58.7 (\pm 11.9 \text{ km} \cdot \text{d}^{-1})$, which allowed us to explicitly incorporate observed variability around movement speeds. We simulated movements for 1000 females and associated daily energy expenditures as follows (Williams, 1999; Wiedenmann et al., 2011; Pirotta et al., 2018b):

$$C_m(d) = COT \cdot W(t) \cdot d$$

where COT is the cost of transport ($\text{kJ} \cdot \text{kg}^{-1} \cdot \text{km}^{-1}$), $W(t)$ is the weight of the individual (kg) and d is the daily distance travelled within the wintering area or for reaching it ($\text{km} \cdot \text{d}^{-1}$). This assumed that individuals were moving (and not feeding) throughout the entire migration period.

3.4.5 Cost of reproduction

The cost of reproduction corresponded to the sum of energy expenditures from gestation and lactation. Direct costs of gestation (in $\text{kJ} \cdot \text{d}^{-1}$) included the production of fetal tissues and heat increment from gestation, which we defined on a daily basis (g) as in Pirotta et al. (2018b):

$$C_g(g) = w_f(g) \cdot c_p + h(g)$$

where w_f is the weight of the fetus on each day of gestation g (kg), c_p is the cost of producing a unit of fetal mass ($\text{kJ} \cdot \text{kg}^{-1}$) and h is the heat increment associated with gestation, which was defined as in Lockyer (1981, 2007):

$$h_{gt}(g) = p(g) \cdot (4,400 \cdot 4.184 \cdot w_b^{1.2})$$

where p is the proportional daily growth of the fetus and w_b is the weight of the calf at birth (kg) (Table 9).

Gestation also incurred indirect costs as a result of the added weight from carrying a fetus and its effect on metabolic rates and cost of transport, which are both mass-specific. The added mass of the growing fetus and corresponding energy expenditures were adjusted daily for pregnant females from the month of conception in wintering areas to parturition the following year (Figure 37).

The mean cost (and 95% confidence interval) for the seven month lactation was estimated from 1000 simulations. The amount of milk delivered each day was drawn from a

uniform distribution assumed to vary between $90 \text{ kg} \cdot \text{d}^{-1}$ (Lockyer, 1981) and $220 \text{ kg} \cdot \text{d}^{-1}$ (Oftedal, 1997). The daily cost of lactation $C_l(lt)$ (in kJ d^{-1}) was calculated as follows:

$$C_l(lt) = M(lt) \cdot e/E$$

where M is the amount of milk delivered (kg) daily by a female, e is the milk energy content ($\text{kJ} \cdot \text{kg}^{-1}$), and E is the mammary gland efficiency (Table 9). This allowed incorporating the uncertainty associated with the effect of body condition of the mother and calf, and phase of lactation into the amount of energy delivered to the calf.

3.4.6 Full reproductive cycle

We then put into perspective the energy accumulated over successive feeding seasons, with the costs associated with migration, time on wintering grounds and reproduction cycle using yearly densities of krill obtained from the hydroacoustic surveys. We modelled an entire reproductive cycle of a female, from the start of pregnancy to the end of lactation, i.e., over 2.5 consecutive feeding seasons with 2011 and 2014 as starting points. Those two years had the highest mean krill densities of *M. norvegica* specifically, positioning the feeding female in the best preyscape years in our time series, and thus in the best conditions to accumulate energy reserves, see below.

Table 9 : Input parameters, associated sampling distributions (where applicable) and/or values used in the model framework.

Parameters	Description (units)	Value	Data source
a	Whale length of an adult female in the northern hemisphere (m)	22	Sears and Calambokidis (2002)
W	Mean mass of a 22 m adult female (kg)	57,000	Lockyer (1976)
g	Whale mean non blubber mass (kg)	42,000	Lockyer (1976)
$W(t)$	Whale mass at time t (kg)	$g + X(t)$	Lockyer (1976)
u	Utilizable energy in blubber ($\text{kJ} \cdot \text{kg}^{-1}$)	31,798	Lockyer (1981)
$RAAMR$	Rorqual average active metabolic rate ($W \cdot \text{kg}^{-1}$)	2.15	Potvin et al. (2012)
$BMR(t)$	Basal daily metabolic rate ($\text{kJ} \cdot \text{d}^{-1}$)	$4 \times W(t)^{0.75} \times 86,400/1,000$	Kleiber (1975)
$RMR(t)$	Resting daily metabolic rate ($\text{kJ} \cdot \text{d}^{-1}$)	$2 \times BMR(t)$	Potvin et al. (2012)
β	Length-specific engulfment volume (m^3)	$0.0011 \times a^{3.56}$	Goldbogen et al. (2010)
Ψ	Forestomach capacity (kg)	$0.47 \times a^{2.88}$	Vikingsson (1997); Wiedenmann et al. (2011)
t_e	Forestomach clearing time (h)	4	Vikingsson (1997)
j_{Tr}	Krill density <i>Thysanoessa</i> spp. ($\text{g} \cdot \text{m}^{-3}$)	Gamma distribution year-specific	Hydroacoustic surveys, this study
j_{Mn}	Krill density <i>M. norvegica</i> ($\text{g} \cdot \text{m}^{-3}$)	Gamma distribution year-specific	Hydroacoustic surveys, this study
ρ_{Tr}	Krill energy content ($\text{kJ} \cdot \text{g}^{-1}$) <i>Thysanoessa</i> spp.	4.3 ± 0.58 Normal distribution	D. Chabot (unpubl.data)
ρ_{Mn}	Krill energy content ($\text{kJ} \cdot \text{g}^{-1}$) <i>M. norvegica</i>	5.2 ± 0.45 Normal distribution	D. Chabot (unpubl.data)
A	Assimilation efficiency	0.84	Goldbogen et al. (2011)
ω	N lunges per hour ($\text{L} \cdot \text{h}^{-1}$)	Weibull distribution Scale = 28 ; shape = 4.8	Guilpin et al. (2019)

Table 9 continued

Parameters	Description (units)	Value	Data source
h_f	Max. n hours available for feeding per day	24	Guilpin et al. (2019)
COT	Cost of transport ($\text{kJ} \cdot \text{kg}^{-1} \cdot \text{km}^{-1}$)	$7.79 * W(t)^{-0.29}$	Williams (1999)
$d(m)$	Daily distance travelled during winter ($\text{km} \cdot \text{day}^{-1}$)	58.7 ± 11.9 Normal distribution	Lesage et al. (2017a), Lesage (unpubl. data)
$w_f(g)$	Foetus mass at time gt of gestation (kg)	$[0.52 * (gt - 73)]^3 / 1000$	Huggett and Widdas (1950)
$h(g)$	Heat of gestation at time gt of gestation (kJ)	$p(gt) * (4400 * 4.184 * w_b^{1.2})$	Lockyer (1981, 2007)
$p(g)$	Proportional daily growth of foetus	$w_f(gt) / w_b$	Huggett and Widdas (1950)
w_b	Final weight of foetus at calf's birth (kg)	2,500	Huggett and Widdas (1950)
c_p	Cost of producing one kg of foetus ($\text{kJ} \cdot \text{kg}^{-1}$)	12,300	Lockyer (1981, 1987, 2007)
M	Amount of milk delivered per day ($\text{kg} \cdot \text{d}^{-1}$)	90–220 Uniform distribution	Lockyer (1981); Oftedal (1997)
e	Milk energy content ($\text{kJ} \cdot \text{kg}^{-1}$)	17,309	Lockyer (1981)
E	Mammary gland efficiency	0.9	Brody (1968)
l	Duration of lactation (days)	212 (i.e. 7 mo)	Lockyer (1984); Tillman and Donovan (1986); Pirota et al. (2018b)
g_{max}	Duration of gestation (days)	334 (i.e. 11 mo)	Lockyer (1984); Sears and Calambokidis (2002); Pirota et al. (2018b)
t_{max}	Duration of feeding season (days)	210 (i.e. 7 mo)	Sears and Calambokidis (2002); Lesage et al. (2017a); Simard et al. (2016)
m_{max}	Duration of migration and overwintering period (days)	150 (i.e. 5 mo)	Lesage et al. (2017a)

3.5 RESULTS

3.5.1 Preyscape–krill density

Over the ten year study period, prey densities that allowed achieving at least neutral energy balance were on average $54 \pm 26 \text{ g} \cdot \text{m}^{-3}$ (mean \pm SD) for *Thysanoessa* spp., and $80 \pm 43 \text{ g} \cdot \text{m}^{-3}$ (mean \pm SD) for *M. norvegica* (Table S1). *Thysanoessa* spp. found in densities suitable for foraging blue whales represented between 1.7 and 26.1% of the densities that were available in the EGSL (i.e., in excess of $4 \text{ g} \cdot \text{m}^{-3}$) depending on years, a proportion that declined to 0.4 and 6.5% when considering only the highest available densities (75th percentile of the yearly maximum; Table 11 in Supplementary information). Similarly, densities leading to at least neutral energy balance varied for *M. norvegica* from 2.9–21.6% of available densities, and declined to 1.2–5.4% when increasing the density threshold to > 75th percentile. Overall, the species offering the highest mean densities varied depending on years for all suitability thresholds, except when considering only the highest suitable densities (> 75th percentile threshold), in which case *M. norvegica* offered higher densities to blue whales than *Thysanoessa* spp. in seven of the ten years of study (Figure 38). However, when considering suitable densities in absolute terms, i.e., when considering the number of bins with densities above minimal suitability, *Thysanoessa* spp. offered almost each year a larger foraging habitat to blue whales than *M. norvegica*, regardless of the threshold used (Figure 38; Figure 42 and Table 11 in Supplementary information).

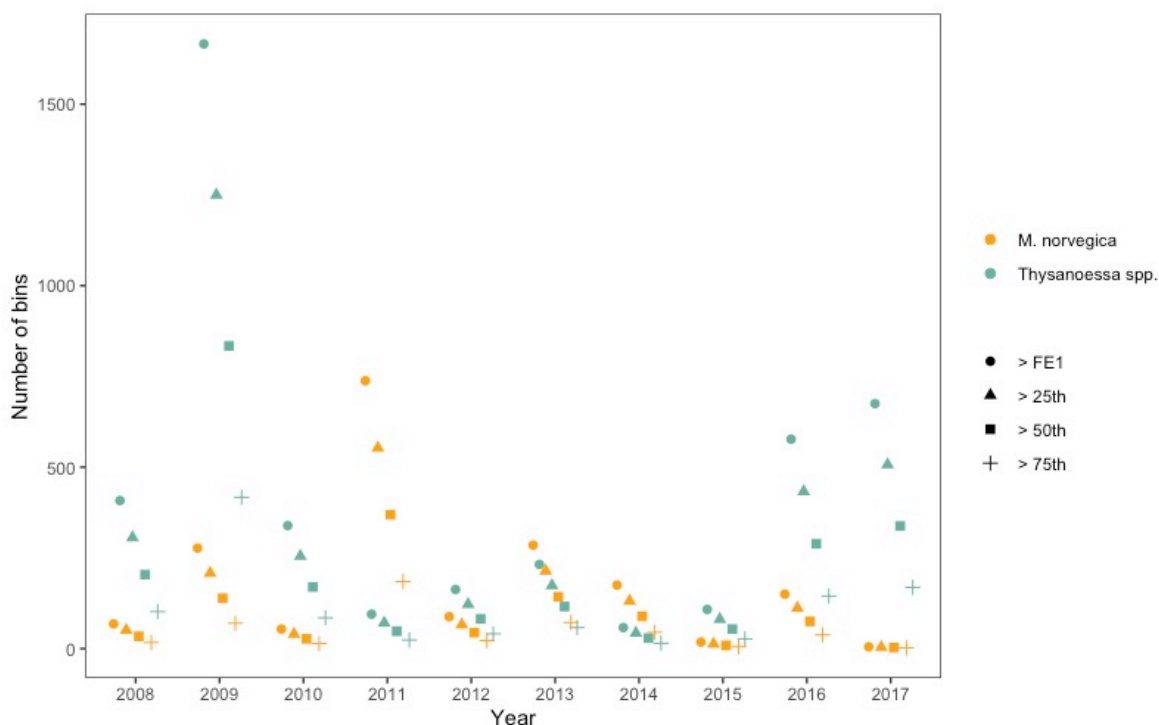


Figure 38 : Number of bins above each threshold ($> FE1$, $> 25^{th}$, 50^{th} and 75^{th} percentiles) for both krill species (*Thysanoessa* spp. and *M. norvegica*) from hydroacoustic surveys conducted yearly from 2008 to 2017.

3.5.2 Energy balance over the feeding season

During the feeding season, we estimated that whales spent on average 63% ($\pm 8\%$ SD) of their time feeding, and 37% ($\pm 9\%$ SD) of their time searching for food or travelling between suitable krill aggregations. The total energy accumulated in the form of blubber at the end of the feeding season varied between years depending on the availability of suitable krill densities, and those targeted by whales (Figure 39, Table 12 in Supplementary information). Details of all simulations are presented in Supplementary information (Figures 43 to 46 in Supplementary information).

In our simulations, blue whales had to seek densities considerably higher than those achieving neutral balance to accumulate energy reserves, i.e., to get above the 15,000 kg (or ~480,000 MJ) initial blubber mass (Figure 4). They had the potential to accumulate on average 2.5 times more energy when feeding on krill densities above the year-specific 75th percentile than on densities achieving neutral energy balance (Table 12 in Supplementary information). However, overall, the capacity of blue whales to reach average or maximum energy reserves remained highly limited over the study period, regardless of the species ingested. To accumulate fat reserves, whales had to seek *M. norvegica* and not *Thysanoessa* spp., and the few bins where krill densities were very high (above 75th percentile). Generally energy reserves accumulated by the end of the feeding season were higher in years when maximum krill densities of either species exceeded $100 \text{ g} \cdot \text{m}^{-3}$ (Figure 39, Table 11, Table 12 in Supplementary information), and when the proportion of *M. norvegica* over *Thysanoessa* spp. increased in the diet (Figure 39, Table 12 in Supplementary information). When whales were assumed to feed solely on *M. norvegica* (ratio 0:100) at densities above the 75th percentile of the maximum suitable densities observed, they were able to reach their maximum energy storage capacity (i.e. the maximum blubber that a whale can accumulate) in only three of the ten years of the study period (Figure 39, Table 12 in Supplementary information). In none of the scenarios where whales were assumed to feed proportionally more on *Thysanoessa* spp. than *M. norvegica* were the maximum energy reserves reached. They could end the feeding season with energy reserves above average (i.e., 15,000 kg of blubber, or ~480,000 MJ) in only two years (2011 and 2016) (Figure 39, Table 12 in Supplementary information). We also found that energy reserves reached average or maximum blubber mass in consecutive years only in simulations with krill densities above the 75th percentile and when krill ratios in the diet were dominated by *M. norvegica* (i.e. ratios of 25:75 and 0:100) (in years 2011–2012 and 2014–2016) (Figure 39 and Table 12 in Supplementary information).

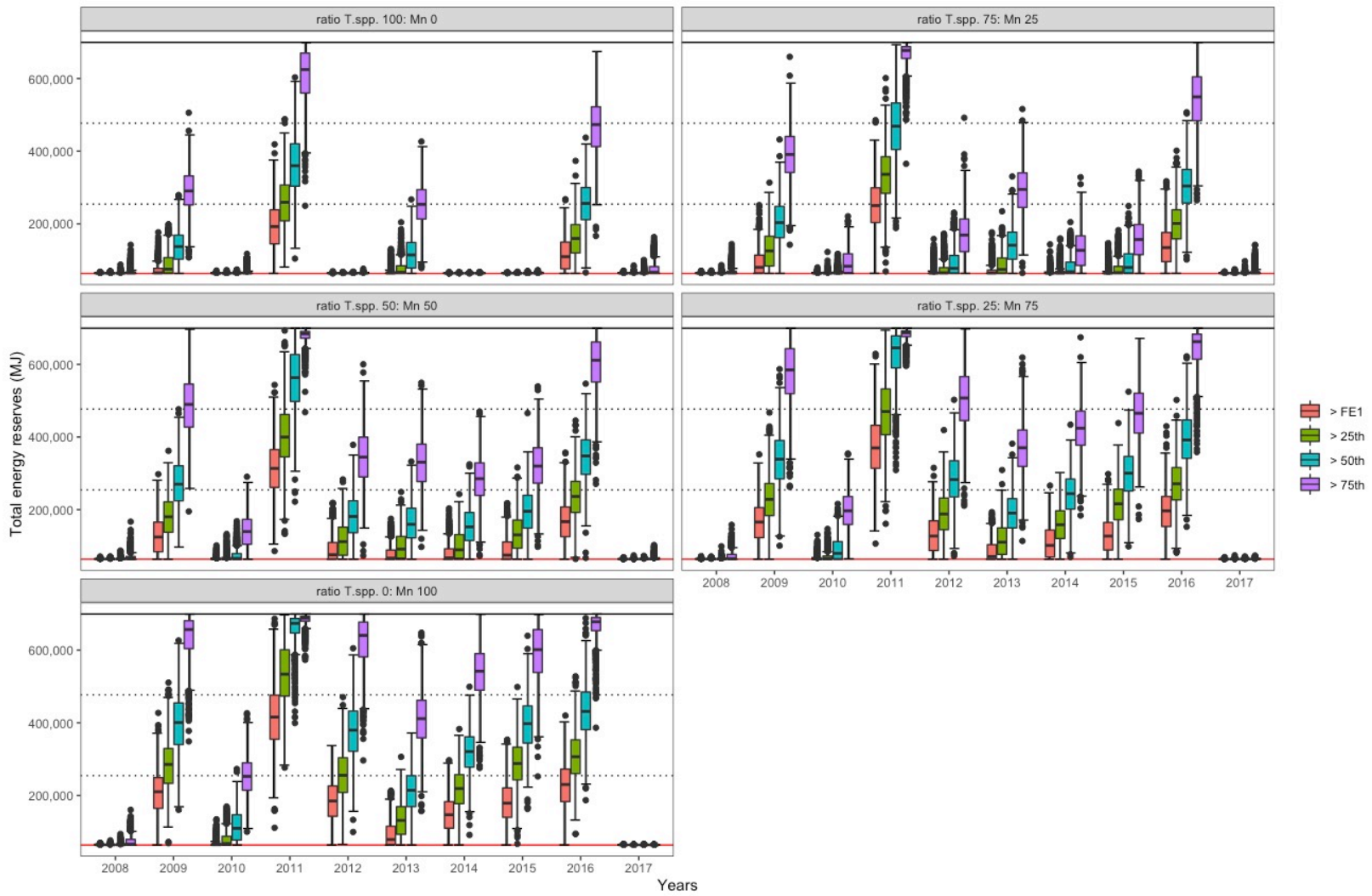


Figure 39 : Yearly variation in total energy stored in blubber (MJ) at the end of a 7-month foraging period according to year-specific krill densities measured during hydroacoustic surveys in the Estuary and Gulf of St. Lawrence. Results are presented for diets comprised of different ratios of *Thysanoessa* spp. (T. spp.) and *M. norvegica* (Mn) (panels) and assuming that whales target prey densities that allow neutral energy balance, or densities allowing higher foraging efficiencies ($> 25^{\text{th}}$, $> 50^{\text{th}}$, $> 75^{\text{th}}$ percentiles of maximum observed densities in a specific year). Boxplots present the median (solid horizontal line), lower and upper quartiles (boxes), extreme values (whiskers) and outliers (points). The black dotted lines indicate the initial range of blubber masses (8,000–15,000 kg or $\sim 255,000$ – $480,000$ MJ) at the beginning of the simulations. Maximum energy reserves (equivalent to 22,000 kg of blubber or $\sim 700,000$ MJ) is indicated by the solid black line while minimum blubber proportion for survival (5% or 2,000 kg, or $\sim 160,000$ MJ) is indicated by the horizontal red solid line. Detailed simulation results for krill densities above all thresholds (FE=1, 25^{th} , 50^{th} and 75^{th}) are presented in Supplementary information.

3.5.3 Costs of migration and movements on wintering grounds

Simulated migrating and overwintering whales travelled an average of 8812 (\pm 140 km) during the 5-months period with an average distance travelled per day of 58.7 (\pm 11.9 km \cdot d⁻¹). The total energetic costs of migrating between feeding and wintering grounds, and of displacements within the wintering grounds was estimated to 163,658 \pm 2,638 MJ (95% CI: 159,312–167,743 MJ) for the 5-months period.

3.5.4 Cost of reproduction

Direct added costs of gestation (i.e., producing fetal tissues and heat of gestation) increased exponentially with gestation time as the weight of the fetus increased (Figure 46 in Supplementary information). They were estimated at 250,822 MJ for a calf weighting 2,500 kg at birth (Figure 46A in Supplementary information), and were mostly incurred during the second half of pregnancy. The increase in energy consumption associated with carrying a fetus was also related to fetus weight (Figure 46B, Table 13 in Supplementary information), the average total added cost over the entire gestation period was estimated on average at 6,653 MJ (95% CI: 2,604–11,012 MJ) (Figure 47 in Supplementary information). Adding these two components led to an estimated cost for this reproductive phase of 257,477 MJ (95% CI: 254,872–268,489). Nevertheless, the gestation phase lasts 11 months; therefore the costs incurred span over the first overwinter period, the second feeding season and the following month migrating back to the wintering grounds (Figure 37) which correspond to 82 MJ, 167,129 MJ and 83,617 MJ for each period, respectively (Table 10).

In the case of lactation, we estimated energy expenditures at 632,185 \pm 10,340 MJ (95% CI: 614,938–649,528 MJ) for a female delivering between 90 and 220 kg of milk per day over the 7-month period (Figure 48 in Supplementary information). The costs associated with the first four months of the lactation period were estimated at 358,088 \pm 7,829 MJ (95%

CI: 345,161–370,784 MJ) while the costs of lactation incurred from the three months of lactation while on the feeding grounds were estimated at $274,097 \pm 2,511$ MJ (95% CI: 269,777–278,743 MJ ; Table 10).

Total reproduction costs including gestation and lactation until weaning reached 889,662 MJ (95% CI: 872,114–918,017 MJ), with lactation accounting for 70% of total costs.

3.5.5 Overall reproductive cycle

To go through parturition in wintering areas and full lactation, a pregnant female would need to accumulate a minimum energy reserve of $\sim 670,000$ MJ (equivalent to $\sim 21,000$ kg of blubber) when they leave the feeding area prior to calving. This includes the minimum of $\sim 63,596$ MJ (or 2,000 kg of blubber) to avoid dying of starvation, the costs associated with the last month of pregnancy ($\sim 83,617$ MJ and $\sim 1,729$ MJ), and the costs of the first four months of lactation ($\sim 358,088$ MJ) (Table 10). The costs of the last three months of the lactation estimated to $274,097$ MJ ($\pm 10,340$ MJ) can be fueled by the last feeding season, considering that they can feed during this time when they are back in feeding areas with their calf. In comparison, a non-pregnant female would need to accumulate at least $227,254 \pm 26,378$ MJ over one feeding season to fuel the costs of migration and overwintering period, which are estimated at $163,658 \pm 26,378$ MJ, and an additional $\sim 63,596$ MJ (or 2,000 kg of blubber) to avoid dying of starvation (Table 10).

Given the variability in krill densities encountered in the simulations, when years were modelled separately, whales could only achieve the minimum energy reserves $\sim 670,000$ MJ ($\sim 21,000$ kg of blubber) when assumed to feed on ratios dominated by *M. norvegica* (ratios of 25:75 or 0:100) and when targeting the highest densities available ($>75^{\text{th}}$ percentile) (Figure 39, Table 12 in Supplementary information). These results are based on years modelled separately, implying that, in each year, whales started from a random initial condition. However, individual body condition carries over from one year to the next, and

the condition at the end of the previous year contributes to the overall energy acquired over an entire reproductive cycle.

Assuming that a pregnant then lactating female was able to feed consistently on the highest densities of *M. norvegica* ($> 75^{\text{th}}$) that prevailed in 2011–2013, such a female would accumulate energy reserves of (\pm SD) 691,912 MJ ($\pm 4,364$) on average at the end of the first feeding season and of 687,671 MJ ($\pm 7,175$) at the end of the second feeding season (Figure 40A). Energy reserves once the calf is weaned after three months into the third feeding season (in 2013) would then be 128,986 MJ ($\pm 43,159$), which is only twice the minimum required to avoid starvation (2,000 kg of blubber $\sim 63,596$ MJ) (Figure 40A). Repeating these simulations using 2014 as a starting point, whales would be able to build energy reserves on average of 683,297 MJ ($\pm 16,775$) after the first feeding season, 687,392 MJ ($\pm 7,769$) after the second season when pregnant, and 417,915 MJ ($\pm 48,371$) after lactating and weaning the calf when seeking *M. norvegica* at the highest densities available in 2014–2016 (Figure 40B).

Table 10 : Mean (\pm SD; when applicable) of all the energetic costs involved in the 27-month reproductive cycle with the temporal periods to which each costs applied to. These costs included, the costs of migrating and time spent on the wintering grounds, gestation and lactation. The indirect costs of gestation represented by the increase in locomotion costs due to the burden of motherhood for cost of transport (COT), the rostral average active metabolic rate (RAAMR), and the resting metabolic rate (RMR) to each temporal periods. na: not applicable.

Costs (MJ)		Periods and months		Feeding season 1			Migration			Overwinter			Migration			Feeding season 2			Migration			Overwinter			Migration			Feeding season 3		
		May to Nov	Dec	Jan	Feb	Mar	Apr	May to Nov	Dec	Jan	Feb	Mar	Apr	May to Nov	Dec	Jan	Feb	Mar	Apr	May to Jul										
Migration and overwintering		na	163,658 \pm 2,638									na	163,658 \pm 2,638									na								
Gestation	direct	na	na	82			167,129	83,617	na						na															
	indirect	COT	na	na			negligible	na	na						na															
		COT	na	na			1,031 \pm 358	na						na																
		RAAMR	na	na			2,238 \pm 1,623	na						na																
		RMR	na	na			1,656 \pm 476	na						na																
		COT	na	na			na	1729 \pm 74	na						na															
Lactation		na	na									na	na	358,088 \pm 7,829						274,097 \pm 10,340										

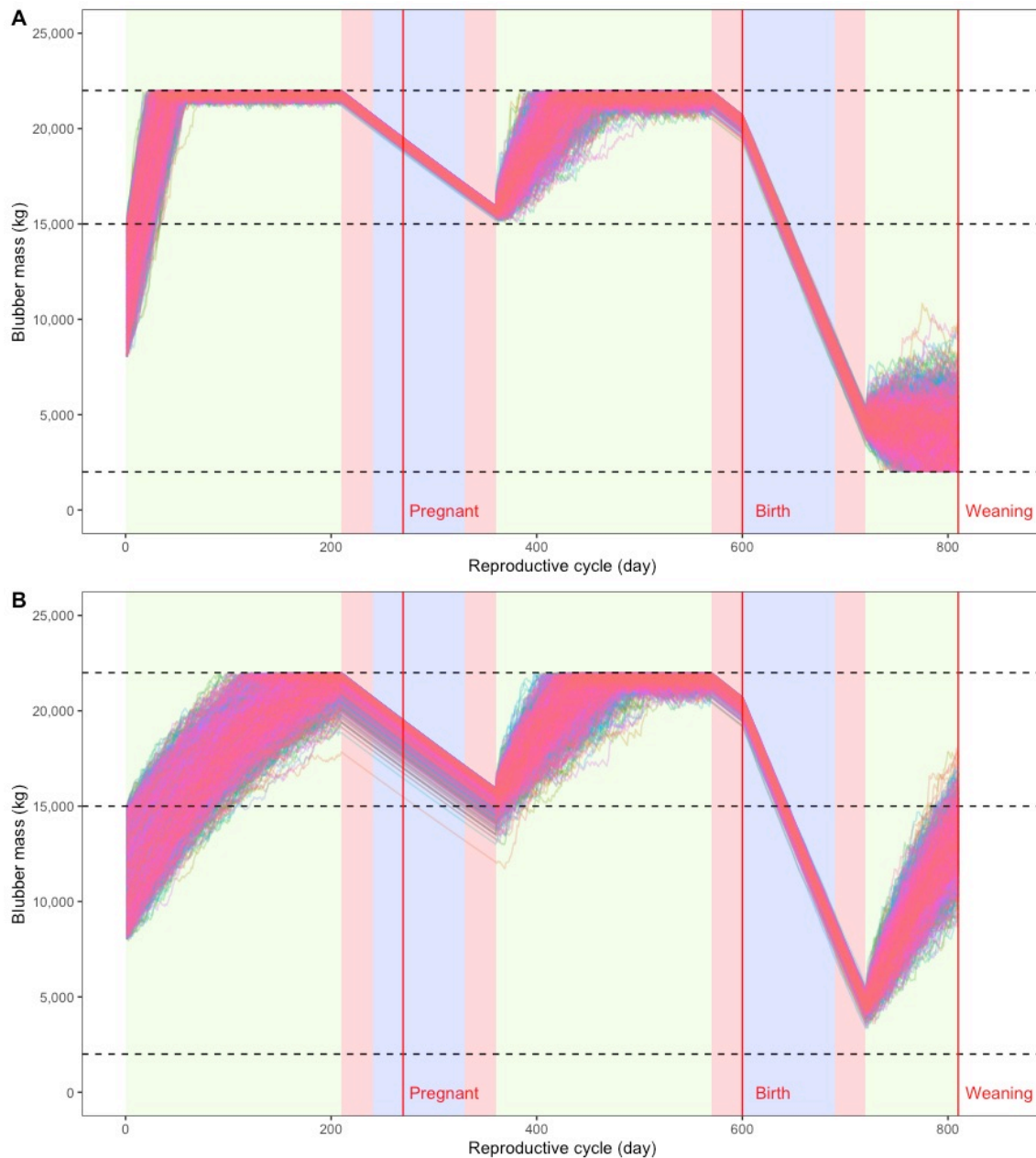


Figure 40 : Blue whale blubber mass (kg) throughout the entire reproduction cycle for whales assumed to feed on densities of *M. norvegica* (ratio 0:100) above the 75th percentile with reproductive cycle starting in (A) 2011 and (B) 2014. The reproductive cycle starts at the first feeding season (2011 or 2014) and carries over in the following years until weaning of a calf. Maximum (35%), average (27%) and minimum (5%) blubber proportions are indicated with the horizontal black dashed lines. Vertical red dashed lines indicate key events such as start of pregnancy, birth and weaning of the calf. Green shaded areas are periods of time spent on the feeding grounds, red shaded areas represent the time spent migrating and blue shaded areas represent on the wintering grounds.

3.6 DISCUSSION

Prey density is a major driver of foraging effort and determines the energy acquisition of individuals (MacArthur and Pianka, 1966). Maximizing energy reserves is critical for capital breeders in particular to fuel survival, growth and reproduction (Costa, 1993). We simulated the energy reserve dynamics of an adult female blue whale based on *in situ* krill densities over a feeding season to investigate their capacity to reproduce. We estimated that blue whales could acquire sufficient energy reserves to reproduce in half of the years modelled, but only when assuming they feed mainly on *M. norvegica* and on densities above the annual 75th percentile as feeding primarily on *M. norvegica* systematically led to higher energy reserves. Since we also found that the volume densities of both *Thysanoessa* spp. and *M. norvegica* were similar in range (Table 11 in Supplementary information), this result is no doubt explained by the higher energy content per gram (~21%) of *M. norvegica* compared to *Thysanoessa* spp. (5.2 ± 0.4 versus 4.3 ± 0.6 kJ · g⁻¹, respectively).

3.6.1 Link between preyscape and energy reserves of whales

Sufficient energy reserves are critical to reproductive success in most species, including large cetaceans (Lockyer, 1986; Houston et al., 2007; Miller et al., 2011; Christiansen et al., 2020), which in turn depends on the annual preyscape in their feeding habitat. For example, body condition of grey whales assessed from imagery from unmanned aerial systems (UAS) on the feeding grounds was shown to increase throughout the feeding season but at a varying rate depending on annual resource availability (Soledade Lemos et al. 2020). In our study simulations of blue whales, krill species-specific density determined individuals' body condition. Indeed, the energy reserves simulated for blue whales were only sufficient to meet the energetic requirements of migration and overwintering on a full reproductive cycle if whales were assumed to target the highest range of prey density (i.e., above the 75th percentile of each distribution) and to feed on species abundance ratios favoring *M. norvegica* over

Thysanoessa spp. Years where whales constantly lost blubber mass through the feeding season (specifically 2008, 2010 and 2017) seemed extreme and unrealistic considering that blue whales in the western North Atlantic regularly visit the EGSL and these results were likely an artefact of model assumptions.

In our simulations, their ability to accumulate sufficient energy reserves to fuel reproduction depended on their ability to target the highest densities of *M. norvegica* (95th percentile). Increasing the density thresholds (25th, 50th and 75th percentiles) forced whales to feed on increasing krill densities leading to higher energy reserves. However, using only the highest krill densities critically assumes that these high densities are regularly available to foraging whales. If these targeted high-density bins are not sufficiently abundant, we are most likely overestimating krill availability—especially in night-time – and overestimate consumption and therefore overestimate energy gain.

Further, the number of exploitable patches of krill decreases as the density threshold increases. Therefore, these higher densities might not be reflective of what is available to foraging blue whales and would need to be linked to the total biomass of krill available. Additionally, the rarity of high krill densities should translate to an increase in the time that whales spent searching for food. On the feeding grounds, we assigned the probability of a whale being in a foraging mode or searching mode based on the matrix of transition probabilities between the two behavioral modes estimated from satellite telemetry data (Lesage et al., 2017a). This matrix of transition probabilities represented an average of the behaviors exhibited by whales in 2002 and between 2010-2015 (except 2011; Lesage et al., 2017a) and therefore could not be linked specifically with yearly krill density and abundance. The probabilities of a whale searching for food should vary with the frequency of occurrence of krill density but also krill patch depletion rate and should be further addressed.

Our simulations indicated that *M. norvegica*, a more temperate species (Sameoto, 1976), is more beneficial to foraging whales (Figure 39, Table 12 in Supplementary information). The 0.6–1.2 °C trend in increasing seawater temperature over the next 50 years (Long et al., 2016; Galbraith et al., 2019) could lead to a niche expansion of this species

(Sameoto, 1976). Therefore, species abundance ratio favoring a dominance of *M. norvegica* could have a positive impact on blue whale energy reserves, body condition, and reproduction success.

Also, our results suggested a clear distinction between the krill preyscape, i.e. the krill present in the environment, and the krill energyscape, i.e. krill densities that are actually energetically suitable to foraging whales. The concept of energy landscapes recently emerged in animal movement ecology as a way to link the spatial distribution of foraging animals to their energy expenditure (Wilson et al., 2012; Shepard et al., 2013). This term was broadened to energyscape to include the energy requirements of foraging individuals as a function of environmental conditions (Amélineau et al., 2018). This study, which examined the energyscape of the little auk (*Alle alle*), highlighted that the predicted suitable habitats were found on a much smaller scale than the scale of distribution of the prey (Amélineau et al., 2018). Prey density and distribution alone are not sufficient to predict habitat suitability; energy requirements and expenditures of foragers are inextricably linked to habitat quality, and drive the preyscape exploitation according to the predator's energetic needs.

3.6.2 Study limitations—krill density and biomass

In our model, krill densities estimated from *in situ* systematic hydroacoustic surveys carried out each August were assumed to be representative of the krill densities that whales could encounter across the entire feeding ground and during the entire feeding period (7 months). Generally the krill densities encountered in the EGSL (0–133 g · m⁻³) were at least 3 fold below densities reported from the Californian current (0–930 g · m⁻³; Pirodda et al., 2018b) or Antarctic regions (2–1,725 g · m⁻³; Miller et al., 2018). The EGSL is possibly not as rich as elsewhere, however the scale of the analysis of hydroacoustic data might not be comparable across studies.

Krill spatial distribution can be affected by oceanic currents and storms (Maps et al., 2015; McQuinn et al., 2015). Further, krill is a highly patchy and dynamic resource, with distribution changing from hours to days, weeks and months (Siegel and Kalinowski, 1994). One survey in August might not capture completely the abundance and densities available in the months surrounding sampling. Weather conditions might also influence the depth of aggregations. Krill might be higher but more dispersed in the water column on foggy and grey days than on bright sunny clear sky days as light penetration influence diel vertical migration (Plourde et al., 2014b). Given the highly dynamic nature of krill, using estimated densities from *in situ* measurements from a single hydroacoustic survey per feeding season represents an annual snapshot and therefore might not necessarily reflect the densities whales could have encountered during the entire feeding season or elsewhere. Similarly, years in which whales constantly lost blubber mass might be an artefact of using one hydroacoustic survey in the EGSL as representative of the entire feeding ground and season. The expansion of systematic hydroacoustic surveys to other periods and to locations outside the EGSL could shed light on the total krill density available to whales.

From our simulations, it appears that blue whales cannot achieve maximum blubber accumulation, or even amounts needed to complete a pregnancy, while feeding on *Thysanoessa* spp., although they are to some extent more successful when feeding on the highest densities of *M. norvegica*. This therefore suggests that blue whales should favor feeding on *M. norvegica*. However, this is contradicted by a previous study which concluded that blue whale diet in the EGSL was comprised of 70% of *Thysanoessa* spp. between 1995–2009 according to quantitative isotopic models (Gavrilchuk et al., 2014) at times when the system was dominated by *Thysanoessa* spp. (i.e. until 2010; McQuinn et al., 2016). This is also contrary to the demonstrated stronger spatial association between *Thysanoessa* spp. and blue whale observations made during combined hydroacoustic-marine mammal surveys from 2009–2013. Further, this pattern of association was observed even in 2013 when *M. norvegica* was more abundant than *Thysanoessa* spp. (McQuinn et al., 2016). Both of these observations, which indicate that *Thysanoessa* spp. are actually favored over *M. norvegica*. suggest that *M. norvegica* densities worth exploiting might not be as common in the EGSL

than assumed by our simulations. This was concluded by McQuinn et al. (2015) who found that *Thysanoessa* spp. had higher volume densities than *M. norvegica* and were typically distributed shallower in the water column.

3.6.3 Study limitations–foraging effort parameters

Depth of feeding was not explicitly taken into account in our model. This caveat should be addressed in future studies considering that the depth of suitable krill density inherently affects the energetics of foraging blue whales (Guilpin et al., 2020). Indeed, the amount of energy reserves at the end of a feeding season depends on both the prey density upon which blue whales feed and the energy expended foraging. The optimal foraging theory predicts that animals should forage by maximizing energy gain while minimizing energy expenditure to increase fitness (Mori, 1998). A study demonstrated that blue whales in the EGSL follow the optimal foraging theory by increasing the number of lunges per dives with increasing feeding depths (Doniol-Valcroze et al., 2011) but lacked sufficient data to link the foraging behavior to krill densities. In our model, the time spent feeding per day depended on the krill density that whales were preying upon. Indeed, the time spent feeding is linked to the time it takes to fill the forestomach which inextricably depends on the density of prey that individuals feed on (Wiedenmann et al., 2011; Pirota et al., 2018b). Nevertheless, both the prey density and the depth at which prey is found influence the feeding behavior of rorquals (Ware et al., 2011; Friedlaender et al., 2016). In the EGSL, feeding depths of blue whales follow a bimodal distribution, with a strong peak near the surface and a weaker peak between 50 and 100 m (Doniol-Valcroze et al., 2012). The depth of feeding was also shown to be significantly different depending on time of day (Guilpin et al., 2019). It is noteworthy that even though the two krill species overlap in their vertical distributions, *M. norvegica* is typically found deeper than *Thysanoessa* spp. (Plourde et al., 2014b; McQuinn et al., 2015).

Further, we did not discriminate between night time and daytime foraging in the model which even though feeding rate (number of lunges per hour) and associated energy

expenditures differ between the two periods (Guilpin et al., 2019). The krill vertical distribution during daytime is significantly different from night time (Sourisseau et al., 2008; Harvey et al., 2009), when krill migrate to the surface and form more diffuse aggregations (Berkes, 1976; Simard et al., 1986b). However, limited nighttime hydroacoustic data was available to us to accurately quantify the night time krill density in the study area. Also, there is the possibility of a limited bias in krill density estimates close to the surface due to the blind zone of a few meters below the echo sounder.

3.6.4 Link between body condition and reproduction

Female body condition is determinant for reproductive success (Guinet et al., 1998; Miller et al., 2011; New et al., 2013b; Williams et al., 2013; Jeanniard-du-Dot et al., 2017). For capital breeders such as baleen whales, ovulation and/or annual reproduction rate was shown to depend on size of blubber stores (Miller et al., 2011; Christiansen et al., 2020). In southern right whales (*Eubalaena australis*), females in better body condition produced longer calves with greater survival rate (Christiansen et al., 2018). In our study, we found that a pregnant female needed to accumulate at least 670,000 MJ to have enough energetic reserves to sustain lactation., and that krill densities limited the capacity of whales to maintain an energetic stasis or to build energy reserves. If we assumed that whales fed exclusively on densities above the 75th percentile of *M. norvegica*, they could accumulate enough energy in about half of the years modelled.

Lactation is the most energetically demanding phase of mammalian reproduction (Gittleman and Thompson, 1988; Christiansen et al., 2016). The simulation results highlighted the need for whales to feed efficiently while lactating their calf when reaching their summer feeding grounds. In a scenario where female blue whales fed exclusively on densities of *M. norvegica* above the 75th percentile during their entire reproductive cycle, from the start of pregnancy to the end of lactation, krill densities were sufficient to support a full reproductive cycle and successfully wean a calf (Figure 40).

In our simulations, lactation costs were assumed to be constant during the entire lactation period given the scarcity of information in the literature on milk composition and daily amount of milk delivered to the calf. Blue whales have a relatively short lactation period (7 months on average) during which they seem to maintain a high rate of energy output. This is in contrast with odontocetes which sustain a much longer lactation period (~years) with a lower energy output (Oftedal, 1997). Blue whales are, in a way, more similar to phocids in their lactation strategies, which invest large amounts of energy in their pup over a short period of time (Schulz and Bowen, 2005).

Fat content of phocid milk such as Weddell seals (*Leptonychotes weddellii*) increases in the first few days to reach a peak (55-60% of fat content) with the decrease in percent water (Eisert et al., 2013). Balaenopterids also produce fat-rich milk (30–50%) (Lockyer, 1984; Oftedal, 1997) however, the lack of information about change in milk composition for balaenopterids precluded us from taking that into account. Nevertheless, it is likely that the amount of milk delivered and fat content changes over the lactation period and with body condition and blubber reserves of the lactating mother (Oftedal, 2000). We could not link this to the body condition of the female as did Pirotta et al. (2018b) because we modelled periods separately, so instead, some variation in the amount of milk delivered per day was incorporated in our model.

Maternal body size and condition was shown to determine body condition of the calf using aerial photogrammetry from UAV imagery in humpback whales and North Atlantic right whales with females in lower body condition producing shorter calves (Christiansen et al., 2018, 2020). Therefore, poor body condition of the lactating mothers might cause reduced growth rates in calves suggesting a reduced calf survival or an increase in calving interval. In the Northwest Atlantic, where relatively few cow-calf pairs have been observed, blue whale calving interval is estimated to be approximately 4 years, almost twice the calving interval observed along the Californian coast in the Pacific (Sears et al., 2013). Body condition of female western North Atlantic blue whales might be linked to the longer calving

interval through periods of anestrus until energy reserves are sufficient again to invest in reproduction, as has been observed for North Atlantic right whales (Wright et al., 1992). Imagery data from unmanned aerial vehicles might provide insights into body condition of blue whales, similarly to what has been done for North Atlantic right whales (Christiansen et al., 2020).

3.6.5 Non-feeding migration periods and the 27-month reproduction cycle

For simplicity and due to limited knowledge about the wintering behavior of this specific blue whales population (Lesage et al., 2017a), we assumed that whales did not feed during winter, which may have underestimated energy reserves left after winter. Recently, studies have shown evidence of sporadic feeding outside the typical feeding grounds or while on their breeding grounds when suitable prey concentrations are encountered. This has been documented in humpback whales (Leaper and Lavigne 2007; Silva et al., 2013; Owen et al., 2016), as well as on fin and blue whales in the Eastern North Atlantic (Silva et al., 2013, 2019) on blue whales from the Eastern North Pacific (Etnoyer et al., 2006; Bailey et al., 2009; Pirotta et al., 2018b). Therefore, migrating whales seem to feed sporadically during migration when suitable locations are encountered, either to meet energy demands or to complement their energy reserves. A satellite telemetry study on western North Atlantic blue whales identified area restricted search (ARS) patterns during migration which could either suggest foraging behavior, or limited movements while socializing (Lesage et al., 2017a). From December to February, ARS was identified 30 % of the time which then increased to 36-37 % in March-April. This compares to ARS representing 53 to 69% of blue whale activity between September and November when whales were on their feeding grounds (Lesage et al., 2017a). Even though the major feeding activity and effort occurs during the peaks of food availability, opportunistic foraging during migration is likely occurring. It is therefore not excluded that western North Atlantic blue whales might also supplement their energy stores throughout the overwintering period, especially when lactating. Complementing energy

reserves during the overwintering period when possible would be beneficial, especially if whales are unable to target the highest densities or if krill are not abundant enough during the feeding season. Additional long-term satellite telemetry data are needed to further characterize behavior during migration and on the wintering grounds to refine the associated energetic costs and potential gain. It would also contribute to uncovering the movements of these large animals across ocean basins, and to further understand their migration routes and potential feeding areas outside the EGSL.

Some of the limitations of our study identified in previous sections are currently being addressed through the improvement of model parameters with data available. Implementing the modelling approach of Pirotta et al. (2018b) using stochastic dynamic programming to determine the optimal decisions and behaviors that whales should be adopting for successful reproduction is a necessary next step. Nevertheless, the present modelling study provides a first approximation of the energetics associated with a reproductive cycle for the western North Atlantic blue whale population. Our study revealed that low krill densities in the EGSL remain a likely candidate as a contributor to the apparent low calving rate of this population.

3.7 ACKNOWLEDGEMENTS

We thank all DFO employees and crewmembers of the *Frederick G. Creed* and of the *Coriolis II* involved with the systematic hydroacoustic surveys. Special thanks to F. Paquet for validating and preparing the hydroacoustic data. We thank A. Ollier for analysis of the satellite tag data from 2017 and 2018. This work and scholarship to MG were funded under the strategic partnership grant (STPGP 447363) from the Natural Sciences and Engineering Research Council of Canada (NSERC) awarded to G.W. and V.L., and by the Species at Risk and Oceans Management programs of Fisheries and Oceans Canada. This study contributes to the program of Québec–Océan, a strategic cluster funded by Fonds de Recherche Québec Nature et Technologie (FRQNT), which also provided MG with travel grants and scientific support.

3.8 SUPPLEMENTARY INFORMATION (CHAPITRE 3)

3.8.1 Supplementary tables

Table 11 : Characteristics of prey densities considered suitable for blue whales foraging in the EGSL, as determined from hydroacoustic surveys conducted yearly from 2008 to 2017. Densities deemed suitable were those allowing blue whales to achieve at least neutral energy balance, and corresponded to 19 g m^{-3} for *Thysanoessa* spp. and 16 g m^{-3} for *Meganyctiphanes norvegica*. Data are also presented while setting suitability at higher thresholds (i.e., 25th, > 50th, > 75th percentiles). The number of bins above the threshold are relative to a distribution that includes all densities above 4 g m^{-3} (McQuinn et al. 2015).

Thresholds	year	<i>Thysanoessa</i>	<i>M.</i>	<i>Thysanoessa</i>	<i>M.</i>
		spp.	<i>norvegica</i>	spp.	<i>norvegica</i>
		mean density of suitable bins (min–max) ($\text{g} \cdot \text{m}^{-3}$)		N. of bins and percent (%) above thresholds	
neutral energy balance	2008	29 (19–95)	24 (16–62)	408 (9.7)	68 (7.5)
	2009	34 (19–243)	34 (16–219)	1666 (26.1)	277 (6.1)
	2010	29 (19–82)	28 (16–102)	339 (1.7)	54 (5.4)
	2011	37 (19–238)	50 (16–243)	95 (8.8)	738 (21.6)
	2012	26 (19–69)	33 (16–179)	163 (5.9)	88 (9.8)
	2013	31 (19–188)	27 (16–231)	232 (11.6)	285 (7.6)
	2014	27 (19–45)	40 (16–95)	58 (6.3)	175 (23.1)
	2015	27 (19–63)	38 (16–113)	108 (8.2)	18 (8.1)
	2016	29 (19–233)	38 (16–173)	577 (16.4)	150 (12.8)
	2017	26 (19–101)	20 (16–23)	675 (16.7)	5 (2.9)
> 25 th	2008	32 (22–95)	26 (18–62)	306 (7.3)	51 (5.6)
	2009	39 (23–243)	39 (19–219)	1250 (19.6)	208 (4.6)
	2010	32 (22–82)	31 (18–102)	255 (1.3)	40 (4)
	2011	43 (22–238)	60 (21–243)	71 (6.6)	553 (16.2)
	2012	29 (21–69)	39 (20–179)	122 (4.4)	66 (7.3)
	2013	35 (22–188)	30 (18–231)	174 (8.7)	214 (5.7)
	2014	30 (22–45)	47 (24–95)	43 (4.7)	131 (17.3)
	2015	29 (21–63)	45 (22–113)	81 (6.1)	13 (5.8)
	2016	43 (23–233)	45 (20–173)	433 (12.3)	112 (9.5)
	2017	34 (22–101)	21 (19–23)	507 (12.6)	4 (2.3)

Table 11 continued

Thresholds	year	<i>Thysanoessa</i>	<i>M.</i>	<i>Thysanoessa</i>	<i>M.</i>
		spp.	<i>norvegica</i>	spp.	<i>norvegica</i>
		mean density of suitable bins (min–max) (g · m ⁻³)		N. of bins and percent (%) above thresholds	
> 50 th	2008	36 (26–95)	30 (20–62)	204 (4.8)	34 (3.8)
	2009	45 (28–243)	48 (24–219)	834 (13.1)	139 (3.1)
	2010	37 (27–82)	36 (23–102)	170 (0.9)	27 (2.7)
	2011	52 (25–238)	77 (32–243)	48 (4.5)	369 (10.8)
	2012	32 (24–69)	47 (25–179)	82 (3)	44 (4.9)
	2013	40 (28–188)	36 (22–231)	116 (5.8)	143 (3.8)
	2014	32 (25–45)	57 (33–95)	29 (3.1)	89 (11.7)
	2015	32 (24–63)	52 (30–113)	54 (4.1)	9 (4.1)
	2016	51 (30–233)	56 (27–173)	289 (8.2)	75 (6.4)
	2017	38 (27–101)	22 (20–23)	338 (8.4)	3 (1.8)
> 75 th	2008	44 (34–95)	37 (28–62)	102 (2.4)	17 (1.9)
	2009	58 (39–243)	68 (36–219)	417 (6.5)	70 (1.5)
	2010	44 (34–82)	45 (30–102)	85 (0.4)	14 (1.4)
	2011	73 (37–238)	107 (65–243)	24 (2.2)	185 (5.4)
	2012	37 (29–69)	65 (36–179)	41 (1.5)	22 (2.4)
	2013	50 (34–188)	47 (28–231)	58 (2.9)	72 (1.9)
	2014	36 (32–45)	71 (54–95)	15 (1.6)	45 (5.9)
	2015	38 (29–63)	67 (38–113)	27 (2.0)	5 (2.2)
	2016	67 (41–233)	79 (46–173)	145 (4.1)	38 (3.2)
	2017	47 (34–101)	23 (22–23)	169 (4.2)	2 (1.2)

Table 12 : Estimates of energy reserves accumulated after one feeding season, according to densities of two krill species documented using hydroacoustic surveys conducted in the EGSL from 2008–2017. Simulations were done assuming a diet composed of different ratios between the two krill species (*Thysanoessa* spp. and *M. norvegica*), and whales seeking to achieve either neutral energy balance, or foraging efficiencies that allow some accumulation of energy reserves (tresholds of > 25th, > 50th, > 75th percentiles of the maximum suitable densities that were observed in a specific year).

Species ratio	krill density thresholds	year	mean energy reserves (MJ)	± SD	95%CI	
					lower	upper
100% <i>Thysanoessa</i> spp.	> FE1	2008	64,193	555	63,638	65,317
		2009	74,196	17,180	63,671	113,099
		2010	62,208	624	63,627	65,388
		2011	193,170	65,525	86,171	299,546
		2012	64,047	453	63,625	64,931
		2013	68,891	10,383	63,652	92,313
		2014	64,007	406	63,623	92,314
		2015	64,061	437	63,627	64,992
		2016	115,911	43,216	63,915	192,237
	2017	64,321	808	63,629	65,577	
	> 25 th	2008	64,314	766	63,639	65,618
		2009	89,466	30,345	63,744	151,001
		2010	64,266	705	63,639	65,490
		2011	258,169	70,454	140,452	370,602
		2012	64,095	484	63,620	65,121
		2013	78,562	22,509	63,704	124,655
		2014	64,025	398	63,620	64,775
		2015	64,109	496	63,623	65,138
		2016	160,374	54,834	70,733	252,860
	2017	64,481	1,326	63,641	66,305	
	> 50 th	2008	64,531	1,529	63,654	65,722
		2009	137,400	45,451	63,324	211,169
		2010	64,428	924	63,641	65,693
		2011	361,842	83,642	228,716	499,424
		2012	64,203	577	63,627	65,348
		2013	117,417	41,808	63,988	188,494
		2014	64,055	413	63,628	64,871
2015		64,211	644	63,638	65,379	
2016		254,547	62,560	149,747	352,796	
2017	65,233	3,172	63,658	69,603		

Table 12 continued

Species ratio	krill density thresholds	year	mean energy reserves (MJ)	± SD	95%CI	
					lower	upper
	> 75 th	2008	68,501	9,453	63,654	90,098
		2009	290,556	60,223	186,361	386,291
		2010	67,680	7,783	63,670	86,248
		2011	604,967	77,420	450,444	689,681
		2012	64,422	900	63,630	65,660
		2013	253,225	60,140	154,073	352,430
		2014	64,136	493	63,630	65,217
		2015	64,456	996	63,334	66,102
		2016	486,983	79,534	334,223	596,893
		2017	76,477	18,571	63,711	118,325
100%	> FE1	2008	64,241	643	63,629	65,431
<i>M. norvegica</i>		2009	20,8113	62,333	106,036	308,780
		2010	68,593	9,874	63,652	92,076
		2011	416,682	89,782	270,652	572,394
		2012	183,815	58,543	82,612	280,080
		2013	93,998	34,420	63,771	164,955
		2014	147,709	50,600	67,122	234,627
		2015	180,212	56,745	86,047	272,596
		2016	227,972	66,727	115,334	338,823
		2017	63,918	300	63,614	64,445
	> 25 th	2008	64,322	905	63,635	65,594
		2009	282,057	70,455	164,279	393,861
		2010	79,984	23,103	63,710	131,949
		2011	533,390	88,217	381,889	672,325
		2012	255,589	66,319	148,080	359,978
		2013	134,144	48,350	64,488	215,770
		2014	217,153	56,688	123,609	309,599
		2015	287,085	65,602	176,930	390,508
		2016	306,794	69,839	191,768	422,610
		2017	63,927	291	63,615	64,447
	> 50 th	2008	64,894	2,412	63,651	67,747
		2009	397,035	82,180	262,867	529,291
		2010	115,702	42,262	64,012	189,044
		2011	658,304	44,262	569,169	695,457
		2012	377,636	80,371	248,634	508,814
		2013	212,244	62,173	106,943	316,008
		2014	320,016	61,244	276,305	516,436
		2015	396,716	73,903	276,305	516,436
		2016	432,805	76,915	310,407	561,247
		2017	63,913	273	63,613	64,403

Table 12 continued

Species ratio	krill density thresholds	year	mean energy reserves (MJ)	± SD	95%CI	
					lower	upper
	> 75 th	2008	74,451	16,808	63,717	113,125
		2009	634,187	61,838	508,919	692,965
		2010	252,430	55,110	161,319	343,229
		2011	683,042	16,500	648,484	697,197
		2012	621,265	68,711	479,078	692,810
		2013	410,530	79,850	279,019	539,646
		2014	538,732	73,630	415,972	652,471
		2015	590,473	78,327	446,670	689,704
		2016	664,283	39,628	589,237	696,549
		2017	63,929	294	63,614	64,445
75 %	> FE1	2008	64,220	678	63,624	65,427
<i>Thysanoessa</i>		2009	94,029	34,989	63,749	165,054
spp. :		2010	64,441	1,194	63,647	66,104
25%		2011	251,332	69,816	140,662	369,536
<i>M. norvegica</i>		2012	69,025	11,927	63,649	96,453
		2013	72,672	16,197	63,680	110,317
		2014	66,404	6,809	63,645	79,447
		2015	68,420	11,082	63,658	93,266
		2016	139,136	52,391	64,885	227,503
		2017	64,236	645	63,631	65,463
	> 25 th	2008	64,279	739	63,636	65,497
		2009	130,135	50,543	64,185	219,977
		2010	64,981	3,182	63,651	68,798
		2011	334,323	77,130	208,417	460,894
		2012	76,046	20,124	63,667	122,344
		2013	88,114	29,189	63,731	147,945
		2014	70,346	13,630	63,676	101,374
		2015	77,864	22,303	63,679	129,651
		2016	200,065	60,335	99,158	294,973
		2017	64,351	977	63,640	65,608

Table 12 continued

Species ratio	krill density thresholds	year	mean energy reserves (MJ)	± SD	95%CI	
					lower	upper
50 % <i>Thysanoessa</i> spp. : 50 % <i>M. norvegica</i>	> 50 th	2008	64,563	1,507	63,644	66,187
		2009	205,241	61,855	101,102	307,208
		2010	67,615	8,106	63,664	85,926
		2011	467,204	92,080	309,313	618,698
		2012	93,297	35,685	63,758	166,713
		2013	141,527	49,401	64,528	225,276
		2014	82,191	25,239	63,685	135,528
		2015	95,372	36,094	63,762	167,590
		2016	303,795	68,293	191,218	416,799
	2017	64,658	2,009	63,645	66,837	
	> 75 th	2008	69,859	11,033	63,686	94,791
		2009	391,132	73,540	268,595	513,494
		2010	94,678	32,489	63,793	158,812
		2011	665,024	35,897	590,432	695,310
		2012	171,552	65,205	70,983	287,325
		2013	292,632	66,922	181,699	398,915
		2014	131,009	51,202	64,246	223,331
		2015	159,285	56,898	70,202	259,332
2016		541,384	83,609	393,709	668,790	
2017	69,841	11,469	63,695	97,864		
	> FE1	2008	64,248	721	63,637	65,478
		2009	128,639	49,705	64,088	214,192
		2010	65,163	3,514	63,651	69,851
		2011	314,025	77,149	192,586	440,453
		2012	90,895	33,310	63,732	160,893
		2013	79,878	22,898	63,685	130,185
		2014	81,560	25,552	63,721	138,643
		2015	91,093	33,256	63,724	157,813
		2016	169,403	58,646	74,379	267,816
	2017	64,143	557	63,627	65,285	
	> 25 th	2008	64,312	753	63,640	65,560
		2009	179,676	59,317	75,891	280,930
		2010	67,214	8,152	63,651	82,677
		2011	402,672	87,690	258,710	546,917
		2012	118,973	47,845	63,919	208,368
		2013	100,820	36,610	63,869	169,761
		2014	102,752	39,285	63,826	178,703
		2015	136,128	53,076	64,182	229,432
2016		235,434	62,991	132,976	339,934	
2017	64,191	661	63,632	65,332		

Table 12 continued

Species ratio	krill density thresholds	year	mean energy reserves (MJ)	± SD	95%CI	
					lower	upper
	> 50 th	2008	64,670	1,771	63,649	66,983
		2009	271,839	68,949	157,409	383,744
		2010	75,955	19,616	63,704	121,683
		2011	556,681	88,207	395,946	683,946
		2012	181,078	61,879	79,183	283,649
		2013	163,939	55,965	73,622	256,453
		2014	154,976	53,002	67,783	244,779
		2015	194,971	62,765	93,541	299,076
		2016	344,691	71,883	222,020	462,175
		2017	64,381	901	63,633	65,672
	> 75 th	2008	71,069	12,861	63,682	100,907
		2009	486,344	84,750	343,087	622,712
		2010	140,381	45,725	66,463	217,432
		2011	677,549	21,427	635,656	696,644
		2012	345,007	77,941	222,595	475,488
		2013	328,843	71,205	211,998	444,798
		2014	283,553	64,785	176,918	385,236
		2015	320,261	72,453	201,359	440,099
		2016	598,859	74,584	464,621	691,256
		2017	65,507	3,957	63,648	71,832
25 % <i>Thysanoessa</i> spp. : 75% <i>M. norvegica</i>	> FE1	2008	64,235	715	63,638	65,473
		2009	166,357	57,782	75,714	267,064
		2010	67,008	7,364	63,663	83,554
		2011	370,286	85,845	229,318	514,555
		2012	132,467	51,097	64,396	225,965
		2013	86,012	27,643	63,737	142,593
		2014	110,812	43,486	63,954	192,531
		2015	131,207	49,843	64,494	222,208
		2016	197,041	61,715	96,007	297,733
		2017	64,061	507	63,620	65,018
	> 25 th	2008	64,369	838	63,637	65,644
		2009	228,959	65,745	117,906	338,620
		2010	71,785	13,784	63,680	104,466
		2011	470,921	92,832	320,025	630,314
		2012	188,342	60,639	88,400	291,264
		2013	117,243	44,796	63,950	198,310
		2014	159,225	52,367	72,527	245,420
		2015	212,419	60,708	109,768	307,159
		2016	271,075	66,028	160,343	377,415
		2017	64,091	582	63,623	65,083

Table 12 continued

Species ratio	krill density thresholds	year	mean energy reserves (MJ)	± SD	95%CI	
					lower	upper
	> 50 th	2008	64,702	1,969	63,649	67,009
		2009	338,220	76,434	213,658	462,322
		2010	92,125	31,776	63,769	157,082
		2011	623,129	69,827	478,895	693,023
		2012	282,723	72,810	163,219	404,139
		2013	191,010	57,075	98,377	284,946
		2014	243,266	57,655	148,417	338,727
		2015	299,413	67,887	188,880	407,639
		2016	393,420	76,257	269,212	512,750
		2017	64,198	732	63,628	65,354
	> 75 th	2008	73,210	14,945	63,696	105,352
		2009	574,112	84,211	421,866	686,531
		2010	196,866	51,717	107,607	274,794
		2011	681,386	16,805	646,082	697,369
		2012	504,629	88,817	354,349	648,627
		2013	369,585	76,655	242,152	493,673
		2014	422,590	71,330	304,518	531,628
		2015	465,184	79,969	331,894	599,956
		2016	640,491	59,096	521,123	694,984
		2017	64,346	872	63,634	65,653

Table 13 : Mean (±SD) indirect costs of gestation represented by the increase in locomotion costs due to the burden of motherhood for cost of transport (COT), the roqual average active metabolic rate (RAAMR), and the resting metabolic rate (RMR) and the temporal periods to which these extra costs applied to.

Costs	Temporal period of extra costs	Mean (MJ)	±SD	95%CI	
				lower	upper
<i>COT</i>	overwinter/migration	negligible	na	na	na
<i>RAAMR</i>	feeding	2,238	1,623	0	5,028
<i>COT</i>	feeding	1,031	358	479	1,644
<i>RMR</i>	feeding	1,656	476	919	2,491
<i>COT</i>	migration	1,729	75	1,607	1,849

3.8.2 Supplementary figures

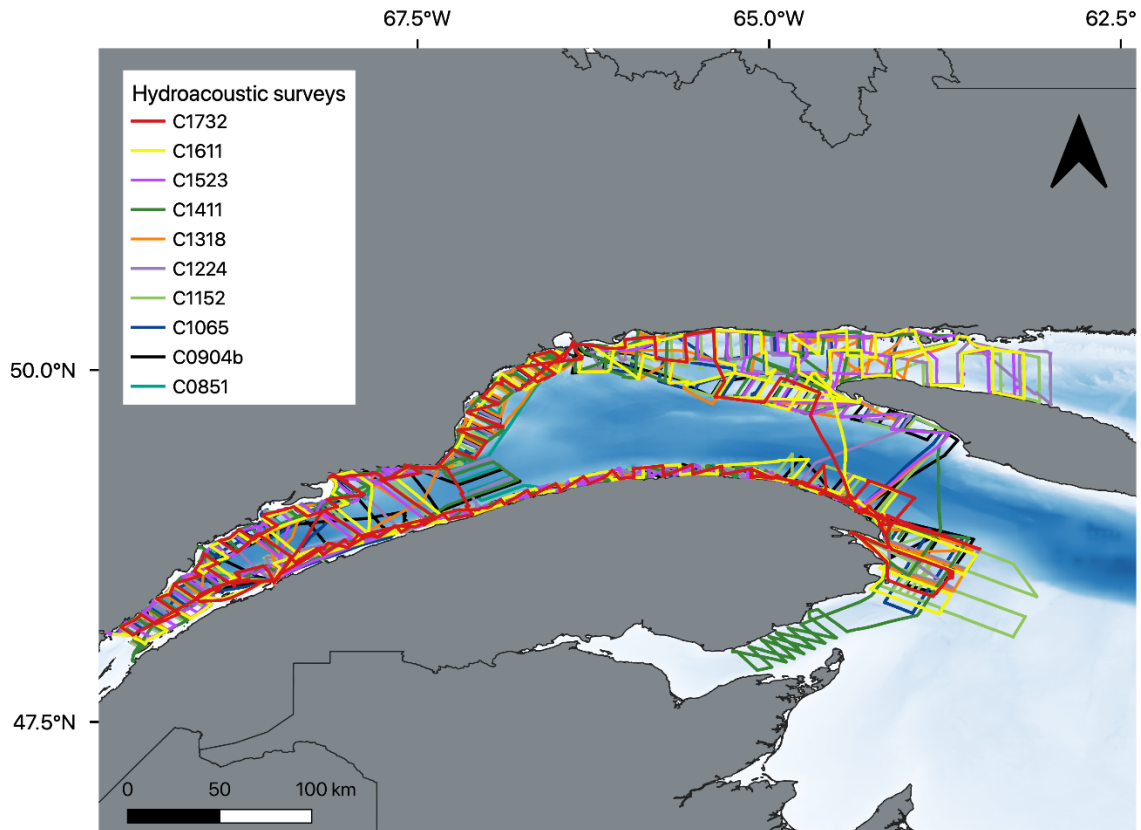
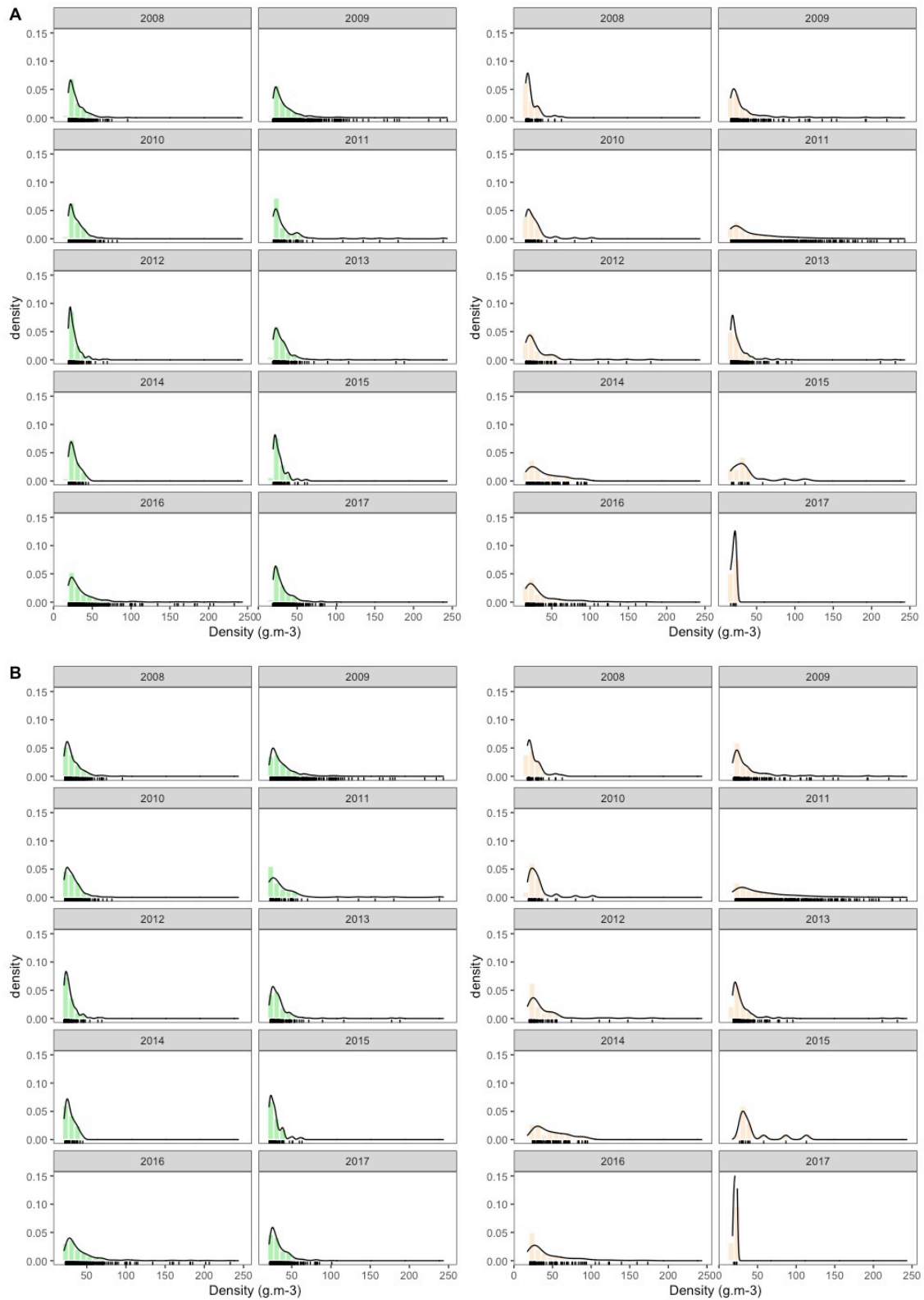


Figure 41 : Locations of hydroacoustic surveys conducted in the Estuary and the North western Gulf of St. Lawrence, from 2008 to 2017. Colored lines represent the transects for each survey year.



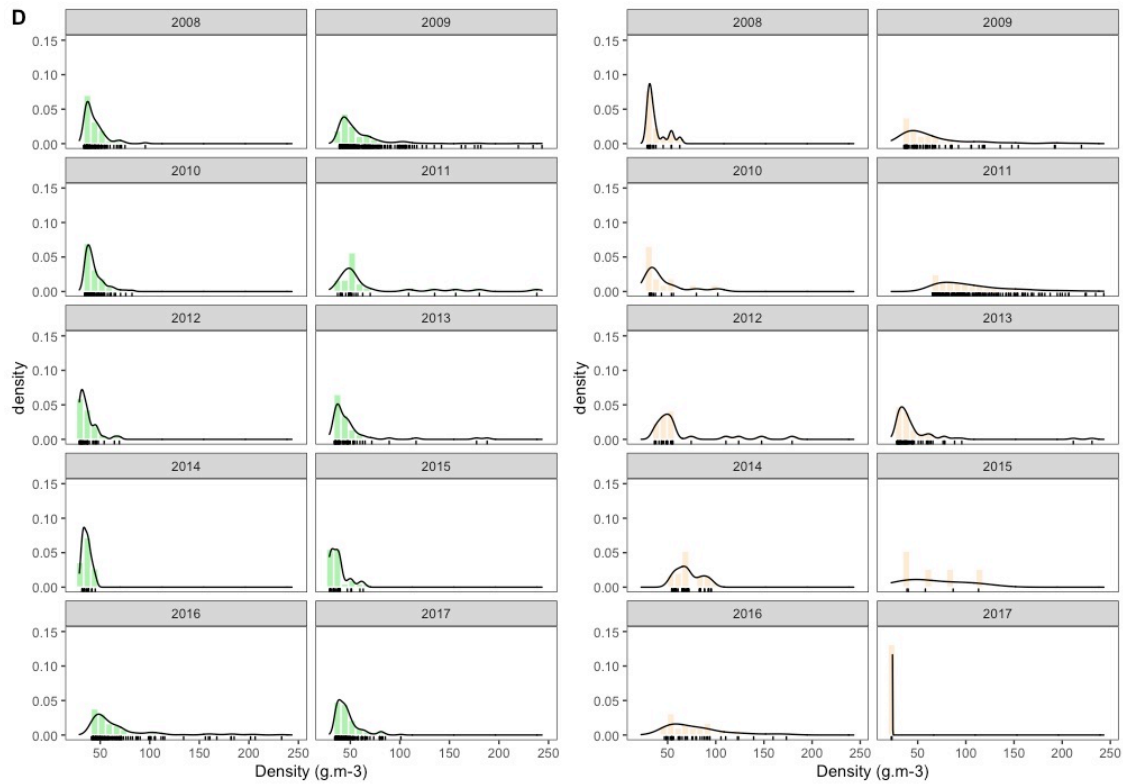
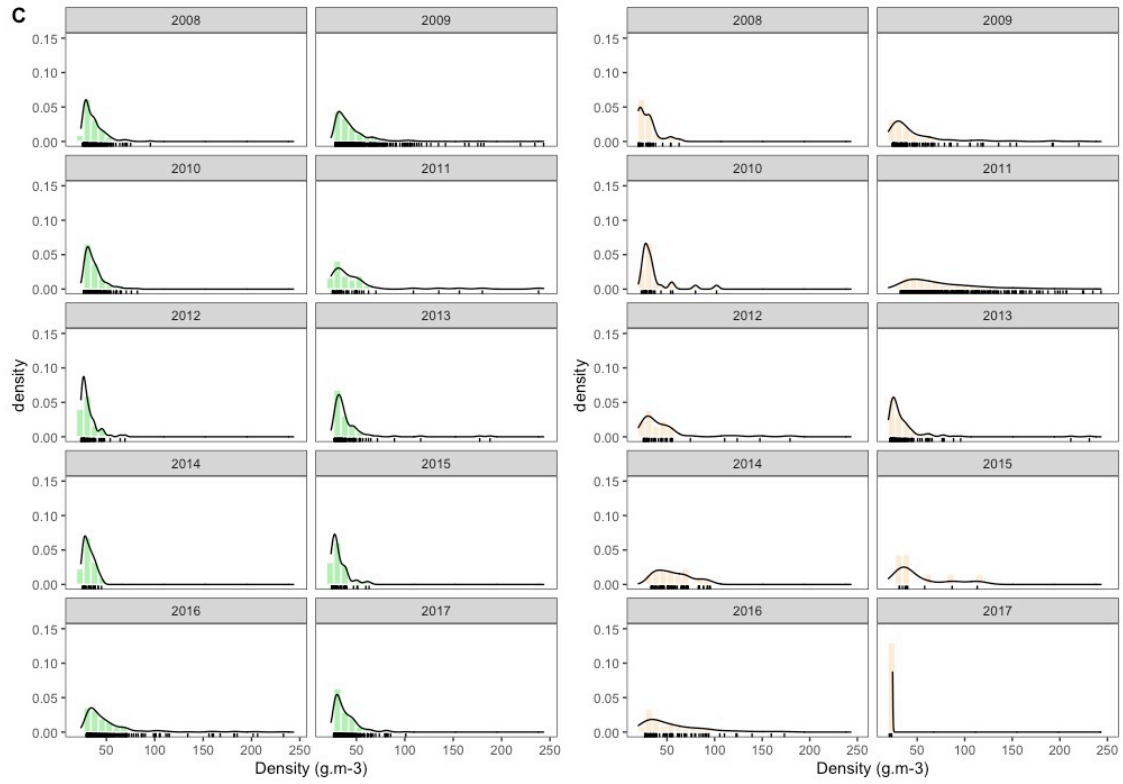


Figure 42 : Probability density distribution of krill densities that exceeded (A) the threshold identified in Guilpin et al. (2019) for blue whale neutral energetic balance (i.e., 16 and 19 $\text{g} \cdot \text{m}^{-3}$) and year-specific (B) 25th, (C) 50th and (D) 75th percentiles thresholds, presented for each of the hydroacoustic surveys conducted between 2008 and 2017, and the two krill species *Thysanoessa* spp. (left panels) and *Meganyctiphanes norvegica* (right panels). Availability is expressed as probability density functions of densities (black line) with associated frequency distributions (colored histograms), and raw data (black vertical lines).

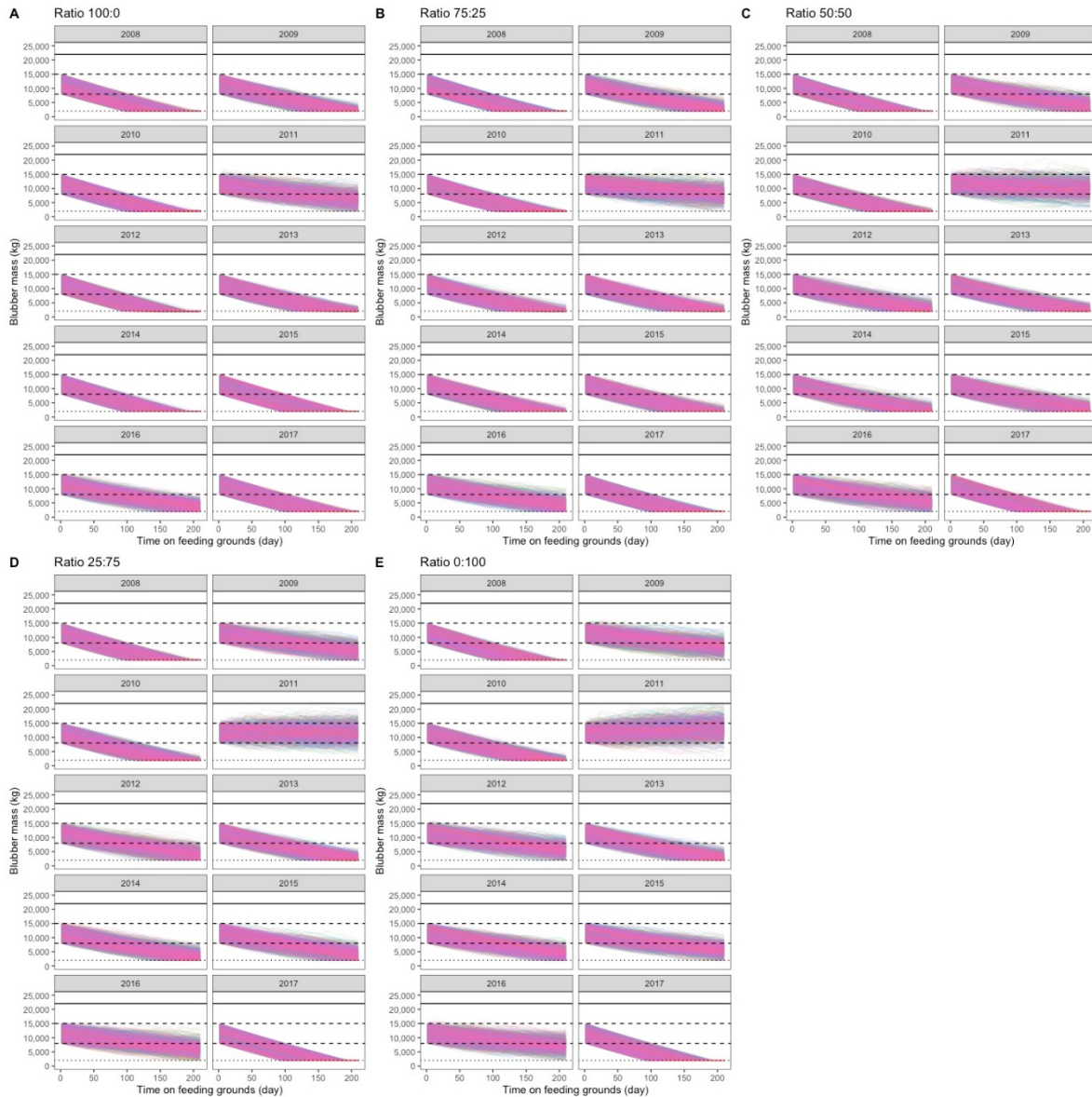


Figure 43 : Blue whale blubber mass (kg) accumulated over a seven-month foraging period, according to year-specific krill densities measured during hydroacoustic surveys conducted in the EGSL between 2008–2017 and for krill densities above the threshold identified in Guilpin et al. (2019) for blue whale neutral energetic balance, while assuming that whales fed on a range of ratios (A) *Thysanoessa* spp. 100:0, (B) 75:25, (C) 50:50, (D) 25:75 or (E) *M. norvegica* 0:100. Body condition in terms of blubber proportion when arriving on feeding grounds was allowed to vary between 16% (lower black dashed line) and the average blubber proportion for a blue whale (27%; upper black dashed line), with a potential maximum of 35% over the course of the seven months (black solid line) and a minimum of 5% blubber (dotted line).

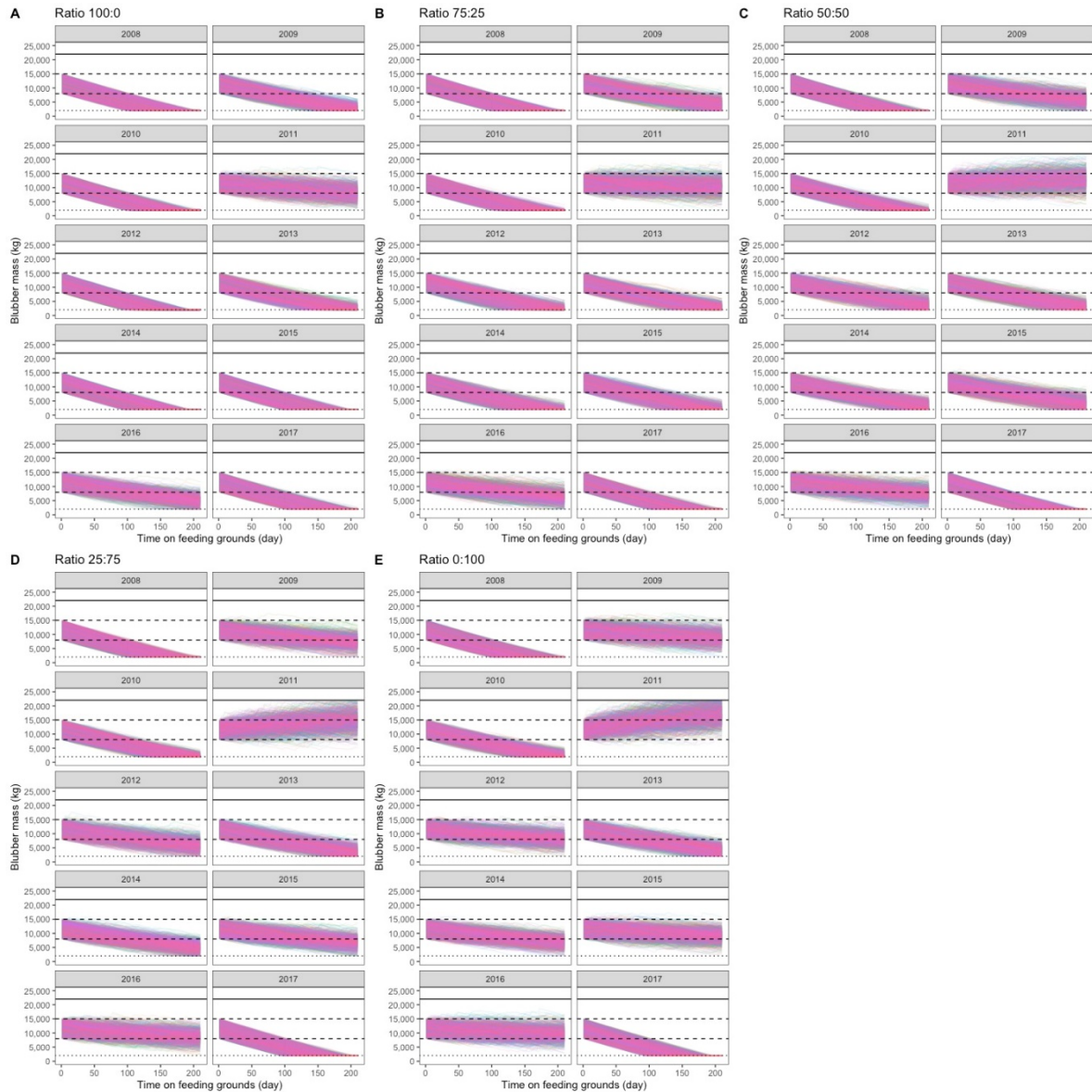


Figure 44 : Blue whale blubber mass (kg) over a seven months foraging period on the feeding ground, according to year-specific krill densities measured during hydroacoustic surveys above the 25th percentile, while assuming that whales fed on a range of ratios (A) *Thysanoessa* spp. 100:0, (B) 75:25, (C) 50:50, (D) 25:75 or (E) *M. norvegica* 0:100. Body condition in terms of blubber proportion when arriving on feeding grounds was allowed to vary between 16% (lower black dashed line) and the average blubber proportion for a blue whale (27%; upper black dashed line), with a potential maximum of 35% over the course of the seven months (black solid line) and a minimum of 5% blubber (dotted line).

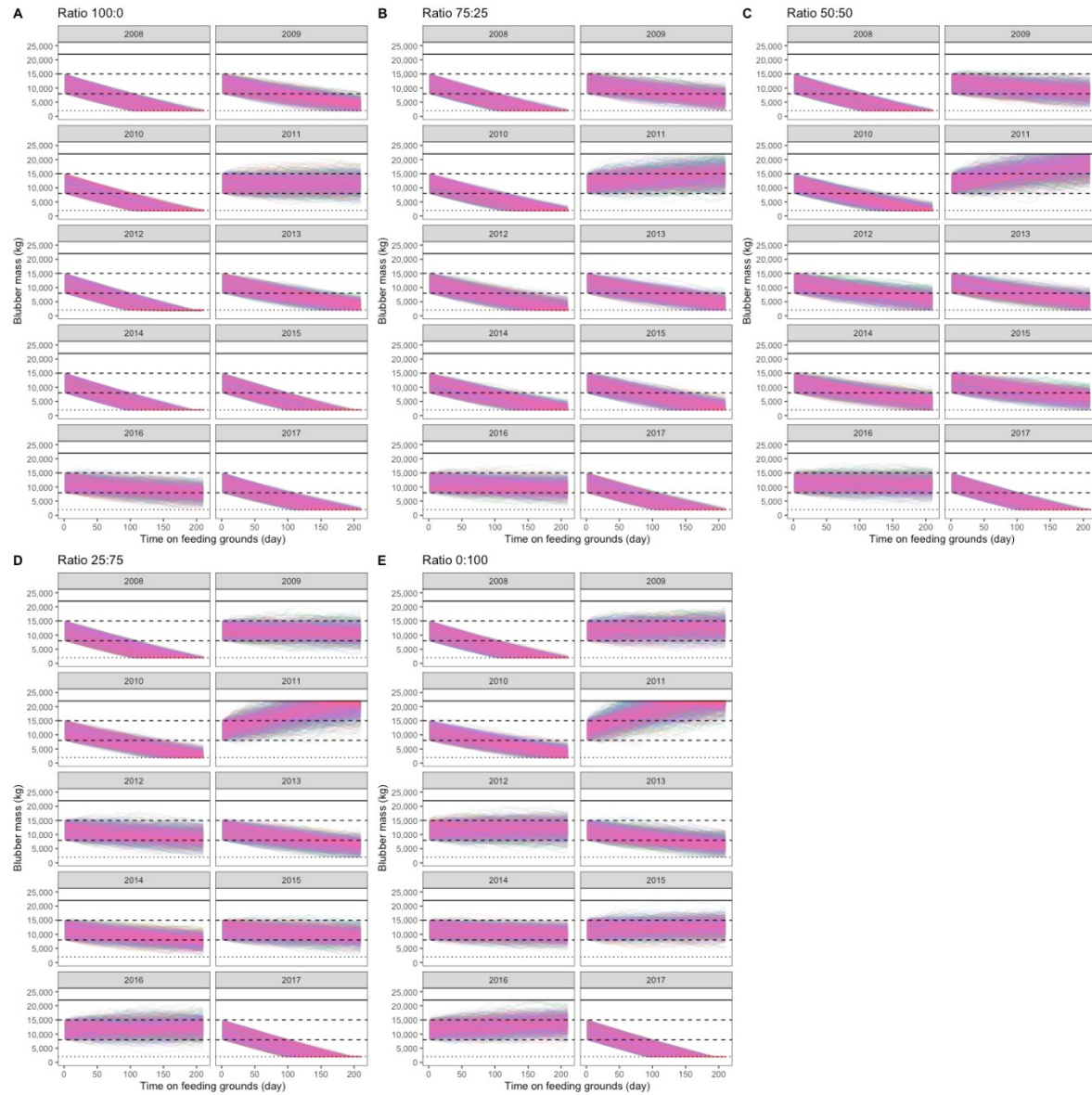


Figure 45 : Blue whale blubber mass (kg) over a seven months foraging period on the feeding ground, according to year-specific krill densities measured during hydroacoustic surveys above the 50th percentile, while assuming that whales fed on a range of ratios (A) *Thysanoessa* spp. 100:0, (B) 75:25, (C) 50:50, (D) 25:75 or (E) *M. norvegica* 0:100. Body condition in terms of blubber proportion when arriving on feeding grounds was allowed to vary between 16% (lower black dashed line) and the average blubber proportion for a blue whale (27%; upper black dashed line), with a potential maximum of 35% over the course of the seven months (black solid line) and a minimum of 5% blubber (dotted line).

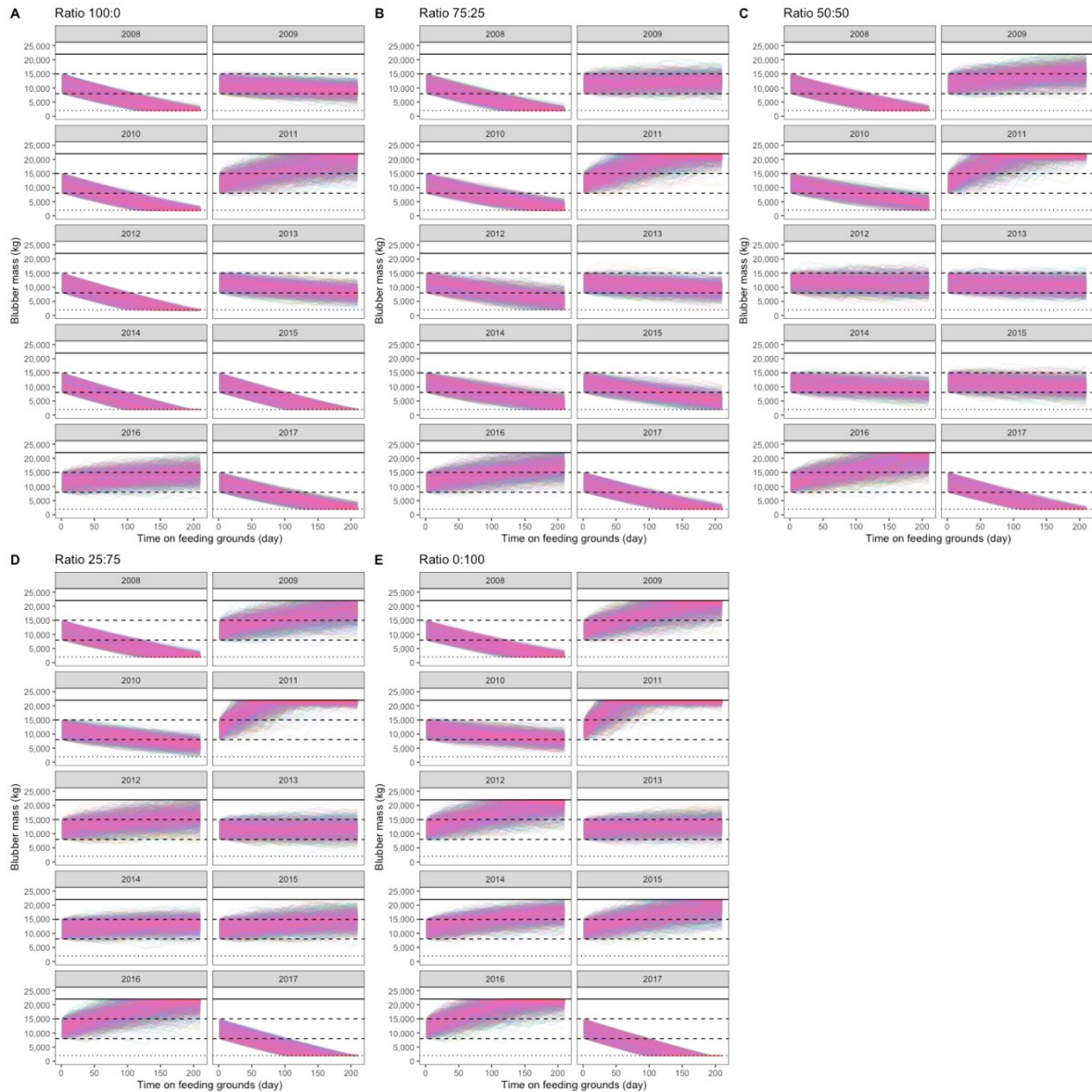


Figure 46 : Blue whale blubber mass (kg) over a seven months foraging period on the feeding ground, according to year-specific krill densities measured during hydroacoustic surveys above the 75th percentile, while assuming that whales fed on a range of ratios (A) *Thysanoessa* spp. 100:0, (B) 75:25, (C) 50:50, (D) 25:75 or (E) *M. norvegica* 0:100. Body condition in terms of blubber proportion when arriving on feeding grounds was allowed to vary between 16% (lower black dashed line) and the average blubber proportion for a blue whale (27%; upper black dashed line), with a potential maximum of 35% over the course of the seven months (black solid line) and a minimum of 5% blubber (dotted line).

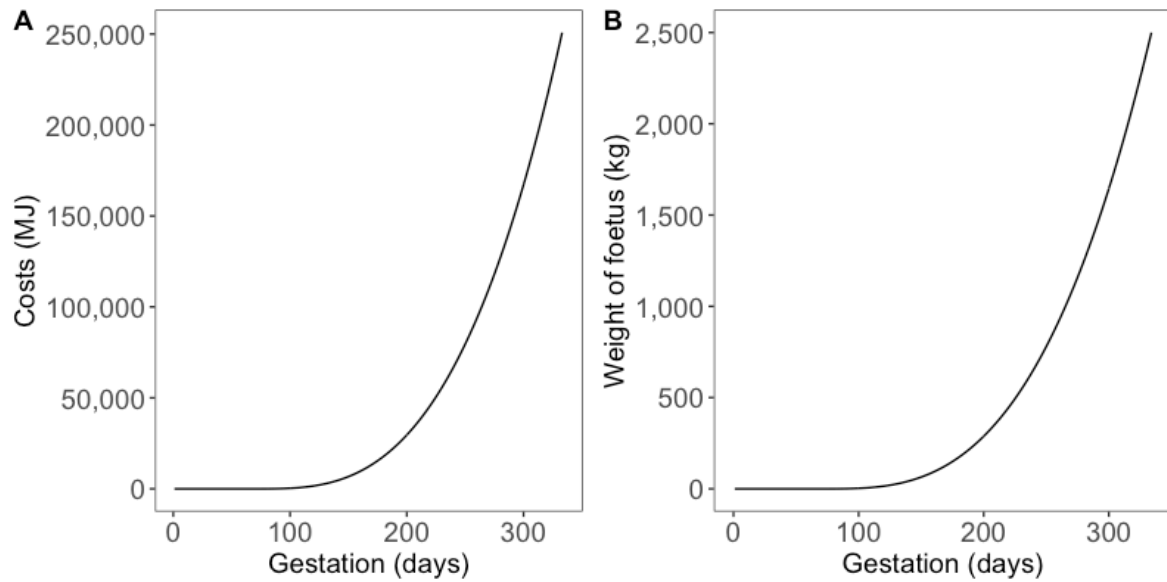


Figure 47 : (A) Cost of gestation (MJ) for the entire gestation period and (B) associated growth curve of the weight of foetus (kg).

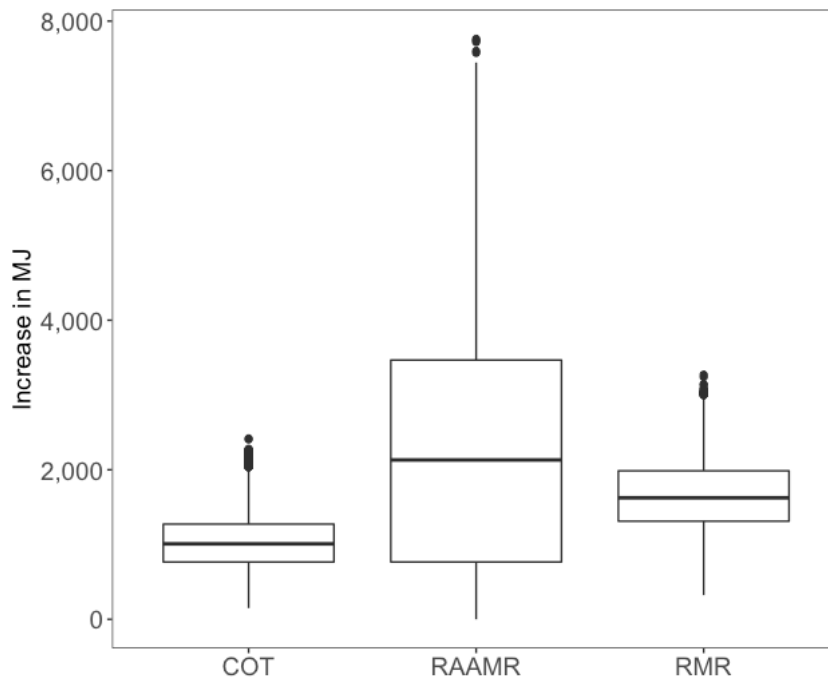


Figure 48 : Increase in locomotion costs due to the burden of motherhood for the cost of transport (COT), the rorqual average active metabolic rate (RAAMR), and the resting metabolic rate (RMR). Boxplots present the median (solid horizontal line), lower and upper quartiles (boxes), extreme values (whiskers) and outliers (points).

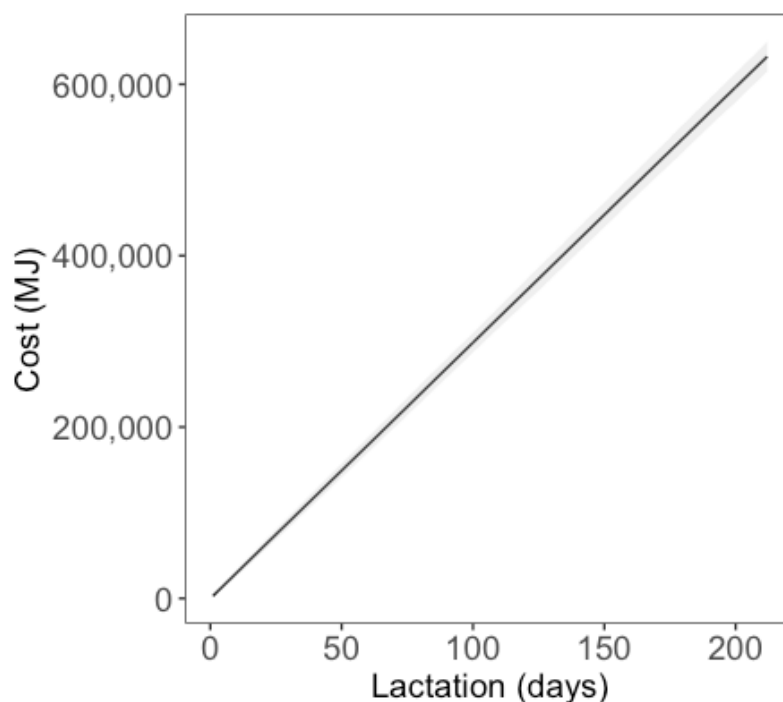


Figure 49 : Mean cost of lactation (MJ) (solid line) including the 95% confidence intervals (ribbon) estimated for 1000 simulated lactating females, with milk delivery variable between 90 and 220 kg of milk per day.

3.8.3 Supplementary data: model parameters

Details of the calculations of the costs of feeding C_f , costs of resting C_r , time spent feeding t_f and time needed to fill the forestomach t_j are provided below.

The cost of feeding (kJ) was (Pirota et al., 2018b):

$$C_f(t) = RAAMR \cdot (3600 \cdot t_f(t)) \cdot W(t)$$

in which $t_f(t)$ is the time spent feeding (h), $RAAMR$ is the rorqual average active metabolic rate ($W \cdot \text{kg}^{-1}$) (Potvin et al., 2012) and $W(t)$ is the weight (kg).

The cost of resting (kJ) was (Pirootta et al., 2018b):

$$C_r(t) = \frac{t_r(t)}{24} \cdot MR_r(t)$$

where $t_r(t)$ is the time spent resting (h) and MR_r is the daily resting metabolic rate ($\text{kJ} \cdot \text{d}^{-1}$) (Kleiber 1975; Potvin et al., 2012).

The time spent feeding and resting was driven by the size of the animal and the krill density preyed upon: length (m) determines the buccal size and forestomach size (Wiedenmann et al., 2011), which, together with krill density, influence the time needed to fill the forestomach and, consequently, the digesting time (i.e. time required to clear the forestomach) (Wiedenmann et al., 2011; Pirootta et al., 2018b). Therefore, the time spent feeding t_f (h) on a day of foraging (t) was defined as (Pirootta et al., 2018b):

$$t_f(t) = t_j(t) \cdot n_j$$

where t_j is the time needed to fill up the forestomach given a krill density j and n_j is the number of times the forestomach can be filled given a krill density j . Therefore, the time spent digesting/resting (h) on a day of foraging (t) was $t_r(t) = 24 - t_f(t)$.

The time needed to fill the forestomach was directly linked to the density of krill and was therefore calculated as follow (Pirootta et al., 2018b):

$$t_j(t) = \frac{\Psi}{(\omega_j \cdot j \cdot \beta)}$$

Where Ψ is the length-specific forestomach capacity (kg), ω_j is the number of lunges per hour, j is the krill density and β is the engulfment volume of a lunge (m^3). The number of lunges per hour was taken from Guilpin et al. (2019) hourly averages (Figure S10), approximated by a Weibull distribution (scale = 28, shape = 4), and could not be linked to krill density in the absence of blue whale behavioural data simultaneous to hydroacoustic surveys.

The number of times the forestomach can be filled n_j depends on krill density j and the time to clear the forestomach $t_e = 4$ h. Therefore, we followed the relation established by Wiedenmann et al. (2011) and Pirotta et al. (2018): if $t_j > t_e$ then $n_j = h_f / t_j$, with h_f being the maximum numbers of hours spent feeding per day (set to 24 h in our case study); in contrast, if $t_j < t_e$ then $n_j = h_f / t_e$.

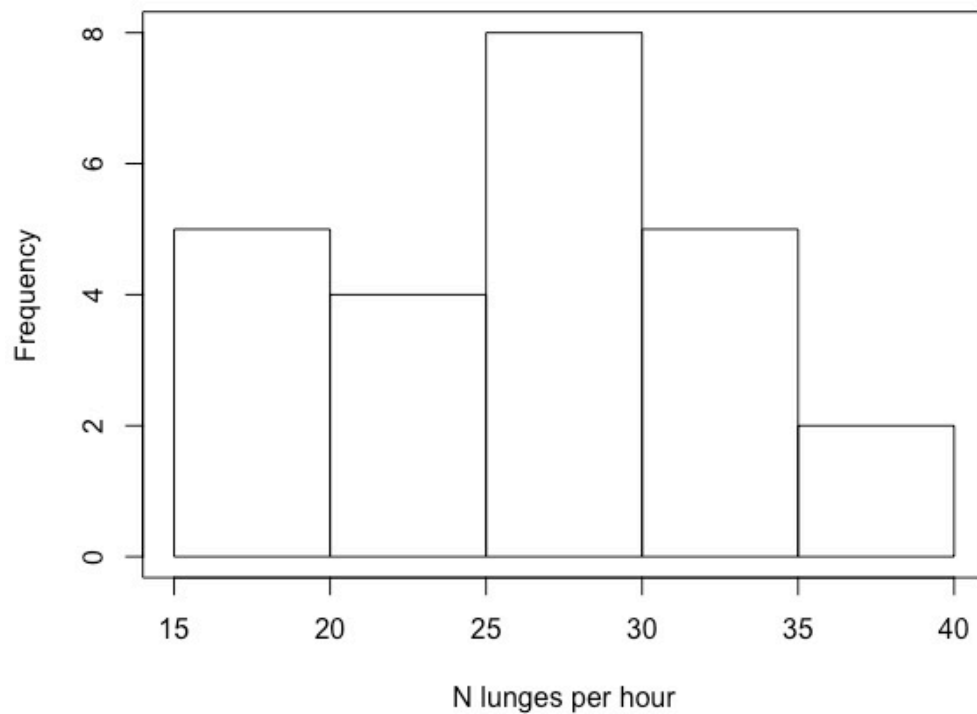


Figure 50 : Frequency distribution the number of lunges performed per hour taken from Guilpin et al. 2019.

CONCLUSION GÉNÉRALE

CONTRIBUTION DE L'ÉTUDE

L'objectif principal de cette thèse de doctorat était de quantifier les besoins énergétiques du rorqual bleu afin de caractériser la capacité du milieu, l'estuaire et le golfe du Saint-Laurent (EGSL), à répondre aux besoins de la population de rorquals bleus de l'Atlantique Nord-Ouest. En parallèle, il s'agissait de déterminer les besoins en krill de ces derniers afin de permettre la mise en place d'une gestion écosystémique des stocks de krill dans l'EGSL. Pour ce faire, des approches de modélisation à plusieurs échelles temporelles (p. ex., heure, jour, mois et année) ont été utilisées. Grâce à l'utilisation de données empiriques du comportement de plongée des rorquals bleus provenant d'enregistreurs de données (*biologgers*), une première estimation de la dépense énergétique par heure liée au comportement alimentaire a été possible. L'absence de données de krill *in situ* en simultané aux données d'enregistreurs de données a mené à une approche innovante visant à estimer les densités de krill requises par heure pour répondre aux besoins énergétiques des rorquals bleus (chapitre 1). Par la suite, les densités estimées ont été comparées aux densités de krill *in situ* mesurées à partir de relevés hydroacoustiques lors d'observations de rorquals bleus en surface. Grâce à une approche de modélisation avec simulations de scénarios probables, nous avons pu investiguer l'effet d'une diminution des densités de krill et d'une diminution du temps de plongée, induite par exemple par la présence d'embarcations à proximité, sur les capacités d'acquisition d'énergie (chapitre 2). Les rorquals bleus étant considérés comme des *capital breeders*, nous avons quantifié l'énergie potentiellement accumulée pendant des saisons complètes d'alimentation (de mai à novembre) et comparé cette dernière aux besoins énergétiques d'un cycle de reproduction (27 mois). Ceci a permis d'estimer la capacité des

rorquals bleus à exploiter les ressources disponibles et à accumuler l'énergie nécessaire à la reproduction (chapitre 3).

Ce projet combinant des approches à différentes échelles temporelles (heure, jour, mois, année) a permis pour la première fois de capter, dans leur globalité, les besoins énergétiques des rorquals bleus de l'EGSL. Nos résultats ont par ailleurs permis 1) d'approfondir les connaissances sur les besoins énergétiques associés à l'alimentation des rorquals bleus dans l'EGSL; 2) de quantifier leurs besoins en krill ; 3) d'évaluer leur vulnérabilité face à une diminution des densités de krill potentiellement en réponse aux changements trophiques à prévoir avec l'augmentation des espèces tempérées au détriment d'espèces arctiques ou à une éventuelle exploitation commerciale des espèces de krill ; et 4) d'investiguer si les densités de krill présentes dans l'EGSL pourraient être un facteur important affectant le statut nutritionnel des rorquals bleus, et pouvant être en cause dans le faible taux de reproduction apparent. Les résultats et conclusions issus de ces trois chapitres apportent ainsi de nouvelles connaissances et visions sur la bioénergétique et l'écologie du rorqual bleu, dont la population de l'Atlantique Nord-Ouest est actuellement désignée comme « en voie de disparition ». Cette thèse de doctorat est la première étude prenant en compte l'énergétique des rorquals bleus dans ce site d'étude pour essayer de comprendre les facteurs limitant leur croissance, et ainsi contribuer aux mesures de protection favorisant le rétablissement de cette population. L'énergétique est centrale à la compréhension des processus écologiques cruciaux à la survie, le maintien et la reproduction des individus (Tomlinson et al., 2014). Ces processus sont associés à des coûts énergétiques que les individus doivent couvrir grâce aux ressources présentes et acquises dans l'environnement dans lequel ils évoluent.

Une première estimation de la dépense énergétique

L'utilisation de données empiriques sur le comportement de plongée des rorquals bleus dans l'EGSL a permis de modéliser la dépense énergétique associée et d'estimer pour la

première fois la dépense énergétique en lien avec l'effort d'alimentation pour chaque heure de la journée (chapitre 1). Nous avons calculé la dépense énergétique de chaque plongée d'alimentation ainsi qu'à plus grande échelle, pour chaque heure de la journée. Le coût énergétique d'une plongée d'alimentation dépend de la profondeur d'alimentation mais aussi du nombre de *lunges* effectués. La dépense énergétique de plongées ayant des caractéristiques similaires (c'est à dire, 3,5 *lunges*) entre les rorquals bleus en alimentation dans l'EGSL et ceux en alimentation le long de la côte californienne résulte en des estimés moyens de coûts énergétiques du même ordre de grandeur (41 130–69 160 kJ et 40 767–77 769 kJ pour l'EGSL et la Californie, respectivement) pour des tailles d'individus modélisés entre 22 et 27 mètres (chapitre 1; Goldbogen et al., 2011). Une étude basée sur les mêmes enregistreurs de données de rorquals bleus dans l'EGSL a aussi démontré que les rorquals bleus suivaient la théorie de l'alimentation optimale, en augmentant le nombre de *lunges* par plongée avec l'augmentation de la profondeur d'alimentation (Doniol-Valcroze et al., 2011). Cependant cette dernière ne prenait pas en compte l'aspect énergétique ni les densités de krill que les individus auraient pu rencontrer. Or, l'effort d'alimentation est lié aux contraintes biologiques et physiologiques d'un prédateur et à la distribution verticale des densités de proies (Witteveen et al., 2015; Ishii et al., 2017; Wright et al., 2017). Les rorquals se nourrissaient plus en profondeur pendant le jour comparativement à la nuit tout en présentant des stratégies d'alimentation distinctes (cette thèse; Doniol-Valcroze et al., 2011). Cependant, même s'ils effectuaient des plongées plus longues avec un nombre de *lunges* plus élevé par plongée le jour, le nombre de *lunges* par heure était plus élevé pendant la nuit car ils effectuaient plus de plongées à plus faible profondeur la nuit. Étonnamment, cette différence dans l'effort d'alimentation n'a pas mené à une différence significative dans la dépense énergétique associée au comportement de plongée d'alimentation, qui est restée stable tout au long de la journée. Cette différence dans l'effort d'alimentation entre le jour et la nuit est liée à la distribution verticale du krill et leurs migrations nycthémerales. Cependant, pendant la journée, il existait une grande variabilité dans la profondeur de plongée des rorquals bleus. Ceci a aussi été démontré dans une étude préalablement réalisée sur les types d'habitats utilisés par des rorquals bleus en alimentation dans la zone d'étude

qui suggérait une profondeur d'alimentation bimodale durant la journée (Doniol-Valcroze et al., 2012). Quantifier la dépense énergétique associée au comportement alimentaire des rorquals bleus dans l'EGSL à l'échelle de la journée constitue donc la première étape dans l'étude des interactions bioénergétiques entre le krill et les rorquals bleus, en vue de déterminer si l'EGSL fournit une capacité de support suffisante, notamment en termes de densité de krill afin de permettre le maintien de la population.

Estimer les besoins en krill

Déterminer les besoins en nourriture d'un prédateur en fonction de ses besoins énergétiques est crucial dans la compréhension des relations bioénergétiques entre les prédateurs et leurs proies. La distribution verticale des proies ainsi que leurs densités sont des facteurs dictant les décisions de quête alimentaire d'un prédateur (MacArthur and Pianka, 1966). La modélisation de la dépense énergétique a permis d'estimer l'apport énergétique requis, qui peut être traduit en consommation de proies lorsque le régime alimentaire et le contenu énergétique des proies sont connus (Boyd, 2002; Noren et al., 2012). Dans notre étude, la dépense énergétique associée à l'activité d'alimentation a pu être modélisée grâce à l'utilisation de données empiriques du comportement de plongée. L'approche innovante utilisée pour pallier l'absence de données de krill *in situ* en simultané aux données empiriques a permis de déterminer les densités de krill minimales requises par les rorquals en fonction de différentes efficacités d'alimentation. Les densités de krill requises varient avec les heures de la journée et sont donc inextricablement liées au nombre de *lunges* effectués (chapitre 1). Nous avons pu prédire les densités nécessaires pour atteindre un équilibre énergétique neutre et pour que celui-ci soit jusqu'à quatre fois plus grand, permettant une accumulation d'énergie sous forme de gras. Nous avons conclu que les densités nécessaires à l'atteinte d'un équilibre énergétique ($14\text{--}40 \text{ g} \cdot \text{m}^{-3}$ et $11\text{--}33 \text{ g} \cdot \text{m}^{-3}$ pour *Thysanoessa* spp. et *Meganyctiphanes norvegica* respectivement) ou à l'accumulation d'énergie ($56\text{--}159 \text{ g} \cdot \text{m}^{-3}$ (*Thysanoessa* spp.) et $46\text{--}131 \text{ g} \cdot \text{m}^{-3}$ (*M. norvegica*)) devaient être plus grandes dans le cas d'une alimentation visant *Thysanoessa* spp. par rapport à Mn. En comparant ces densités

estimées à celles mesurées dans l'EGSL nous avons pu démontrer que seul 1,5% des agrégations de krill permettaient le stockage d'énergie. En comparaison avec d'autres environnements, la population de rorquals bleus de l'EGSL semblerait atteindre une efficacité d'alimentation plus faible que les autres populations dans le monde, probablement en raison des faibles densités de krill rencontrées. Dans l'EGSL, les densités de krill mesurées par relevés hydroacoustiques et utilisées dans cette thèse variaient en général entre 0–250 $\text{g}\cdot\text{m}^{-3}$. En comparaisons, celles mesurées en Californie et sur lesquelles les rorquals bleus s'alimentaient étaient plutôt de l'ordre de 150–4500 $\text{g}\cdot\text{m}^{-3}$ leur permettant d'atteindre des efficacités d'alimentation de 2,6 à 77 (pour un individu moyen de 25 m) (Goldbogen et al., 2011). Cependant, dans leur cas, l'efficacité d'alimentation est calculée à l'échelle de la plongée seulement et par conséquent ne tiens pas compte des périodes autres qu'alimentaires qui ne comportent que des dépenses énergétiques contrairement à la méthode adoptée dans cette présente thèse. En Antarctique, un exercice de modélisation a prédit que des rorquals bleus ne s'alimenteraient pas sur des densités de krill en deçà de 110 $\text{g}\cdot\text{m}^{-3}$ (Wiedenmann et al., 2011). Ces estimés s'accordent avec les densités minimales estimées pour des rorquals bleus dans le Pacifique (Goldbogen et al., 2011).

La vulnérabilité face à une diminution de la densité de krill et au dérangement anthropique

Les prédateurs marins sont capables de moduler leurs efforts d'alimentation en fonction de la densité et de la distribution des proies (Friedlaender et al., 2009; Goldbogen et al., 2015), mais aussi en fonction de leurs contraintes physiologiques (Booth et al., 2018; Hückstädt et al., 2018), suggérant une certaine flexibilité et plasticité. Cependant cette flexibilité n'est pas toujours suffisante pour pallier à la rareté ou à la faible abondance de proies (Ronconi & Burger, 2008), ce qui va indéniablement avoir des conséquences énergétiques (McHuron et al., 2018a). L'utilisation d'une approche de modélisation avec simulations de scénarios a permis d'explorer les conséquences énergétiques de changements de comportements d'alimentation liés à des perturbations humaines ainsi que des variations

du paysage du krill sur le gain net d'énergie du rorqual bleu dans l'EGSL (chapitre 2). Des scénarios ont permis d'étudier les effets de tels changements par rapport aux conditions de base incluant des données *in situ* de krill, tout en tenant compte des profondeurs de recherche de nourriture sur une période de 10 h.

Compte tenu de la distribution verticale des densités de krill mesurées *in situ* par relevés hydroacoustiques, le plus grand potentiel d'accumulation d'énergie était prédit lorsque les individus se nourrissaient sur des pics de densité peu profonds, ou lorsque le double des densités était trouvé en profondeur, ou que les individus ciblaient *M. norvegica* plutôt que *Thysanoessa* spp. En général, les effets variaient avec la densité et la profondeur des agrégations de krill accessibles aux rorquals bleus, et augmentaient avec l'ampleur des réductions de densité de krill et avec la durée de la proximité des bateaux d'excursion. Il est intéressant de noter que, plus les densités initiales sur lesquelles les individus s'alimentaient étaient grandes, moins l'effet d'une réduction de krill était important. Une diminution des densités de krill de 25 à 50% ne permettait plus aucun gain net d'énergie. Les activités d'observation en mer, quant à elles, peuvent réduire l'activité de recherche de nourriture des mammifères marins en déclenchant des réponses d'évitement et en modifiant leurs comportements de plongée (Christiansen et al., 2013; Senigaglia et al., 2016; Schuler et al., 2019). Nous avons démontré qu'un dérangement d'une durée de 3 h avait des effets négligeables ou faibles tandis qu'un dérangement de 10 h représentait une perturbation importante menant à une diminution significative du gain net énergétique de 47 à 85% selon la profondeur d'alimentation et les densités de krill disponibles. La proximité des bateaux d'excursion à moins de 400 m diminuait le temps de plongée (Lesage et al., 2017b), limitant ainsi la profondeur d'alimentation des individus. L'effet du dérangement par les bateaux d'excursion dépendait donc du comportement alimentaire dans lequel se trouvait l'individu avant d'être dérangé et de l'accessibilité des ressources. La combinaison des deux facteurs a aboutit à une addition des impacts de chacune des deux perturbations. Cependant, il n'est pas exclus qu'il s'agisse d'un effet synergique et que les deux facteurs s'amplifient mutuellement, mais cet effet n'a pas été testé. Un des points majeurs de cette étude (chapitre 2) réside dans le fait que les impacts du dérangement et de la réduction du krill dépendaient

tous les deux des densités de krill les plus bénéfiques et des profondeurs auxquelles elles se situaient. Nous avons également démontré que le déficit énergétique causé par les réductions de densité de krill, la proximité des bateaux d'excursion, ou leur combinaison, pouvait être important, même lorsque les bateaux d'excursion étaient à proximité pendant des périodes relativement courtes (3 h). Cette étude souligne l'importance des limites de distance et de durée d'interactions lors des excursions d'observation des baleines pour assurer une alimentation efficace, ainsi que la vulnérabilité de ce spécialiste face aux fluctuations des densités de krill (chapitre 2).

Il existe fort probablement une distinction d'échelle temporelle sur laquelle une diminution des densités de krill suite à une exploitation commerciale ou suite aux changements climatiques s'opèrerait. Ainsi, une diminution de densité suite à une exploitation commerciale peut être vue comme un changement beaucoup plus abrupt dans le temps tandis que des changements liés aux changements climatiques s'étalent vraisemblablement sur des années. La flexibilité des prédateurs à faire face à des conditions environnementales dynamiques pourrait leur permettre de pallier à des diminutions évoluant sur le long terme et non à des perturbations abruptes ou accélérées dans un système pour lequel les densités retrouvées sont déjà faibles en comparaison à d'autres régions (voir section précédente). La plasticité comportementale pourrait à elle seule être insuffisante pour atténuer les conséquences du changement climatique, qui accélère et exacerbe la variabilité naturelle des proies (Ronconi and Burger, 2008; Sydeman et al., 2013). Ces deux dernières décennies, les changements climatiques semblent agir négativement sur l'abondance et la distribution du krill, la composition des espèces et le cycle de vie dans les deux pôles (en Arctique et Antarctique) en affectant la température de l'eau, l'étendue de la glace de mer et d'autres facteurs environnementaux (Flores et al., 2012; McBride et al., 2014). Dans l'EGSL, l'épaisseur de la couche intermédiaire froide pourrait diminuer avec le réchauffement des eaux ce qui se traduirait par une perte d'habitat pour *Thysanoessa* spp. en termes de température (Galbraith et al., 2019). Par contre, *M. norvegica*, une espèce adaptée à des eaux tempérées (Sameoto, 1976), verrait son habitat augmenter. Nous ne pouvons que supputer quant à l'effet des changements climatiques en cours dans l'EGSL sur les densités de krill

dont les espèces dominantes occupent des niches de températures différentes (Sameoto, 1976; Mauchline and Fisher, 1980).

La disponibilité des proies peut également moduler les impacts des perturbations en agissant en synergie. Une étude de simulation impliquant des rorquals bleus a indiqué qu'au-delà du déficit potentiel instantané de gain énergétique net associé à un événement perturbateur, la récurrence de perturbations anthropiques (par exemple, chaque année) et son effet combiné avec de mauvaises conditions environnementales pourraient entraîner de forts effets négatifs sur leur succès reproducteur, puisqu'ils priorisent leur propre survie au lieu d'investir dans la reproduction (Pirotta et al., 2019). Dans la zone d'étude de l'EGSL, les résultats ne permettent pas d'indiquer si les changements modélisés pourraient affecter la capacité du rorqual bleu à accumuler des réserves d'énergie adéquates pour se reproduire avec succès ou pour survivre, puisque cela dépend de la persistance des interactions avec les bateaux d'excursion et de l'abondance de nourriture. Les besoins énergétiques à long terme et notamment ceux associés à la reproduction doivent être estimés afin de quantifier l'impact d'un déficit énergétique lié au dérangement sur le succès reproducteur des individus.

Les densités de krill comme indice d'un faible succès reproducteur

Une modélisation sur un cycle de reproduction au complet (27 mois) a permis de démontrer que les rorquals bleus pouvaient acquérir des réserves énergétiques suffisantes pour la production d'un veau au cours de la moitié des années modélisées. C'était le cas, notamment, uniquement lorsqu'ils se nourrissaient principalement de *M. norvegica* et sur des densités supérieures au 75^{ème} percentile de la distribution de krill. Ces résultats vont toutefois à l'encontre de résultats préalablement publiés et devront être investigués davantage. Par exemple, une étude isotopique identifie *Thysanoessa* spp. comme l'espèce dominante (70%) le régime alimentaire des rorquals bleus entre 1992 et 2010 (Gavrilchuk et al., 2014). De plus, une autre étude a démontré une plus grande association spatiale des rorquals bleus avec les densités de *Thysanoessa* spp. (McQuinn et al., 2016). La condition corporelle des

femelles est un facteur déterminant dans le succès reproducteur de nombreuses espèces de mammifères marins (Guinet et al., 1998; Miller et al., 2011; New et al., 2013b; Williams et al., 2013; Jeanniard-du-Dot et al., 2017). Pour les *capital breeders*, l'accumulation suffisante de réserves énergétiques afin de permettre une reproduction est cruciale (Lockyer, 1986; Miller et al., 2011; Christiansen et al., 2020). De plus, les taux d'ovulation et de reproduction dépendent de la quantité de réserves énergétiques comme démontré chez certaines espèces de rorquals (Miller et al., 2011; Christiansen et al., 2020). D'autre part, la lactation est l'étape de la reproduction la plus coûteuse en énergie chez les mammifères (Gittleman and Thompson, 1988; Christiansen et al., 2016). L'approvisionnement en énergie du veau et son taux de croissance lors de la lactation dépendent des réserves énergétiques de la mère, ainsi des femelles en meilleure condition physique produisent des veaux plus grands avec un taux de survie plus élevé (Christiansen et al., 2018). Dans l'Atlantique Nord-Ouest et l'EGSL en particulier, seules quelques observations de paires mère-veau ont été faites (28 en 40 ans d'observation ; Sears, données non publiées) et l'intervalle de mise bas est estimé à environ 4 ans (Sears et al., 2013), alors que l'intervalle de mise bas des rorquals bleus dans le Pacifique le long de la côte californienne est estimé en moyenne à 2,37 ans (Sears et al., 2013). Le faible taux de natalité apparent pourrait être expliqué par des densités de krill limitantes, menant à une condition corporelle ne permettant pas un intervalle de mise bas semblable à celui de la population de rorquals bleus du Pacifique Nord-Est.

LIMITATIONS ET PERSPECTIVES

Limitation de l'étude

Cette thèse de doctorat est basée sur des données empiriques du comportement alimentaire des rorquals bleus dans l'EGSL et de densités de krill. Il y a cependant une importante partie de modélisation qui repose inévitablement sur des hypothèses ou sur la simplification de processus et paramètres. La plupart de ces hypothèses limitent l'étude, mais sont autant de sujets identifiés et de perspectives sur lesquelles concentrer les prochains

efforts de recherche. Cette section détaille les principales limitations identifiées au fil de ce travail doctoral ainsi que des propositions afin de pallier ces limitations.

- *Taille d'échantillon du comportement alimentaire des rorquals bleus*

L'analyse de sensibilité du chapitre 1 indique que la plus grande source d'incertitude réside dans le nombre de *lunges* faits par heure, qui se propage ensuite au coût énergétique de l'activité d'alimentation par heure. L'incertitude dans le nombre de *lunges* par heure peut être lié à l'hétérogénéité de la durée de déploiement des enregistreurs de données, mais réside aussi dans la variabilité interindividuelle du comportement en terme de budget d'activité et de profondeur de plongée des rorquals bleus. La taille d'échantillon réduite ($n = 10$) des données empiriques de comportements de plongées ne permet pas de lisser cette variabilité interindividuelle inhérente. L'augmentation de la taille de l'échantillon pourrait réduire cette incertitude. Cependant, la grande variabilité observée dans l'effort de recherche de nourriture horaire (nombre de plongées d'alimentation par heure, nombre de *lunges* par plongée et nombre de *lunges* par heure) pourrait également être écologique. Les individus de différent sexe, d'âge et de statut reproducteur différents ont des besoins énergétiques propres (Winship et al., 2002; Hammill et al., 2010; Fortune et al., 2013; Villegas-Amtmann et al., 2015) et devraient adopter différents comportements et stratégies de recherche de nourriture (Hoskins and Arnould, 2013; Hückstädt et al., 2018). De plus, une étude précédente a démontré que les rorquals bleus utilisent trois types d'habitats différents pour l'alimentation dans l'estuaire du Saint-Laurent (Doniol-Valcroze et al., 2012). Une augmentation de la taille de l'échantillon éliminerait cette variabilité qui a aussi un fondement écologique, ou il s'agirait d'avoir un échantillon pour lequel le sexe et des informations sur l'histoire des individus.

- *Les senseurs des enregistreurs de données limitent la précision des coûts énergétiques*

Les senseurs des enregistreurs de données ont permis la détection et l'extraction du nombre de *lunges* par plongée notamment par l'utilisation de la vitesse de nage (Doniol-Valcroze et al., 2011, 2012). Toutefois, le nombre limité et le type de senseurs sur les enregistreurs de données n'ont pas permis d'obtenir toutes les caractéristiques de plongée d'alimentation, comme la durée des *lunges* et les manœuvres effectuées, qui ont une influence majeure sur le coût énergétique estimé (Goldbogen et al., 2013a, 2015; Kot et al., 2014). L'utilisation d'accéléromètre triaxial n'était pas encore très répandu dans le domaine des mammifères marins lorsque le travail de terrain a commencé en 2002 sur les rorquals bleus de l'EGSL (Bograd et al., 2010). Le déploiement d'enregistreurs de données avec des senseurs tels qu'un accéléromètre triaxial permettrait d'estimer plus précisément les coûts énergétiques associés au comportement d'alimentation en ayant des caractéristiques d'alimentation encore plus détaillées (Halsey et al., 2009; Bograd et al., 2010). En effet, les taux métaboliques spécifiques à l'alimentation des rorquals sont issus de modèles hydrodynamiques robustes et ont été estimés spécifiquement pour chaque phase d'un *lunge* (Potvin et al., 2010, 2012; Goldbogen et al., 2012).

- *L'absence de caractérisation des densités de krill réellement ciblées*

L'approche innovante utilisée dans le chapitre 1 a permis une estimation des densités requises en fonction des coûts énergétiques en l'absence de données hydroacoustiques en simultané aux données de comportements alimentaires des rorquals bleus. Cependant, ce manque de données ne permet pas la caractérisation du type de densités de krill ciblées par les rorquals. Des mesures *in situ* de densités de krill en simultané aux données de comportements de recherche et d'alimentation sont essentielles afin de pouvoir affirmer, corroborer ou infirmer les densités requises estimées dans le chapitre 1.

- *Variabilité intra-annuelle des densités de krill*

Les densités de krill *in situ* estimées à partir de données de relevés hydroacoustiques et utilisées dans les chapitres 2 et 3 proviennent d'une seule mission par année ayant lieu en août. La distribution horizontale du krill peut être affectée par les courants océaniques et les tempêtes (Maps et al., 2015; McQuinn et al., 2015) tandis que la distribution verticale est davantage influencée par la température et la pénétration de la lumière, mais aussi liée à la salinité (Plourde et al., 2014b). De plus, le krill est une ressource très dynamique, dont la distribution varie d'heures en jours, semaines et mois (Siegel and Kalinowski, 1994). Un relevé effectué en août pourrait ne pas capturer l'abondance et les densités disponibles au cours des semaines entourant l'échantillonnage. Étant donné la distribution hétérogène et hautement dynamique du krill, l'utilisation de densités estimées à partir de mesures *in situ* d'un seul relevé hydroacoustique par saison d'alimentation pourrait ne représenter qu'un instantané et donc une caractérisation globale biaisée du paysage des proies. D'autre part, la présence et qualité de données de krill *in situ* durant la nuit sont limitées. En effet, il n'existe pas ou peu de relevés hydroacoustiques systématiques de nuit. De plus, l'obtention d'estimés de densité précis pendant la nuit est difficile étant donné que les mesures hydroacoustiques peuvent être biaisées négativement en raison de la zone aveugle de quelques mètres sous les échosondeurs lorsque le krill se trouve au plus proche de la surface.

- *Variabilité intra-annuelle du contenu énergétique du krill*

Le contenu énergétique spécifique aux deux espèces de krill (*Thysanoessa* spp. et *M. norvegica*) a été utilisé dans les trois chapitres de cette thèse. Ces contenus énergétiques, issus d'échantillons prélevés l'estuaire du Saint-Laurent entre mai et septembre, ont été mesurés par bombe calorimétrique et représente une moyenne du contenu énergétique global des deux espèces ($4,3 \pm 0,6$ versus $5,2 \pm 0,4$ kJ · g⁻¹ pour *Thysanoessa* spp. et *M. norvegica* respectivement) durant toute la période d'alimentation des rorquals bleus (D. Chabot, données non publiées). Cependant le comportement alimentaire, la composition et densité

énergétique différent entre les deux espèces de krill mais varient aussi de manière saisonnière (Cabrol et al., 2019a, 2019b). En général, *Thysanoessa* spp. a une densité énergétique (c'est-à-dire la quantité de lipides par microgram de poids frais) plus élevée que celui de *M. norvegica* (Cabrol et al., 2019b), qui atteint son maximum en été et à l'automne. Cette variabilité du contenu et de la composition lipidique des deux espèces pourrait avoir un impact sur le gain énergétique des rorquals bleus mais aussi sur leur comportement alimentaire. Le régime alimentaire des rorquals bleus entre 1990 et 2010 était dominé par *Thysanoessa* spp. à 70% selon des études isotopiques (Gavrilchuk et al., 2014), et l'indice d'association spatial entre les densités de krill et des observations de rorquals bleus à la surface démontre une plus grande association des rorquals bleus avec *Thysanoessa* spp. (McQuinn et al., 2016). Ainsi, compte tenu de la variabilité saisonnière du contenu lipidique des deux espèces de krill (Cabrol et al., 2019b), il pourrait ainsi être plus bénéfique pour des rorquals bleus de s'alimenter sur *Thysanoessa* spp. selon les mois de la saison d'alimentation dépendamment de la quantité et du type de lipides contenus (Cabrol et al., 2019a, 2019b). Une estimation du contenu énergétique tenant compte des différentes classes de lipides contenues dans chaque espèce de krill et de la variabilité intra annuelle (Cabrol et al., 2019b, 2019a) pourrait aboutir à des estimés de contenus énergétiques plus précis. Cependant, la modélisation des réserves énergétiques des rorquals bleus sur une saison d'alimentation complète basées sur les densités de krill mesurées entre 2008 et 2017 à partir de relevés hydroacoustiques indique que les rorquals bleus accumuleraient seulement la moitié du temps des réserves énergétiques suffisantes pour assurer la reproduction uniquement s'ils s'alimentaient majoritairement sur *M. norvegica* et en ciblant les plus hautes densités. Ces résultats contredisent les résultats préalablement publiés sur le régime alimentaire et l'indice d'association (Gavrilchuk et al., 2014; McQuinn et al., 2016) et seront davantage examinés.

Perspectives de recherche

Plusieurs avenues pourraient être explorées afin de pallier aux lacunes de cette étude, d'élargir davantage les connaissances sur l'écologie alimentaire et d'apporter de nouvelles informations essentielles au rétablissement de la population de rorquals bleus de l'Atlantique Nord-Ouest (Figure 51). Certaines de ces propositions de recherche reposent sur l'analyse de données déjà récoltées tandis que d'autres pourraient représenter des futurs projets de recherche à part entière.

- *Estimation plus précise des coûts énergétiques*

Estimer de manière la plus précise possible le coût énergétique des différentes activités est essentiel afin de diminuer l'incertitude de ce paramètre, même s'il y aura toujours une variabilité interindividuelle inhérente. L'utilisation d'enregistreurs de données avec des senseurs tels qu'un accéléromètre triaxial et magnétomètre pourrait permettre de raffiner le comportement d'alimentation et ainsi les coûts énergétiques associés. Il a été démontré que les rorquals bleus en Californie effectuent plus de manœuvres quand ils se nourrissent sur des densités plus faibles (Goldbogen et al., 2013a, 2015). Le recours aux manœuvres permet à l'individu de concentrer les proies au moment de l'engouffrement, augmentant ainsi la densité de krill sur laquelle ils s'alimentent. Il serait intéressant d'avoir une telle information, puisque les densités de krill estimées dans cette étude sont bien en deçà de celles retrouvées dans le Pacifique ou en Antarctique et nous pourrions donc émettre l'hypothèse que les rorquals bleus dans l'EGSL utilisent davantage de manœuvres lorsqu'ils s'alimentent. Cela permettrait aussi d'étudier la vitesse de *lunge* proche de la surface versus en profondeur ou la durée d'engouffrement et de déterminer si l'alimentation proche de la surface est plus ou moins coûteuse en énergie que les plongées effectuées en profondeur. Des données plus précises quant à l'effort d'alimentation et la durée d'un *lunge* permettrait de s'assurer que les calculs ne surestiment pas les coûts énergétiques des plongées d'alimentation (Figure 51–perspective 1).

- *Quantifier les densités de krill ciblées par les rorquals bleus en alimentation*

L'utilisation d'enregistreurs de données équipés de sonar/échosondeurs permettrait de quantifier les densités de krill ciblées et engouffrées par les rorquals bleus (Lawson et al., 2015; Goulet et al., 2019) (Figure 51–perspective 2). Testé sur des éléphants de mer du Sud *Mirounga leonine* (Goulet et al., 2019) et du Nord *Mirounga angustirostris* (Lawson et al., 2015) ces outils représentent une avancée majeure dans la description et la quantification des champs de proies directement visés par les prédateurs. Cependant, un sonar multifréquence n'est pas encore disponible sur ce genre d'appareil (Goulet et al., 2019), et ne permettrait pas de différencier les deux espèces de krill dans l'EGSL, ce qui requiert une approche multifréquence (McQuinn et al., 2013). L'utilisation de caméras vidéos miniatures combinées aux enregistreurs de données permettent de visualiser les manœuvres d'un prédateur en alimentation et le champ de proies ciblé par un prédateur mais ne permettent pas forcément de quantifier précisément les densités de proies ciblées (Akiyama et al., 2019; Cade et al., 2020). De plus, l'utilisation de caméras vidéos peut être limitée en termes de profondeur en fonction de la pénétration de la lumière (Akiyama et al., 2019). Cependant, une mission permettant le déploiement d'enregistreurs de données (avec accéléromètre triaxial) en simultané à des relevés hydroacoustiques permettrait de mieux qualifier les densités de krill ainsi que les espèces de krill ciblées par les rorquals bleus en alimentation (Figure 51–perspective 2). En effet, la distribution des prédateurs est ainsi aussi déterminée par la capacité du milieu à répondre à leurs besoins énergétiques (Wilson et al., 2012). Le concept de paysage énergétique ou « energy landscape », a récemment émergé dans l'écologie du mouvement comme un moyen de relier la distribution spatiale des prédateurs à leurs dépenses énergétiques en fonction des conditions environnementales (Wilson et al., 2012; Shepard et al., 2013; Amélineau et al., 2018). Ainsi, la sélection de l'habitat dépend à la fois de la densité des proies, des besoins énergétiques et de l'interaction entre ces deux paramètres (Amélineau et al., 2018). La densité et la distribution des proies à elles seules ne suffisent pas à prédire la pertinence d'un habitat pour les individus. Les besoins énergétiques

d'un prédateur et donc par extension de la population sont inextricablement liés et influencent l'exploitation du paysage des proies ou « preyscape », par un prédateur en fonction de ses besoins énergétiques. Connaître les besoins énergétiques d'un prédateur et les densités de proies dont il dépend permet de cartographier les zones d'importance et de mieux appliquer les efforts de conservation. De plus, il s'agit de s'assurer que les prélèvements par la pêche n'entravent pas les besoins des prédateurs.

- *Dérangement par la proximité des bateaux d'excursion*

Une étude préalable a démontré que la proximité de bateaux d'excursion à moins de 400 m des rorquals bleus limite leur durée de plongée (Lesage et al., 2017b). Cependant cette étude basée sur des observations de surface n'est pas en mesure d'indiquer si les individus dérangés réduisent leur temps de plongée tout en continuant à s'alimenter, ou s'ils cessent toutes activités alimentaires. L'analyse des enregistreurs de données avec les suivis focaux de surface pourrait permettre d'identifier le type de plongée exécuté lorsque les individus sont dérangés (Figure 51–perspective 3). De plus, les résultats de cette thèse (chapitre 2), indiquent qu'un dérangement d'une durée de 3 h peut avoir un effet négligeable ou faible, mais que lorsque combinés à une diminution des densités de krill ou de longue durée (10 h) les effets peuvent être très importants. L'effet est inextricablement lié à l'habitat dans lequel se nourrissent les rorquals bleus et à la distribution des ressources dans la colonne d'eau. Ces résultats appuient également la réglementation actuellement en vigueur dans le parc marin du Saguenay–Saint-Laurent, qui impose une zone d'exclusion de 400 m pour les bateaux d'excursion autour du rorqual bleu. Cette mesure vise à atténuer les impacts potentiels sur cette espèce en voie de disparition. Il serait souhaitable, nécessaire et recommandé d'étendre ces limites à d'autres habitats importants pour le rorqual bleu, où les interactions avec les bateaux d'excursion peuvent aboutir à des effets chroniques. Les résultats du chapitre 2 soulignent également l'importance de limiter la durée de proximité des bateaux d'excursion, en particulier si les bateaux d'excursion se trouvent à moins de 400 m d'un individu et dans des conditions où les densités de krill pourraient être réduites. Dans le parc marin du

Saguenay–Saint-Laurent, il existe une limitation d’une heure d’observation par navire, avec un intervalle d’une heure entre les observations successives (Règlement du parc marin du Saguenay–Saint-Laurent) (Figure 51–perspective 4). Une mesure de gestion potentielle pourrait être de mettre en œuvre des limites cumulatives du temps d’observation des bateaux d’excursion par jour autour des rorquals bleus afin de réduire la durée totale des perturbations potentielles. De plus, en supplément à la limitation de distance d’approche et de durée d’observation, le niveau sonore émis par les bateaux d’excursions devraient être considéré. En effet, le niveau sonore des bateaux d’excursion pourrait être l’un des éléments déclencheur de changements de comportement des mammifères marins mais dépend grandement du contexte de l’exposition au bruit et de l’espèce (Gomez et al., 2016 ; Erbe et al., 2019). Des femelles avec leurs petits exposées à un niveau sonore supérieur à 172 dB montraient une diminution de 30% du temps de repos, une augmentation de 50% de la fréquence de respiration et une augmentation de 37% de la vitesse de nage (Sprogis et al., 2020). Ces changements de comportements ont probablement un effet sur le budget énergétique des individus. Ainsi, ils préconisent l’utilisation de bateaux d’excursion dont le niveau d’émission sonore est inférieur à 150 dB. Une étude sur le dérangement acoustique des bateaux d’excursion sur le comportement alimentaire du rorqual bleu pourrait être envisagée afin d’améliorer la régulation des activités d’observations.

- *Évaluer les effets à long terme d’une diminution de densité de krill et du dérangement*

Afin de comprendre les effets de réductions de densité de krill et du dérangement sur le gain net énergétique des rorquals bleus sur le long terme (+ de 10 h), les résultats pourraient être incorporés et extrapolés à un modèle de conséquences des perturbations sur les populations « Population Consequences of Disturbances PCoD » (Pirota et al., 2018a) (Figure 51–perspective 5). Le cadre de ce modèle permet de relier l’effet de différents types de perturbations (p. ex. acoustiques, comportementales) et d’évaluer les conséquences sur le long terme aussi bien au niveau individuel qu’au niveau populationnel.

- *Comportement durant le cycle annuel*

La durée de déploiement de balises télémétriques satellites est limitée dans le temps et n'a permis jusqu'à lors que quelques suivis de plusieurs mois durant les périodes de migration et périodes d'hivernage (Lesage et al., 2017a). La continuation de l'étude du suivi par télémétrie satellite est essentielle à la compréhension des mouvements des rorquals bleus de la population de l'Atlantique Nord-Ouest (Figure 51–perspective 6). Les coûts énergétiques estimés de la migration et du temps passé sur les aires d'hivernage dans le chapitre 3 sont basés sur une distribution de vitesse de nage et de distance parcourue par jour sans aucune activité d'alimentation. Néanmoins, l'analyse par Lesage et al. (2017a) des données de suivis télémétriques par satellite indique des zones de recherche restreintes « area restricted search (ARS) » aux environs des monts sous-marins de la Nouvelle-Angleterre. Il existe une incertitude quant à la signification de ces zones de recherche restreintes, qui peuvent être une indication de comportements d'alimentation ou de comportements ayant les mêmes caractéristiques (déplacement à faible vitesse, taux de rotation élevé). La présence de ces zones de recherche restreintes proches de caractéristiques topographiques reconnues comme étant propices à l'alimentation du rorqual bleu pourrait indiquer un comportement alimentaire. Il a été démontré que les rorquals communs et bleus de l'Atlantique Nord-Ouest s'alimentent de façon sporadique aux Açores durant leurs migrations (Silva et al., 2013). De futurs suivis télémétriques de longues durées permettront de mieux comprendre les comportements et les distances parcourues afin de mieux quantifier les coûts énergétiques de la période hivernale incluant la migration, mais aussi les gains énergétiques potentiels. De plus, même s'ils sont rares, il existe un exemple d'échange entre l'Atlantique Nord-Est et l'Atlantique Nord-Ouest. En effet, un rorqual bleu photo-identifié en septembre 1984 par la station de recherche des îles Mingan (MICS) dans l'EGSL a été photographié au large de Pico (Açores) en juin 2014. Ce rorqual a été de nouveau observé par le MICS en août et septembre 2015 (Sears et al., 2015). Les rorquals bleus de la population de l'Atlantique Nord-Ouest pourraient utiliser le bassin atlantique comme leur domaine vital tout entier. Ils

pourraient alterner des patrons de migration entre les lieux de recherche de nourriture, comme le suggèrent les données de télémétrie par satellite et les zones de recherche restreintes « area restricted search (ARS) » (Lesage et al., 2017a).

- *Estimation in situ de la condition corporelle et taux de reproduction*

Depuis 2018, des relevés aériens sont effectués dans le cadre du monitoring et de la conservation de la baleine franche de l'Atlantique Nord. Ces relevés, durant lesquels les observations d'autres mammifères marins, incluant les grands rorquals, sont aussi enregistrées, couvrent la quasi-totalité de la saison estivale, aussi bien spatialement que temporellement (avril/mai à novembre). Cet effort de surveillance accru pourrait servir à raffiner la distribution temporelle des rorquals bleus dans l'EGSL. L'augmentation de l'effort d'observation pourrait ainsi aider à une meilleure quantification du taux de natalité et aider à déterminer si le faible taux d'observation de paires de mère-veau est vraiment dû à un faible taux de natalité ou s'il s'agit d'un biais d'observation. De même, une étude de Lesage et al. est en cours pour déterminer le taux de grossesse des rorquals bleus dans l'EGSL grâce aux dosages d'hormones associées à la reproduction, il sera intéressant de comparer ces chiffres avec le taux de natalité apparent tiré des observations (Figure 51–perspective 7).

Récemment l'utilisation de véhicules aériens sans pilote (ou drones) a permis d'estimer et de monitorer la condition corporelle de plusieurs espèces de cétacés. Christiansen et al. (2020) ont ainsi démontré grâce à de la photogrammétrie aérienne que la population de baleines franches de l'Atlantique Nord était en moins bonne condition corporelle que trois populations de baleines franches australes (Argentine, Australie et Nouvelle-Zélande). Soledade Lemos et al. (2020) ont pu suivre l'évolution de la condition corporelle de baleines grises du Pacifique Nord-Est *Eschrichtius robustus* au cours d'une saison d'alimentation grâce à des données de photogrammétrie aérienne. L'acquisition d'imagerie par véhicules aériens sans pilote et l'application de méthodes d'analyse de photogrammétrie serait un axe

de recherche à développer afin de qualifier la condition corporelle des rorquals bleus dans la zone d'étude avec des données empiriques (Figure 51–perspective 8).

- *Nouvelles avenues de recherche*

Cette thèse de doctorat pourra servir à informer certains aspects du programme des espèces en péril, en particulier concernant les menaces qui pèsent sur la population de rorquals bleus de l'Atlantique Nord-Ouest et qui se portent sur l'effet de la réduction de la disponibilité et de la densité des proies et le dérangement par la proximité des bateaux d'excursion (Lesage et al., 2018). Le travail de modélisation de ce projet de doctorat a permis l'avancée des connaissances sur la bioénergétique des rorquals bleus dans l'EGSL en relation avec le krill. De plus, il s'agit d'un bon moyen pour reconnaître les limitations et visualiser les problématiques pour faire avancer les recherches empiriques. Ce travail de modélisation a également permis d'identifier les limitations rencontrées durant cette thèse, et qui ont été présentées dans les sections ci-dessus avec des perspectives et solutions associées. Les perspectives présentées ci-dessus s'appliquent à différentes échelles temporelles et spatiales et pour certaines, il s'agit de projets déjà en cours (p. ex. les perspectives 6 et 7, Figure 51). Les perspectives 1, 2 et 8 (Figure 51) qui sont : 1) affiner les coûts énergétiques avec des informations plus précises sur les manœuvres et le comportement alimentaire grâce à l'utilisation d'enregistreurs avec un accéléromètre triaxial ; 2) effectuer une meilleure quantification des densités de krill ciblées par les individus en utilisant des "sonar tags" ou relevés hydroacoustiques en simultané aux données d'enregistreurs ; et 8) déterminer la condition corporelle par le biais d'analyses de photogrammétrie aérienne obtenue par véhicules aériens sans pilote ; seraient à mettre en place. Ces perspectives pourraient d'ailleurs faire partie d'un seul et même projet de recherche entrepris durant la saison d'alimentation. Ce projet de grande envergure serait la suite logique de ce travail de doctorat et permettrait d'approfondir encore plus notre compréhension des interactions bioénergétiques entre le rorqual bleu et le krill. Les résultats pourraient ensuite, avec ceux déjà acquis durant cette thèse et ceux des projets en cours, être intégrés à plus grande échelle temporelle sur le cycle de vie des rorquals bleus.

- *Application générale des approches présentées*

Dans le domaine de l'écologie marine, il est souvent difficile de collecter des données sur l'effort de recherche de nourriture d'un prédateur en simultané à l'environnement de proie mais aussi de quantifier la dépense énergétique et les besoins énergétiques à court et long terme. Les outils de modélisation, et en particulier les modèles bioénergétiques permettent malgré des simplifications inévitables de certains mécanismes, de comprendre et de quantifier au mieux les interactions bioénergétiques entre les prédateurs et leurs proies (Winship et al., 2002; Hammill et al., 2010; Noren et al., 2012; Fortune et al., 2013; Pirota et al., 2018b). Dans la présente thèse, des approches telles qu'une approche de rétro-ingénierie pour déterminer les exigences de densité de krill par un grand prédateur marin, estimées à partir de la modélisation des dépenses énergétiques dérivées de données de comportement de plongée, mais aussi des approches de simulations mécanistes paramétrées avec des données empiriques et de la littérature ont été utilisées. Ici, les modèles et simulations utilisés ont été paramétrés avec le comportement et les caractéristiques biologiques du rorqual bleu en alimentation dans l'EGSL pour répondre spécifiquement aux objectifs de recherche de cette thèse de doctorat. Cependant, ces approches pourraient être applicables à d'autres espèces de mammifères marins ou prédateurs dans l'étude des interactions bioénergétiques entre les prédateurs et leurs proies ; et plus spécifiquement lors de problématique de conservation ou pour la mise en place d'une gestion durable d'un écosystème.

Pour conclure, ce travail doctoral constitue la première étude se concentrant sur la bioénergétique de cette population de rorqual bleu. Les résultats obtenus font état de nouvelles connaissances sur la bioénergétique des rorquals bleus et de leurs besoins en krill lorsqu'ils s'alimentent dans l'EGSL. De plus, ces résultats constituent une base de connaissances solides et pourront contribuer aux mesures de conservation nécessaires au

rétablissement de la population de rorquals bleus de l'Atlantique Nord-Ouest et seront donc grandement pertinents lors de la prochaine évaluation du statut de cette population. L'ensemble de ces résultats contribue à une approche écosystémique dans la gestion des stocks de krill présents dans l'EGSL, en y apportant la première quantification des besoins en krill des rorquals bleus. Ces résultats permettront également de mieux appréhender les conséquences de futurs changements des communautés zooplanctoniques et de façon plus générale sur les espèces qui dépendent du krill comme ressource principale.

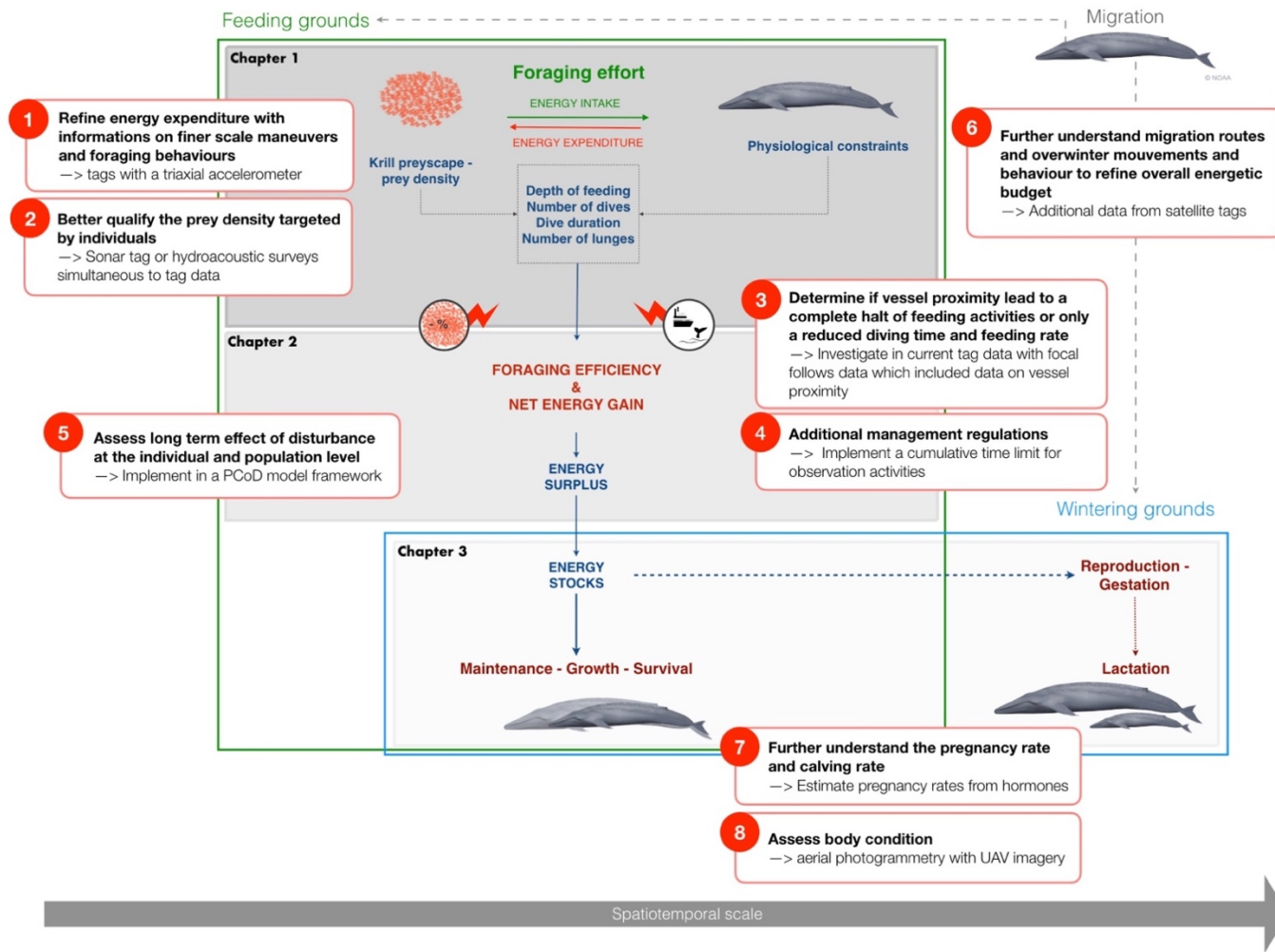


Figure 51 : Perspectives de recherche proposées basées sur le schéma conceptuel de la thèse. Les perspectives de recherches et leurs utilités afin de pallier aux limitations/problématiques soulevées dans les différents chapitres sont proposées dans les encadrés numérotés rouge.

RÉFÉRENCES BIBLIOGRAPHIQUES

- Abrahms, B., Hazen, E. L., Aikens, E. O., Savoca, M. S., Goldbogen, J. A., Bograd, S. J., et al. (2019). Memory and resource tracking drive blue whale migrations. *Proc Natl Acad Sci U S A* 116, 5582–5587. doi:10.1073/pnas.1819031116.
- Acevedo-Gutiérrez, A., Croll, D. A., and Tershy, B. R. (2002). High feeding costs limit dive time in the largest whales. *J Exp Biol* 205, 1747–1753.
- Akiyama, Y., Akamatsu, T., Rasmussen, M. H., Iversen, M. R., Iwata, T., Goto, Y., et al. (2019). Leave or stay? Video-logger revealed foraging efficiency of humpback whales under temporal change in prey density. *PLoS One* 14, e0211138. doi:10.1371/journal.pone.0211138.
- Alonzo, S. H., Switzer, P. V, and Mangel, M. (2003). An ecosystem-based approach to management: using individual behaviour to predict the indirect effects of Antarctic krill fisheries on penguin foraging. *J Appl Ecol* 40, 692–702. doi:10.1046/j.1365-2664.2003.00830.x.
- Amélineau, F., Fort, J., Mathewson, P. D., Speirs, D. C., Courbin, N., Perret, S., et al. (2018). Energyscapes and prey fields shape a North Atlantic seabird wintering hotspot under climate change. *R Soc Open Sci* 5. doi:10.1098/rsos.171883.
- Arnould, J. P. Y., Boyd, I. L., and Speakman, J. R. (1996). The relationship between foraging behaviour and energy expenditure in Antarctic fur seals. *J Zool* 239, 769–782. doi:10.1111/j.1469-7998.1996.tb05477.x.
- Aulanier, F., Simard, Y., Roy, N., Gervaise, C., and Bandet, M. (2016). Spatial-temporal exposure of blue whale habitats to shipping noise in St. Lawrence system. *DFO Can. Sci. Advis. Sec. Res. Doc.* 2016/090. vi + 26 p.
- Avgar, T., Street, G., and Fryxell, J. M. (2014). On the adaptive benefits of mammal migration. *Can J Zool* 92, 481–490. doi:10.1139/cjz-2013-0076.
- Bailey, H., Mate, B., Palacios, D., Irvine, L., Bograd, S., and Costa, D. (2009). Behavioural estimation of blue whale movements in the Northeast Pacific from state-space model analysis of satellite tracks. *Endanger Species Res* 10, 93–106. doi:10.3354/esr00239.

- Beauchamp, J., Bouchard, H., de Margerie, P., Otis, N., and Savaria, J.-Y. (2009). Recovery Strategy for the blue whale (*Balaenoptera musculus*), Northwest Atlantic population, in Canada. Species at Risk Act Recovery Strategy Series. Fisheries and Oceans Canada, Ottawa. 62 pp.
- Bejarano, A. C., Wells, R. S., and Costa, D. P. (2017). Development of a bioenergetic model for estimating energy requirements and prey biomass consumption of the bottlenose dolphin *Tursiops truncatus*. *Ecol Modell* 356, 162–172. doi:10.1016/j.ecolmodel.2017.05.001.
- Benkort, D., Plourde, S., Winkler, G., Cabrol, J., Ollier, A., Cope, L.-E., et al. (2019). Individual-based modeling explains the contrasted seasonality in size, growth, and reproduction of the sympatric Arctic (*Thysanoessa raschii*) and Nordic krill (*Meganyctiphanes norvegica*) in the St. Lawrence Estuary, eastern Canada. *Limnol Oceanogr*, 1–21. doi:10.1002/lno.11032.
- Benoit-Bird, K. J., Battaile, B. C., Heppell, S. a., Hoover, B., Irons, D., Jones, N., et al. (2013). Prey patch patterns predict habitat use by top marine predators with diverse foraging strategies. *PLoS ONE* 8(1): e53348. doi:10.1371/journal.pone.0053348.
- Berkes, F. (1976). Ecology of Euphausiids in the Gulf of St. Lawrence. *J Fish Res Board Canada* 33, 1894–1905. doi:10.1139/f76-242.
- Biuw, M., Boehme, L., Guinet, C., Hindell, M., Costa, D., Charrassin, J. B., et al. (2007). Variations in behavior and condition of a Southern Ocean top predator in relation to in situ oceanographic conditions. *Proc Natl Acad Sci U S A* 104, 13705–13710. doi:10.1073/pnas.0701121104.
- Blais, M., Galbraith, P. S., Plourde, S., Scarratt, M., Devine, L., and Lehoux, C. (2019). Chemical and Biological Oceanographic Conditions in the Estuary and Gulf of St. Lawrence during 2017. DFO Can Sci Advis Sec Res Doc 2019/009 iv + 56 pp.
- Bograd, S. J., Block, B. A., Costa, D. P., and Godley, B. J. (2010). Biologging technologies: New tools for conservation. Introduction. *Endanger Species Res* 10, 1–7. doi:10.3354/esr00269.
- Booth, C. G., Sinclair, R. R., and Harwood, J. (2020). Methods for monitoring for the Population Consequences of Disturbance in Marine Mammals: A Review. *Front Mar Sci* 7, 1–18. doi:10.3389/fmars.2020.00115.

- Booth, J. M., Steinfurth, A., Fusi, M., Cuthbert, R. J., and McQuaid, C. D. (2018). Foraging plasticity of breeding Northern Rockhopper Penguins, *Eudyptes moseleyi*, in response to changing energy requirements. *Polar Biol.* doi:10.1007/s00300-018-2321-6.
- Bowen, W. D., Tully, D., Boness, D. J., Bulheier, B. M., and Marshall, G. J. (2002). Prey-dependent foraging tactics and prey profitability in a marine mammal. *Mar Ecol Prog Ser* 244, 235–245. doi:10.3354/meps244235.
- Boyd, I. L. (1996). Temporal scales of foraging in a marine predator. *Ecology* 77, 426–434. doi:10.2307/2265619.
- Boyd, I. L. (2002). Estimating food consumption of marine predators: Antarctic fur seals and macaroni penguins. *J Appl Ecol* 39, 103–119. doi:10.1046/j.1365-2664.2002.00697.x.
- Boyd, I. L., Arnould, J. P. Y., Barton, T., and Croxall, J. P. (1994). Foraging behaviour of Antarctic fur seals during periods of contrasting prey abundance. *J Anim Ecol* 63, 703–713. doi:10.2307/5235
- Boyd, I. L., Kato, A., and Ropert-coudert, Y. (2004). Bio-logging science : sensing beyond the boundaries. *Mem Natl Inst Polar Res Spec Issue* 58, 1–14.
- Braithwaite, J. E., Meeuwig, J. J., Letessier, T. B., Jenner, K. C. S., and Brierley, A. S. (2015). From sea ice to blubber: linking whale condition to krill abundance using historical whaling records. *Polar Biol* 38, 1195–1202. doi:10.1007/s00300-015-1685-0.
- Brodie, P. (1975). Cetacean energetics, an overview of intraspecific size variation. *Ecology* 56, 152–161. doi:doi:10.2307/1935307.
- Brody, S. (1968) *Bioenergetics and growth*. New York: Hafner Publishing Co.
- Bronson, F. H. (1989) *Mammalian reproductive biology*. The University of Chicago Press, Chicago, IL
- Butler, P. J., and Jones, D. R. (1997). The physiology of diving of birds and mammals. *Physiol. Rev.* 77:837–99. doi:10.1152/physrev.1997.77.3.837

- Cabrol, J., Nadalini, J. B., Tremblay, R., Galbraith, P. S., Nozais, C., Starr, M., et al. (2019a). Seasonal and large-scale spatial variability of the energy reserves and the feeding selectivity of *Meganyctiphanes norvegica* and *Thysanoessa inermis* in a Subarctic environment. *Prog Oceanogr* 179, 102203. doi:10.1016/j.pocean.2019.102203.
- Cabrol, J., Trombetta, T., Amaudrut, S., Aulanier, F., Sage, R., Tremblay, R., et al. (2019b). Trophic niche partitioning of dominant North-Atlantic krill species, *Meganyctiphanes norvegica*, *Thysanoessa inermis*, and *T. raschii*. *Limnol Oceanogr* 64, 165–181. doi:10.1002/lno.11027.
- Cade, D. E., Carey, N., Domenici, P., Potvin, J., and Goldbogen, J. A. (2020). Predator-informed looming stimulus experiments reveal how large filter feeding whales capture highly maneuverable forage fish. *Proc Natl Acad Sci U S A* 117, 472–478. doi:10.1073/pnas.1911099116.
- Cade, D. E., Friedlaender, A. S., Calambokidis, J., and Goldbogen, J. A. (2016). Kinematic diversity in rorqual whale feeding mechanisms. *Curr Biol* 26, 2617–2624. doi:10.1016/j.cub.2016.07.037.
- Caraco, T. (1980). On foraging time allocation in a stochastic environment. *Eco.* 61, 119–128.
- Case, T. J. (1979). Optimal body size and an animal's diet. *Acta Biotheor* 28, 54–69. doi:10.1007/BF00054680.
- Charnov, E. L. (1976). Optimal foraging, the marginal value theorem. *Theor Popul Biol* 9, 129–136. doi:10.1016/0040-5809(76)90040-X.
- Chion, C., Turgeon, S., Michaud, R., Landry, J.-A., and Parrott, L. (2009). Portrait de la navigation dans le parc marin du Saguenay–Saint-Laurent. Caractérisation des activités sans prélèvement de ressources entre le 1er mai et le 31 octobre 2007. Présenté à Parcs Canada. 86 pages.
- Christiansen, F., Dawson, S., Durban, J., Fearnbach, H., Miller, C., Bejder, L., et al. (2020). Population comparison of right whale body condition reveals poor state of the North Atlantic right whale. *Mar Ecol Prog Ser* 640, 1–16. doi:10.3354/meps13299.
- Christiansen, F., Dujon, A. M., Sprogis, K. R., Arnould, J. P. Y., and Bejder, L. (2016). Noninvasive unmanned aerial vehicle provides estimates of the energetic cost of reproduction in humpback whales. *Ecosphere* 7. doi:10.1002/ecs2.1468.

- Christiansen, F., Rasmussen, M. H., and Lusseau, D. (2014). Inferring energy expenditure from respiration rates in minke whales to measure the effects of whale watching boat interactions. *J Exp Mar Bio Ecol* 459, 96–104. doi:10.1016/j.jembe.2014.05.014.
- Christiansen, F., Rasmussen, M., and Lusseau, D. (2013). Whale watching disrupts feeding activities of minke whales on a feeding ground. *Mar Ecol Prog Ser* 478, 239–251. doi:10.3354/meps10163.
- Christiansen, F., Vivier, F., Charlton, C., Ward, R., Amerson, A., Burnell, S., et al. (2018). Maternal body size and condition determine calf growth rates in Southern right whales. *Mar Ecol Prog Ser* 592, 267–282. doi:10.3354/meps12522.
- Cochrane, N. A., Sameoto, D. D., and Herman, A. W. (2000). Scotian Shelf euphausiid and silver hake population changes during Scotian Shelf euphausiid and silver hake population changes during 1984 – 1996 measured by multi-frequency acoustics. *ICES J Mar Sci* 57, 122–132. doi:10.1006/jmsc.1999.0563.
- Cochrane, N. A., Sameoto, D., Herman, A. W., and Neilson, J. (1991). Multiple-frequency acoustic backscattering and zooplankton aggregations in the Inner Scotian Shelf Basins. *Can J Fish Aquat Sci* 48, 340–355. doi:10.1139/f91-046.
- Cohen, J. (1977). *Statistical power analysis for the behavioral science*. Academic Press, New York City, NY.
- Costa, D. P. (1993). The relationship between reproductive and foraging energetics and the evolution of the Pinnipedia. *Symp Zool Soc London* 66, 293–314.
- Costa, D. P. (2009) Energetics. In: Perrin WF, Würsig B, Thewissen JGM (eds) *Encyclopedia of marine mammals*. Academic Press, San Diego, CA, p 383–391
- Costa, D. P., Croxall, J. P., and Duck, C. D. (1989). Foraging energetics of Antarctic fur seals in relation to changes in prey availability. *Ecology* 70, 596–606. doi:10.2307/1940211.
- Cresswell, K. A., Wiedenmann, J., and Mangel, M. (2008). Can macaroni penguins keep up with climate- and fishing-induced changes in krill? *Polar Biol* 31, 641–649. doi:10.1007/s00300-007-0401-0.
- Crocker, D. E., Williams, J. D., Costa, D. P., and Le Boeuf, B. J. (2001). Maternal traits and reproductive effort in northern elephant seals. *Ecology* 82, 3541–3555. doi:10.1890/0012-9658(2001)082[3541:MTAREI]2.0.CO;2

- Croll, D. A., Acevedo-Gutiérrez, A., Tershy, B. R., and Urbán-Ramírez, J. (2001). The diving behavior of blue and fin whales: is dive duration shorter than expected based on oxygen stores? *Comp Biochem Physiol Part A Mol Integr Physiol* 129, 797–809. doi:10.1016/S1095-6433(01)00348-8.
- Croll, D. A., Marinovic, B., Benson, S., Chavez, F. P., Black, N., Ternullo, R., et al. (2005). From wind to whales: Trophic links in a coastal upwelling system. *Mar Ecol Prog Ser* 289, 117–130. doi:10.3354/meps289117.
- Demer, D. A., Berger, L., Bernasconi, M., Bethke, E., Boswell, K. M., Chu, D., et al. (2015). Calibration of acoustic instruments. ICES Cooperative Research Report No. 326. 133 pp.
- Deruiter, S. L., Langrock, R., Skirbutas, T., Goldbogen, J. A., Calambokidis, J., Friedlaender, A. S., et al. (2017). A multivariate mixed hidden markov model for blue whale behaviour and responses to sound exposure. *Ann Appl Stat* 11, 362–392. doi:10.1214/16-AOAS1008.
- Di Clemente, J., Christiansen, F., Pirotta, E., Steckler, D., Wahlberg, M., and Pearson, H. C. (2018). Effects of whale watching on the activity budgets of humpback whales, *Megaptera novaeangliae* (Borowski, 1781), on a feeding ground. *Aquat Conserv Mar Freshw Ecosyst*, 1–11. doi:10.1002/aqc.2909.
- Doniol-Valcroze, T., Berteaux, D., Larouche, P., and Sears, R. (2007). Influence of thermal fronts on habitat selection by four rorqual whale species in the Gulf of St. Lawrence. *Mar Ecol Prog Ser* 335, 207–216. doi:10.3354/meps335207.
- Doniol-Valcroze, T., Lesage, V., Giard, J., and Michaud, R. (2011). Optimal foraging theory predicts diving and feeding strategies of the largest marine predator. *Behav Ecol* 22, 880–888. doi:10.1093/beheco/arr038.
- Doniol-Valcroze, T., Lesage, V., Giard, J., and Michaud, R. (2012). Challenges in marine mammal habitat modelling: Evidence of multiple foraging habitats from the identification of feeding events in blue whales. *Endanger Species Res* 17, 255–268. doi:10.3354/esr00427.
- Dufour, R., Benoît, H., Castonguay, M., Chassé, J., Devine, L., Galbraith, P., et al. (2010). Ecosystem status and trends report: estuary and gulf of St. Lawrence ecozone. MPO Sec Can Cons Sci Doc Res 2010/030, v + 187 p.
- Dunn, R. E., Wanless, S., Daunt, F., Harris, M. P., and Green, J. A. (2020). A year in the life of a North Atlantic seabird: behavioural and energetic adjustments during the annual cycle. *Sci Rep* 10, 1–11. doi:10.1038/s41598-020-62842-x.

- Eisert, R., Oftedal, O. T., and Barrell, G. K. (2013). Milk composition in the Weddell seal *Leptonychotes weddellii*: Evidence for a functional role of milk carbohydrates in pinnipeds. *Physiol Biochem Zool* 86, 159–175. doi:10.1086/669036.
- Erbe, C., Marley, S. A., Schoeman, R. P., Smith, J. N., Trigg, L. E., and Embling, C. B. (2019). The Effects of Ship Noise on Marine Mammals—A Review. *Front Mar Sci* 6. doi:10.3389/fmars.2019.00606.
- EI-Sabh, M. I. & Silverberg, N. (1990). *Oceanography of a Large-Scale Estuarine System: The St. Lawrence*. Springer-Verlag, New York.
- Emlen, J. M. (1966). The role of time and energy in food preference. *Am Nat* 100, 611–617. doi:10.1086/282455.
- Etnoyer, P., Canny, D., Mate, B. R., Morgan, L. E., Ortega-Ortiz, J. G., and Nichols, W. J. (2006). Sea-surface temperature gradients across blue whale and sea turtle foraging trajectories off the Baja California Peninsula, Mexico. *Deep Res Part II Top Stud Oceanogr* 53, 340–358. doi:10.1016/j.dsr2.2006.01.010.
- Fagan, W. F. (2019). Migrating whales depend on memory to exploit reliable resources. *Proc Natl Acad Sci U S A* 116, 5217–5219. doi:10.1073/pnas.1901803116.
- Fahlman, A., van der Hoop, J., Moore, M. J., Levine, G., Rocho-Levine, J., and Brodsky, M. (2016). Estimating energetics in cetaceans from respiratory frequency: why we need to understand physiology. *Biol Open* 5, 436–442. doi:10.1242/bio.017251.
- Falk-Petersen, S., Hagen, W., Kattner, G., Clarke, A., and Sargent, J. (2000). Lipids, trophic relationships, and biodiversity in Arctic and Antarctic krill. *Can J Fish Aquat Sci* 57, 178–191. doi:10.1139/cjfas-57-S3-178.
- Fisheries and Oceans Canada (2020). Policy on new fisheries for forage species. Available online at: <https://www.dfo-mpo.gc.ca/reports-rapports/regs/sff-cpd/forage-eng.htm>
- Flores, H., Atkinson, A., Kawaguchi, S., Krafft, B. A., Milinevsky, G., Nicol, S., et al. (2012). Impact of climate change on Antarctic krill. *Mar Ecol Prog Ser* 458, 1–19. doi:10.3354/meps09831.
- Fortune, S. M. E., Trites, A. W., Mayo, C. A., Rosen, D. A. S., and Hamilton, P. K. (2013). Energetic requirements of North Atlantic right whales and the implications for species recovery. *Mar Ecol Prog Ser* 478, 253–272. doi:10.3354/meps10000.

- Friedlaender, A. S., Goldbogen, J. A., Hazen, E. L., Calambokidis, J., and Southall, B. L. (2015). Feeding performance by sympatric blue and fin whales exploiting a common prey resource. *Mar Mammal Sci* 31, 345–354. doi:10.1111/mms.12134.
- Friedlaender, A. S., Halpin, P., Qian, S., Lawson, G., Wiebe, P., Thiele, D., et al. (2006). Whale distribution in relation to prey abundance and oceanographic processes in shelf waters of the Western Antarctic Peninsula. *Mar Ecol Prog Ser* 317, 297–310. doi:10.3354/meps317297.
- Friedlaender, A. S., Hazen, E. L., Nowacek, D. P., Halpin, P. N., Ware, C., Weinrich, M. T., et al. (2009). Diel changes in humpback whale *Megaptera novaeangliae* feeding behavior in response to sand lance *Ammodytes* spp. behavior and distribution. *Mar Ecol Prog Ser* 395, 91–100. doi:10.3354/meps08003.
- Friedlaender, A. S., Johnston, D. W., Tyson, R. B., Kaltenberg, A., Goldbogen, J. A., Stimpert, A. K., et al. (2016). Multiple-stage decisions in a marine central-place forager. *R Soc Open Sci* 3, 160043. doi:10.1098/rsos.160043.
- Friedlaender, A. S., Tyson, R. B., Stimpert, A. K., Read, A. J., and Nowacek, D. P. (2013). Extreme diel variation in the feeding behavior of humpback whales along the western Antarctic Peninsula during autumn. *Mar Ecol Prog Ser* 494, 281–289. doi:10.3354/meps10541.
- Galbraith, P., Pettipas, R., Chassé, J., Gilbert, D., Larouche, P., Pettigrew, B., et al. (2019). Physical Oceanographic Conditions in the Gulf of St. Lawrence in 2018. DFO Can. Sci. Advis. Sec. Res. Doc. 2019/046. iv + 79 p.
- Galbraith, P. S., Chassé, J., Caverhill, C., Nicot, P., Gilbert, D., Lefaivre, D., et al. (2018). Physical Oceanographic Conditions in the Gulf of St. Lawrence during 2017. DFO Can. Sci. Advis. Sec. Res. Doc. 2018/050. v + 79 p.
- Gavrilchuk, K., Lesage, V., Ramp, C., Sears, R., Bérubé, M., Bearhop, S., et al. (2014). Trophic niche partitioning among sympatric baleen whale species following the collapse of groundfish stocks in the Northwest Atlantic. *Mar Ecol Prog Ser* 497, 285–301. doi:10.3354/meps10578.
- Gibbens, J., Parry, L. J., and Arnould, J. P. Y. (2010). Influences on fecundity in Australian fur seals (*Arctocephalus pusillus doriferus*). *J Mammal* 91, 510–518. doi:10.1644/08-mamm-a-377.1.
- Gittleman, J. L., and Thompson, S. D. (1988). Energy allocation in mammalian reproduction. *Integr Comp Biol* 28, 863–875. doi:10.1093/icb/28.3.863.

- Goldbogen, J. A., Calambokidis, J., Croll, D. A., Harvey, J. T., Newton, K. M., Oleson, E. M., et al. (2008). Foraging behavior of humpback whales: kinematic and respiratory patterns suggest a high cost for a lunge. *J Exp Biol* 211, 3712–3719. doi:10.1242/jeb.023366.
- Goldbogen, J. A., Calambokidis, J., Croll, D. A., Mckenna, M. F., Oleson, E., Potvin, J., et al. (2012). Scaling of lunge-feeding performance in rorqual whales: Mass-specific energy expenditure increases with body size and progressively limits diving capacity. *Funct Ecol* 26, 216–226. doi:10.1111/j.1365-2435.2011.01905.x.
- Goldbogen, J. A., Calambokidis, J., Friedlaender, A. S., Francis, J., DeRuiter, S. L., Stimpert, A. K., et al. (2013a). Underwater acrobatics by the world's largest predator: 360 rolling manoeuvres by lunge-feeding blue whales. *Biol Lett* 9, 20120986–20120986. doi:10.1098/rsbl.2012.0986.
- Goldbogen, J. A., Calambokidis, J., Oleson, E., Potvin, J., Pyenson, N. D., Schorr, G., et al. (2011). Mechanics, hydrodynamics and energetics of blue whale lunge feeding: efficiency dependence on krill density. *J Exp Biol* 214, 131–146. doi:10.1242/jeb.054726.
- Goldbogen, J. A., Calambokidis, J., Shadwick, R. E., Oleson, E. M., McDonald, M. a, and Hildebrand, J. a (2006). Kinematics of foraging dives and lunge-feeding in fin whales. *J Exp Biol* 209, 1231–1244. doi:10.1242/jeb.02135.
- Goldbogen, J. A., Hazen, E. L., Friedlaender, A. S., Calambokidis, J., DeRuiter, S. L., Stimpert, A. K., et al. (2015). Prey density and distribution drive the three-dimensional foraging strategies of the largest filter feeder. *Funct Ecol* 29, 951–961. doi:10.1111/1365-2435.12395.
- Goldbogen, J. A., Potvin, J., and Shadwick, R. (2010). Skull and buccal cavity allometry increase mass-specific engulfment capacity in fin whales. *Proc Biol Sci* 277, 861–868. doi:10.1098/rspb.2009.1680.
- Goldbogen, J. A., Pyenson, N. D., and Shadwick, R. E. (2007). Big gulps require high drag for fin whale lunge feeding. *Mar Ecol Prog Ser* 349, 289–301. doi:10.3354/meps07066.
- Goldbogen, J. A., Southall, B. L., DeRuiter, S. L., Calambokidis, J., Friedlaender, A. S., Hazen, E. L., et al. (2013b). Blue whales respond to simulated mid-frequency military sonar. *Proc Biol Sci* 280, 20130657. doi:10.1098/rspb.2013.0657.

- Gomez, C., Lawson, J. W., Wright, A. J., Buren, A. D., Tollit, D., and Lesage, V. (2016). A systematic review on the behavioural responses of wild marine mammals to noise: the disparity between science and policy. *Can J Zool* 94, 801–819. doi:10.1139/cjz-2016-0098.
- Goulet, P., Guinet, C., Swift, R., Madsen, P. T., and Johnson, M. (2019). A miniature biomimetic sonar and movement tag to study the biotic environment and predator-prey interactions in aquatic animals. *Deep Res Part I Oceanogr Res Pap* 148, 1–11. doi:10.1016/j.dsr.2019.04.007.
- Griffiths, D. (1980). Foraging Costs and Relative Prey Size. *Am Nat* 116, 743–752. doi:10.2307/2678832.
- Guilpin, M., Lesage, V., McQuinn, I., Goldbogen, J., Potvin, J., Jeanniard-du-Dot, T., Doniol-Valcroze, T., Michaud, R., Moisan, M. and Winkler, G. (2019). Foraging energetics and prey density requirements of western North Atlantic blue whales in the Estuary and Gulf of St. Lawrence, Canada. *Mar Ecol Prog Ser* 625, 205–223. doi:10.3354/meps13043.
- Guilpin, M., Lesage, V., McQuinn, I., Brosset, P., Doniol-Valcroze, T., Jeanniard-du-Dot, T., and Winkler, G. (2020). Repeated vessel interactions and climate- or fishery-driven changes in prey density limit energy acquisition by foraging blue whales. *Front Mar Sci*. 7, 1–16. doi:10.3389/fmars.2020.00626
- Guinet, C., Roux, J. P., Bonnet, M., and Mison, V. (1998). Effect of body size, body mass, and body condition on reproduction of female South African fur seals (*Arctocephalus pusillus*) in Namibia. *Can J Zool* 76, 1418–1424. doi:10.1139/z98-082.
- Halsey, L. G., Green, J. A., Wilson, R. P., and Frappell, P. B. (2009). Accelerometry to estimate energy expenditure during activity: Best practice with data loggers. *Physiol Biochem Zool* 82, 396–404. doi:10.1086/589815.
- Hammill, M. O., Ryg, M., and Chabot, D. (2010). Seasonal Changes in Energy Requirements of Harp Seals. *J Northwest Atl Fish Sci* 42, 135–152. doi:10.2960/J.v42.m660.
- Harvey, M., Galbraith, P. S., and Descroix, A. (2009). Vertical distribution and diel migration of macrozooplankton in the St. Lawrence marine system (Canada) in relation with the cold intermediate layer thermal properties. *Prog Oceanogr* 80, 1–21. doi:10.1016/j.pocean.2008.09.001.

- Hazen, E. L., Friedlaender, A. S., and Goldbogen, J. A. (2015). Blue whales (*Balaenoptera musculus*) optimize foraging efficiency by balancing oxygen use and energy gain as a function of prey density. *Sci Adv* 1, e1500469. doi:10.1126/sciadv.1500469.
- Heaslip, S. G., Bowen, W. D., and Iverson, S. J. (2014). Testing predictions of optimal diving theory using animal-borne video from harbour seals (*Phoca vitulina concolor*). *Can J Zool* 318, 309–318. doi:10.1139/cjz-2013-0137.
- Hemmingsen, A. M. (1960). Energy metabolism as related to body size and respiratory surfaces, and its evolution. *Rep. Stem Meml. Hosp. Nordisk Insulin Lab.* 9:110.
- Higginson, A. D., Fawcett, T. W., Trimmer, P. C., McNamara, J. M., and Houston, A. I. (2012). Generalized optimal risk allocation: Foraging and antipredator behavior in a fluctuating environment. *Am Nat* 180, 589–603. doi:10.1086/667885.
- Higginson, A. D., and Ruxton, G. D. (2015). Foraging mode switching: the importance of prey distribution and foraging currency. *Anim Behav* 105, 121–137. doi:10.1016/j.anbehav.2015.04.014.
- Hin, V., Harwood, J., and de Roos, A. M. (2019). Bio-energetic modeling of medium-sized cetaceans shows high sensitivity to disturbance in seasons of low resource supply. *Ecol Appl* 29, 1–19. doi:10.1002/eap.1903.
- Hindell, M. A., Crocker, D., Mori, Y., and Tyack, P. (2010) Foraging behaviour. In : *Marine mammal ecology and conservation—A handbook of techniques*. Boyd Ian L., Bowen W. Don, Iverson Sarah J, eds. Oxford. pp. 241–262
- Holling, C. S. (1965). The functional response of predators to prey density and its role in mimicry and population regulation. *Mem Entomol Soc Canada* 97, 5–60. doi:10.4039/entm9745fv.
- Hoskins, A. J., and Arnould, J. P. Y. (2013). Temporal allocation of foraging effort in female Australian fur seals (*Arctocephalus pusillus doriferus*). *PLoS One* 8, e79484. doi:10.1371/journal.pone.0079484.
- Houston, A. I., and Carbone, C. (1992). The optimal allocation of time during the dive cycle. *Behav Ecol* 3, 255–265. doi:10.1093/beheco/3.3.255.
- Houston, A. (1985). Central-place foraging: some aspects of prey choice for multiple-prey loaders. *Am Nat* 125, 811–826. doi:10.1086/284381

- Houston, A. I., and McNamara, J. M. (1985). A general theory of central place foraging for single-prey loaders. *Theor Popul Biol* 28, 233–262. doi:10.1016/0040-5809(85)90029-2
- Houston, A. I., Prosser, E., and Sans, E. (2012). The cost of disturbance: A waste of time and energy? *Oikos* 121, 597–604. doi:10.1111/j.1600-0706.2011.19594.x.
- Houston, A. I., Stephens, P. A., Boyd, I. L., Harding, K. C., and McNamara, J. M. (2007). Capital or income breeding? A theoretical model of female reproductive strategies. *Behav Ecol* 18, 241–250. doi:10.1093/beheco/arl080.
- Hückstädt, L. A., Holser, R. R., Tift, M. S., and Costa, D. P. (2018). The extra burden of motherhood: reduced dive duration associated with pregnancy status in a deep-diving mammal, the northern elephant seal. *Biol Lett* 14, 20170722. doi:10.1098/RSBL.2017.0722.
- Huggett, A. S. G., and Widdas, W. F. (1950). The relationship between mammalian foetal weight and conception age. *J Physiol* 4, 306–307. doi:10.1113/jphysiol.1951.sp004622
- Hutchings, J. A., Côté, I. M., Dodson, J. J., Fleming, I. A., Jennings, S., Mantua, N. J., et al. (2012). Climate change, fisheries, and aquaculture: trends and consequences for Canadian marine biodiversity. *Environ Rev* 20, 220–311. doi:10.1139/a2012-013.
- Irvine, L. M., Palacios, D. M., Lagerquist, B. A., and Mate, B. R. (2019). Scales of blue and fin whale feeding behavior off California, USA, with implications for prey patchiness. *Front Ecol Evol* 7, 1–16. doi:10.3389/fevo.2019.00338.
- Ishii, M., Murase, H., Fukuda, Y., Sawada, K., Sasakura, T., Tamura, T., et al. (2017). Diving behavior of sei whales *Balaenoptera borealis* relative to the vertical distribution of their potential prey. *Mammal Soc Japan*, 191–199. doi:10.3106/041.042.0403.
- Iwasa, Y., Higashi, M., and Yamamura, N. (1981). Prey distribution as a factor determining the choice of optimal foraging strategy. *Am Nat* 117, 710. doi:10.1086/283754.
- Jeanniard-du-Dot, T., Guinet, C., Arnould, J. P. Y., Speakman, J. R., and Trites, A. W. (2016). Accelerometers can measure total and activity-specific energy expenditures in free-ranging marine mammals only if linked to time-activity budgets. *Funct Ecol* 31, 377–386. doi:10.1111/1365-2435.12729.

- Jeanniard-du-Dot, T., Trites, A., Arnould, J., Speakman, J., and Guinet, C. (2018). Trade-offs between foraging efficiency and pup feeding rate of lactating northern fur seals in a declining population. *Mar Ecol Prog Ser* 600, 207–222. doi:10.3354/meps12638.
- Jeanniard-du-Dot, T., Trites, A. W., Arnould, J. P. Y., and Guinet, C. (2017). Reproductive success is energetically linked to foraging efficiency in Antarctic fur seals. *PLoS One* 12, e0174001. doi:10.1371/journal.pone.0174001.
- Jeanniard-du-dot, T., Trites, A. W., Arnould, J. P. Y., Speakman, J. R., and Guinet, C. (2017). Activity-specific metabolic rates for diving, transiting, and resting at sea can be estimated from time–activity budgets in ranging marine mammals. *Ecol Evol* 7, 2969–2976. doi:10.1002/ece3.2546.
- Johnson, M. P., and Tyack, P. L. (2003). A digital acoustic recording tag for measuring the response of wild marine mammals to sound. *IEEE J Ocean Eng* 28, 3–12. doi:10.1109/JOE.2002.808212.
- Jonsson, K. I. (1997). Capital and income breeding as alternative tactics of resource use in reproduction. *Oikos* 78, 57–66. doi:10.2307/3545800.
- Kawamura, A. (1980). A Review of food of balaenopterid whales. *Sci Reports Whales Res Inst* 32, 155–197.
- King, S. L., Schick, R. S., Donovan, C., Booth, C. G., Burgman, M., Thomas, L., et al. (2015). An interim framework for assessing the population consequences of disturbance. *Methods Ecol Evol* 6, 1150–1158. doi:10.1111/2041-210X.12411.
- Kingsley, M., and Reeves, R. R. (1998). Aerial surveys of cetaceans in the Gulf of St. Lawrence in 1995 and 1996. *Can J Zool* 76, 1529–1550. doi:10.1139/z98-054.
- Kleiber, M. (1975). *The Fire of Life: an introduction to animal energetics*. R.E. Kreiger Publishing Co., Huntington, NY. 453pp.
- Kooyman, G. L. (1965). Techniques used in measuring diving capacities of Weddell seals. *Polar Record*, 12(79), 391–394. doi:10.1017/S003224740005484X
- Kooyman, G. L. (2004). Genesis and evolution of bio-logging devices: 1963–2002. *Mem Natl Polar Res Inst*, 15–22.
- Kooyman, G. L., and Ponganis, P. J. (1998). The physiological basis of diving to depth: birds and mammals. *Annu Rev Physiol* 60, 19–32. doi:10.1146/annurev.physiol.60.1.19.

- Kot, B. W., Sears, R., Zbinden, D., Borda, E., and Gordon, M. S. (2014). Rorqual whale (*balaenopteridae*) surface lunge-feeding behaviors: Standardized classification, repertoire diversity, and evolutionary analyses. *Mar Mammal Sci* 30, 1335–1357. doi:10.1111/mms.12115.
- Koutitonsky, V. G., and Bugden, G. L. (1991). The physical oceanography of the Gulf of St. Lawrence: A review with emphasis on the synoptic variability of the motion, in *The Gulf of St. Lawrence: Small Ocean or Big Estuary?*, edited by J.-C. Theriault, *Can. Spec. Publ. Fish. Aquat. Sci.*, 113, 57–90, 1991.
- Krebs, J. R., Erichsen, J. T., and Webber, M. I. (1977). Optimal prey selection in the great tit (*Parus major*). *Anim Behav* 25, 30–38. doi: 10.1016/0003-3472(77)90064-1.
- Kulka, D. W., Corey, S., and Iles, T. D. (1982). Community Structure and Biomass of Euphausiids in the Bay of Fundy. *Can J Fish Aquat Sci* 39, 326–334. doi:10.1139/f82-045.
- Labarbera, M. (1984). Feeding currents and particle capture mechanisms in suspension feeding animals. *Am Zool* 24, 71–84. doi:10.1093/icb/24.1.71.
- Lambertsen, R., Ulrich, N., and Straley, J. (1995). Frontomandibular stay of *Balaenopteridae*: A mechanism for momentum recapture during feeding. *J Mammal* 76, 877–899. doi:10.2307/1382758.
- Lawson, G. L., Hückstädt, L. A., Lavery, A. C., Jaffré, F. M., Wiebe, P. H., Fincke, J. R., et al. (2015). Development of an animal-borne “sonar tag” for quantifying prey availability: Test deployments on northern elephant seals. *Anim Biotelemetry* 3. doi:10.1186/s40317-015-0054-7.
- Leaper, R., and Lavigne, D. (2007). How much do large whales eat? *J Cetacean Res Manag* 9, 179–188.
- Lesage, V., Gavrilchuk, K., Andrews, R. D., and Sears, R. (2017a). Foraging areas, migratory movements and winter destinations of blue whales from the western North Atlantic. *Endanger Species Res* 34, 27–43. doi:10.3354/esr00838.
- Lesage, V., Gosselin, J.-F., Hammill, M., Kingsley, M. C. ., and Lawson, J. (2007). Ecologically and Biologically Significant Areas (EBSAs) in the Estuary and Gulf of St. Lawrence – A marine mammal perspective. *DFO Can. Sci. Advis. Sec., Sci. Adv. Rep.* 2007/016.

- Lesage, V., Gosselin, J., Lawson, J. W., Mcquinn, I., Moors-Murphy, H., Plourde, S., et al. (2018). Habitats Important to Blue Whales (*Balaenoptera musculus*) in the Western North Atlantic. DFO Can. Sci. Advis. Sec. Res. Doc. 2016/080. iv + 50 p.
- Lesage, V., Omrane, A., Doniol-Valcroze, T., and Mosnier, A. (2017b). Increased proximity of vessels reduces feeding opportunities of blue whales in the St. Lawrence Estuary, Canada. *Endanger Species Res* 32, 351–361. doi:10.3354/esr00825.
- Lewis, R. J., and Kappeler, P. M. (2005). Seasonality, body condition, and timing of reproduction in *Propithecus verreauxi verreauxi* in the Kirindy Forest. *Am J Primatol* 67, 347–364. doi:10.1002/ajp.20187.
- Lockyer, C. (1976). Body weights of some species of large whales. *ICES J Mar Sci* 36, 259–273. doi:10.1093/icesjms/36.3.259.
- Lockyer, C. (1981). Growth and energy budgets of large baleen whales from the Southern Hemisphere. *Mamm seas*, vol 3, (FAO Fish Ser no 5), 379–487.
- Lockyer, C. (1984). Review of baleen whale (*Mysticeti*) reproduction and implications for management. *Reports Int Whal Comm Spec*, 27–50.
- Lockyer, C. (1986). Body fat condition in Northeast Atlantic fin whales, *Balaenoptera physalus*, and its relationship with reproduction and food resource. *Can J Fish Aquat Sci* 43, 142–147. doi:10.1139/f86-015
- Lockyer, C. (2007). All creatures great and smaller: a study in cetacean life history energetics. *J Mar Biol Assoc UK* 87, 1035–1045. doi:10.1017/S0025315407054720.
- Lockyer, C. H., McConnell, L. C., and Waters, T. D. (1985). Body condition in terms of anatomical and biochemical assessment of body fat in North Atlantic fin and sei whales. *Can J Zool* 63, 2328–2338. doi:10.1139/z85-345.
- Loncarevic, B. D., Piper, D. J. W., and Fader, G. B. J. (1999). Application of high-quality bathymetry to geological interpretation on the Scotian Shelf. *Geosci Canada* 19, 5–13.
- Long, Z., Perrie, W., Chassé, J., Brickman, D., Guo, L., Drozdowski, A., et al. (2016). Impacts of climate change in the Gulf of St. Lawrence. *Atmosphere-Ocean* 54, 337–351. doi:10.1080/07055900.2015.1029869.

- Lusseau, D., Bain, D. E., Williams, R., and Smith, J. C. (2009). Vessel traffic disrupts the foraging behavior of southern resident killer whales *Orcinus orca*. *Endanger Species Res* 6, 211–221. doi:10.3354/esr00154.
- MacArthur, R. H., and Pianka, E. R. (1966). On optimal use of a patchy environment. *Am Nat* 100, 603–609. doi:10.1086/282454.
- Madsen, T., and Shine, R. (1999). The adjustment of reproductive threshold to prey abundance in a capital breeder. *J Anim Ecol* 68, 571–580. doi:10.1046/j.1365-2656.1999.00306.x.
- Maps, F., Plourde, S., Lavoie, D., McQuinn, I. H., and Chasse, J. (2012). Modelling the influence of daytime distribution on the transport of two sympatric krill species (*Thysanoessa raschii* and *Meganyctiphanes norvegica*) in the Gulf of St Lawrence, eastern Canada. *ICES J Mar Sci* 69, 1205–1217. doi:10.1093/icesjms/fst048.
- Maps, F., Plourde, S., McQuinn, I. H., St-Onge-Drouin, S., Lavoie, D., Chassé, J., et al. (2015). Linking acoustics and finite-time lyapunov exponents reveals areas and mechanisms of krill aggregation within the gulf of St. Lawrence, eastern Canada. *Limnol Oceanogr* 60, 1965–1975. doi:10.1002/lno.10145.
- Mårtensson, P. E., Nordøy, E. S., and Blix, A. S. (1994). Digestibility of krill (*Euphausia superba* and *Thysanoessa* sp.) in minke whales (*Balaenoptera acutorostrata*) and crabeater seals (*Lobodon carcinophagus*). *Br J Nutr* 72, 713–716. doi:10.1079/BJN19940073.
- Martins, C. C. A. (2012). Study of baleen whales' ecology and interaction with maritime traffic activities to support management of a complex socio-ecological system. Ph.D. thesis, Université de Montréal, Montréal.
- Mate, B. R., Lagerquist, B. A., and Calambokidis, J. (1999). Movements of North Pacific Blue Whales during the feeding season off Southern California and their southern fall migration. *Mar Mammal Sci* 15, 1246–1257. doi:10.1111/j.1748-7692.1999.tb00888.x
- Mauchline, J., and Fisher, L. R. (1980). *The biology of euphausiids*. London: Academic Press.
- McBride, M. M., Dalpadado, P., Drinkwater, K. F., Godø, O. R., Hobday, A. J., Hollowed, A. B., et al. (2014). Krill, climate, and contrasting future scenarios for Arctic and Antarctic fisheries. *ICES J Mar Sci* 71, 1934–1955. doi:10.1093/icesjms/fsu002.

- McHuron, E. A., Peterson, S. H., Hückstädt, L. A., Melin, S. R., Harris, J. D., and Costa, D. P. (2018a). The energetic consequences of behavioral variation in a marine carnivore. *Ecol Evol* 8, 4340–4351. doi:10.1002/ece3.3983.
- McHuron, E. A., Schwarz, L. K., Costa, D. P., and Mangel, M. (2018b). A state-dependent model for assessing the population consequences of disturbance on income-breeding mammals. *Ecol Modell* 385, 133–144. doi:10.1016/j.ecolmodel.2018.07.016.
- McKenzie, J., Parry, L. J., Page, B., and Goldsworthy, S. D. (2005). Estimation of pregnancy rates and reproductive failure in New Zealand fur seals (*Arctocephalus Forsteri*). *J Mammal* 86, 1237–1246. doi:10.1644/05-mamm-a-085r.1.
- McQuinn, I. H., Dion, M., and St. Pierre, J.-F. (2013). The acoustic multifrequency classification of two sympatric euphausiid species. *ICES J Mar Sci* 69, 1205–1217. doi:10.1093/icesjms/fst048.
- McQuinn, I. H., Gosselin, J., Bourassa, M., Mosnier, A., St-Pierre, J.-F., Plourde, S., et al. (2016). The spatial association of blue whales (*Balaenoptera musculus*) with krill patches (*Thysanoessa* spp. and *Meganyctiphanes norvegica*) in the estuary and northwestern Gulf of St. Lawrence. *DFO Can. Sci. Advis. Sec. Res. Doc.* 2016/104. iv + 19 p.
- McQuinn, I. H., Plourde, S., St. Pierre, J.-F., and Dion, M. (2015). Spatial and temporal variations in the abundance, distribution, and aggregation of krill (*Thysanoessa raschii* and *Meganyctiphanes norvegica*) in the lower estuary and Gulf of St. Lawrence. *Prog Oceanogr* 131, 159–176. doi:10.1016/j.pocean.2014.12.014.
- McWilliams, S. R., Guglielmo, C., Pierce, B., and Klaassen, M. (2004). Flying, fasting, and feeding in birds during migration: A nutritional and physiological ecology perspective. *J Avian Biol* 35, 377–393. doi:10.1111/j.0908-8857.2004.03378.x.
- Meyer-Gutbrod, E. L., and Greene, C. H. (2018). Uncertain recovery of the North Atlantic right whale in a changing ocean. *Glob Chang Biol* 24, 455–464. doi:10.1111/gcb.13929.
- Miller, C. A., Reeb, D., Best, P. B., Knowlton, A. R., Brown, M. W., and Moore, M. J. (2011). Blubber thickness in right whales *Eubalaena glacialis* and *Eubalaena australis* related with reproduction, life history status and prey abundance. *Mar Ecol Prog Ser* 438, 267–283. doi:10.3354/meps09174.

- Miller, D. G. M., and Hampton, I. (1989). Krill aggregation characteristics: Spatial distribution patterns from hydroacoustic observations. *Polar Biol* 10, 125–134. doi:10.1007/BF00239157.
- Miller, E. J., Potts, J., Cox, M. J., Miller, B. S., O’Driscoll, R., Kelly, N., et al. (2018). The characteristics of krill swarms in relation to aggregating Antarctic blue whales. *Int Whal Comm Sci Comm Pap SC/67b/EM*, 1–13. doi:10.1038/s41598-019-52792-4.
- Miller, P. J. O., Biuw, M., Watanabe, Y. Y., Thompson, D., and Fedak, M. a. (2012). Sink fast and swim harder! Round-trip cost-of-transport for buoyant divers. *J Exp Biol* 215, 3622–3630. doi:10.1242/jeb.070128.
- Moors-Murphy, H. B., Lawson, J. W., Rubin, B., Marotte, E., Renaud, G., and Fuentes-Yaco, C. (2019). Occurrence of Blue Whales (*Balaenoptera musculus*) off Nova Scotia, Newfoundland, and Labrador. *DFO Can. Sci. Advis. Sec. Res. Doc.* 2018/007. iv + 55 p.
- Mori, Y. (1998). The optimal patch use in divers: Optimal time budget and the number of dive cycles during bout. *J Theor Biol* 190, 187–199. doi:10.1006/jtbi.1997.0550.
- Morissette, L., Castonguay, M., Savenkoff, C., Swain, D. P., Chabot, D., Bourdages, H., et al. (2009). Contrasting changes between the northern and southern Gulf of St. Lawrence ecosystems associated with the collapse of groundfish stocks. *Deep Sea Res Part II Top Stud Oceanogr* 56, 2117–2131. doi:10.1016/j.dsr2.2008.11.023.
- Naito, Y. (2004). New steps in bio-logging science. *Mem Natl Inst Polar Res Spec Issue* 58, 50–57.
- Narazaki, T., Isojunno, S., Nowacek, D. P., Swift, R., Friedlaender, A. S., Ramp, C., et al. (2018). Body density of humpback whales (*Megaptera novaengliae*) in feeding aggregations estimated from hydrodynamic gliding performance. *PLoS One* 13, 1–23. doi:10.1371/journal.pone.0200287.
- New, L. F., Clark, J. S., Costa, D. P., Fleishman, E., Hindell, M. A., Klanjšček, T., et al. (2014). Using short-term measures of behaviour to estimate long-term fitness of Southern elephant seals. *Mar Ecol Prog Ser* 496, 99–108. doi:10.3354/meps10547.
- New, L. F., Harwood, J., Thomas, L., Donovan, C., Clark, J. S., Hastie, G., et al. (2013a). Modelling the biological significance of behavioural change in coastal bottlenose dolphins in response to disturbance. *Funct Ecol* 27, 314–322. doi:10.1111/1365-2435.12052.

- New, L. F., Moretti, D. J., Hooker, S. K., Costa, D. P., and Simmons, S. E. (2013b). Using energetic models to investigate the survival and reproduction of beaked whales (family *Ziphiidae*). *PLoS One* 8, e68725. doi:10.1371/journal.pone.0068725.
- Nicol, S., and Endo, Y. (1999). Krill fisheries: Development, management and ecosystem implications. *Aquat Living Resour* 12, 105–120. doi:10.1016/S0990-7440(99)80020-5
- Nicol, S., and Foster, J. (2003). Recent trends in the fishery for Antarctic krill. *Aquat living Resour* 16, 42–45. doi:10.1016/S0990-7440(03)00004-4
- Nicol, S., Foster, J., and Kawaguchi, S. (2012). The fishery for Antarctic krill – recent developments. *Fish Fish* 13, 30–40. doi:10.1111/j.1467-2979.2011.00406.x.
- Nordøy, E. S., Folkow, L. P., Mårtensson, P.-E., and Blix, A. S. (1995). Food requirements of Northeast Atlantic minke whales. In: *Whales, Seals, Fish and Man*. A. S. Blix, L. Walløe, and Ø. Ulltang (eds.). *Dev. Mar. Bio.*, 4: 307–317.
- Noren, S. R., Udevitz, M. S., and Jay, C. V (2012). Bioenergetics model for estimating food requirements of female Pacific walrus *Odobenus rosmarus divergens*. *Mar Ecol Prog Ser* 460, 261–275. doi:10.3354/meps09706.
- Oftedal, O. T. (1997). Lactation in whales and dolphins: Evidence of divergence between baleen- and toothed-species. *J Mammary Gland Biol Neoplasia* 2, 205–230. doi:10.1023/A:1026328203526.
- Oftedal, O. T. (2000). Use of maternal reserves as a lactation strategy in large mammals. *Proc Nutr Soc* 59, 99–106. doi:10.1017/S0029665100000124
- Øigård, T. A., Lindstrøm, U., Haug, T., Nilssen, K. T., & Smout, S. (2013). Functional relationship between harp seal body condition and available prey in the Barents Sea. *Mar Ecol Prog Ser*, 484, 287–301. doi.org/10.3354/meps10272
- Ollier, A., Chabot, D., Audet, C., and Winkler, G. (2018). Metabolic rates and spontaneous swimming activity of two krill species (*Euphausiacea*) under different temperature regimes in the St. Lawrence Estuary, Canada. *J Crustac Biol*, 1–10. doi:10.1093/jcbiol/ruy028.
- Olsen, M. A., Blix, A. S., Utsi, T. H., Sørmo, W., and Mathiesen, S. D. (2000). Chitinolytic bacteria in the minke whale forestomach. *Can J Microbiol* 46, 85–94. doi:10.1139/w99-112.

- Owen, K., Kavanagh, A. S., Warren, J. D., Noad, M. J., Donnelly, D., Goldizen, A. W., et al. (2016). Potential energy gain by whales outside of the Antarctic: prey preferences and consumption rates of migrating humpback whales (*Megaptera novaeangliae*). *Polar Biol.* doi:10.1007/s00300-016-1951-9.
- Peters, R. H. (1983). *The ecological implications of body size*. Cambridge, UK: Cambridge University Press
- Phillipson, J. (1964). A miniature bomb calorimeter for small biological samples. *Oikos* 15, 130–139. doi: 10.2307/3564751.
- Piatt, J. F., and Methven, D. A. (1992). Threshold foraging behavior of baleen whales. *Mar Ecol Prog Ser* 84, 205–210. doi:10.3354/meps084205.
- Pinheiro J, Bates D, DebRoy S, Sarkar D, R Core Team (2013) nlme: linear and nonlinear mixed effects models. R package version 3.1-131. <https://CRAN.R-project.org/package=nlme>
- Pirotta, E., Booth, C. G., Costa, D. P., Fleishman, E., Kraus, S. D., Lusseau, D., et al. (2018a). Understanding the population consequences of disturbance. *Ecol Evol*, 1–13. doi:10.1002/ece3.4458.
- Pirotta, E., Mangel, M., Costa, D. P., Goldbogen, J., Harwood, J., Hin, V., et al. (2019). Anthropogenic disturbance in a changing environment: modelling lifetime reproductive success to predict the consequences of multiple stressors on a migratory population. *Oikos* 128, 1340–1357. doi:10.1111/oik.06146.
- Pirotta, E., Mangel, M., Costa, D. P., Mate, B., Goldbogen, J. A., Palacios, D. M., et al. (2018b). A dynamic state model of migratory behavior and physiology to assess the consequences of environmental variation and anthropogenic disturbance on marine vertebrates. *Am Nat* 191, E40–E56. doi:10.1086/695135.
- Pitcher, K. W., Calkins, D. G., and Pendleton, G. W. (1998). Reproductive performance of female Steller sea lions: an energetics-based reproductive strategy? *Can J Zool* 76, 2075–2083. doi:10.1139/cjz-76-11-2075.
- Pivorunas, A. (1979). The feeding mechanisms of baleen whales. *Am Sci* 67, 432–440.
- Plourde, S., Grégoire, F., Lehoux, C., Galbraith, P. S., Castonguay, M., and Ringuette, M. (2014a). Effect of environmental variability on the Atlantic Mackerel (*Scomber scombrus* L.) stock dynamics in the Gulf of St. Lawrence. doi:10.1111/fog.12113.

- Plourde, S., Lehoux, C., McQuinn, I. H., and Lesage, V. (2016). Describing krill distribution in the western North Atlantic using statistical habitat models. DFO Can. Sci. Advis. Sec. Res. Doc. 2016/111. v + 34 p.
- Plourde, S., McQuinn, I. H., Maps, F., St-Pierre, J.-F., Lavoie, D., and Joly, P. (2014b). Daytime depth and thermal habitat of two sympatric krill species in response to surface salinity variability in the Gulf of St Lawrence, eastern Canada. *ICES J Mar Sci* 71, 272–281. doi:10.1093/icesjms/fst023.
- Plourde, S., Starr, M., Devine, L., St-Pierre, J.-F., St-Amand, L., Joly, P., et al. (2014c). Chemical and biological oceanographic conditions in the Estuary and Gulf of St. Lawrence during 2011 and 2012. DFO Can Sci Advis Sec Res Doc 2014/049, v + 46 p.
- Potvin, J., Goldbogen, J. A., and Shadwick, R. E. (2010). Scaling of lunge feeding in rorqual whales: An integrated model of engulfment duration. *J Theor Biol* 267, 437–453. doi:10.1016/j.jtbi.2010.08.026.
- Potvin, J., Goldbogen, J. A., and Shadwick, R. E. (2012). Metabolic expenditures of lunge feeding rorquals across scale: Implications for the evolution of filter feeding and the limits to maximum body size. *PLoS One* 7, e44854. doi:10.1371/journal.pone.0044854.
- Potvin, J., and Werth, A. J. (2017). Oral cavity hydrodynamics and drag production in balaenid whale suspension feeding. *PLoS One* 12, e0175220. doi:10.1371/journal.pone.0175220.
- Pujol G, Iooss B Janon A, Boumhaout K and others (2016) sensitivity: global sensitivity analysis of model outputs. R package version 1.12.1. <https://CRAN.R-project.org/package=sensitivity>
- Pyke, G. (1984). Optimal Foraging Theory: A critical review. *Annu Rev Ecol Syst* 15, 523–575. doi:10.1146/annurev.ecolsys.15.1.523.
- Pyke, G., Pulliam, H. R., and Charnov, E. L. (1977). Optimal Foraging: A selective review of theory and tests. *Q Rev Biol* 52, 137–154.
- R Development Core Team (2017) R: a language and environment for statistical computing. R Foundation for Statistical Computing, Vienna

- Reid, K., Watkins, J. L., Murphy, E. J., Trathan, P. N., Fielding, S., and Enderlein, P. (2010). Krill population dynamics at South Georgia: Implications for ecosystem-based fisheries management. *Mar Ecol Prog Ser* 399, 243–252. doi:10.3354/meps08356.
- Richardson, A. J. (2008). In hot water: Zooplankton and climate change. *ICES J Mar Sci* 65, 279–295. doi:10.1093/icesjms/fsn028.
- Riisgård, H. U., and Larsen, P. S. (1995). Filter-feeding in marine macro-invertebrates: pump characteristics, modelling and energy cost. *Biol Rev Camb Philos Soc* 70, 67–106. doi:10.1111/j.1469-185X.1995.tb01440.x.
- Ronconi, R. A., and Burger, A. E. (2008). Limited foraging flexibility : increased foraging effort by a marine predator does not buffer against scarce prey. *Mar Ecol Prog Ser* 366, 245–258. doi:10.3354/meps07529.
- Ropert-Coudert, Y., and Wilson, R. (2005). Trends and perspectives in animal-attached remote sensing. *Front Ecol Env* 3, 437–444.
- Ropert-coudert, Y., and Wilson, R. P. (2004). Subjectivity in bio-logging science : do logged data mislead? *Mem Natl Polar Res Inst* 58, 23–33.
- Rosenberg, D. K., and McKelvey, K. S. (1999). Estimation of habitat selection for central-place foraging animals. *J Wildl Manage* 63, 1028–1038. doi:10.2307/3802818
- Runge J., and P. Joly, 1995. Zooplancton (euphausiacés et Calanus) de l'estuaire et du golfe du Saint-Laurent. In *Rapport sur l'état des invertébrés en 1994: crustacés et mollusques des côtes du Québec, crevette nordique et zooplancton de l'estuaire et du golfe du Saint-Laurent*. Edited by L. Savard. *Rapp. Manuscrit Can. Sci. Halieut. Aquat.* 2323:124-132.
- Rutz, C., and Hays, G. C. (2009). New frontiers in biologging science. *Biol Lett* 5, 289–292. doi:10.1098/rsbl.2009.0089.
- Saguenay-St. Lawrence Marine Park (2020). Regulations. Available online at:http://parcmarin.qc.ca/wp-content/uploads/2016/10/ParcMarin-Regulations_v2_www-1.pdf
- Sameoto, D. D. (1976). Distribution of sound scattering layers caused by Euphausiids and their relationship to chlorophyll a concentrations in the Gulf of St . Lawrence Estuary. *J Fish Res Board Canada* 33, 681–687. doi:10.1139/f76-084.

- Saucier, F. J., Roy, F., and Gilbert, D. (2003). Modeling the formation and circulation processes of water masses and sea ice in the Gulf of St. Lawrence, Canada. *J Geophys Res* 108, 1–20. doi:10.1029/2000JC000686.
- Savenkoff, C., Comtois, S., and Chabot, D. (2013). Trophic interactions in the St. Lawrence Estuary (Canada): Must the blue whale compete for krill? *Estuar Coast Shelf Sci* 129, 136–151. doi:10.1016/j.ecss.2013.05.033.
- Schneider, J. E. (2004). Energy balance and reproduction. *Physiol Behav* 81, 289–317. doi:10.1016/j.physbeh.2004.02.007.
- Schoenherr, J. R. (1991). Blue whales feeding on high concentrations of euphausiids around Monterey Submarine Canyon. *Can J Zool* 69, 583–594. doi:10.1139/z91-088.
- Schuler, A. R., Piwetz, S., Di Clemente, J., Steckler, D., Mueter, F., and Pearson, H. C. (2019). Humpback whale movements and behavior in response to whale-watching vessels in Juneau, AK. *Front Mar Sci* 6, 1–13. doi:10.3389/fmars.2019.00710.
- Schulz, T. M., and Bowen, W. D. (2005). The evolution of lactation strategies in pinnipeds: A phylogenetic analysis. *Ecol Monogr* 75, 159–177. doi:10.1890/04-0319.
- Sears, R., and Calambokidis, J. (2002). Update COSEWIC status report on the Blue Whale *Balaenoptera musculus* in Canada, in COSEWIC assessment and update status report on the Blue Whale *Balaenoptera musculus* in Canada. Committee on the Status of Endangered Wildlife in Canada. Ottawa. 1-32 pp.
- Sears R, Perrin WF (2009) Blue whale (*Balaenoptera musculus*). In: Perrin WF, Würsig B, Thewissen JGM (eds) Encyclopedia of marine mammals. Academic Press, San Diego, CA, p 120–124
- Sears, R., Ramp, C., Douglas, a B., and Calambodikis, J. (2013). Reproductive parameters of eastern North Pacific blue whales *Balaenoptera musculus*. *Endanger Species Res* 22, 23–31. doi:10.3354/esr00532.
- Sears, R., Ramp, C., Santos, R., Silva, M. A., Steiner, L., Vikingson, G. A. (2015). Comparison of the Northwest Atlantic-NWA and Northeast Atlantic-NEA blue whale (*Balaenoptera musculus*) photo-identification catalogs. Poster presented as a poster at the 21st Biennial Society for Marine Mammalogy Conference; 13–18 December; San Francisco, USA.

- Sears, R., Williamson, M. J., Wenzel, F. W., Bérubé, M., Gendron, D., and Jones, P. (1990). Photographic identification of the Blue Whale (*Balaenoptera musculus*) in the Gulf of St. Lawrence, Canada. Rep Int Whal Comm Spec Issue, 335–342.
- Senigaglia, V., Christiansen, F., Bejder, L., Gendron, D., Lundquist, D., Noren, D. P., et al. (2016). Meta-analyses of whale-watching impact studies: Comparisons of cetacean responses to disturbance. Mar Ecol Prog Ser 542, 251–263. doi:10.3354/meps11497.
- Sergeant, D. E. (1966). Populations of large whale species in the western North Atlantic with special reference to the fin whale. Journal de l'Office des recherches sur les pêcheries, Station de biologie arctique. circulaire no 9.
- Seyboth, E., Groch, K. R., Dalla Rosa, L., Reid, K., Flores, P. A. C., and Secchi, E. R. (2016). Southern Right Whale (*Eubalaena australis*) Reproductive Success is Influenced by Krill (*Euphausia superba*) Density and Climate. Sci Rep 6, 28205. doi:10.1038/srep28205.
- Shaw, A. K., and Couzin, I. D. (2013). Migration or residency? the evolution of movement behavior and information usage in seasonal environments. Am Nat 181, 114–124. doi:10.1086/668600.
- Shepard, E. L. C., Wilson, R. P., Rees, W. G., Grundy, E., Lambertucci, S. A., and Vosper, S. B. (2013). Energy landscapes shape animal movement ecology. Am Nat 182, 298–312. doi:10.1086/671257.
- Sibly, R. M., Nott, H. M. R., and Fletcher, D. . (1990). Splitting behaviour into bouts. Anim Behav 39, 63–69. doi:10.1016/S0003-3472(05)80726-2.
- Siegel, V. (2000). Krill (*Euphausiacea*) demography and variability in abundance and distribution. Can J Fish Aquat Sci 57, 151–167. doi:10.1139/f00-184.
- Siegel, V., Kalinowski, J. (1994) Southern Ocean ecology: the BIOMASS perspective, El-Sayed Sayed Z., BIOMASS Program, Germany) Biomass Colloquium (1991 Bremerhaven Cambridge University Press, Feb. 24, 1994 - Nature - 399 pages
- Sigler, M. F., Tollit, D. J., Vollenweider, J. J., Thedinga, J. F., Csepp, D. J., Womble, J. N., et al. (2009). Steller sea lion foraging response to seasonal changes in prey availability. Mar Ecol Prog Ser 388, 243–261. doi:10.3354/meps08144.

- Sigurjónsson, J. and T. Gunnlaugsson. (1990). Recent trends in abundance of blue (*Balaenoptera musculus*) and humpback whales (*Megaptera novaeangliae*) off west and southwest Iceland, with a note on occurrence of other cetacean species. Report - International Whaling Commission. 40:537-551.
- Silva, M. A., Borrell, A., Prieto, R., Gauffier, P., Bérubé, M., Palsbøl, P. J., et al. (2019). Stable isotopes reveal winter feeding in different habitats in blue, fin and sei whales migrating through the Azores. R Soc Open Sci 6: 181800. doi:10.1098/rsos.181800
- Silva, M. A., Prieto, R., Jonsen, I., Baumgartner, M. F., and Santos, R. S. (2013). North Atlantic blue and fin whales suspend their spring migration to forage in middle latitudes: Building up energy reserves for the journey? PLoS ONE 8(10):e76507. doi:10.1371/journal.pone.0076507.
- Simard, Y., de Ladurantaye, R., and Therriault, J. (1986a). Aggregation of euphausiids along a coastal shelf in an upwelling environment. Mar Ecol Prog Ser 32, 203–215. doi:10.3354/meps032203.
- Simard, Y., Lacroix, G., and Legendre, L. (1986b). Diel vertical migrations and nocturnal feeding of a dense coastal krill scattering layer (*Thysanoessa raschii* and *Meganyctiphanes norvegica*) in stratified surface waters. Mar Biol 91, 93–105. doi:10.1007/BF00397575.
- Simard, Y., and Lavoie, D. (1999). The rich krill aggregation of the Saguenay–St. Lawrence Marine Park: hydroacoustic and geostatistical biomass estimates, structure, variability, and significance for whales. Can J Fish Aquat Sci 56, 1182–1197. doi:10.1139/f99-063.
- Simard, Y., Roy, N., Aulanier, F., and Giard, S.. (2016). Blue whale continuous frequentations of St . Lawrence habitats from multi-year PAM series. DFO Can. Sci. Advis. Sec. Res. Doc. 2016/091. v + 14 p.
- Simard, Y., Roy, N., Giard, S., and Yayla, M. (2014). Canadian year-round shipping traffic atlas for 2013: Volume 1, East Coast marine waters. Can. Tech. Rep. Fish. Aquat. Sci. 3091((Vol.1) E): xviii + 327 p.
- Sims, D. W., Witt, M. J., Richardson, A. J., Southall, E. J., and Metcalfe, J. D. (2006). Encounter success of free-ranging marine predator movements across a dynamic prey landscape. Proc Biol Sci 273, 1195–1201. doi:10.1098/rspb.2005.3444.

- Skagen, S. K. (2006). Migration stopovers and the conservation of Arctic-breeding Calidridine sandpipers. *Auk* 123, 313. doi:10.1642/0004-8038(2006)123[313:msatco]2.0.co;2.
- Soledade Lemos, L., Burnett, J. D., Chandler, T. E., Sumich, J. L., and Torres, L. G. (2020). Intra- and inter-annual variation in gray whale body condition on a foraging ground. *Ecosphere* 11. doi:10.1002/ecs2.3094.
- Sourisseau, M., Simard, Y., and Saucier, F. J. (2006). Krill aggregation in the St. Lawrence system, and supply of krill to the whale feeding grounds in the estuary from the gulf. *Mar Ecol Prog Ser* 314, 257–270. doi:10.3354/meps314257.
- Sourisseau, M., Simard, Y., and Saucier, F. J. (2008). Krill diel vertical migration fine dynamics, nocturnal overturns, and their roles for aggregation in stratified flows. *Can J Fish Aquat Sci* 65, 574–587. doi:10.1139/f07-179.
- Sparling, C. E., Georges, J. Y., Gallon, S. L., Fedak, M., and Thompson, D. (2007). How long does a dive last? Foraging decisions by breath-hold divers in a patchy environment: a test of a simple model. *Anim Behav* 74, 207–218. doi:10.1016/j.anbehav.2006.06.022.
- Sprogis, K. R., Videsen, S., and Madsen, P. T. (2020). Vessel noise levels drive behavioural responses of humpback whales with implications for whale-watching. *Elife* 9, 1–17. doi:10.7554/eLife.56760.
- Stephens, D., & Krebs, J. (1986) *Foraging theory*. Princeton University Press, Princeton, N.J.
- Sweeney, D. A., DeRuiter, S. L., McNamara-Oh, Y. J., Marques, T. A., Arranz, P., and Calambokidis, J. (2019). Automated peak detection method for behavioral event identification: detecting *Balaenoptera musculus* and *Grampus griseus* feeding attempts. *Anim Biotelemetry* 7, 7. doi:10.1186/s40317-019-0169-3.
- Sydeman, W. J., Santora, J. A., Thompson, S. A., Marinovic, B., and Lorenzo, E. Di (2013). Increasing variance in North Pacific climate relates to unprecedented ecosystem variability off California. *Glob Chang Biol* 19, 1662–1675. doi:10.1111/gcb.12165.
- Szesciorka, A. R., Ballance, L. T., Rice, A., Hildebrand, J., Širović, A., and Franks, P. J. (2019). Timing is everything: Drivers of interannual variability in blue whale migration. *J Acoust Soc Am* 146, 2804–2805. doi:10.1121/1.5136714.

- Tarling, G. A., Cuzin-Roudy, J., and Buchholz, F. (1999). Vertical migration behavior in the northern krill *Meganyctiphanes norvegica* is influenced by moult and reproductive processes. *Mar Ecol Prog Ser* 190, 253–262. doi:10.3354/meps190253.
- Thompson, D., and Fedak, M. A. (2001). How long should a dive last? A simple model of foraging decisions by breath-hold divers in a patchy environment. *Anim Behav* 61, 287–296. doi:http://dx.doi.org/10.1006/anbe.2000.1539.
- Thompson D, Hiby AR, Fedak MA (1993) How fast should I swim? Behavioural implications of diving physiology. In: Boyd IL (ed) *Marine mammals: advances in behavioural and population biology*. Clarendon Press, Oxford, p 349–368
- Thums, M., Bradshaw, C. J. A., and Hindell, M. A. (2011). In situ measures of foraging success and prey encounter reveal marine habitat-dependent search strategies. *Ecology* 92, 1258–1270. doi:10.1890/09-1299.1.
- Thums, M., Bradshaw, C. J. A., Sumner, M. D., Horsburgh, J. M., and Hindell, M. A. (2013). Depletion of deep marine food patches forces divers to give up early. *J Anim Ecol* 82, 72–83. doi:10.1111/j.1365-2656.2012.02021.x.
- Tillman, M. F. and G. P. Donovan. (1986). Behaviour of whales in relation to management: report of the workshop. *Rapports de la Commission baleinière internationale*. Numéro spécial 8:1-56.
- Tomlinson, S., Arnall, S. G., Munn, A., Bradshaw, S. D., Maloney, S. K., Dixon, K. W., et al. (2014). Applications and implications of ecological energetics. *Trends Ecol Evol* 29, 280–290. doi:10.1016/j.tree.2014.03.003.
- Vikingsson, G. A. (1990). Energetic studies on fin and sei whales caught off Iceland. (*Balaenoptera physalus*, *Balaenoptera borealis*). *Rep Int Whal Comm* 40, 365–373.
- Villegas-Amtmann, S., Schwarz, L. K., Sumich, J. L., and Costa, D. P. (2015). A bioenergetics model to evaluate demographic consequences of disturbance in marine mammals applied to gray whales. *Ecosphere* 6, art183. doi:10.1890/ES15-00146.1.
- Visser, F., Hartman, K. L., Pierce, G. J., Valavanis, V. D., and Huisman, J. (2011). Timing of migratory baleen whales at the Azores in relation to the North Atlantic spring bloom. *Mar Ecol Prog Ser* 440, 267–279. doi:10.3354/meps09349.

- Ward, E. J., Holmes, E. E., and Balcomb, K. C. (2009). Quantifying the effects of prey abundance on killer whale reproduction. *J Appl Ecol* 46, 632–640. doi:10.1111/j.1365-2664.2009.01647.x.
- Ware, C., Friedlaender, A. S., and Nowacek, D. P. (2011). Shallow and deep lunge feeding of humpback whales in fjords of the West Antarctic Peninsula. *Mar Mammal Sci* 27, 587–605. doi:10.1111/j.1748-7692.2010.00427.x.
- Ware, C., Trites, A. W., Rosen, D. A. S., and Potvin, J. (2016). Averaged Propulsive Body Acceleration (APBA) can be calculated from biologging tags that incorporate gyroscopes and accelerometers to estimate swimming speed, hydrodynamic drag and energy expenditure for Steller sea lions. *PLoS One* 11, e0157326. doi:10.1371/journal.pone.0157326.
- Watanabe, Y. Y., Ito, M., and Takahashi, A. (2014). Testing optimal foraging theory in a penguin-krill system. *Proceeding R Soc London Ser B* 281, 20132376. doi:10.1098/rspb.2013.2376.
- Watkins, J. L., and Murray, A. W. A. (1998). Layers of Antarctic krill, *Euphausia superba*: Are they just long krill swarms? *Mar Biol* 131, 237–247. doi:10.1007/s002270050316.
- Webb, P. W. (1984). Body form, locomotion and foraging in aquatic vertebrates. *Am Zool* 24, 107–120. doi:10.1093/icb/24.1.107
- Wheatley, K. E., Bradshaw, C. J. A., Harcourt, R. G., and Hindell, M. A. (2008). Feast or famine: Evidence for mixed capital-income breeding strategies in Weddell seals. *Oecologia* 155, 11–20. doi:10.1007/s00442-007-0888-7.
- Wiedenmann, J., Cresswell, K. A., Goldbogen, J. A., Potvin, J., and Mangel, M. (2011). Exploring the effects of reductions in krill biomass in the Southern Ocean on blue whales using a state-dependent foraging model. *Ecol Modell* 222, 3366–3379. doi:10.1016/j.ecolmodel.2011.07.013.
- Williams, R., Lusseau, D., and Hammond, P. S. (2006). Estimating relative energetic costs of human disturbance to killer whales (*Orcinus orca*). *Biol Conserv* 133, 301–311. doi:10.1016/j.biocon.2006.06.010.
- Williams, R., Vikingsson, G. A., Gislason, A., Lockyer, C., New, L., Thomas, L., et al. (2013). Evidence for density-dependent changes in body condition and pregnancy rate of North Atlantic fin whales over four decades of varying environmental conditions. *ICES J Mar Sci* 70, 1273–1280. doi:10.1093/icesjms/fst059.

- Williams, T. M. (1999). The evolution of cost efficient swimming in marine mammals: Limits to energetic optimization. *Philos Trans R Soc B Biol Sci* 354, 193–201. doi:10.1098/rstb.1999.0371.
- Williams, T. M., Davis, R. W., Fuiman, L. A., Francis, J., LeBoeuf, B. J., Horning, M., et al. (2000). Sink or swim: strategies for cost-efficient diving by marine mammals. *Science* (80-) 288, 133–136. doi:10.1126/science.288.5463.133.
- Wilson, R. P., Quintana, F., and Hobson, V. J. (2012). Construction of energy landscapes can clarify the movement and distribution of foraging animals. *Proc R Soc B Biol Sci* 279, 975–980. doi:10.1098/rspb.2011.1544.
- Winship, A. J., Trites, A. W., and Rosen, D. A. S. (2002). A bioenergetic model for estimating the food requirements of Steller sea lions *Eumetopias jubatus* in Alaska, USA. *Mar Ecol Prog Ser* 229, 291–312. doi:10.3354/meps229291.
- Witteveen, B. H., De Robertis, A., Guo, L., and Wynne, K. M. (2015). Using dive behavior and active acoustics to assess prey use and partitioning by fin and humpback whales near Kodiak Island, Alaska. *Mar Mammal Sci* 31, 255–278. doi:10.1111/mms.12158.
- Womble, J. N., Horning, M., Lea, M. A., and Rehberg, M. J. (2013). Diving into the analysis of time-depth recorder and behavioural data records: A workshop summary. *Deep Res Part II Top Stud Oceanogr* 88–89, 61–64. doi:10.1016/j.dsr2.2012.07.017.
- Wood S (2006) Mixed GAM computation vehicle with automatic smoothness estimation. R package version 1.8-17. <https://CRAN.R-project.org/package=mgcv>
- Wright, B. M., Ford, J. K. B., Ellis, G. M., Deecke, V. B., Shapiro, A. D., Battaile, B. C., et al. (2017). Fine-scale foraging movements by fish-eating killer whales (*Orcinus orca*) relate to the vertical distributions and escape responses of salmonid prey (*Oncorhynchus* spp.). *Mov Ecol* 5, 3. doi:10.1186/s40462-017-0094-0.
- Wright, I. A., Rhind, S. M., Whyte, T. K., and Smith, A. J. (1992). Effects of body condition at calving and feeding level after calving on LH profiles and the duration of the post-partum anoestrous period in beef cows. *Anim Prod* 55, 41–46. doi:10.1017/S0003356100037259.
- Yochem, P.K., Leatherwood, S. (1985). Blue whale *Balaenoptera musculus* (Linnaeus 1758). In *Handbook of marine mammals, Volume 3, The sirenians and baleen whales*. S. H. Ridgway and Sir R. Harrison (Editors). Academic Press Limited, London, 362 p.

Zuur, A.F., Ieno, E.N., Walker, N.J., Saveliev, A.A. & Smith, G.M. (2009) *Mixed Effects Models and Extensions in Ecology with R*. Springer, New-York.

